PB88-208178

Effect of Fuel Sulfur on Nitrogen Oxide Formation in Combustion Processes

Arizona Univ., Tucson

Prepared for

Environmental Protection Agency
Research Triangle Park, NC

May 88

U.S Department of Commerce
National Technical Information Service
NTIS

TECHNICAL REPORT DATA

(Please read Instructions on the reverse before completing)

1. REPORT NO. EPA/600/7-88/007

2.

3. RECIPIENT'S ACCESSION NO. PB88-208178/AS

4. TITLE AND SUBTITLE Effect of Fuel Sulfur on Nitrogen Oxide Formation in Combustion Processes

5. REPORT DATE May 1988

6. PERFORMING ORGANIZATION CODE

7. AUTHOR(S) J.O.L. Wendt, T.L. Corley, and J.T. Morcomb

8. PERFORMING ORGANIZATION REPORT NO.

9. PERFORMING ORGANIZATION NAME AND ADDRESS
The University of Arizona
Department of Chemical Engineering
Tucson, Arizona 85721

10. PROGRAM ELEMENT NO.

11. CONTRACT/GRANT NO. EPA Grant R803715

12. SPONSORING AGENCY NAME AND ADDRESS
EPA, Office of Research and Development
Air and Energy Engineering Research Laboratory
Research Triangle Park, NC 27711

13. TYPE OF REPORT AND PERIOD COVERED Final; 1/76 - 12/80

14. SPONSORING AGENCY CODE **EPA/600/13**

15. SUPPLEMENTARY NOTES Project officer W.S. Lanier is no longer with the Agency. For details, contact William P. Linak, Mail Drop 65, 919/541-5792.

16. ABSTRACT The report gives results of research that focuses on the questions: is the sulfur content of a fuel likely to have a major influence on the resulting NOx emissions? and does the presence of fuel sulfur cause major changes in mechanisms of fuel NO formation? (NOTE: Chemically bound nitrogen in fossil fuels has been shown to be an important contributor to nitrogen oxide (NOx) emissions from combustion processes. Many fuels containing chemically bound nitrogen also contain sulfur in various amounts.) Research results will aid in the interpretation of data on effects of fuel quality and composition on pollutant formation and will help in the development of combustion modifications for pollutant control from burning dirty fuels. The most important conclusion is that the presence of fuel sulfur will increase the ultimate conversion of fuel nitrogen to NOx under poorly mixed flame conditions that are often typical of combustion modifications. The influence of sulfur is to increase the total amount of XN species ($NO + NH_3 + HCN$) under rich conditions, and this effect is most pronounced at high temperatures. The mechanisms occur in the post-flame or at fairly long residence times and probably involve interactions between the hydrocarbon chemistry, sulfur, and nitrogenous species.

17. KEY WORDS AND DOCUMENT ANALYSIS

a. DESCRIPTORS	b. IDENTIFIERS/OPEN ENDED TERMS	c. COSATI Field/Group
Pollution	Pollution Control	13B
Fossil Fuels	Stationary Sources	21D
Sulfur	Fuel Sulfur	07B
Nitrogen Oxides		
Combustion		21B

18. DISTRIBUTION STATEMENT **Release to Public**

19. SECURITY CLASS *(This Report)* Unclassified

20. SECURITY CLASS *(This page)* Unclassified

21. NO. OF PAGES 251

22. PRICE

EPA Form 2220-1 (9-73)

EPA/600/7-88/007
May 1988

PB88-208178

EFFECT OF FUEL SULFUR ON NITROGEN OXIDE FORMATION IN COMBUSTION PROCESSES

by

J.O.L. Wendt, T.L. Corley and J.T. Morcomb
Department of Chemical Engineering
University of Arizona
Tucson, Arizona 85721

EPA Grant No. R803715

EPA Project Officer: W. Steven Lanier
Combustion Research Branch
Air and Energy Engineering Research Laboratory
Research Triangle Park, N.C. 27711

AIR AND ENERGY ENGINEERING RESEARCH LABORATORY
OFFICE OF RESEARCH AND DEVELOPMENT
U.S. ENVIRONMENTAL PROTECTION AGENCY
RESEARCH TRIANGLE PARK, NC 27711

REPRODUCED BY
U.S. DEPARTMENT OF COMMERCE
National Technical Information Service
SPRINGFIELD, VA. 22161

NOTICE

This document has been reviewed in accordance with U.S. Environmental Protection Agency policy and approved for publication. Mention of trade names or commercial products does not constitute endorsement or recommendation for use.

ABSTRACT

Chemically bound nitrogen in fossil fuels has been shown to be an important contributor to nitrogen oxide (NO_x) emissions from combustion processes. Many fuels containing chemically bound nitrogen also contain sulfur in various amounts. The research reported here focuses on the question whether the sulfur content of a fuel is likely to have a major influence on the resulting NO_x emissions and specfcally whether the presence of fuel sulfur causes major changes in mechanisms of fuel NO formation. Results will aid in the interpretation of data on effects of fuel quality and composition on pollutant formation and will help in the development of combustion modifications for pollutant control from the burning of dirty fuels.

The research was divided into four phases, and so this report is divided into four parts. Part 1 is concerned with exhaust emission measurements from turbulent diffusion flames; Part 2 with NO profiles in premixed rich methane flames; Part 3 with detailed results on rich premixed CO flames; and Part 4 with detailed results on rich CH_4 flames. Parts 3 and 4 also contain details of the chromatographic procedure utilized to help close the nitrogen balance.

The most important conclusion is that the presence of fuel sulfur will increase the ultimate conversion of fuel nitrogen to nitrogen oxides under poorly mixed flame conditions that are often typical of combustion modifications. The influence of sulfur is to increase the total amount of XN species (CO + NH_3 + HCN) under rich conditions, and this effect is most pronounced at high temperatures. The mechanisms occur in the post flame or at fairly long residence times and probably involve interactions between the hydrocarbon chemistry, sulfur and nitrogenous species.

TABLE OF CONTENTS

Page

ABSTRACT iii

FIGURES vi

TABLES xii

CONVERSION FACTORS xiii

NOMENCLATURE xiii

EXECUTIVE SUMMARY. xiv

1. FUEL SULFUR EFFECTS ON NO_X FORMATION IN TURBULENT DIFFUSION FLAMES 1

1.1 Background 1

1.2 Combustion Facility 10

1.3 Definition of Terms 26

1.4 Thermal NO 30

1.5 Fuel NO-Fuel Sulfur Interactions 56

1.6 Fuel Nitrogen Conversion to NO 78

1.7 Discussion 85

1.8 Conclusions 99

1.9 References 104

2. INTERACTIONS OF FUEL SULFUR AND FUEL NITROGEN IN FUEL RICH PREMIXED LAMINAR FLAMES 109

2.1 Purpose and Scope 109

2.2 Background 110

2.3 Hardware 114

2.4 Flame Temperature Measurement 128

2.5 Interferences in Sampling and Analysis System 136

2.6 Results 148

2.7 Discussion 166

2.8 References 177

TABLE OF CONTENTS (Continued)

Page

3. POST FLAME BEHAVIOR OF NITROGENOUS SPECIES IN THE PRESENCE OF FUEL SULFUR. I. RICH, MOIST, $CO/Ar/O_2$ FLAMES. 179

3.1 Introduction 179

3.2 Experimental Burner 181

3.3 Experimental Results 184

3.4 Kinetic Modeling 191

3.5 Conclusions 203

3.6 References 205

4. POST FLAME BEHAVIOR OF NITROGENOUS SPECIES IN THE PRESENCE OF FUEL SULFUR. II. RICH, $CH_4/He/O_2$ FLAMES . . 207

4.1 Introduction 207

4.2 Experimental Apparatus 208

4.3 Experimental Results 211

4.4 Conclusions 230

4.5 References 231

LIST OF FIGURES

Figure Page

1.2-1 Experimental Furnace -- From Pershing (1976). 11

1.2-2 Multifuel Burner -- From Pershing (1976) 13

1.2-3 Swirl Vanes -- From Pershing (1976) 14

1.2-4 Schematic of Natural Gas Fuel Injector 16

1.2-5 Schematic of Distillate Oil Fuel Injector 17

1.2-6 Air Supply System 18

1.2-7 Fuel Oil/Additive System 21

1.2-8 Typical High-Pressure, Oil Atomizing Nozzle and Resulting Spray Cone Pattern. 23

1.2-9 Analytical System -- From Pershing (1976) 24

1.4-1 Natural Gas/Axial Injector: Effect of SO_2 on Thermal NO (37% Swirl; 120°F Air Proheat) 33

1.4-2 Natural/Gas/ Axial Injector: Effect of Swirl on Fuel S Inhibition of Thermal NO (11.4% Excess Air; 100°F Preheat). 35

1.4-3 Natural Gas/Axial Injector: Effect of SO_2 at High Air Preheat (40% Swirl; 440°F Air Preheat). 37

1.4-4 Natural Gas/Axial Injector: Effect of SO_2 at High Air Preheat (44% Swirl; 430°F Air Heat). 38

1.4-5 Natural Gas/Axial Injector: Effect of Swirl on Fuel S Inhibition of Thermal NO at high Air Preheat (15.0% Excess Air; 430°F Air Preheat).. 43

1.4-6 Natural Gas/Radial Injector: Effect of SO_2 on Thermal NO (38% Swirl; 100°F Air Preheat). 45

1.4-7 Natural Gas/Radial Injector: Effect of Swirl on Fuels Inhibition of Thermal N (15.9% Excess Air; 110°F Air Preheat). 47

1.4-8 Natural Gas/Radial Injector: Effect of SO_2 at High Air Preheat (42% Swirl; 440°F Air Preheat). 49

1.4-9 Distillate Oil: Replacement of Some Distillate Oil by Benzene Does Not Affect Thermal NO (59% Swirl; 100°F Air Preheat; 80°R Nozzle). 52

LIST OF FIGURES (Continued)

Figure Page

1.4-10 Distillate Oil: Thiophene Inhibits Thermal NO at Low Air Preheat (60% Swirl; 100°F Air Preheat; 80°R Nozzle). 54

1.4-11 Distillate Oil: Effect of SO_2 Addition to Air on Thermal NO at High Air Preheat (44% Swirl; 310°F Air Preheat; 30°R Nozzle) 55

1.5-1 Distillate Oil: Effect of Benzene Addition and Fuel S on Fuel NO (44% Swirl; 130°F Air Preheat; 30°R Nozzle). . . 62

1.5-2 Distillate Oil: Thiophene Does Not Affect Fuel NO at Low Air Preheat (43% Swirl; 100°F Air Preheat; 30°R Nozzle). 64

1.5-3 Distillate Oil: Effect of Fuel S and Fuel N on Fuel NO (44% Swirl; 100°F Air Preheat; 30°R Nozzle). 65

1.5-4 Distillate Oil: Effect of Swirl and Fuel S on Fuel NO (15.1% Excess Air; 100°F Air Preheat; 30°R Nozzle) . . . 67

1.5-5 Distillate Oil: Benzene Does Not Affect Fuel NO at High Air Preheat (44% Swirl; 315°F Air Preheat; 330°R Nozzle). 69

1.5-6 Distillate Oil: Thiophene Increases Fuel NO at High Air Preheat (40% Swirl; 310°F Preheat; 30°R Nozzle) 70

1.5-7 Distillate Oil: Fuel S and Fuel N Interactions of High Air Preheat (44% Swirl; 315°F Air Preheat; 30°R Nozzle). 72

1.5-8 Distillate Oil: Effect of Swirl on Thiophene Enhancement of Fuel NO at High Air Preheat (21.3% Excess Air; 310°F Air Preheat; 30°R Nozzle). 75

1.5-9 Natural Gas/Ammonia -- Axial Injector: SO_2 Increases Fuel NO at High Air Preheat (44% Swirl; 430°F Air Preheat). 76

1.6-1 Distillate Oil: Conversion of Fuel N to Fuel NO at Various Fuel N Levels (15.0% Excess Air; 42% Swirl; 100°F Air Preheat; 30°R Nozzle; Thermal NO = 100 ppm) 79

1.6-2 Comparison of nitrogen Conversion to NO with That of Other Workers -- Selected data taken from Sarofim and Flagan (1975) 81

LIST OF FIGURES (Continued)

Figure Page

2.3-1 Schematic of Burner and Position of Probe 115

2.3-2 Schematic of Hot Quartz Probe and Probe Holder. 117

2.3-3 Schematic of Water Cooled Quartz Sampling Probe and Its Holder. 119

2.3-4 Schematic of the Sampling and Analysis System 121

2.3-5 Schematic of Flow System 125

2.4-1 Optical System for Flame Temperature Determination 131

2.4-2 Chart Recorder Traces of a Temperature Determination by Sodium Reversal Method. -- Peaks of sodium doublet appear at 5886A and 5891A. Chart speed set at 6 A/inch. . 135

2.5-1 Units and Their Substitutes in the Sampling and Analysis System to Determine Possible Interferences. . . . 137

2.5-2 Hot Probe Effect Shown at a 0.46 Stoichiometric Ratio. -- Initial (i) and final (f) indices refer to base NO values before and after sulfur addition. 140

2.5-3 Behavior of Cooled Probe Sampling at a 0.46 Stoichiometric Ratio. -- Initial (i) and final (f) indices refer to base NO values before and after sulfur additions 142

2.5-4 Effect of Cooled Probe on Temperature at a Point Low Temperature Study, S.R. = 0.50 143

2.5-5 Effect of Cooled Probe on Temperature at a Point High Temperature Study, S.R. = 0.69. = Peak temperature of 2114 K at grid level with probe removed 144

2.5-6 Effect of Hot Probe on Temperature at a Point Low Temperature Study, S.R. = 0.50. = Peak Temperature of 2022 K at grid level 146

2.5-7 Effect of Hot Probe on Temperature at a Point High Temperature Study, S.R. = 0.72. -- Peak temperature of 2076 K at grid level with probe removed. 147

2.6-1 Laminar Premixed Flame: Stoichiometric Ratio 0.40 (0.21% Fuel N, 100% Conversion = 554 ppm, 1 cm = 7.56 ms at 1930 K, SO_2, H_2S, as Fuel S). 150

LIST OF FIGURES (Continued)

Figure Page

2.6-2 Laminar Premixed Flame: Stoichiometric Ratio 0.46 (0.21% Fuel N, 100% Conversion = 553 ppm, 1 cm = 7.67 ms at 1900 K, SO_2 as Fuel S). 151

2.6-3 Laminar Premixed Flame: Stoichiometric Ratio 0.46 (0.21% Fuel N, 100% Conversion = 509 ppm, 1cm = 6.81 ms at 1970 K, SO_2 as Fuel S). 152

2.6-4 Laminar Premixed Flame: Stoichiometric Ratio (0.46 (0.21% Fuel N, 100% Conversion = 553 ppm, 1 cm = 7.67 ms at 1900 K, H_2S as Fuel S). 153

2.6-5 Laminar Premixed Flame: Stoichiometric Ratio 0.54 (0.21% Fuel N, 100% Conversion = 399 ppm, 1 cm = 4.10 ms at 2150 K, SO_2 as Fuel S). 154

2.6-6 Laminar Premixed Flame: Stoichiometric Ratio 0.54 (0.21% Fuel N, 100% Conversion = 399 ppm, 1 cm = 410 ms at 2150 K, H_2S as Fuel S) 155

2.6-7 Laminar Premixed Flame: Stoichiometric Ratio 0.61 (0.21% Fuel N, 100% Conversion = 357 ppm, 1 cm = 4.47ms at 2100 K, SO_2, H_2S as Fuel S) 156

2.6-8 Laminar Premixed Flame: Stoichiometric Ratio 0.68 (0.21% Fuel N, 100% Conversion = 300 ppm 1 cm = 4.00 ms at 1980 K, SO_2, H_2S as Fuel S). 157

2.6-9 Laminar Premixed Flame: Stoichiometric Ratio 0.80 (0.21% Fuel N, 100% Conversion = 245 ppm, 1 cm = 3.53 ms at 1830 K, SO_2 as Fuel S). 158

2.6-10 Laminar Premixed Flame: Stoichiometric Ratio 1.2 (0.21% Fuel N, 100% Conversion = 208 ppm NO, 1 cm = 2.74 ms at 2000 K, SO_2 as Fuel S). 159

2.6-11 Laminar Premixed Flame: Stoichiometric Ratio 0.46 (1.05% Fuel N, 100% Conversion = 2559 ppm, 1 cm = 6.68 ms at 2000 K, SO_2 as Fuel S). 160

2.6-12 Laminar Premixed Flame: Stoichiometric Ratio 0.61 (1.05% Fuel N, 100% Conversion = 1751 ppm, 1 cm = 4.74 ms at 1940 K, SO_2 as Fuel S). 161

2.7-1 Enhancement of Peak Fuel NO by Sulfur Additives at Fuel-Rich Conditions. -- Sulfur given as mole percent of inlet fuel 169

LIST OF FIGURES (Continued)

Figure Page

2.7-2 Higher Mole Percent Fuel Sulfur Contents Increase Peak Fuel NO Yields for Two Rich Stoichiometric Ratios. 171

2.7-3 Sulfur Additives Cause a Greater Reduction in Exhaust Fuel NO at Most Stoichiometric Ratios 172

2.7-4 Peak NO Yields in the Presence of SO_2 Decrease With Increasing Peak Flame Temperatures. -- 0.46 stoichiometric ratio. 175

3.2-1 Schematic of Flat Flame Apparatus and Analysis System . . . 183

3.2-2 Sample Chromatogram for Trace N_2 Analysis 185

3.3-1 Major species profiles for flame 1, $\phi = 2.17$ Shaded symbols denote equilibrium values at the local tempertures 188

3.3-2 Nitrogenous species and nitrogen balance in post flame: Effect of Fuel nitrogen species type. Flames 1 and 2, $\phi = 2.17$ 189

3.3-3 Nitrogenous species and nitrogen balance in the post flame: Effect of fuel sulfur and fuel nitrogen level 192

3.4-1 Experimental and predicted NO and N_2 profiles in the high temperature (2400-2000K) post flame. 196

3.4-2 Experimental and predicted NO and N_2 profiles in the low temperature (2000-1700K) post flame. The role of $HNO + CO \rightarrow CO_2 + NH$ 198

4.2-1 Chromatograms for N_2/He Mixtures N_2 appears at 2.0 minutes. 210

4.3-1 Influence of SO_2 on NO Profiles with Argon Diluent [Zero SO_2: $C_2N_2^o$ = 1906 ppm; with SO_2: $C_2N_2^o$ = 1409 ppm; SO_2^o = 9436 ppm; CH_4 = 6.08 ℓ/min; O_2 = 5.62 ℓ/min; Ar = 10.84 ℓ/min] 212

4.3-2 Influence of SO_2 on NO Profiles with Helium Diluent [Zero SO_2: $C_2O\ N_2^o$ = 1906; with SO_2: $C_2N_2^o$ = 1884 ppm; SO_2^o = 11570 ppm]. 213

LIST OF FIGURES (Continued)

Figure Page

4.3-3 Influence of Sulfur on Major Species Profiles: SR = 0.458, Flame A [CH_4 = 6.18 ℓ/min O_2 = 5.68 ℓ/min, He = 12.20 ℓ/min, SO_2 = 8850 ppm] 215

4.3-4 Effect of Sulfur on Nitrogenous Species SR = 0.458, Flame A [C_2N_2 = 1350 ppm, 1340 ppm with SO_2] 216

4.3-5 Influence of Sulfur on Major Species Profiles: SR = 0458, Flame B [CH_4 = 7.12 ℓ/min, O_2 = 6.55 ℓ/min, He = 13.64 ℓ/min, SO_2 = 242 ℓ/min] 218

4.3-6 Influence of Sulfur on Nitrogenous Species Profiles: SR = 0.458, Flame B [C_2N_2 = 53.6 mℓ/min]. 219

4.3-7 Major Species, SR = 0.585 [CH_4 = 7.12 ℓ/min, O_2 = 8.39 ℓ/min, He = 26.99 ℓ/min, SO_2 = 215 mℓ/min] . . . 221

4.3-8 Temperature Profile: SR = 0.585 222

4.3-9 Comparison of Measured Temperature and Temperature Consistent with Water Gas Shift Equilibrium. 223

4.3-10 Influence of Sulfur on Nitrogenous Species, SR = 0.585 [C_2N_2 = 50.9 mℓ/min]. 224

4.3-11 Closure of the Nitrogen Balance 226

4.3-12 Decay of (Inferred) N_2O Concentration 227

4.3-13 Nitrogenous Species Profiles, SR = 0.693 [CH_4 = 5.03 ℓ/min, O_2 = 7.04 ℓ/min, He = 39.67 ℓ/m, C_2N_2 = 983 ppm (979 ppm with SO_2), SO_2 = 4135 ppm] . . 229

LIST OF TABLES

Table		Page
1.3-1	#2 Diesel Oil Composition	27
1.3-2	Natural Gas Composition	28
1.7-1	Summary of Proposed Reactions	93
3.3-1	High Temperature Flame Conditions	186
3.3-2	Low Temperature Flame Conditions	186
3.4-1	Inlet, Calculated Plug Flow Inlet and Equilibium Mole . . Fractions. Flame 1	195
3.4-2	Sulfur Chemistry	200

CONVERSION FACTORS

To convert from	To	Multiply by
British thermal unit	gram calories	252
degrees Fahrenheit-32	degrees Centigrade	0.5555
feet	centimeters	30.48
cubic feet	cubic meters	0.02832
feet per minute	centimeters per second	0.508
cubic feet per minute	cubic meters per second	0.000472
gallons	liters	3.785
gallons per minute	liters per second	0.06308
grains per cubic foot	grams per cubic meter	2.228
pounds	kilograms	0.4536
tons (short)	metric tons	0.90718
tons per hour	kilograms per second	0.252

NOMENCLATURE

Å = Angstroms

cc = cm^3

gph = gallons per hour

u = micrometers

psi = pounds per square inch

psig = pounds per square inch gauge

" = inches

EXECUTIVE SUMMARY

Because chemically bound nitrogen in fossil fuels has been shown to be an important contributor to nitrogen oxide (NO_x) emmisions, much research has been focused on mechanisms governing the oxidation of fuel nitrogen to fuel NO. This has been done in the hope that the insight and understanding gained thereby will lead to development of new combustion modifications for NO_x control. However, many fuels containing chemically bound nitrogen also contain sulfur in various amounts. Indeed, insofar as pulverized coal is concerned, a wide variation in sulfur content is possibble, even from coals with similar nitrogen contents. The question can, therefore, be posed whether the sulfur content of a fuel is likely to have a major influence on the resulting NO_x emissions and specifically whether the presence of fuel sulfur will cause major changes in mechanisms of fuel NO formation. Furthermore, since there exists a wide variety of possible combustion conditions and combustion modifications, it is to be expected that the potential importance of SO_x/NO_x interactions depends not only on the fuel quality. but also on the conditions under which the fuel is burned.

This report describes results of a far ranging study to determine first, if sulfur has a measurable effect on fuel nitrogen conversion in practical combustion configurations and second, the mechanisms through which this effect, if it exists, is implemented. The results from the practical turbulent diffusion flame studies did in fact indicate that sulfur may have a first order influence on fuel NO emissions when the fuel is burned under hot, poorly mixed combustion conditions in which fuel nitrogen processing occurs in long-lived hot rich zones. These results, which are of practical significance, prompted further studies on fuel nitrogen processing in hot rich premixed laminar flames environments.

The project was divided into four phases:

1. Fuel sulfur effects on NO_x formation in turbulent diffusion flames.
2. Interactions of fuel sulfur and fuel nitrogen in fuel-rich premixed laminar flames.
3. Post flame behavior of nitrogenous species in the presence of fuel sulfur. I. Rich, Moist, $CO/Ar/O_2$ flames.
4. Post flame behavior of nitrogenous species in the presence of fuel sulfur. II. Rich, Moist, $CH_4/He/O_2$ flames.

It is apparent that each phase followed on from the previous one and originated from the need to obtain ever more fundamental data to understand and generalize the effects observed. Phase 1 was concerned only with exhaust NO measurements, Phase 2 with NO profiles, Phase 3 with NO, HCN, $NH_3$and N_2 profiles in CO flames and the kinetic modeling thereof, and Phase 4 with profiles of the same species in CH_4 flames. Summaries of further details of each phase are delineated below.

Phase 1: Turbulent Diffusion Flames

Interactions between certain fuel sulfur compounds and nitric oxide (NO) in turbulent gaseous and distillate oil diffusion flames were experimentally investegated utilizing a 75,000 Btu/hr (22 kW) laboratory combustor. Aerodynamics, air preheat conditions, and overall excess air conditions were varied to determine their role in any such interaction.

Results indicated that addition of sulfur dioxide (SO_2) to natural gas flames could enhance or inhibit NO emmissions. Local flame stoichiometry and temperature, which were influenced by fuel injector type, determined which effect was observed and the extent to which it occurred. Thiophene (C_4H_4S) and pyridine (C_5H_5N) were added to #2 diesel oil to determine effects of fuel sulfur on conversion of chemically bound fuel nitrogen to NO. No discernible effect was observed at "zero" air preheat conditions. NO emissions were enhanced at high air preheat conditions. Addition of SO_2 to natural gas flames doped with ammonia (NH_3) produced a significant increase in conversion of NH_3 to NO at high air preheat conditions.

Inhibition effects were explained in terms of homogeneous catalysis of recombination reactions by SO_2. Hydrogen abstraction reactions involving reduced form, were considered to explain the enhancement effect.

Phase 2: NO Profiles in Premixed Laminar Flames

Significant fuel sulfur and fuel nitrogen interactions were observed in the post reaction zone of premixed flat flames. Methane/oxygen/argon flames of stoichiometric ratios between 0.40 (ϕ= 2.5) and 1.2 (ϕ= 0.833) were doped with cyanogen and with sulfur additives of SO_2 and H_2S. The resulting profiles of NO in fuel-rich studies exhibited an enhancement of peak NO formation due to sulfur species. These peak NO values decayed rapidly in the later portions of the flame, indicating the continuation of low temperature (below 1600 K) reactions. In some instances, the presence of sulfur species caused the decay or reduction of NO to proceed below the base line values at very long (greater that 0.1 second) residence times.

Phase 3: Nitrogenous Species Profiles in CO Flames

Experimental measurements of NO, N_2 and other nitrogenous species in the post flame gases of rich (ϕ=2.17) premixed laminar CO/Ar/O_2 (trace H_2) flames, with fuel nitrogen as NO, C_2N_2 and NH_3 and fuel sulfur as SO_2, allowed the nitrogen balance to be closed to within 7%. In the absence of hydrocarbons, and with only a trace of hydrogen, NO decayed homogeneously to form N_2 at high temperatures, and the fate of the fuel nitrogen was independent of the type of fuel nitrogen species. The effect of fuel sulfur was to decrease post flame NO levels and increase N_2 more rapidly. The observed decay in NO and formation of N_2 were consistent with detailed kinetic calculations employing only the reverse Zeldovich mechanisms to form N and N_2. There was no evidence of other N_2 formation mechanisms being important for these hydrogen poor flames, at either high or low temperatures. Calculations also showed that the most plausible effect of SO_2 in the mixture was to increase the steady state N atom concentration through direct interactions between N, NO, S and SO.

Phase 4: Nitrogenous Species Profiles in CH_4 Flames

Profiles of NH_3, HCN, NO, and N_2 in premixed CH_4/He/O_2/C_2N_2 flames allowed the nitrogen balance to be closed to within 3% in the far post flame region of rich flames at stoichiometric ratios greater than 0.58 ($\phi<1.72$). In the flame front and the near post flame, a (decaying) discrepancy in the nitrogen balance was attributed to N_2O which was being destroyed to form N_2. For exceedingly rich sooting flames (SR=0.46,ϕ=2.17), closure was impossible due to nitrogenous species adsorbed on solid particles. In all cases the effect of sulfur was to increase the sum of NO + HCN + NH_3 and to decrease N_2. This is consistent with the previous data on hydrocarbon flames decribed above.

Results showed that sulfur accelerates hydrocarbon decay rates, thereby inhibiting hydrocarbon breakthrough, which apparently influences the XN species profiles in the post flame. Certainly, hydrocarbons and possibly hydrogen play a critical role in the enhancement effect that fuel sulfur has on fuel nitrogen conversion.

Results from this project, taken as a whole, indicate that, under hot rich conditions often considered optimum for NO abatement by staged combustion, fuel sulfur tends to increase the conversion of fuel nitogen in hydrocarbon fuels.

1. FUEL SULFUR EFFECTS ON NO_x FORMATION IN TURBULENT DIFFUSION FLAMES

1.1 Background

1.1-1 Introduction

The combustion of many fossil fuels gives rise to emissions of sulfur oxides and nitrogen oxides. Control of these pollutants will become increasingly important with the anticipated increase in usage of coal and low-grade residual oils, since significant amounts of chemically bound sulfur and/or nitrogen are usually present. The potential increase in usage of low-Btu fuels, derived from coal gasification, for on-site energy needs, may also result in increased interest in abatement techniques of sulfur and nitrogen oxides since, in the absence of hot gas, cleanup processes, substantial amounts of ammonia and hydrogen sulfide may remain in the gas.

Sulfur oxide pollution may be abated by either fuel desulfurization or stack gas scrubbing. The choice of abatement method is usually dictated by economic considerations. However, in calculating cost effectiveness of various sulfur oxide abatement strategies, it is important to determine the extent to which the technology used has an adverse effect on other pollutants, such as nitrogen oxides (NO_x). Should sulfur compounds in the flame front have an inhibition influence on the formation of NO_x (Wendt and Ekmann, 1974), this would indicate that fuel desulfurization might require additional NO_x abatement methods to be implemented, and that this would involve additional costs which would not occur with stack gas scrubbing, where the sulfur species are removed after the combustion process.

This work focuses on the possibility of interaction of fuel sulfur with nitrogen oxide (NO) formation in gaseous and distillate oil turbulent diffusion flames. The project should, therefore, be viewed as an extension of previous work (Wendt and Ekmann, 1974), which showed that high levels of fuel sulfur did inhibit thermal NO formation in premixed gaseous flames. The goal here was to determine whether fuel sulfur did influence the formation of NO in turbulent diffusion flames. In the event that an interaction between fuel sulfur and NO formation was observed, the objective was to identify and investigate those factors which were important in the interaction.

The formation of nitrogen oxides in "clean" systems (gaseous fuels) has been extensively investigated and is reviewed in sections 1.2 and 1.3. Information concerning fuel sulfur is presented in section 1.4.

1.1-2 Thermal NO Formation

During the combustion of fossil fuels, nitrogen oxides are formed by the high temperature, thermal fixation of molecular oxygen, and nitrogen present in the combustion air. NO is the favored oxide form because the residence time in most stationary combustion processes is too short for the oxidation of NO to NO_2, even though NO_2 is thermodynamically favored at lower temperatures (Bartok et al., 1969). NO, however, does oxidize in the atmosphere to NO_2, which is a primary participant in photochemical smog. NO resulting from the oxidation of atmospheric nitrogen, N_2, is defined to be thermal NO.

For many years, it was generally assumed that the thermal fixation of atmospheric nitrogen to produce NO occurred according to the mechanism suggested by Zeldovich, Sadovnikov, and Frank-Kamenetskii (1947):

$$O + N_2 = NO + N$$

$$N + O_2 = NO + O$$

plus the reaction

$$N + OH = NO + H$$

taken together with the assumption that the combustion reactions have equilibrated prior to the initiation of nitric oxide formation. Although the data of Fenimore (1971), Bowman (1973), and Pershing and Berkau (1973) support this simplified equilibrium Zeldovich mechanism scheme for post combustion zone formation of NO, it does not allow absolute prediction of NO emissions, especially under fuel-rich conditions, and does not agree with measured profiles near the flame front.

Fenimore (1971) found a substantial amount of "prompt" NO which formed very rapidly in the methane-air and ethylene-air flame fronts. This prompt NO could not be explained based on the extended Zeldovich mechanism with equilibrated radical concentrations. Prompt NO has subsequently been observed experimentally in gaseous systems by Bowman and Seery (1972); Iverach, Basden, and Kirov (1973); Wendt and Ekmann (1974); and Malte and Pratt (1975). It has been suggested that prompt NO is the consequence of nonequilibrium radical concentrations in the vicinity of the combustion zone (Bowman, 1971; Sarofim and Pohl, 1973; de Soete, 1972). Mitchell and Sarofim (1975), Malte and Pratt (1975), and Bowman (1975) have experimentally observed "super-equilibrium" radical concentrations in gaseous systems. The inclusion of nonequilibrium free radical concentrations in the Zeldovich mechanism improves the agreement between predicted and measured NO profiles under fuel-lean conditions. Wendt and Ekmann (1974) indicated that the rapid rate of formation of NO in the flame (i.e., prompt NO) can be attributed to super-equilibrium oxygen atom concentrations under fuel-lean conditions. However, the inclusion of nonequilibrium radical concentrations does not explain the observed rate of formation of NO in fuel-rich hydrocarbon flames (Engleman, 1976).

Fenimore (1971) and Iverach et al. (1973) have attributed prompt NO to reactions other than those in the Zeldovich mechanism. In particular, a cyanide mechanism was proposed in which the cyanide radical (CN) was an intermediate. Considerable evidence exists which indicates that under fuel-rich conditions reactions of N_2 with methyl radicals can cause rupture of the nitrogen bond (N≡N) and lead to the formation of NO with hydrogen cyanide (HCN) as an intermediate (Haynes, Iverach, and Kirov, 1975; Engleman, 1976). A reaction scheme in which the controlling reaction is:

$$N_2 + CH \rightarrow HCN + N$$

together with the nonequilibrium Zeldovich mechanism has produced kinetic predictions which are in agreement with data from an adiabatic well-stirred reactor (Engleman, 1976).

To summarize, thermal NO formation in gaseous flames may occur via the extended Zeldovich mechanism and/or via the prompt NO mechanism. In the post flame region, NO formation is adequately explained by the equilibrated Zeldovich scheme. This means that post flame NO is formed through a relatively slow, very temperature-dependent reaction, where the resultant NO emissions are likely to depend upon the time-temperature history throughout the entire length of a combustor. Near the flame, or in the flame, NO formation occurs via the prompt NO mechanism. The non-equilibrium Zeldovich mechanism is important in this region. For hydrocarbon flames and under fuel-rich conditions, the cyanide mechanism is of great importance in prompt NO formation.

1.1-3 Fuel NO Formation

It was assumed for many years that NO was formed only by high temperature fixation of atmospheric nitrogen and oxygen; recent experimental studies, however, have indicated that the conversion of chemically bound nitrogen in the fuel to NO is of greater importance in the formation of NO_x during coal and residual oil combustion. Martin, Pershing, and Berkau (1971) noted, in an evaluation of fuel additives in a small experimental furnace, that nitogen-containing additives, notably amines and nitrates, increased NO_x emissions through approximately 50 percent conversion of the nitrogen in the additive to NO.

A number of experimental studies have been conducted on the addition of various nitrogeneous compounds to flat, laboratory flames (Wendt and Sternling, 1974; Axworthy, 1975; Sarofim et al., 1975; de Soete, 1975; Haynes et al., 1975; Merryman and Levy, 1975). The data indicate that fuel nitrogen is a large potential source of NO emissions, and that the oxidation of many nitrogen-containing species to NO is rapid, occurring on a time scale comparable to that of the combustion reactions (Bowman, 1973). Axworthy (1975) found that, above 80 percent of stoichiometric air requirements, greater than 50 percent of the fuel nitrogen was converted to NO.

Investigators have also attempted to determine the importance of fuel nitrogen conversion to NO in practical systems by examining emission data from distillate and residual oils doped with typical nitrogen compounds. Turner, Andrews, and Siegmund (1972) measured NO emissions from a package boiler burning oils doped with twenty nitrogen additives and measured 40 to 80 percent conversions under normal operating conditions. Martin and Berkau (1972) used a small experimental furnace to determine the amount of NO produced from burning a distillate oil doped with pyridine, quinoline, and piperidine; conversions ranged from 20 to 70 percent. With rapid initial mixing, almost complete conversion of the bound nitrogen to NO was observed by Appleton and Heywood (1973) in studies conducted on kerosene doped with pyridine in a one-dimensional spray combustor. Pershing, Martin, and Berkau (1975) burned a low-sulfur residual oil in argon/oxygen and inferred that about half of the total NO measured under normal conditions was the result of fuel nitrogen oxidation.

Available evidence indicates that increased oxygen availability results in increased fuel nitrogen conversion. In premixed systems, nearly quantitative conversion to NO is achieved for fuel-lean conditions. Substoichiometric (i.e., fuel-rich) conditions, however, result in significantly reduced conversions. Appleton and Heywood (1973) found that imperfect fuel-air mixing causes inhomogeneities and, consequently, the average fuel nitrogen conversion is determined by local stoichiometry. The data of Martin and Berkau (1972), and Turner et al. (1972) further demonstrate the importance of local oxygen concentration in fuel NO production during oil combustion.

Data from premixed gaseous experiments (Sarofim et al., 1975) indicate there is only a slight dependence of conversion on the type of nitrogeneous compound. Data on oil flames show a similar insensitivity to speciation. Martin and Berkau (1972), investigating both unsaturated single-ring and saturated multi-ring nitrogen compounds, observed only a slight effect of composition on fuel nitrogen conversion in distillate oil flames. Turner et al. (1972) tested twenty different nitrogen-containing additives, including amines and heterocyclics with similar results.

The amount of nitrogen chemically bound in the fuel is also believed important in determining the conversion to NO. Evidence indicates that nitrogen conversion to NO decreases with increasing nitrogen content. Martin and Berkau (1972) and Turner et al. (1972) experimentally observed this phenomenon for prototype nitrogen compounds.

Although the experimental studies conducted indicate that fuel nitrogen contributes substantially to NO emissions, and to some extent those factors which influence conversion of fuel nitrogen to NO, the mechanisms of fuel nitrogen oxidation are presently quite imperfectly understood. Various nitrogeneous species have been identified in experimental studies conducted on the combustion of gaseous fuels doped with typical nitrogen compounds: HCN, NH_3 (Fenimore, 1976); CN (Appleton and Heywood, 1973); NH, CN (Merryman and Levy, 1975); NH_3, NH (Duxbury and Pratt, 1975). However, how such species are formed or participate in NO formation is still under discussion with little agreement.

1.1-4 Fuel Sulfur -- Formation of SO_x and Interaction with NO Formation

Although oxidation of chemically bound sulfur in the fuel can result in significant sulfur oxide emissions, there is little or no data concerning the pertinent mechanisms involved. The combustion of H_2S has been studied extensively (Levy and Merryman, 1965; Merryman and Levy, 1967; Sachyan, Gershenzon, and Nalbandyan, 1967). There is good agreement on the mechanisms involved in forming SO_2 from H_2S and concerning the sulfur species present at different stages of the combustion process. The limited data available on combustion of organic sulfur compounds indicate the presence of sulfur species identified in the combustion of H_2S (Cullis and Mulcahey, 1972). Due to the general lack of data, it would appear necessary to treat bound sulfur in the fuel as if it were H_2S to analyze the possible interactions with NO formation.

The possibility of interactions between sulfur and nitrogen oxides at low temperatures is not new (Wendt and Sternling, 1974). This interaction results in the catalysis, by NO, of the oxidation of SO_2 to SO_3. At higher temperatures, typical of combustion conditions, free radicals are produced in super-equilibrium concentrations. Since free radicals are important in NO formation, and since it has been shown (Durie, Johnson, and Smith, 1971) that sulfur dioxide is an effective catalyst in reducing super-equilibrium free radical concentrations, it is reasonable to expect that sulfur dioxide, and possibly other fuel sulfur compounds, inhibit the formation of NO in flames. Indeed, Wendt and Ekmann (1974) found that the addition of SO_2 or H_2S to premixed, flat, methane-air flames inhibited thermal NO formation significantly. The inhibition effect was attributed to the catalysis of super-equilibrium oxygen atom recombination reactions by SO_2.

Literature on flame interactions between species derived from fuel sulfur and fuel nitrogen in the flame front is quite meager. Due to the uncertainties in the mechanisms of fuel nitrogen oxidation, and since the role of super-equilibrium oxygen atoms in these mechanisms is unclear, only speculative remarks are possible concerning the effect of fuel sulfur on fuel NO formation. However, recent work by Flagan, Galant, and Appleton (1974) indicates that super-equilibrium concentrations of atoms and free radicals may play a role in the formation of NO from bound nitrogen. It may, therefore, be tentatively speculated that sulfur dioxide may have an inhibitory effect similar to that observed by Wendt and Ekmann (1974) for thermal NO. Preliminary indications from studies conducted by Wendt and Ekmann (1974)on fuel sulfur interactions with fuel NO formation are that, although the effect is not significant under fuel-lean conditions, it may, under fuel-rich conditions, have a marked influence on the rate at which fuel NO is formed.

1.2 Combustion Facility

1.2-1 Introduction

The facility used in this study was designed and constructed by D. W. Pershing for studies of pulverized coal combustion. Details can be found in Pershing and Wendt (1976).

1.2-2 Furnace

The experimental furnace is shown in Figure 1.2-1. The vertical combustion chamber is 76" long and 6" in diameter inside. The overall outer diameter is approximately 27". In the lower half of the furnace, the walls consist of an outer steel shell, 1/4" of rollboard insulation, 8" of Harbison-Walker Lightweight 26 insulating castable (2600°F maximum service temperature), and 2" of Harbison-Walker Castolast G 3200°F castable refractory. In the upper half of the furnace, the walls consist of 6" of insulating castable and 4" of the high-temperature Castolast G. This casting pattern was used to provide the capability of working at very hot combustion conditions (fuel in argon/oxygen), but at the same time having minimal heat losses.

There are four 6" wide x 10" long observation ports and three 2" diameter ports spaced down the length of the furnace for flame photography and visual observation.

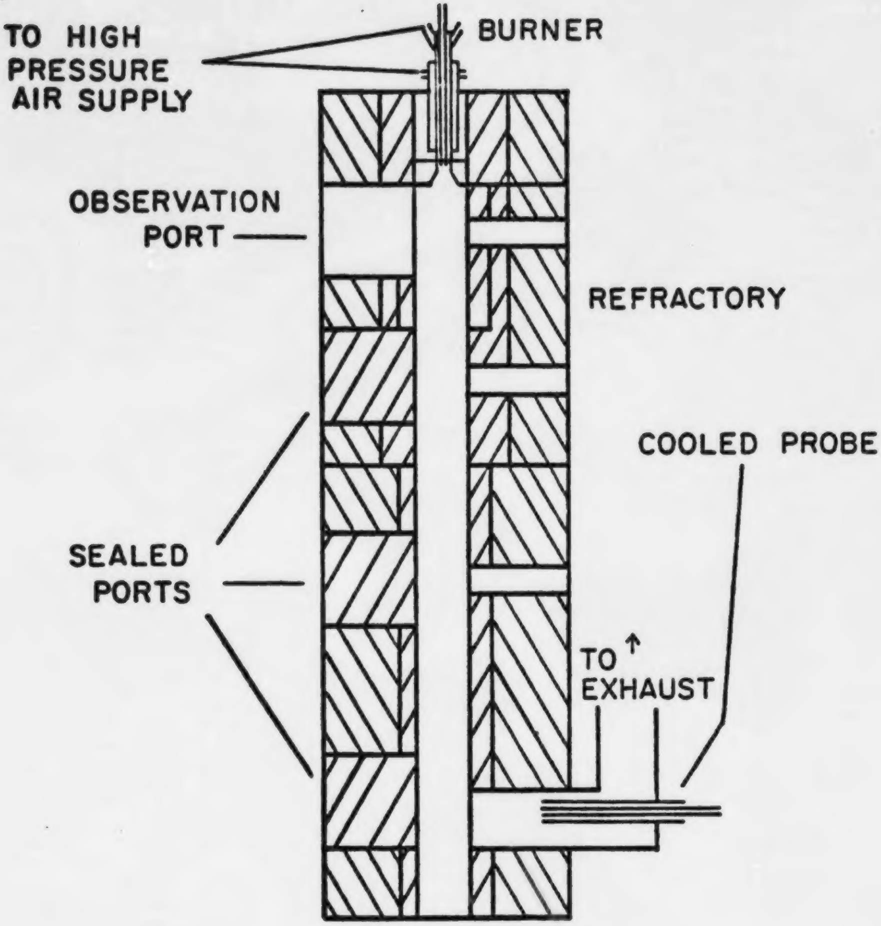
TO HIGH PRESSURE AIR SUPPLY
BURNER
OBSERVATION PORT
REFRACTORY
COOLED PROBE
SEALED PORTS
TO EXHAUST

Figure 1.2-1 Experimental furnace. -- From Pershing (1976).

Fuel and air enter the combustion chamber at the top via a water-cooled burner to be described in detail below. The combustion gases leave the furnace through a 6" diameter exhaust port and flow through approximately forty feet of water and air, double pipe, heat exchangers. The flue gas temperature is less than 300°F upon exiting the exchangers. The gases are then exhausted into a fume duct.

System start-up is initiated with an 18" Eclipse extended pilot. The pilot is located in a horizontal port approximately 5" below the top of the furnace. It normally extends about halfway through the refractory wall and is a long, internally spark-ignited pilot burner. A long, horizontal flame is produced directly across the main burner when the pilot is ignited. When either the main gas or the fuel oil is turned on, ignition occurs immediately and the pilot is turned off.

1.2-3 Multifuel Burner

The specially designed water-cooled burner is illustrated in Figure 1.2-2. It has separate axial and swirl air inlets. The axial air enters through two 1/2" angled ports into the center pipe. Swirl air enters a vaned swirl chamber via two tangential ports 180 degrees opposed and passes through eight 0.100" curved swirl vanes as shown in Figure 1.2-3. The inside diameter of the burner itself is 1.38"; however, several burner inserts were prepared so that axial air velocity could be maintained at 60 ft/sec for a variety of mass flows and air preheats. The burner throat is water-cooled and the exit is fitted with a 30-degree refractory (Castolast G) quarl that has an L/D ratio of unity. The top of the burner has a removable collar designed to accept fuel injectors for natural gas and fuel oils.

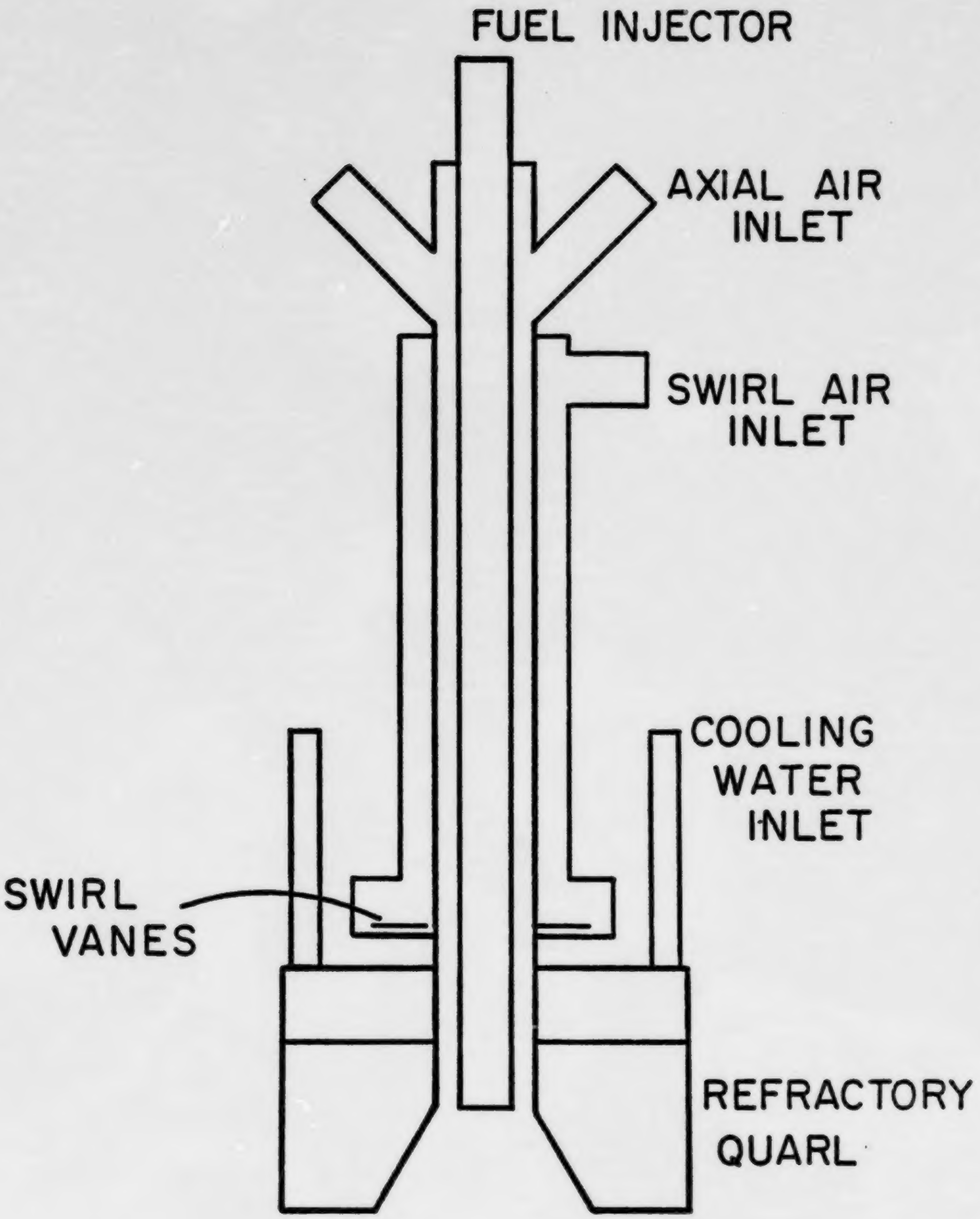
FUEL INJECTOR
AXIAL AIR INLET
SWIRL AIR INLET
COOLING WATER INLET
SWIRL VANES
REFRACTORY QUARL

Figure 1.2-2 Multifuel Burner. -- From Pershing (1976).

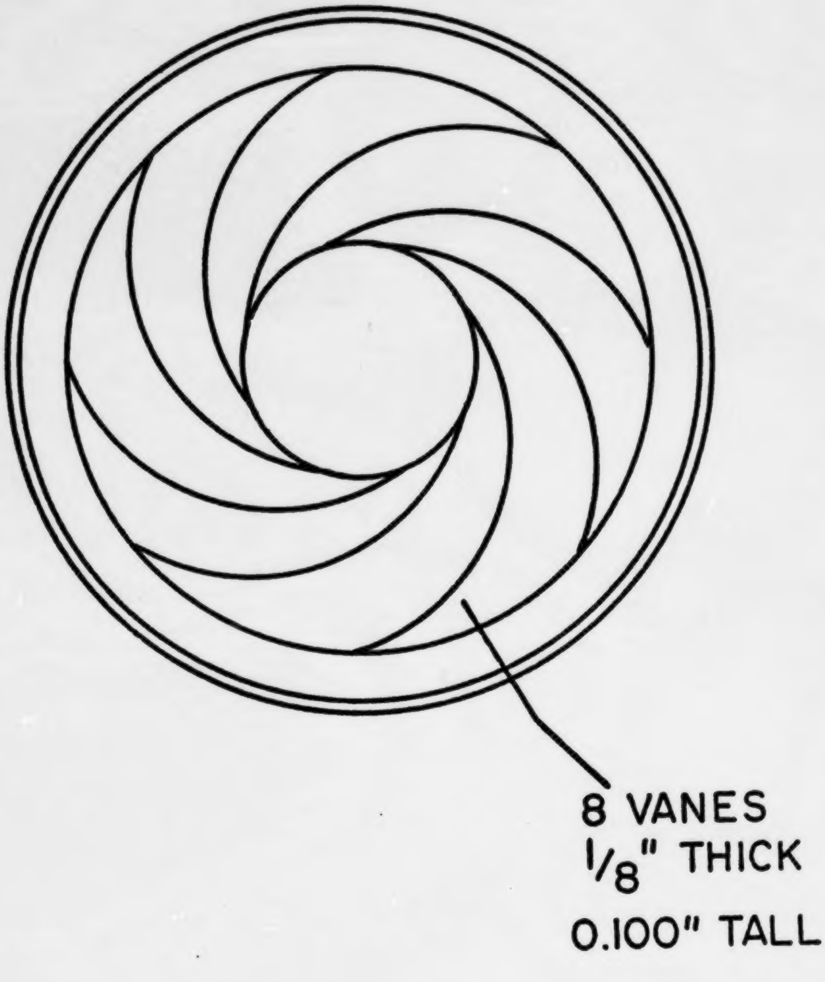
8 VANES
1/8" THICK
0.100" TALL

Figure 1.2-3 Swirl Vanes. -- From Pershing (1976).

1.2-4 Fuel Injectors

The fuel injectors used in this study are shown in Figures 1.2-4 and 1.2.5. Both injectors were fabricated from stainless steel tubing with end plugs. The natural gas injector allows the fuel to be introduced in a radial or an axial direction. Such an arrangement permits comparisons between rapidly mixed short flames and long, poorly mixed flames, respectively. The total area of the six holes for the radial case is equivalent to the area of the single-hole, axial case.

The oil injector used in this study was water-cooled. Preliminary calculations indicated a potential temperature rise in the oil of about 150°F. Two problems were anticipated due to a temperature increase of this size:

1. Significant changes in the kinematic viscosity with corresponding effects on the Sauter mean diameter of the oil droplets.
2. Fuel vaporization within the injector.

Further calculations, assuming the Sauter mean diameter to be proportional to kinematic viscosity to the 0.25 power (Perry, Chilton, and Kirkpatrick, 1963), showed a possible reduction of 15% in the mean droplet diameter. As the droplet size could possibly influence the results obtained, it was concluded that the oil injector would have to be water-cooled.

1.2-5 Air Supply System

The air supply system for the furnace is shown in Figure 1.2-6. Under normal operating conditions, a 100 psig air compressor supplies the combustion air. After being filtered and partially dried, the air

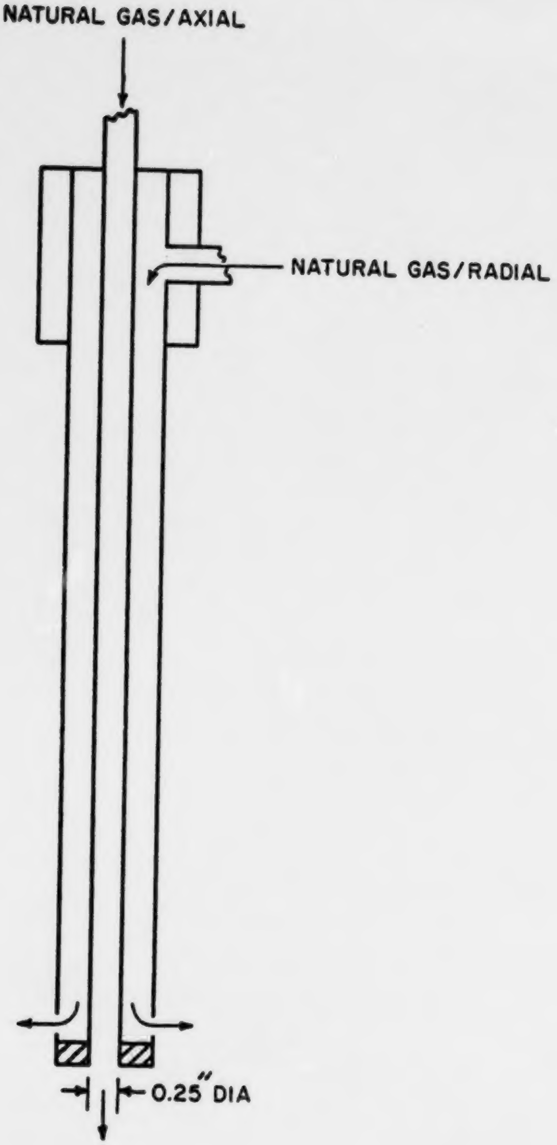
NATURAL GAS/AXIAL
NATURAL GAS/RADIAL
0.25" DIA

Figure 1.2-4 Schematic of Natural Gas Fuel Injector.

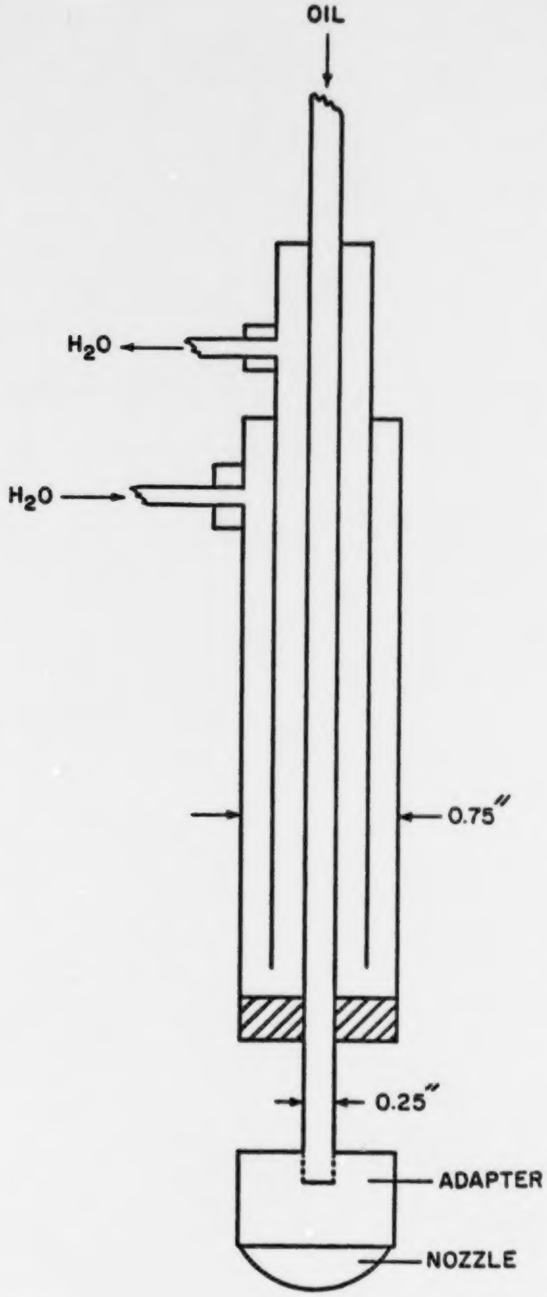
OIL
H$_2$O
H$_2$O
0.75"
0.25"
ADAPTER
NOZZLE

Figure 1.2-5 Schematic of Distillate Oil Fuel Injector.

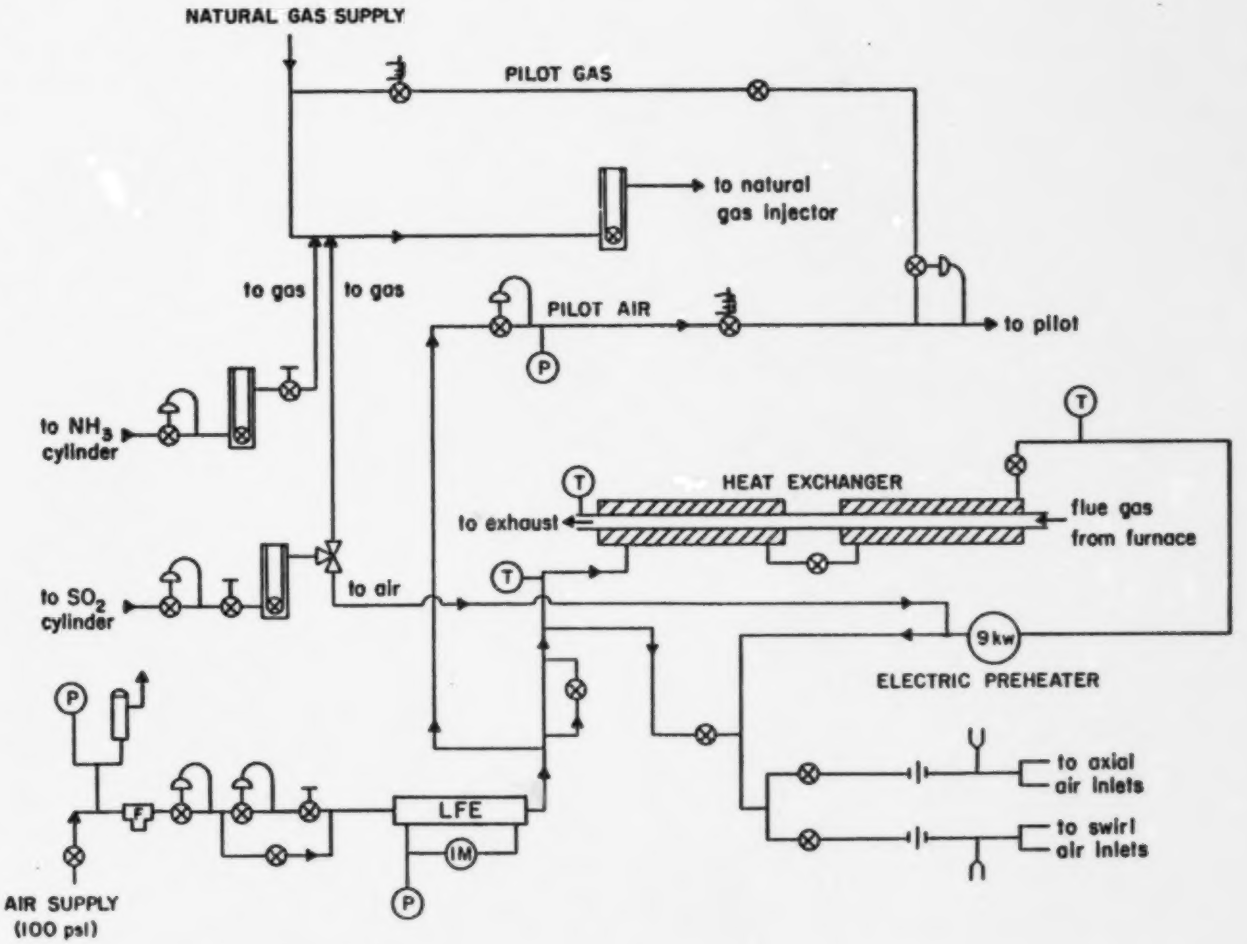
NATURAL GAS SUPPLY
PILOT GAS
to natural gas injector
to gas
to gas
PILOT AIR
P
to pilot
to NH$_3$ cylinder
T
HEAT EXCHANGER
T
to exhaust
flue gas from furnace
to SO$_2$ cylinder
to air
T
9kw
ELECTRIC PREHEATER
P
F
LFE
IM
P
to axial air inlets
to swirl air inlets
AIR SUPPLY (100 psi)

Figure 1.2-6 Air Supply System

passes through two high-volume regulators where the pressure is stepped down to approximately 30 psig.

Once the pressure has been reduced, the air passes through a 3/4" micro-needle valve for total flow control and a laminar flow element. The pressure drop across the laminar flow element is measured by a 10" H_2O inclined manometer. Relatively accurate measurement of the inlet flow is thus obtained.

After the pilot stream is split off, the remaining flow goes to the preheater. The temperature is raised from 70°F to the desired level. This is accomplished by first passing it through the shellside of a double pipe, heat exchanger (the inner pipe contains hot combustion gas from the furnace). The air is about 300°F at the outlet of this exchanger. A 9 Kw Chromalox circulation heater is used to provide the final preheating and temperature control. The heater was constructed with a 304 stainless steel shell and Incoloy elements so that air preheats of up to 1000°F would be feasible.

Once the air has the desired temperature, it is split into axial and swirl air streams. The flow in each line is controlled with a high-temperature, globe valve and metered with a calibrated orifice. Two 0.036" exposed bead, iron-constantan thermocouples, located just before the burner inlets, are used for measuring the temperature of each stream and for the input to the proportional temperature controller on the electric preheater.

For special tests, the air or natural gas may be doped with SO_2. The SO_2 (Matheson, C. P.) is supplied from a 250 cubic feet high pressure cylinder. A calibrated rotameter is downstream of the SO_2 cylinder. Unfortunately, the O-rings of this rotameter deteriorated and introduced large errors in the measured SO_2 flow rates. As a result, desired SO_2 levels were achieved by monitoring flue emissions.

1.2-6 Fuel Oil/Additive System

The fuel oil/additive system (see Figure 1.2-7) was designed to facilitate doping of a representative #2 diesel oil with accurately measured amounts of nitrogen and/or sulfur compounds without changing the total liquid fuel flow rate. A Harvard Apparatus model 915, multispeed syringe pump was selected for addition of the doping agents. Flow rates were accurate to ±0.5%. It was decided that 200 cc B-D Luer Lok syringes would be used with this pump as the drive mechanism had been designed for such syringes. Stainless steel #13 needles were welded to 1/8" stainless steel tubing to connect the syringes to the 1/4" Teflon lines.

Twelve gearbox settings permit flow rates of 0.024 to 120.0 cc/min to be selected when the 200 cc syringes are used. The sulfur or nitrogen compound may be added separately by disengaging one of the syringes from the drive mechanism or the compounds may be added simultaneously at identical flow rates.

After passing through a 60 μ, stainless steel filter, the fuel mixture is fed to the furnace by a Webster model 2M34CB-3 oil pump. The discharge pressure of this pump is factory set at 100 psi. An important

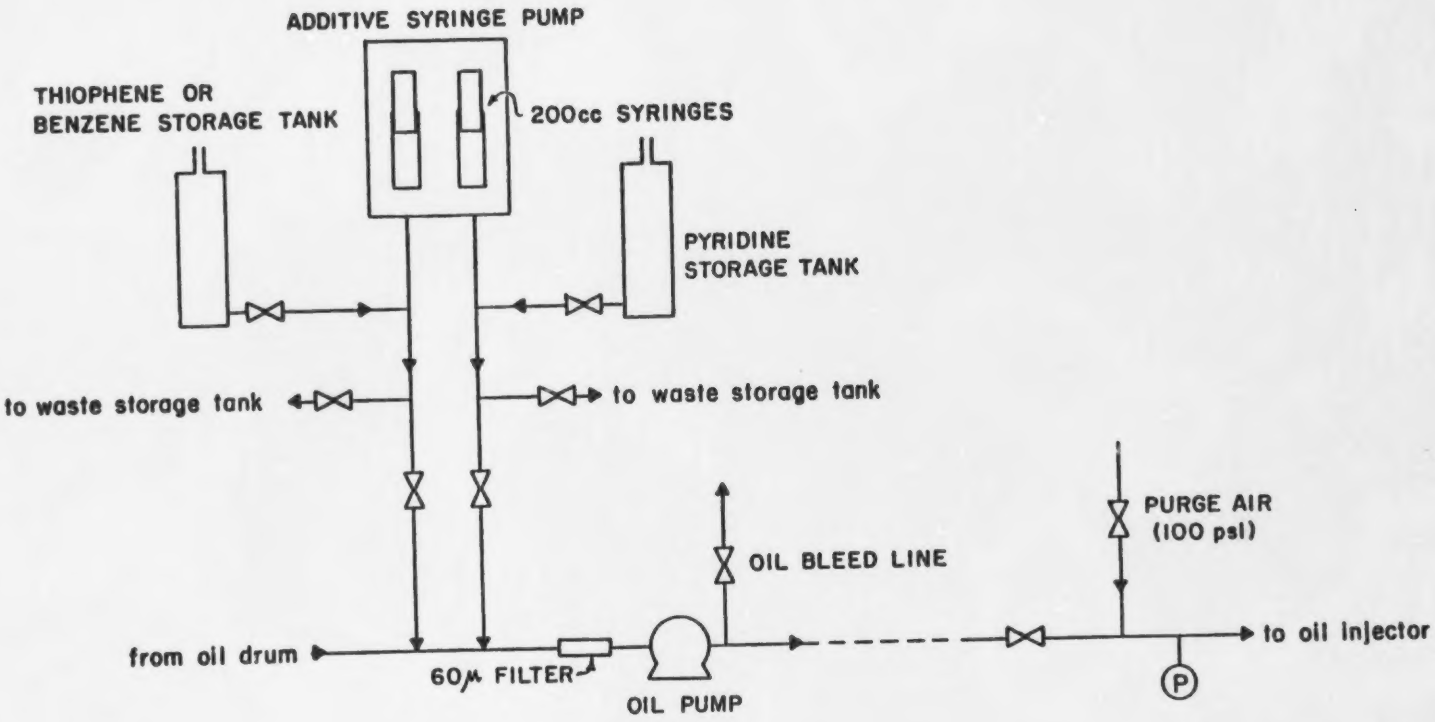
ADDITIVE SYRINGE PUMP
THIOPHENE OR
BENZENE STORAGE TANK
200cc SYRINGES
PYRIDINE
STORAGE TANK
to waste storage tank
to waste storage tank
PURGE AIR
(100 psi)
OIL BLEED LINE
from oil drum
60µ FILTER
OIL PUMP
to oil injector
P

Figure 1.2-7 Fuel Oil/Additive System.

feature of the system is that total flow rate remains constant whether or not additives are present.

Monarch nozzles rated at 0.5 gph at 100 psi were used to achieve mechanical atomization of the fuel. Figure 2.8 shows the internal construction of a typical high-pressure, oil atomizing nozzle; the spray cone pattern of the nozzles used in this study is also shown. The majority of the tests were conducted with 30°R solid cone nozzles. This reduced impingement of the fuel spray on the walls of the furnace and on the quarl. A maximum error of +10% in the flow rate is possible according to the manufacturer.

1.2-7 Analytical System

The analytical system was designed to provide continuous monitoring of NO, NO_2, CO, CO_2, O_2, and SO_2. Figure 1.2-9 shows a schematic of the sampling and analysis system. The flue gas was withdrawn from the stack through a 3/8" water-cooled, stainless steel probe. During the initial shakedown testing, both cooled and uncooled quartz probes were compared to the water-cooled, stainless steel probe. No difference in the measured NO was observed, even with the presence of CO and unburned carbon. However, the flue gas had cooled to below 1000°F at the point of sampling.

Sample conditioning consisted of a refrigerated dryer (water condenser), two glass wool filters, a 60 μ stainless steel filter (50°F), a stainless/Teflon sampling pump and a 7 μ stainless steel filter. All sample lines were 1/4" Teflon and all fittings were 316 stainless steel.

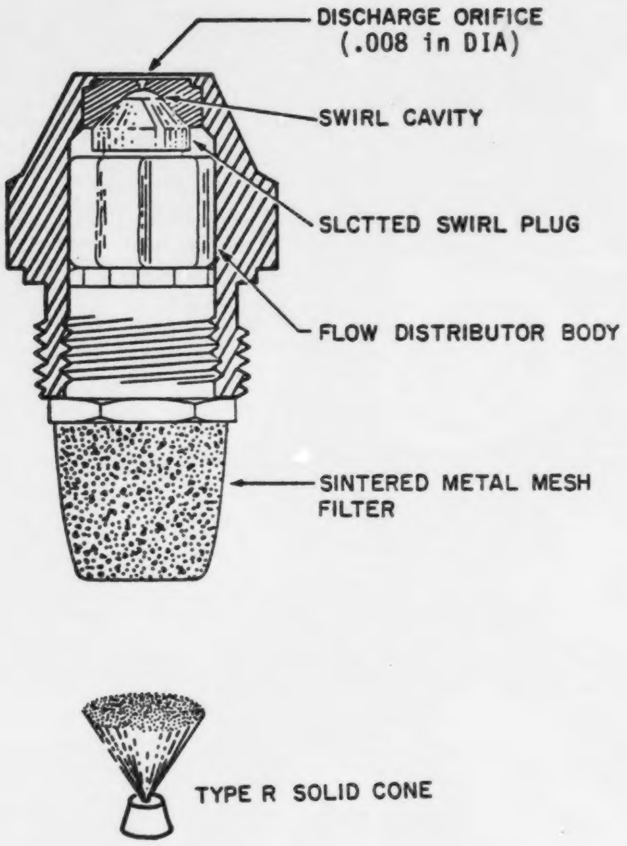
DISCHARGE ORIFICE
(.008 in DIA)
SWIRL CAVITY
SLCTTED SWIRL PLUG
FLOW DISTRIBUTOR BODY
SINTERED METAL MESH FILTER
TYPE R SOLID CONE

Figure 1.2-8 Typical High-Pressure, Oil Atomizing Nozzle and Resulting Spray Cone Pattern.

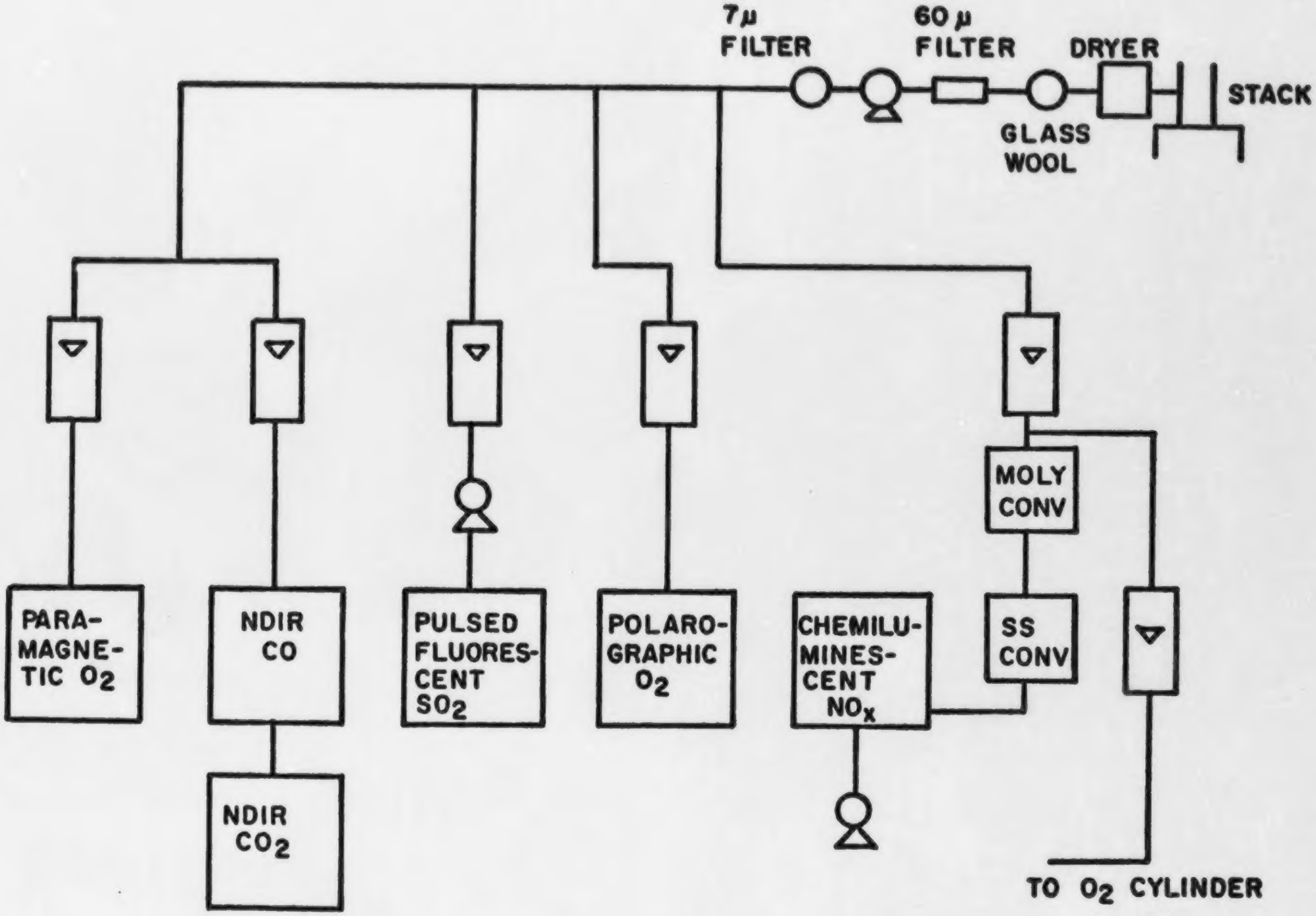
7μ FILTER
60 μ FILTER
DRYER
STACK
GLASS WOOL
PARA-MAGNE-TIC O_2
NDIR CO
NDIR CO_2
PULSED FLUORES-CENT SO_2
POLARO-GRAPHIC O_2
CHEMILU-MINES-CENT NO_x
MOLY CONV
SS CONV
TO O_2 CYLINDER

Figure 1.2-9 Analytical System. -- From Pershing (1976).

The analysis system consisted of the following instrumentation:

1. Beckman Model F3 Paramagnetic Oxygen Analyzer.
2. Beckman Model 864 Nondispersive Infrared CO Analyzer.
3. Beckman Model 864 Nondispersive Infrared CO_2 Analyzer.
4. Thermo Electron Model 40 Pulsed Fluorescent SO_2 Analyzer.
5. Beckman Model 715 Polarographic Oxygen Analyzer.
6. Thermo Electron Model 10AR ChemiLuminescent NO-NO_x Analyzer with Model 300 Molybdenum Convertor.

All instruments were calibrated with zero and span gas every four hours. Details regarding the zero and span gases are presented in Appendix B.

1.2-8 Safety Control System

The furnace is equipped with an electrical interlock safety system to insure both safe start-up and proper shutdown in case of a variety of operational problems. The facility was designed so that it could be operated continuously without an attendant and thereby maintain thermal steady state. It monitors the outlet temperature and flow of the cooling loops to insure system integrity. In the event of a poor or unstable flame, it automatically shuts off all fuel flow. The system also monitors the inlet air and in the event of a compressor failure shuts down both the furnace and the electric preheater (to protect the Incoloy elements from overheating).

1.3 Definition of Terms

The material presented in this chapter is a necessary background for Sections 1.4 through 1.6.

1.3-1 Fuels

The compositions of the #2 diesel oil and natural gas used in this study are shown in Table 1.3-1 and 1.3-2, respectively. Physical properties as well as heat of combustion data are included. The fuel oil was selected on the basis of low sulfur content.

1.3-2 Data Reduction

The data presented and discussed in Sections 1.4 through 1.6 are listed in Appendices C and D. The emission data are reported as parts per million (ppm) by volume on a dry basis and reduced to stoichiometric conditions (zero percent excess air).

Variations in the composition of a fuel due to the addition of doping agents were taken into account when reducing the emission data to stoichiometric conditions. In calculating theoretical air requirements, the following combustion products were assumed: 1) CO_2, 2) H_2O, 3) SO_2, 4) N_2, and 5) O_2.

Table 1.3-1 #2 Diesel Oil Composition.*

C	86.78 wt %
H	12.91 wt %
S	0.30 wt %
N: total	106 ppm by weight
basic	41 ppm by weight
O	300 ppm by weight
Ash	0.001 wt %
H_2O	214 ppm by weight
Gravity: 36.3 °API	
Heating value (Btu/lb, dry): 18308	

*Analysis conducted by Gulf Research and Development Company, Pittsburgh, Pennsylvania.

Table 1.3-2 Natural Gas Composition.

Specie	Mole %
Methane	89.72
Iso-butane	0.09
n-butane	0.16
Ethene	6.4
Propane	1.31
Iso-pentane	0.02
n-pentane	0.02
He	0.02
CO_2	0.35
N_2	1.91

Heating value (btu/ft^3): 1047, wet
1064, dry

Specific gravity: .615

Volatile sulfur content: 0.07 grains/100 ft^3

1.3-3 Additives

Thiophene (reagent grade; Matheson, Coleman & Bell) and pyridine (reagent grade; J. T. Baker) were selected for use in this study as both are representative of classes of sulfur and nitrogen compounds in petroleum and synthetic fuels (Martin and Berkau, 1972; Turner et al., 1972; Satterfield, Modell, and Mayer, 1975). Thiophene is an aromatic five-membered heterocyclic compound: C_4H_4S. It behaves like extremely reactive benzene derivatives. Pyridine is a six-membered aromatic heterocyclic compound: C_5H_5N. The electronegativity of nitrogen makes pyridine unreactive toward electrophilic substitution but highly reactive toward nucleophilic substitution.

Thiophene is about 39% sulfur by weight; pyridine is about 18% nitrogen by weight. The use of these compounds as doping agents allowed investigation of significant levels of sulfur and nitrogen in a fuel oil without requiring the injection of excessively large amounts of either additive.

Sulfur dioxide and NH_3 (Matheson, C. P.) were used to simulate fuel sulfur and fuel nitrogen in the natural gas studies. The selection of SO_2 as a doping agent was based on the desire to compare the results of these turbulent diffusion flame studies to the results of premixed flame studies conducted by Ekmann (1974). Since NH_3 has been used extensively in premixed studies (Wendt and Sternling, 1974; Sternling and Wendt, 1974; Fenimore, 1972; and others), it was selected as the model fuel nitrogen compound in these studies. Safety factors also dictated the use of only semitoxic compounds.

1.3-4 Definitions of Miscellaneous Terms

To avoid confusion, it is necessary to explicitly define terminology used in this study:

1. Percent swirl is the ratio of the volumetric flow of air introduced through the swirl vanes to the total volumetric air flow (swirl plus axial) times one hundred percent.
2. Air preheat is a weighted volumetric average of the swirl and axial air temperatures; percent swirl is used to weight the respective temperatures.

1.4 "Thermal" NO

This chapter is concerned with the effect of fuel sulfur on "thermal" NO emissions from turbulent gaseous and distillate oil diffusion flames. "Thermal" NO denotes the nitrogen oxide emissions resulting from the thermal fixation of molecular oxygen and nitrogen present in the combustion air.

1.4-1 Introduction

In work already published (Wendt and Ekmann, 1974), it was shown that, in a laboratory premixed methane-air flat flame, the addition of SO_2 (6400 ppm SO_2 in the exhaust) or H_2S (6300 ppm SO_2 in the exhaust) to the fuel inhibited the formation of thermal NO. The inhibition was significant at all air/fuel ratios and especially at high air preheats (464°F). This form of inhibition was attributed to catalysis of oxygen atom recombination reactions by SO_2.

However, there are distinct differences in the premixed environment investigated in that work and the environment controlling NO formation in turbulent diffusion flames. In a premixed flame, the fuel and oxidizer are mixed prior to ignition. The physical processes of convection and diffusion are important, since a substantial amount of back diffusion into the unburned gases is crucial in allowing a stable flame front to be maintained and in allowing ignition to occur.

In a turbulent diffusion flame, the fuel and oxidizer are usually injected separately, mix, and subsequently react. The turbulent flame structure consists of macroscale-sized regions composed of fuel, of oxidizer, or of combustion products, and of thin interfacial zones in which the combustion reaction occurs. Since concentration gradients leading to the reaction zone are determined by turbulent mixing, the local oxidant levels within the flame will be affected by the degree of turbulence.

The present study, therefore, examines the effect of fuel sulfur on thermal NO formation in more practical turbulent diffusion gaseous and oil flames in order to determine whether a similar adverse effect on thermal NO, as was established for premixed flames, would be observed under typical furnace combustion conditions.

1.4-2 Natural Gas -- Axial Injector

The axial injector permits a long, poorly mixed, gaseous turbulent diffusion flame to be studied; the extent of mixing can be increased by increasing the percent swirl. At low percent swirl values, this flame should have characteristics similar to tangentially fired furnaces which are also poorly mixed.

This particular set of experiments was designed to investigate the effect of SO_2 on thermal NO formation as well as to provide insight into how physical hardware and flame parameters affected the results. For this latter reason, SO_2 was also injected into the air. The rationale was that information concerning how to model the kinetic environment important in a turbulent diffusion flame could be gained.

Effect of SO_2 on Thermal NO at "Zero" Air Preheat

To insure that the observed effects on thermal NO were due to the presence of fuel sulfur and not to transients caused by the introduction of SO_2, efforts were made to maintain all other conditions constant. The baseline point was first determined at a particular excess air condition as indicated by the percent oxygen in the flue. SO_2 was then injected into the air stream. The natural gas rotameter was checked to determine that the fuel flow rate had not changed. The CO_2 and O_2 monitors were used to verify that the fuel rate remained constant; these monitors also permitted minor adjustments in the natural gas rate to be made to give identical readings as the baseline point. SO_2 was then added to the natural gas and similar checks and adjustments were made. Finally, the original baseline point was checked to determine that it had not changed. Checks were also made of the air temperature and the percent swirl.

Figure 1.4-1 shows the effect of SO_2 addition at "zero" air preheat and a moderate percent swirl. From this data it can be concluded that 3000 to 4000 ppm SO_2 in the exhaust can inhibit thermal NO formation by 10 to 20 percent. The inhibition effect is more pronounced when SO_2 is added to the air (the fuel-lean side) even though the level of SO_2 is lower.

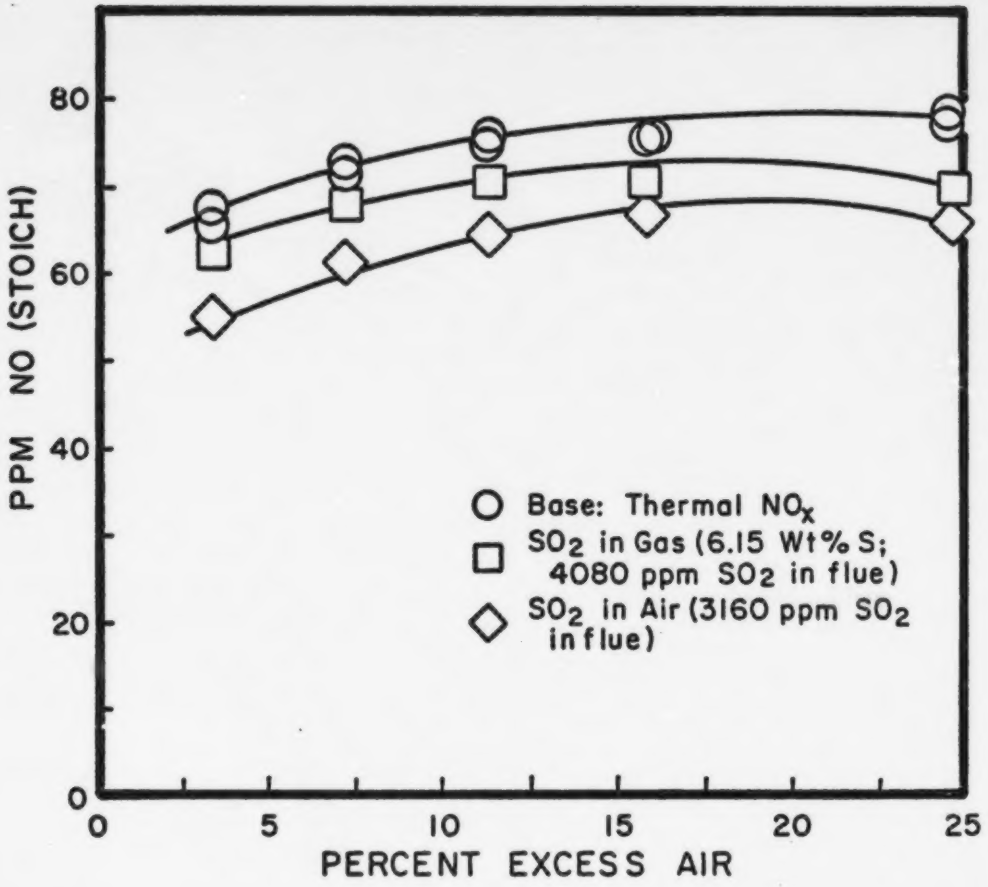

Figure 1.4-1 Natural Gas/Axial Injector: Effect of SO_2 on Thermal NO (37% Swirl; 120°F Air Preheat).

It would also appear that the inhibition effect of SO_2 becomes less when added to the fuel as stoichiometric conditions are approached. Since, in this case, the SO_2 is present on the fuel-rich side of the flame front, it is not unreasonable to assume that the SO_2 is at least partially reduced to species such as H_2S. Wendt and Ekmann (1974) report that H_2S must be converted to SO_2 before inhibition is important and that this occurs rapidly under fuel-lean conditions. This point is consistent with the data reported on Figure 1.4-1 as the curves showing the effect of SO_2 addition approach one another as excess air increases. It is reasonable to expect oxygen concentration on the fuel-rich side of the flame front to increase with increasing excess air due to greater driving forces for diffusion. Fuel-rich eddies are also broken up by the higher air velocities associated with increasing excess air. An increase in the oxygen level would decrease the reduction of SO_2 or increase the conversion of H_2S to SO_2. Therefore, the inhibition effect would be greater at high excess air conditions than near stoichiometric when SO_2 is present in the fuel.

The inhibition effect of SO_2 on thermal NO formation can still be attributed to the catalysis of oxygen atom recombination reactions by SO_2.

The inhibition effect of SO_2 was further examined by varying the percent swirl at a fixed excess air condition (11.4% excess air). The findings are shown in Figure 1.4-2. At high percent swirl values, it makes little difference whether SO_2 is introduced in the fuel or in the air stream. Since mixing is rapid at these conditions, the SO_2 concentration may not be significantly higher on either the fuel-lean or fuel-rich side of the flame front. However, the concentration of SO_2, as measured in the exhaust, is 40 percent greater when added to the fuel than when

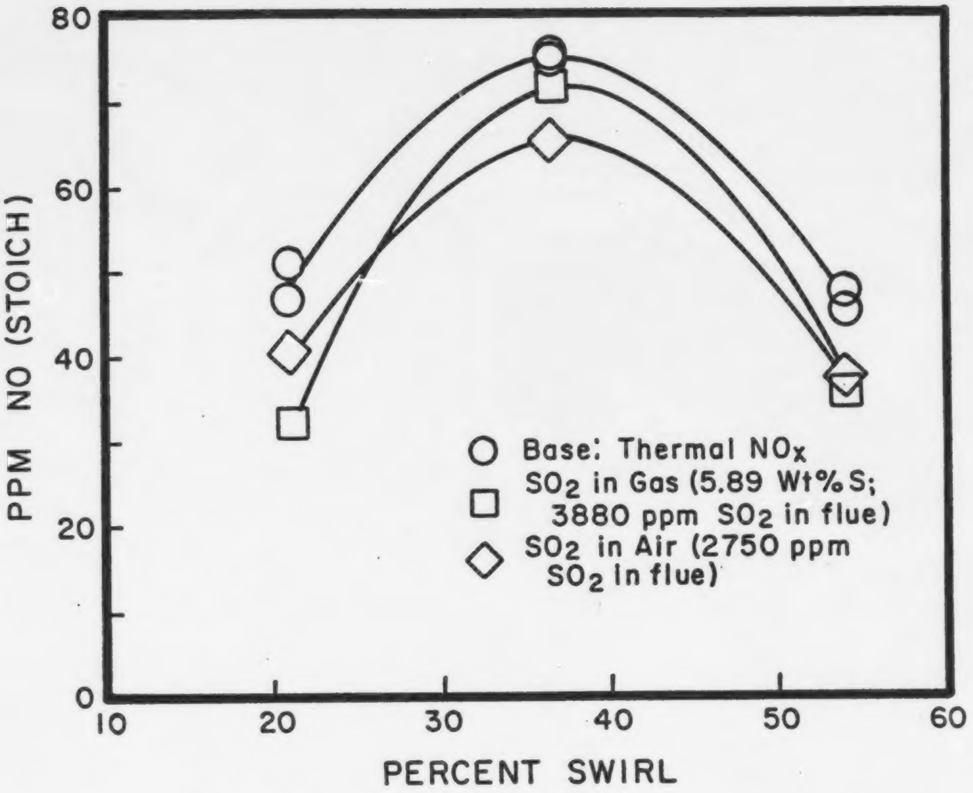

Figure 1.4-2 Natural Gas/Axial Injector: Effect of Swirl on Fuel S Inhibition of Thermal NO (11.4% Excess Air; 100°F Air Preheat)

added to the air. That a greater effect was not observed, for this high percent swirl value when SO_2 was added to the fuel, probably indicates the continued existence of fuel-rich zones within the flame where reduction of SO_2 can take place. Extrapolation of the curves to 60 percent swirl shows that the higher concentration of SO_2 present in the gas would have a greater effect than the SO_2 added to the air.

At low percent swirl values, the "normal" situation is reversed and SO_2 addition to the fuel has a larger effect than SO_2 in the air. Under these conditions, the bulk of the NO may be fuel-rich induced prompt NO, in which case a large concentration of SO_2 in the fuel would be expected to have a larger effect. However, at these low percent swirl values (less than 30 percent swirl), recirculation eddies were observed; these recirculation zones extended the length of the furnace. With the greater mixing generated by such recirculation, fuel-rich regions within the flame should be rapidly broken up. Also, the concentration of SO_2 should not be significantly greater on either the fuel-rich or fuel-lean side of the flame. Since the level of SO_2 is higher for addition to the fuel, it would be expected that a larger effect should be observed.

Effect of SO_2 on Thermal NO at High Air Preheat

The results of studies conducted at high air preheats and moderate percent swirl values are shown in Figures 1.4-3 and 1.4-4. A comparison of the baseline data in these two figures indicates an apparent discrepancy of 50 ppm NO, over the entire excess air range, for similar air preheats and percent swirl values. However, the data in Figure 4.4 was taken about six months after the data shown in Figure 4.3.

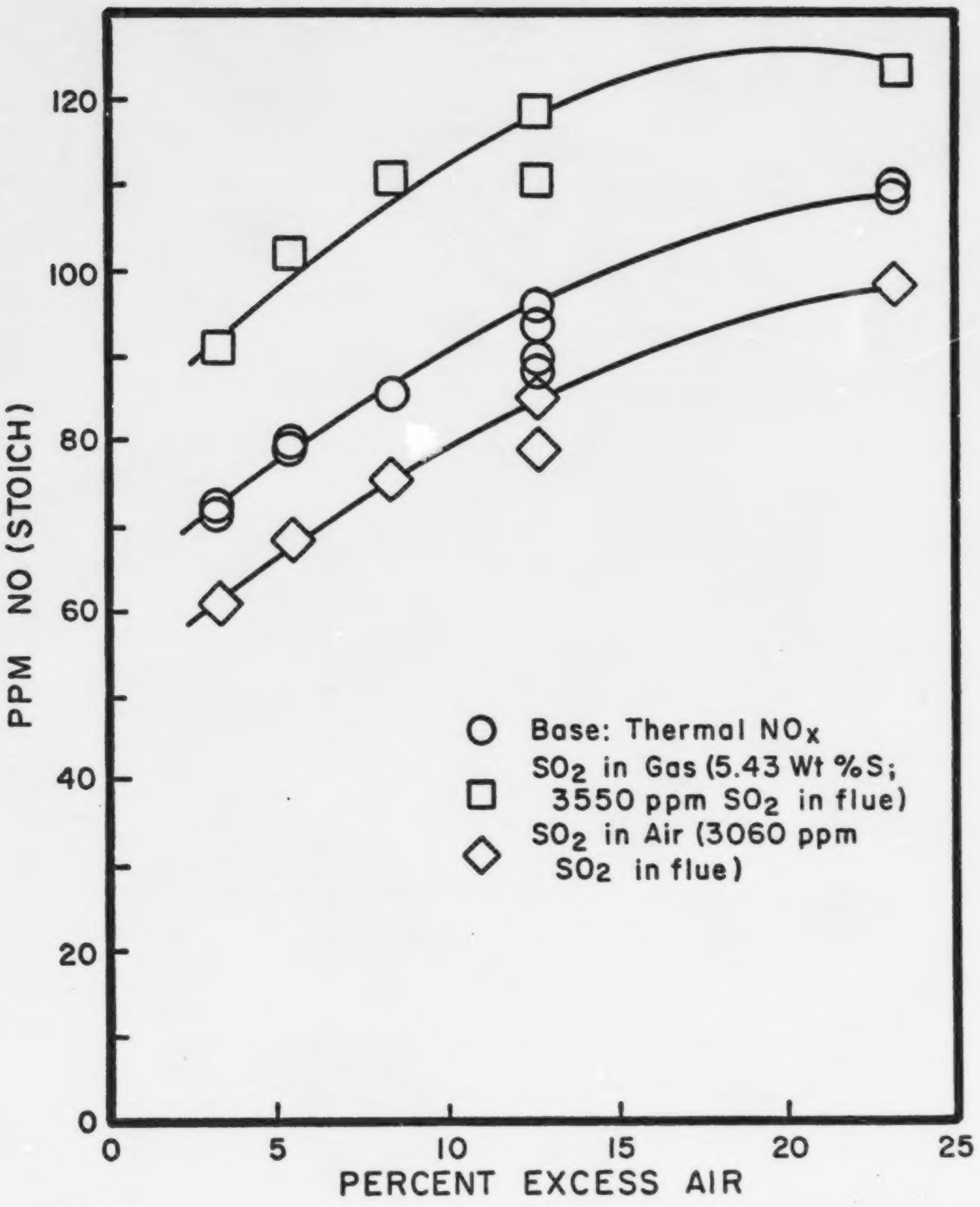

Figure 1.4-3 Natural Gas/Axial Injector: Effect of SO_2 at High Air Preheat (40% Swirl; 440° Air Preheat).

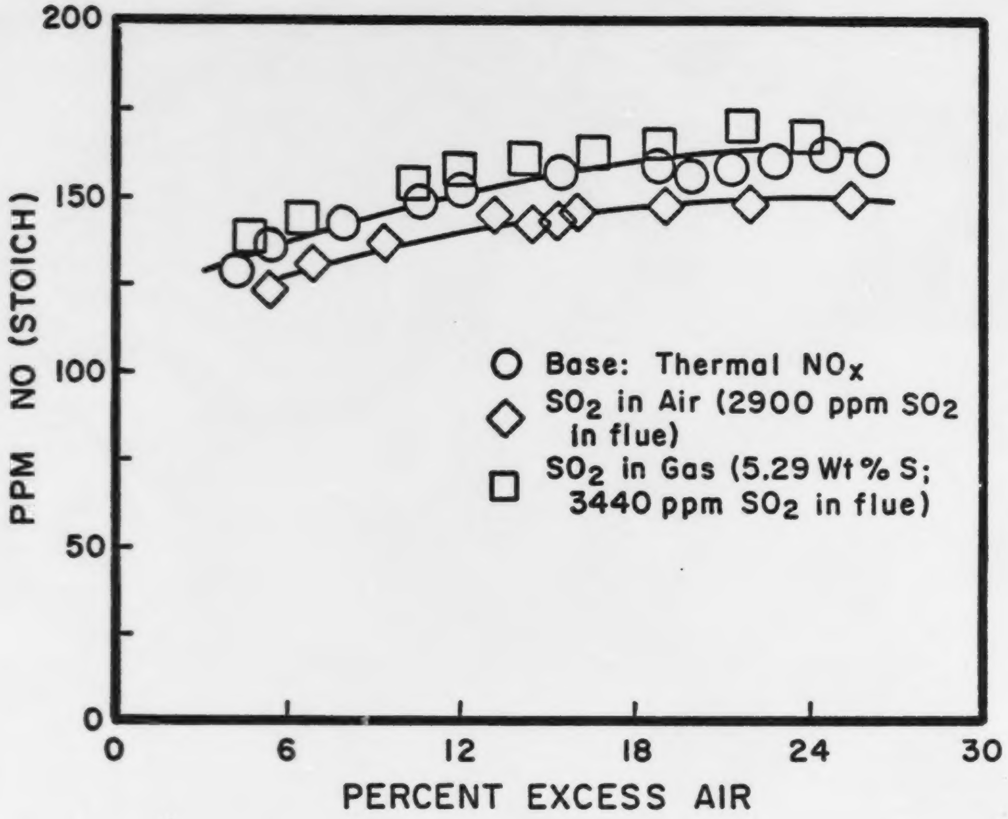

Figure 1.4-4 Natural Gas/Axial Injector: Effect of SO_2 at High Air Preheat (44% Swirl; 430°F Air Preheat).

During the interim, other studies on coal combustion caused deposition of slag on the furnace walls; the effective diameter of the lower half of the furnace was, therefore, reduced. The gas firing rate for the data in Figure 1.4-4 was about 51,000 Btu/hr, as compared to 49,000 Btu/hr for the data in Figure 1.4-3.

More significant than the changes in physical hardware and the differences in firing rates were the radically dissimilar flames produced in each investigation. The flame associated with the data presented in Figure 1.4-3 was short, bushy, and luminous. The yellow color of this flame is produced by the pyrolysis and incomplete combustion of hydrocarbon species. The color, therefore, indicates the presence of locally substoichiometric conditions within the flame which indicates that the flame is poorly mixed. This flame was located in the top two feet of the combustion chamber.

In contrast, the flame associated with the data in Figure 4.4 was long, narrow, and jetlike in the top section of the furnace. The jet expanded and produced intense mixing in the lower two-thirds of the furnace. The bright, blue-violet color of this flame indicates near-stoichiometric combustion conditions within the flame. This flame was better mixed as compared to the flame associated with the data of Figure 1.4-3.

Although there is no immediately obvious reason for the differences in the flame shapes, the changes in local flame stoichiometry, as indicated by color, and in local flame temperatures, induced by the differences in aerodynamics, could readily explain the higher baseline data reported in Figure 1.4-4.

Figure 1.4-3 and 1.4-4 indicate an apparent anomaly for the high air preheat studies. The addition of SO_2 to the fuel causes an increase of 5 to 20 percent in thermal NO emissions. The enhancement is greater for the short, bushy flame than for the long, narrow, jetlike flame. Since the air preheats, the percent swirl values, and the levels of SO_2 added to the fuel are almost identical, it can be inferred that the differences in local flame stoichiometry and, therefore, the local flame temperatures are responsible for the disparity observed in the extent to which this enhancement effect occurs in these flames.

The fact that this enhancement effect is greater for the flame with locally substoichiometric conditions may indicate that SO_2 in the fuel increases the formation of fuel-rich induced prompt NO. Since it would be expected that SO_2 would be reduced more in a fuel-rich flame than in a flame near stoichiometric conditions, it is possible that the observed increase in NO emissions is due to the interaction of reduced species, such as SH or S, with the prompt NO formation mechanism.

This enhancement effect at high air preheat provides an alternative explanation for the "zero" air preheat data presented in section 1.4-2. In that case, the addition of SO_2 to the fuel decreased NO emissions, but not as much as when SO_2 was added to the air, even though the level of SO_2 was higher in the fuel. The flame associated with the data in Figure 1.4-1 was short, bushy, and luminous. It may be that a competition exists between inhibition of thermal NO and enhancement of fuel-rich induced prompt NO. Since the inhibition effect of SO_2 in the fuel decreased as overall stoichiometric conditions were approached, it can be inferred that the subsequent decrease in local flame stoichiometry is also an important factor. If SO_2 is reduced to species which then interact with the prompt NO mechanism, it is reasonable to expect SO_2 to be reduced to a greater extent as the overall stoichiometric ratio approaches unity.

Although an increase in NO emissions was observed when SO_2 was added to the fuel, the addition of SO_2 to the air, as Figures 1.4-3 and 1.4-4 show, produced a decrease in NO emissions. For the luminous flame, a constant reduction of 11 ppm NO was observed over the entire excess air range investigated. The reduction in NO emissions for the jetlike flame ranged from about 10 ppm NO at 5 percent excess air to about 15 ppm NO at 25 percent excess air.

The data presented in this section for SO_2 addition to the fuel appear to be inconsistent with the results reported by Wendt and Ekmann (1974) for SO_2 or H_2S addition to premixed methane-air flat flames. Overall NO emissions were reduced by the presence of SO_2 or H_2S; the inhibition was observed at all fuel/air ratios and was especially significant at air preheat conditions (464°F air preheat). The inhibition of thermal NO was observed for levels of SO_2 or H_2S addition, producing levels of SO_2 in the exhaust similar to those of this study (3200 to 3300 ppm SO_2 in the exhaust as compared to 3400 to 3600 ppm SO_2 in the exhaust). The inhibition effect was more significant at flue SO_2 levels approximately double those of this study. It may be that differences in aerodynamics, local flame temperatures, local flame stoichiometries, and heat losses are responsible for the disparity in effects observed in these different flames.

However, Wendt and Ekmann (1974) also present results for the effect of SO_2 or H_2S on prompt NO formation. Their findings indicate SO_2 inhibits prompt NO formation at all fuel/air ratios and to a greater degree at high air preheat. In contrast, the addition of H_2S inhibits prompt NO to a greater extent for near stoichiometric or fuel-lean conditions. Below approximately 90 percent of stoichiometric requirements, there appears to be little effect or a slight enhancement of prompt NO formation as conditions become more fuel-rich. From this information, it can be inferred that for sufficiently fuel-rich regions in a flame reduced forms of SO_2 can enhance the formation of prompt NO. If the enhancement were large enough, it would be expected that overall NO emissions would also increase.

The effect of SO_2 addition was examined further in this study by varying the percent swirl value while maintaining a constant excess air value (15.0% excess air). The results are shown in Figure 1.4-5; this area was taken with the jetlike flame. The inhibition or enhancement effect of SO_2 remains roughly constant for the range of swirl values investigated. The increase in NO emissions as the percent swirl value decreases is probably due to longer residence times at a higher local flame temperature, since the decreased residence time in the furnace reduces radiative heat losses. The flame was detached below 30% swirl and was severely distorted above 50% swirl.

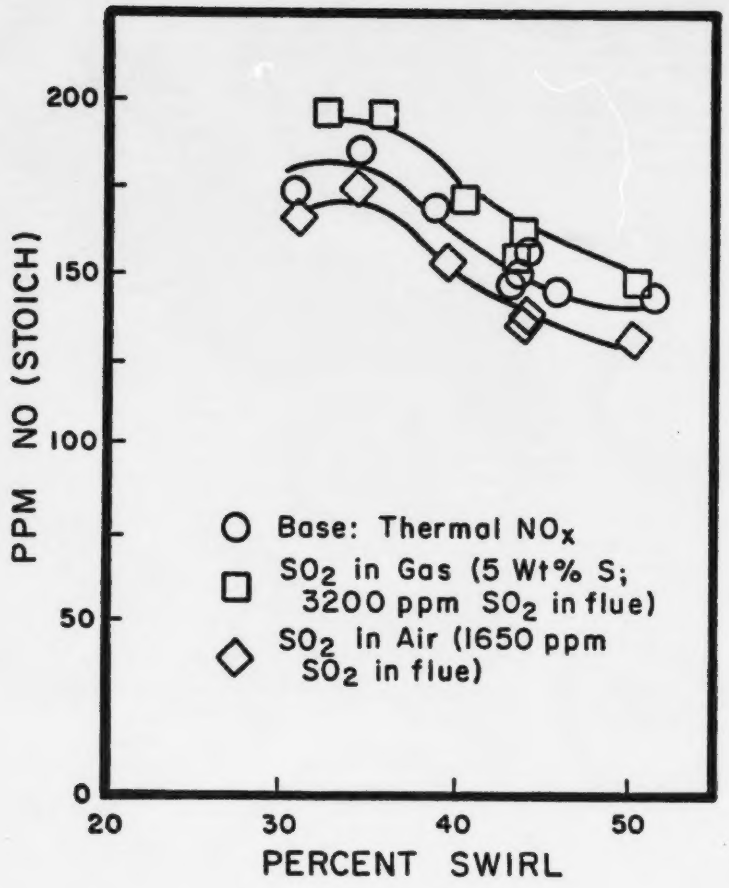

Figure 1.4-5 Natural Gas/Axial Injector: Effect of Swirl on Fuel S Inhibition of Thermal NO at High Air Preheat (15.0% Excess Air; 430°F Air Preheat).

1.4-3 Natural Gas -- Radial Injector

The radial injector permits a more highly mixed turbulent diffusion flame than that produced by the axial injector to be studied. The flame produced using this injector should have similarities to some high efficiency burners.

This set of experiments was designed to determine whether the effect of SO_2 on thermal NO formation would be dependent on the type of fuel injector used. Insight into how physical hardware and flame parameters affected the results was also sought. To provide information concerning how to model the kinetic environment, important in a turbulent diffusion flame, SO_2 was also injected into the air.

The same cycling procedure that was employed with the axial injector was used to insure that the observed effects were due to SO_2 and not to transients or other phenomena introduced by the addition of SO_2. The CO_2 and O_2 monitors were used to verify that the fuel flow rate did not change when SO_2 was added.

Effect of SO_2 on Thermal NO at "Zero" Air Preheat

Figure 1.4-6 shows the results of the study at "zero" air preheat and a moderate percent swirl value. The flame associated with this data was short and conical in shape. Near-stoichiometric local combustion conditions in the flame were indicated by the intense blue-violet color of the flame.

It can be concluded from Figure 1.4-6 that the additon of SO_2, to produce about 4000 ppm SO_2 in the flue, inhibits thermal NO formation by

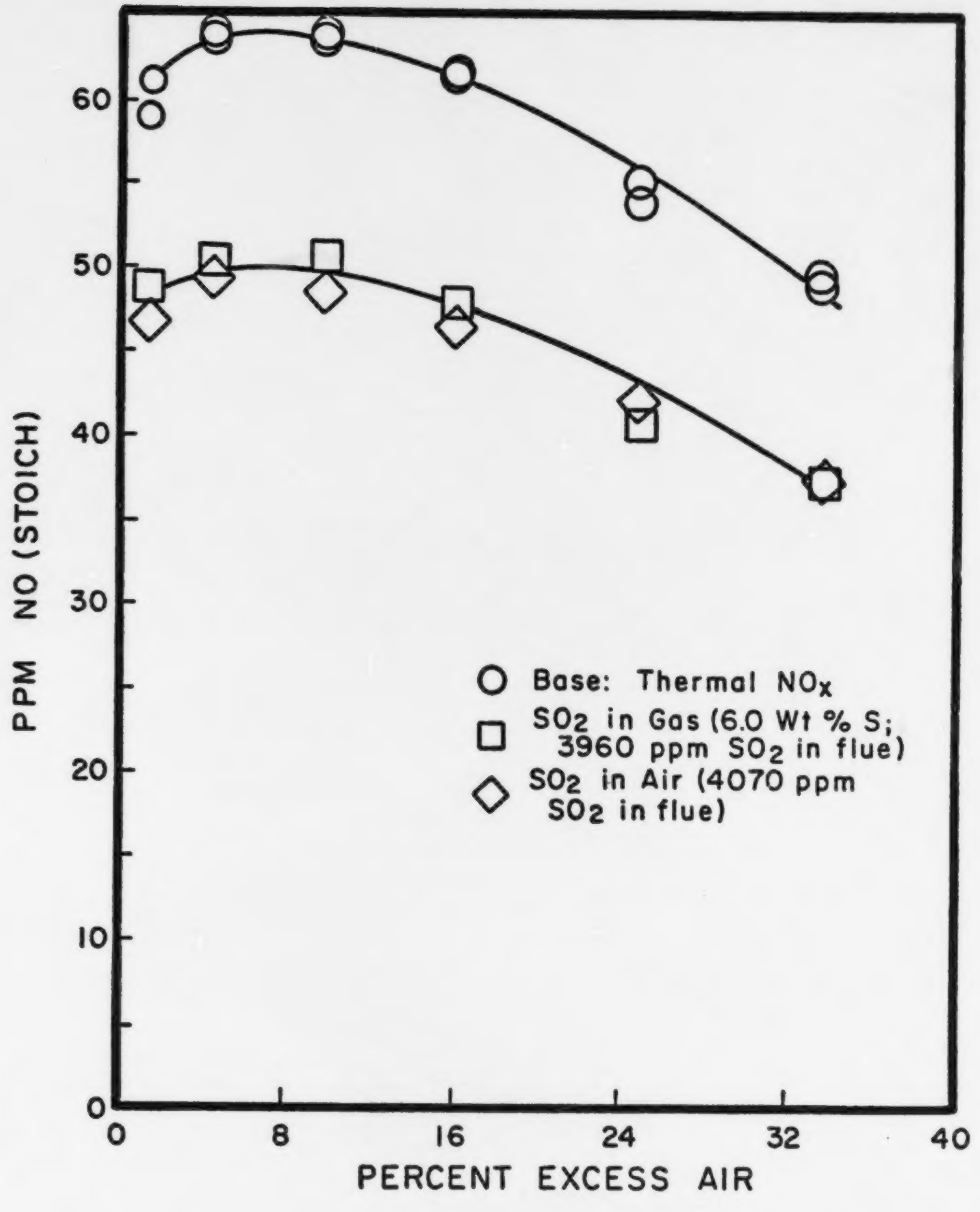

Figure 1.4-6 Natural Gas/Radial Injector: Effect of SO_2 on Thermal NO (38% Swirl; 100°F Air Preheat).

20 percent. The reduction is approximately constant, 12 to 14 ppm NO, over the entire range of excess air conditions investigated. As can be seen, it makes no difference whether SO_2 is added to the air or to the fuel. This point indicates that mixing is rapid in this flame.

Another indication of rapid mixing between air and fuel streams is the shape of the excess air curve. At excess air conditions above 10 percent, NO emissions decrease. Rapid mixing would result in more entrainment of air at higher excess air conditions. Local temperatures in the flame would decrease due to dilution resulting from greater entrainment of air. Since thermal NO is very temperature sensitive, it would be expected that emissions would decrease as flame temperature also decreased. The curvature noted is, therefore, an indication of "rapid" mixing.

The effect of SO_2 on thermal NO was further examined by varying the percent swirl value at a fixed excess air condition (15.9% excess air). The results are presented in Figure 1.4-7. The curve is similar in shape to that observed for the axial injector (see Figure 1.4-2) except here mixing was sufficiently rapid to eliminate any differences between the addition of SO_2 to the air or to the fuel. The decrease in NO emissions with increasing percent swirl can be attributed to the increase of air entrainment which reduces local flame temperatures. The decrease in NO as the percent swirl value falls below 40% swirl may be due to increased radiative heat losses which also would decrease local flame temperatures.

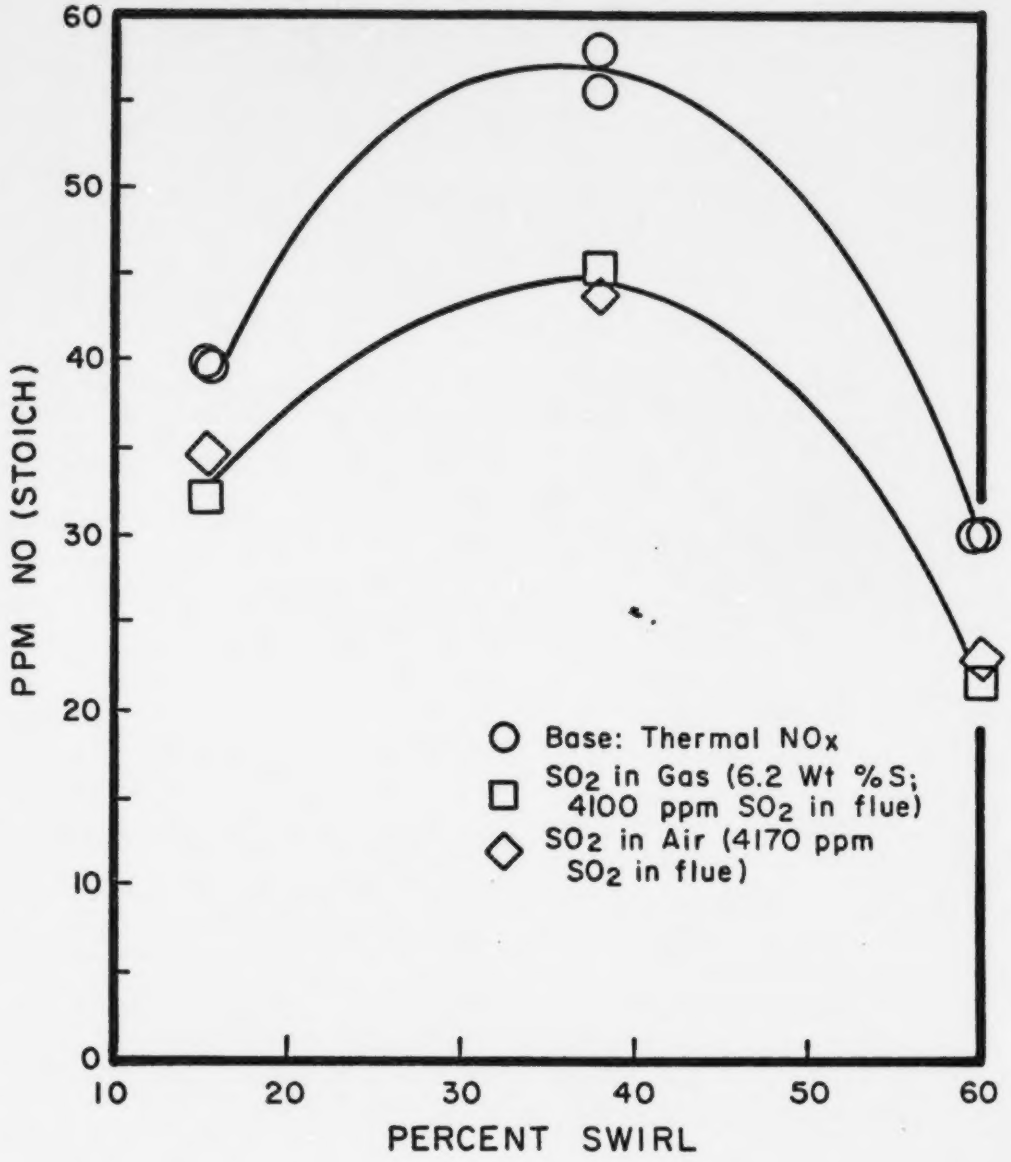

Figure 1.4-7 Natural Gas/Radial Injector: Effect of Swirl on Fuel S Inhibition of Thermal NO (15.9% Excess Air; 110°F Air Preheat).

Effect of SO_2 on Thermal NO at High Air Preheat

Figure 1.4-8 presents the results of the study at high air preheat conditions and a moderate percent swirl value. At low excess air conditions, the addition of SO_2 to the fuel has a smaller effect than when SO_2 is added to the air. The differences in the inhibition effect decrease with increasing excess air; at 20 percent excess air there is no difference in the inhibition effect. The reduction in thermal NO caused by the presence of SO_2 in the air decreases with increasing excess air. In contrast, the reduction in NO emissions increases with increasing excess air when SO_2 is added to the fuel.

The decrease in inhibition, as excess air increases, when SO_2 is added to the air stream may be due to an increase in the concentration of oxygen atoms at the higher excess air conditions. An alternative explanation is that at higher excess air conditions local SO_2 concentrations are lower than for low excess air conditions, due to dilution.

The decrease in the inhibition effect, as excess air conditions decrease, when SO_2 is added to the fuel may indicate that mixing is less rapid compared to kinetics at high air preheats. Slower mixing, as compared to NO formation kinetics, could affect the availability of SO_2 in the region of the flame where oxygen atom recombination is important. The resulting lower local concentrations of SO_2 would have less of an inhibition effect on thermal NO.

There is another explanation for this phenomenon. Since SO_2 is added to the fuel-rich side of the flame front, it is possible that an enhancement of fuel-rich induced prompt NO is responsible for the

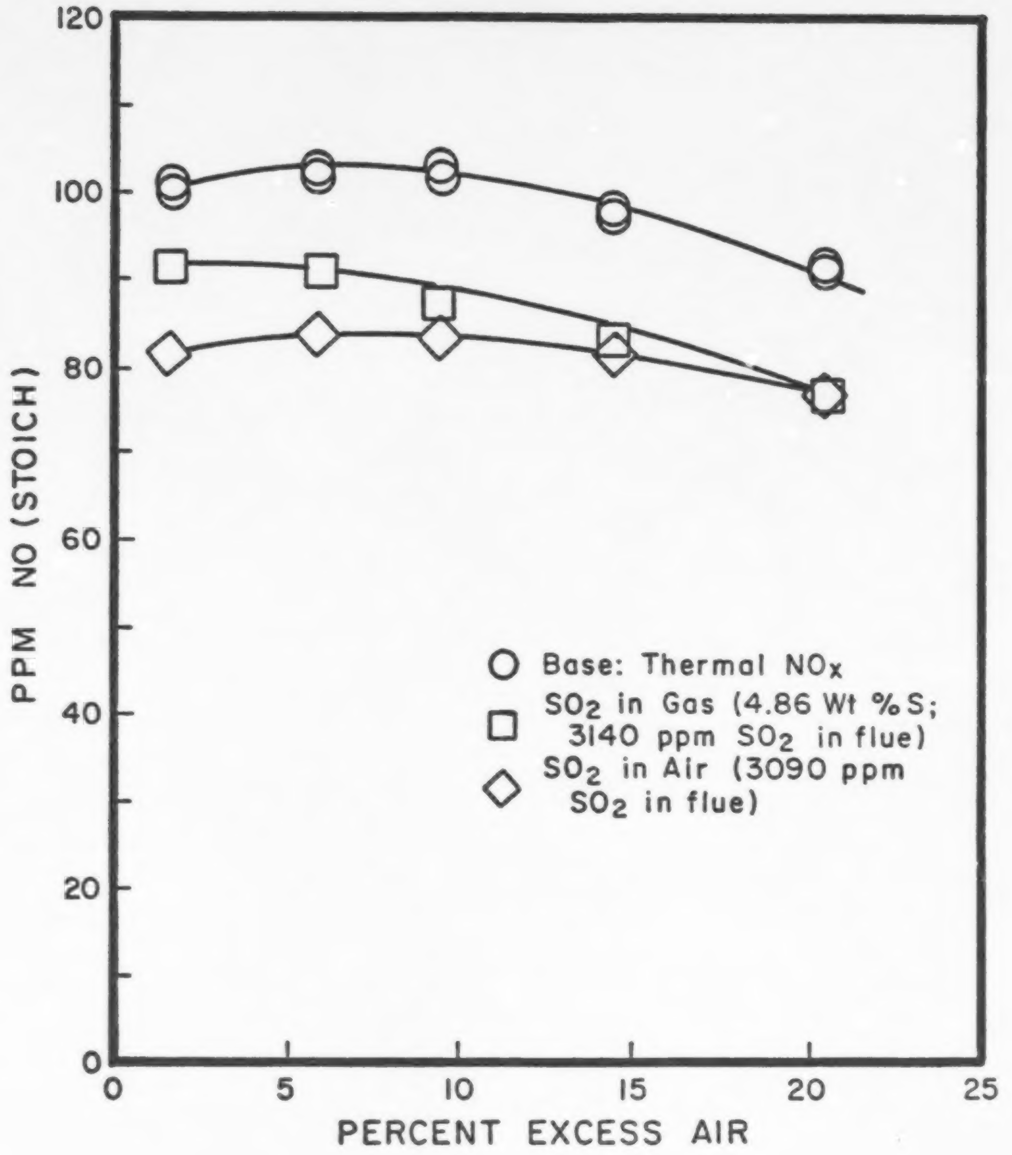

Figure 1.4-8 Natural Gas/Radial Injector: Effect of SO_2 at High Air Preheat (42% Swirl; 440°F Air Preheat).

decrease in inhibition of NO emissions. Locally fuel-rich conditions in the flame may partially reduce SO_2 to species which then interact with the prompt NO mechanism. As excess air increases, the oxygen concentration on the fuel-rich side of the flame front should also increase due to an increased driving force for diffusion. The higher air velocities associated with higher excess air conditions should promote the break-up of fuel-rich zones. It could, therefore, be expected that NO_2 would not be reduced to as great an extent as at lower excess air conditions and, therefore, SO_2 in the fuel would have the same inhibition effect as when added to the air.

1.4-4 Distillate Oil

The effect of fuel sulfur on thermal NO emissions from distillate oil flames was examined by doping the oil with thiophene, which is a representative fuel oil sulfur compound. Onuma and Ogasawara (1975) conducted studies on the structure of a spray combustion flame. Their results indicate that a typical spray combustion flame may be considered to consist of three regions. In the first region, which is located near the nozzle, a heterogeneous mixture containing many droplets burns. It may be that the droplets do not burn individually but that the vapor cloud formed by the evaporation of the droplets burns like a turbulent gaseous diffusion flame. In the second region, only combustible gas fed from the first region burns steadily. The final region burns the remaining combustible gas from the second region intermittently. A gas diffusion flame was observed in the second and third regions where droplets are very few.

Since it appears that droplets first evaporate before combustion occurs, the rate at which evaporation takes place may be an important parameter. Local stoichiometry could possibly be affected if the evaporation rate is slow or rapid. If fuel sulfur remains in the droplet for relatively long times, subsequent interaction with the thermal NO formation mechanism could be affected. It is also possible that pyrolysis-type reactions increase in importance in a spray combustion flame.

The distillate oil used in this study contained some chemically bound nitrogen. The maximum contribution to NO emissions, if all fuel nitrogen were converted to NO, would be 13 ppm NO.

Effect of Fuel Sulfur on Thermal NO at "Zero" Air Preheat

The injection of a doping agent such as thiophene could possibly affect the NO emissions by changing local stoichiometry or by changing the physical properties of the fuel. Changes in physical properties could affect the size distribution of droplets, the burning properties, and the rate of evaporation of droplets. Therefore, any effect on the NO emissions would not necessarily have to be due to the chemical interactions with sulfur. For these reasons, it was first determined that replacement of distillate oil by an aromatic compound, such as benzene, had no effect on thermal NO emissions. As Figure 1.4-9 shows, the injection of benzene, at the same flow rate as was later used for thiophene addition, has no effect on thermal NO emissions. Since the volume of oil displaced by benzene was the same as that displaced later by thiophene,

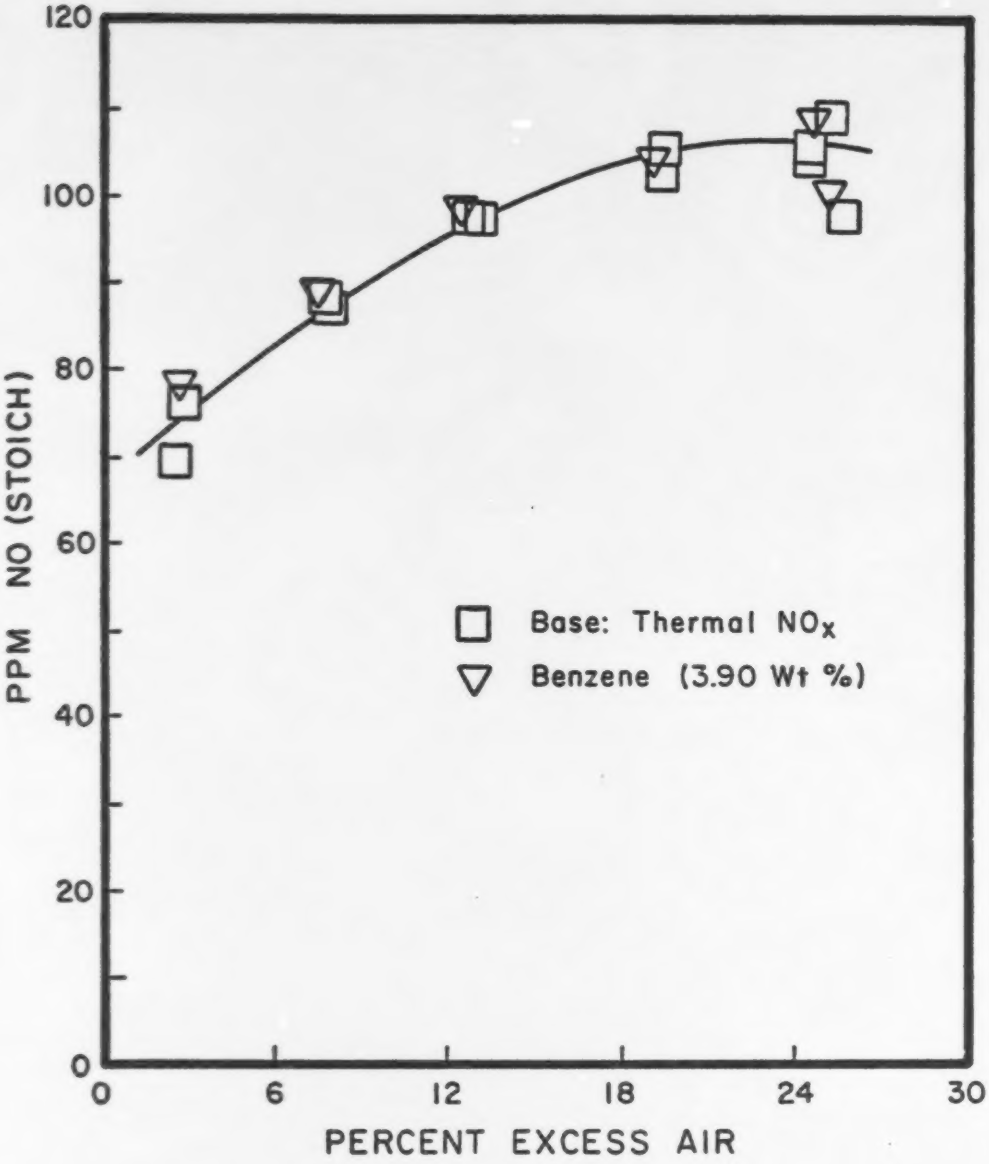

Figure 1.4-9 Distillate Oil: Replacement of Some Distillate Oil by Benzene Does Not Affect Thermal NO (59% Swirl; 100°F Air Preheat; 80°R Nozzle).

these data indicate that thiophene should only have an effect on NO emissions by virtue of its sulfur content.

Figure 1.4-10 presents the results of the study of the effect of thiophene addition to distillate oil on NO emissions. A reduction of 12 to 15 percent in emissions was observed; the reduction was of the order of 10 ppm NO. It can be seen that the effect was essentially independent of excess air conditions which indicates mixing is less rapid than kinetics. The flame associated with these data was bushy and luminous. These findings indicate that fuel desulfurization may have an adverse effect on NO emissions regardless of whether the fuel is introduced as a spray or in a gaseous state. The level of thiophene addition produced about 2000 ppm SO_2 in the exhaust.

Effect of SO_2 Addition to the Air at High Air Preheat

To gain information concerning how to model the kinetic environment, important in a turbulent distillate oil diffusion flame, SO_2 was added to the air stream. Figure 1.4-11 shows the results of this study at 310°F air preheat and a moderate percent swirl value. A reduction of 10 to 15 percent in NO emissions was observed when the SO_2 level was 3000 ppm SO_2 in the exhaust. The inhibition was approximately 10 ppm NO over the entire excess air range investigated. The flame was bushy and luminous.

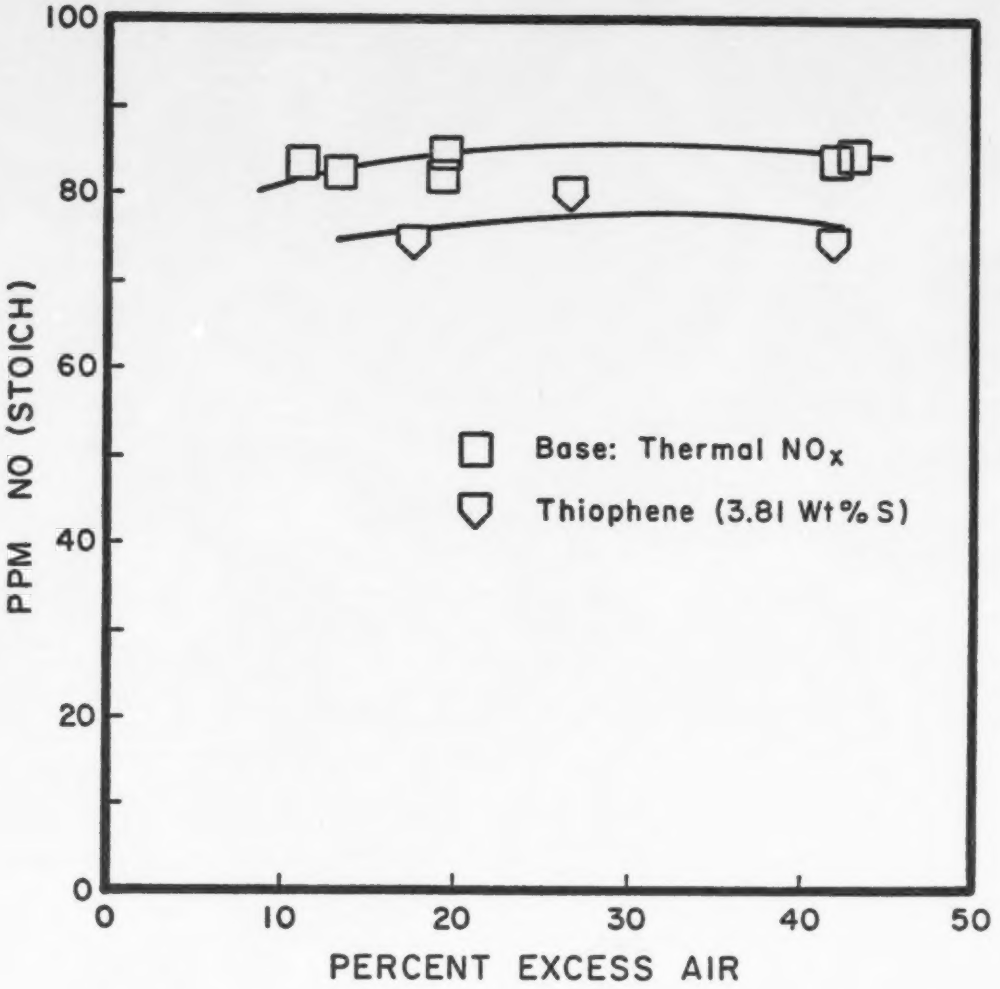

Figure 1.4-10 Distillate Oil: Thiophene Inhibits Thermal NO at Low Air Preheat (60% Swirl; 100°F Air Preheat; 80°R Nozzle).

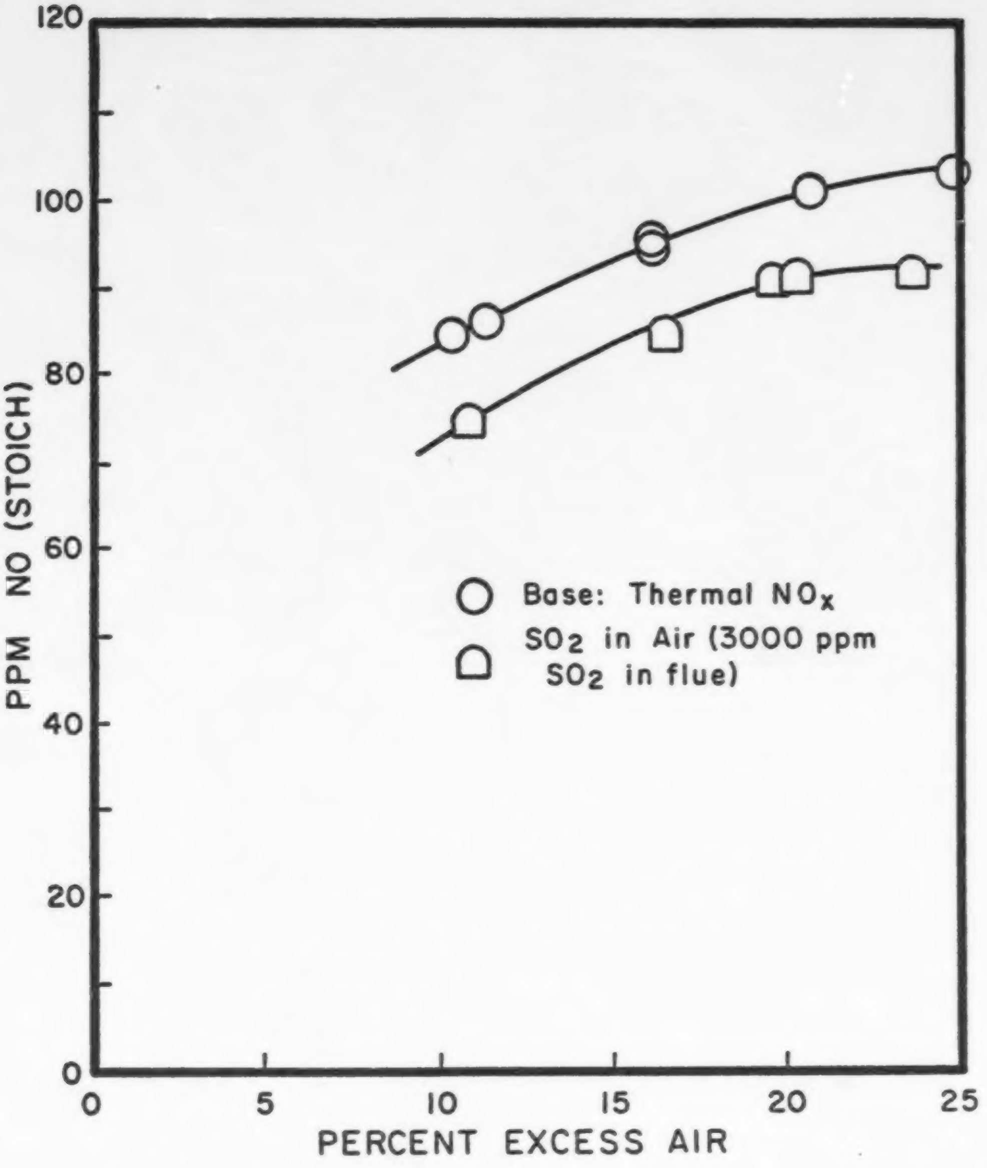

Figure 1.4-11 Distillate Oil: Effect of SO_2 Addition to Air on Thermal NO at High Air Preheat (44% Swirl; 310°F Air Preheat; 30°R Nozzle).

1.5 Fuel NO-Fuel Sulfur Interactions

The effect of fuel sulfur on "fuel" NO (i.e., NO emissions resulting from the oxidation of chemically bound fuel nitrogen) in turbulent oil and gaseous diffusion flames is presented in this chapter. Thiophene addition to mixtures of pyridine and distillate oil was examined to determine possible interactions in oil flames. Addition of SO_2 to an ammonia-natural gas mixture was examined to determine possible effects in gaseous fuels.

1.5-1 Introduction

The data presented in the previous chapter indicated that fuel sulfur could significantly affect thermal NO emissions from turbulent gaseous and oil diffusion flames. A potentially more significant problem is the possibility of similar type interactions between fuel sulfur and fuel NO, since most fuels that contain sulfur also contain chemically bound nitrogen. The possibility that fuel sulfur may inhibit or enhance fuel NO formation would be important in deciding whether to desulfurize the fuel before combustion, or to use stack gas scrubbing to remove the resulting SO_2 after combustion. Determination of possible interactions between fuel sulfur and fuel NO is also important, since fuel desulfurization can be accomplished without removing an equivalent amount of chemically bound nitrogen.

Wendt and Ekmann (1974) conducted studies with premixed methane-air flat flames doped with cyanogen (C_2N_2) or NO to determine the effect of fuel sulfur, introduced as SO_2, on fuel NO emissions. The results obtained were inconclusive due to phenomena occurring in the uncooled quartz sampling probe under fuel-rich conditions. However, preliminary indications were that, although the effect of fuel sulfur on fuel NO emissions was not significant under fuel-lean conditions, fuel sulfur might, under fuel-rich conditions, have a marked influence on the rate at which fuel NO is formed.

The present study examines the effect of fuel sulfur on fuel NO formation in more practical turbulent oil and gaseous diffusion flames. Since the mechanisms of fuel nitrogen oxidation are presently quite imperfectly understood, and since the role of super-equilibrium concentrations of atoms and free radicals in these mechanisms is unclear, it is not possible to speculate whether fuel sulfur may have effects on fuel NO similar to those observed with thermal NO under typical combustion conditions.

1.5-2 Distillate Oil

The addition of thiophene to a pyridine-distillate oil fuel mixture was used to investigate the effect of fuel sulfur on fuel NO emissions. For the majority of studies conducted, the fuel sulfur level was 2.05 wt % S, corresponding to about 1100 ppm SO_2 in the exhaust for complete conversion; the fuel nitrogen level was .78 wt % N, corresponding to approximately 960 ppm NO in the flue for complete conversion.

These levels are representative of fuel sulfur and fuel nitrogen contents of low-grade crudes or residual oils.

The oil firing rate was about 70,000 Btu/hr. The fuel was mechanically atomized after passing through a water-cooled injector. The same injector was used for all studies although the nozzle was changed before each study. The flames produced were short, bushy, and luminous. These flames were attached to the nozzle about 1/4" above the orifice of the nozzle. For the majority of studies, 30° solid cone nozzles were used.

To insure that the observed effects on fuel NO were due to the presence of fuel sulfur, and not to transients introduced by the addition of thiophene, efforts were made to ascertain that all other conditions remained constant. As a result of the relatively long lag times involved in the feed line (about 15 minutes), the cycling procedure used with the thermal NO studies was not employed. Also, thiophene is itself a fuel and changes in the stoichiometric air requirements would be expected when it was introduced into the pyridine-oil fuel mixture. The following procedure was therefore employed in these studies:

1. Baseline thermal NO data were taken over the excess air range of interest without the presence of pyridine.
2. Pyridine was added to the fuel and excess air conditions were varied over the range of interest.
3. Thiophene was added to the pyridine-oil mixture and NO measurements were made over a range of excess air conditions.

4. Thiophene addition was stopped and NO measurements were again taken for the pyridine-oil mixture at selected excess air conditions.
5. Finally, pyridine addition to the oil was stopped, and thermal NO readings were taken to compare with the original baseline data.

The most important problem encountered in the studies conducted with #2 diesel oil was coke formation on the oil nozzles. The severity of coke formation increased with air preheat, decreasing excess air conditions, and when fuel nitrogen was present. A reduction in coking was observed when thiophene was added to the pyridine-oil mixture. Since the presence of SO_2 or H_2S in premixed and diffusion flames has been found to reduce carbon formation (Cullis and Mulcahey, 1972), this is not unexpected.

Carbon formation on the nozzles caused variations in the flow rate of the fuel; this was indicated by the CO and CO_2 monitors and the oxygen monitor. The angle of the spray was also restricted and in severe cases a single stream of fuel was observed. It was also noted that coking caused exhaust measurements of NO to be insensitive to changes in the inlet air flow rate, i.e., excess air conditions.

To minimize coking in these studies, 30°R solid cone nozzles were used. A burner insert was used in the preheat cases to increase the axially directed air velocity. Both measures were taken to prevent recirculation of fuel or combustion gases to the relatively cooler region about the nozzle. Even with these modifications, it was still necessary to physically jar the coke from the nozzles by rapping on the oil injector.

It was also necessary to change oil nozzles before each run as a result of fouling caused by carbon formation. Variations of 5 to 25 percent in baseline NO levels with pyridine in the fuel were observed for the same operating conditions. These effects may have been caused by differences in the atomization characteristics of the nozzles. However, similar relative effects on fuel NO emissions due to the presence of fuel sulfur were observed regardless of the baseline data.

Effect of Fuel Sulfur on Fuel NO at "Zero" Air Preheat

The experimental procedure used in these investigations established that only minor changes in operating conditions (i.e., the temperature history of the furnace, the air preheats, and the percent swirl value) would be observed for the entire duration of a particular run. These changes in operating conditions did not influence the NO emissions observed with and without thiophene and/or pyridine. However, it was still necessary to establish that the introduction of thiophene, which causes a change in fuel composition, did not affect the NO emissions due only to the anticipated changes in local flame stoichiometry. Also, the introduction of a more volatile specie to the pyridine-oil mixture could affect the mass flux of pyridine to the gas phase as the droplets in the spray evaporate. This is a potential problem since the evaporation of a multicomponent droplet is analogous to multicomponent distillation (Newbold and Amundson, 1973); the saturated vapor pressure of pure thiophene is two to three times that of pyridine.

Therefore, before determining any effects of fuel sulfur on NO emissions, benzene addition to the pyridine-oil mixture was investigated. The saturated vapor pressure of pure benzene is about ten times that of thiophene. Figure 1.5-1 shows the results of the benzene addition study at "zero" air preheat and a moderate percent swirl value. Scatter in data is due to coking. It is apparent that benzene has no influence on the NO exhaust emissions. Since benzene was introduced at the same flow rate as thiophene was later, these data indicate that any effect of thiophene on fuel NO emissions should only be related to the presence of fuel sulfur. The fact that the introduction of a compound with a vapor pressure twenty to thirty times that of pyridine did not affect the overall NO emissions may indicate rapid vaporization of the droplets, or that the evaporation process occurs on a much shorter time scale than fuel NO formation kinetics.

Figure 1.5-1 also indicates that the introduction of fuel sulfur as thiophene has no discernible effect on overall NO emissions at zero preheat. However, it has previously been demonstrated that fuel sulfur as thiophene reduces thermal NO emissions from turbulent oil diffusion flames. Although it may, therefore, be postulated that fuel sulfur causes a small increase in fuel NO emissions, which is then compensated for by a reduction in thermal NO, the scatter in the data does not permit conclusive inferences to be drawn. Also, the sulfur level in the thermal NO study was higher than that with this fuel NO study (approximately

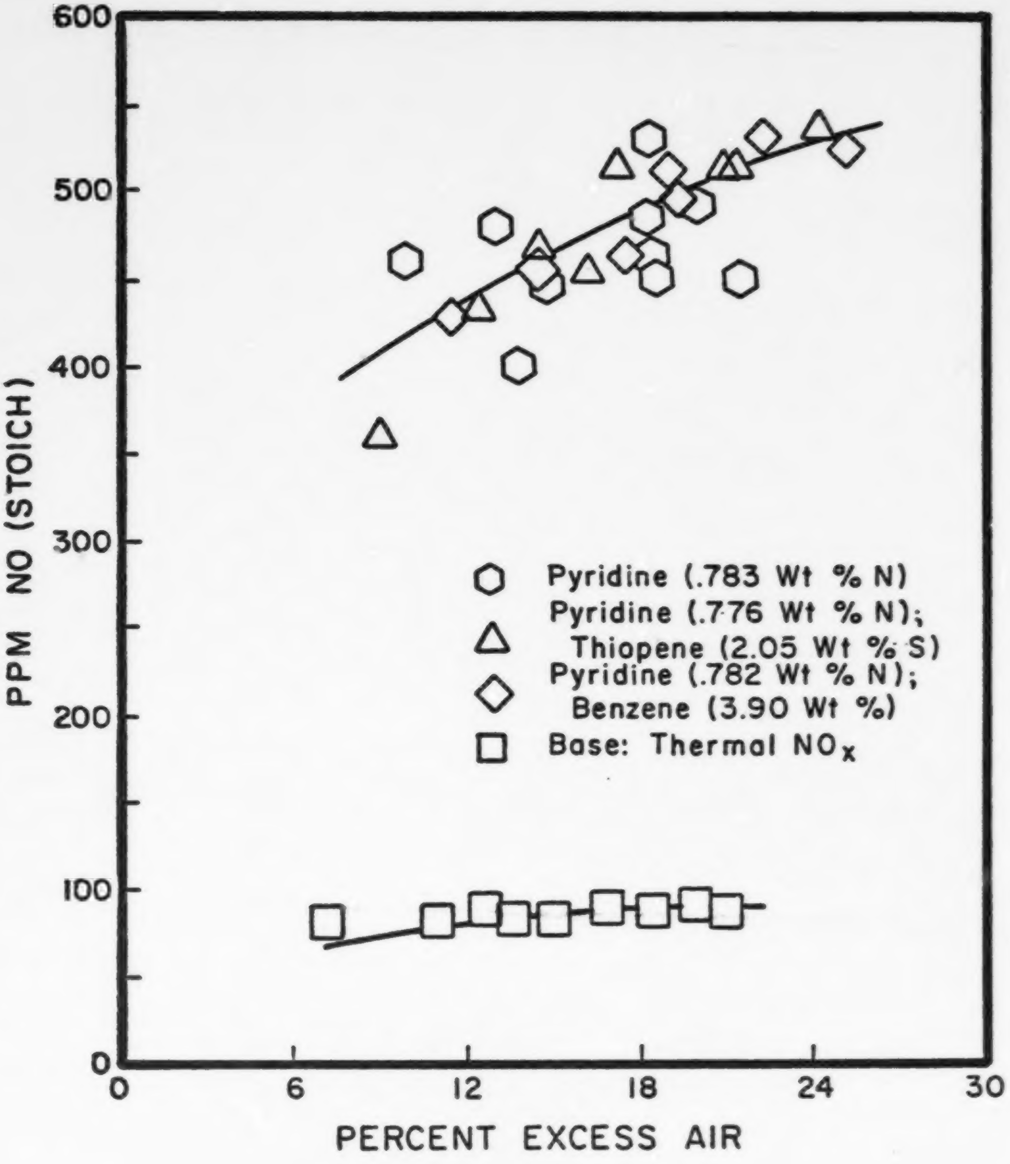

Figure 1.5-1 Distillate Oil: Effect of Benzene Addition and Fuel S on Fuel NO (44% Swirl; 130°F Air Preheat; 30°R Nozzle).

2200 ppm SO_2 in the exhaust compared to 1100 ppm SO_2 in the exhaust). The reduction in thermal NO was about 10 ppm NO; it is apparent that the resolution of data in this fuel NO study would not permit such small effects to be observed.

It should be noted that the apparent discrepancies in weight percent nitrogen in the fuel reported on Figure 1.5-1 are due only to dilution when benzene or thiophene is introduced to the pyridine-oil mixture. The pyridine flow rate was constant throughout. It should also be noted that the scatter in the data is due to coke formation on the nozzle.

Further substantiation of the finding that fuel sulfur has little or no effect on NO emissions, at "zero" air preheat and a moderate percent swirl value, is provided in Figure 1.5-2. For the same fuel nitrogen and fuel sulfur contents, but slightly different air preheat and percent swirl value, it is again concluded that there is no discernible effect of fuel sulfur at these operating conditions. Since different nozzles were used, the NO emissions in Figure 1.5-2 are different than those in Figure 1.5-1. The slight scatter in the data is due to some coke formation.

Figure 1.5-3 shows that for fuel sulfur and fuel nitrogen contents more typical of coals the presence of fuel sulfur has no effect on overall NO emissions. The data presented on this figure also allow comparison between NO emissions resulting from two nitrogen levels. Such a comparison indicates that approximately doubling the fuel nitrogen content does not produce the same doubling in NO emissions. This implies a decrease in conversion with increasing fuel nitrogen content and is

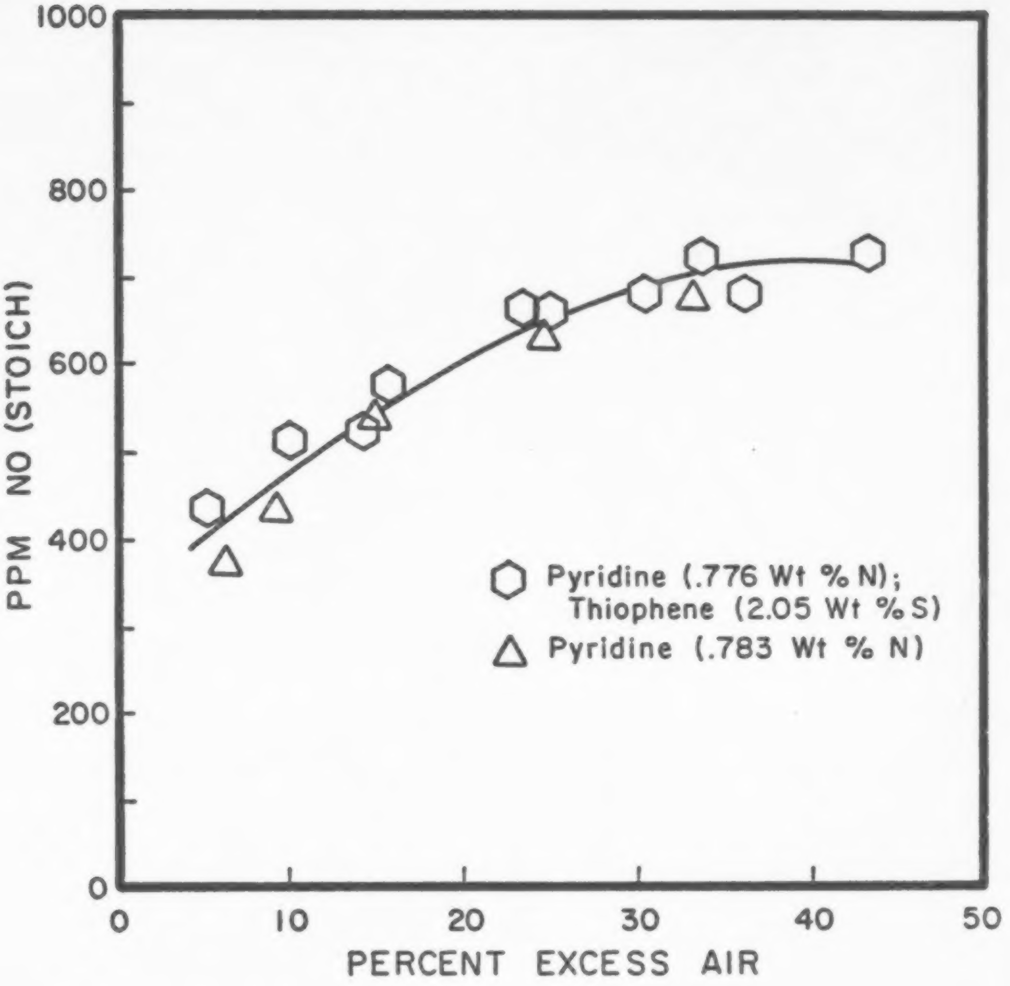

Figure 1.5-2 Distillate Oil: Thiophene Does Not Affect Fuel NO at Low Air Preheat (43% Swirl; 100°F Air Preheat; 30°R Nozzle).

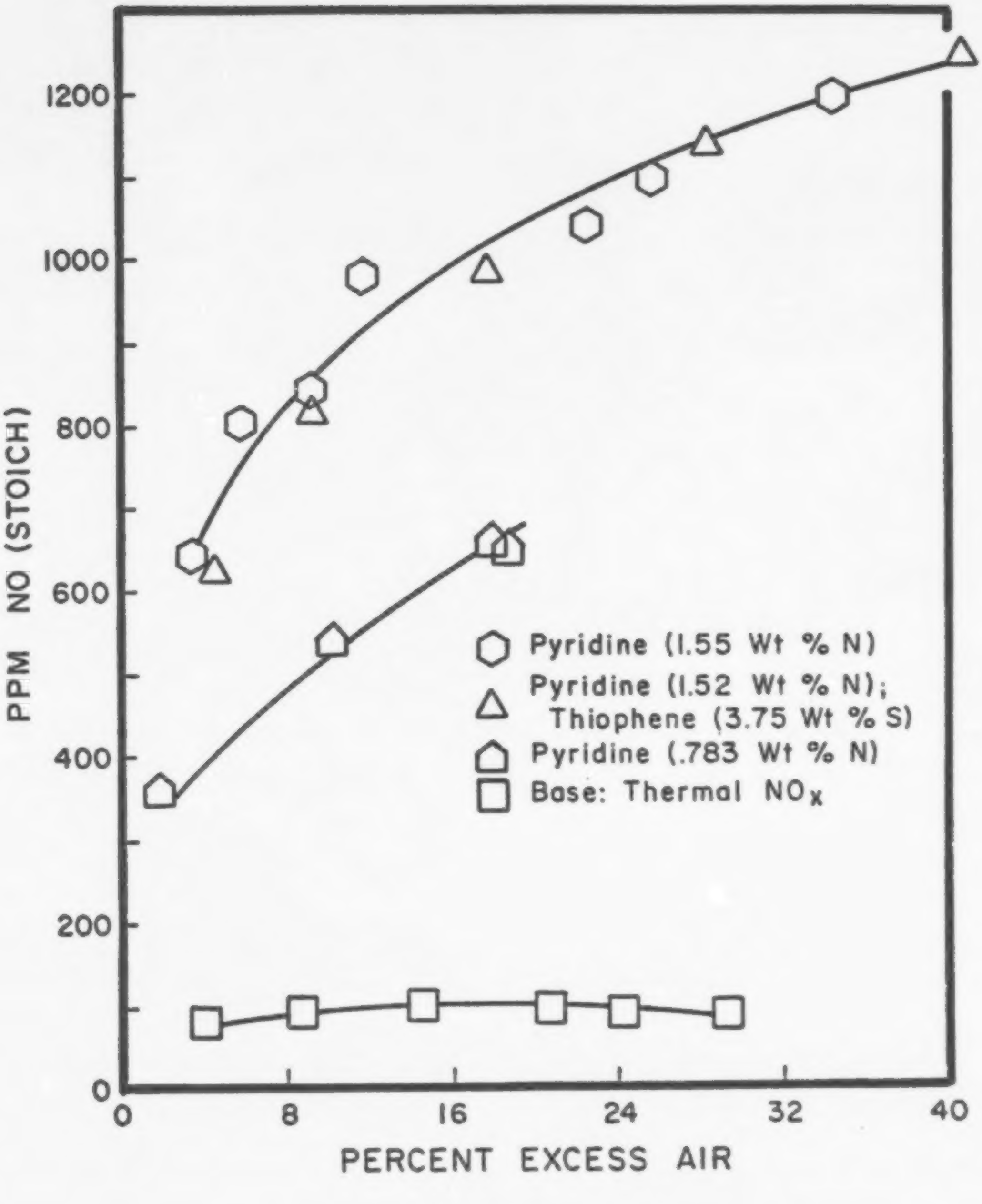

Figure 1.5-3 Distillate Oil: Effect of Fuel S and Fuel N on Fuel NO (44% Swirl; 100°F Air Preheat; 30°R Nozzle).

consistent with the findings of other workers (Pershing et al., 1975; Martin and Berkau, 1972; Fenimore, 1971, 1976; Sarofim et al., 1975).

Although the data presented show that fuel sulfur has little effect on fuel NO emissions, it may be that at different operating conditions the results would be different. For this reason, the phenomenon was further investigated by varying the percent swirl value while maintaining a constant excess air condition (15.1% excess air). Figure 1.5-4 indicates that fuel sulfur has little or no effect on fuel NO emissions over a large range of percent swirl values. A minimum in NO emissions occurs at about 40 percent swirl; at greater percent swirl values, NO emissions increase. Since the extent of mixing between air and fuel streams is expected to increase for these operating conditions, the increase may be associated with increasing local oxidant levels within the flame. The increase in NO exhaust levels as the percent swirl value approaches zero may be caused by a decrease in residence time (Myerson, 1975; Martin and Berkau, 1972). Since local flame temperatures should also increase with decreasing percent swirl values, as a result of lower radiative heat losses, the observed increase in overall NO emissions may be caused by this temperature increase.

Effect of Fuel Sulfur on Fuel NO at High Air Preheat

The next series of studies were undertaken to determine whether fuel sulfur would have any effect on fuel NO at a moderately high air preheat. Since coke formation increased with increasing air preheat, it was necessary to select an air preheat at which coking did not seriously

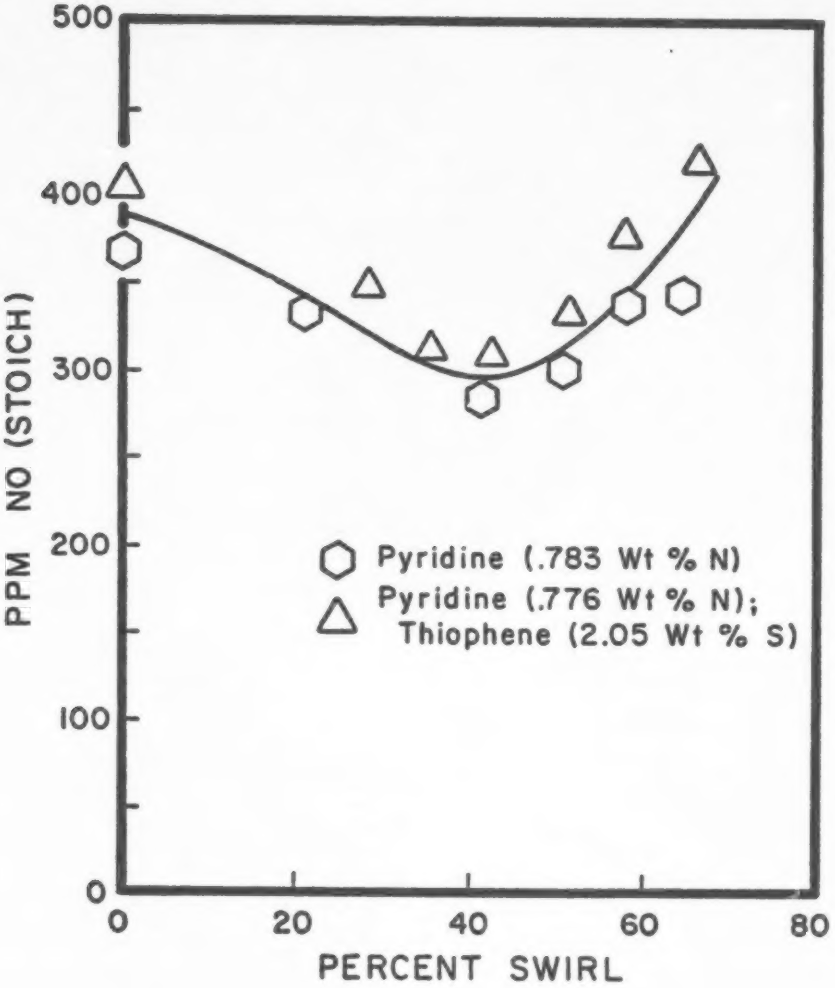

Figure 1.5-4 Distillate Oil: Effect of Swirl and Fuel S on Fuel NO (15.1% Excess Air; 100°F Air Preheat; 30°R Nozzle).

interfere with the determination of possible interactions between fuel sulfur and fuel NO. A burner insert was used in these studies to increase the axially directed air velocity and, therefore, to reduce the extent of coke formation. The resulting velocity increase was about two-and-one-half times that for the "zero" air preheat studies.

To determine that changes in the fuel composition, with resulting changes in local flame stoichiometry, as well as the introduction of a more volatile specie, did not affect overall NO emissions, benzene was again added to the pyridine-oil mixture. Figure 1.5-5 shows that benzene addition does not effect NO emissions at high air preheat and a moderate percent swirl value. These results indicate that any effects on NO emissions observed when thiophene is added to the fuel should only be caused by virtue of its sulfur content.

Figure 1.5-6 shows the results of the study conducted at a high air preheat and a moderate percent swirl value. It appears that increases of 30 to 50 percent in NO emissions can occur due to the presence of fuel sulfur. The increase is about 150 ppm NO at 10 percent excess air and decreases to about 120 ppm NO at 24 percent excess air. It should be noted that this flame was luminous which indicates locally substoichiometric conditions within the flame. Since at higher excess air conditions the break-up of fuel-rich regions is promoted, and since the enhancement effect decreases with increasing excess air, it may be postulated that fuel sulfur interacts with fuel nitrogen to enhance NO emissions in fuel-rich regions within the flame. Note that the fuel

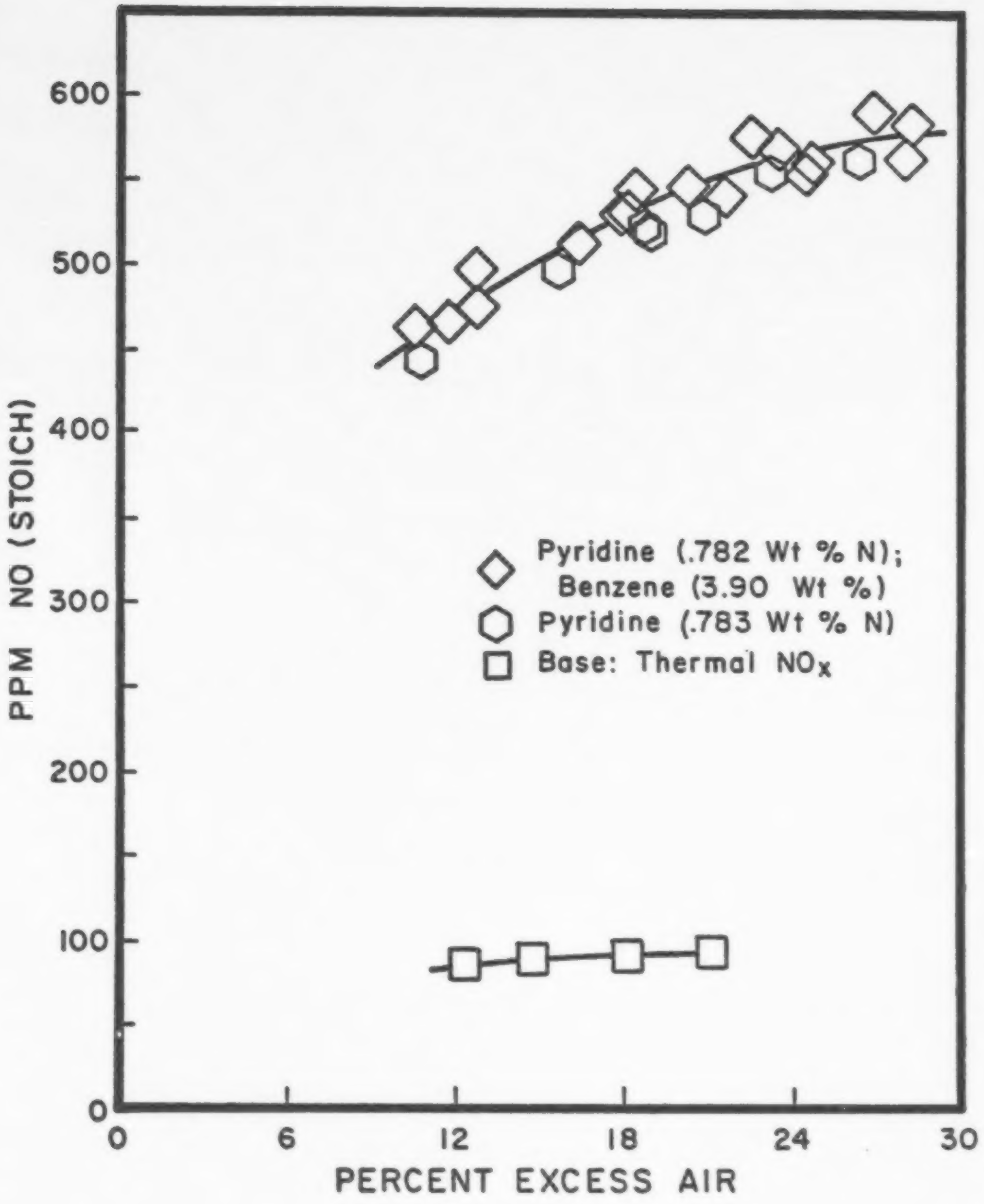

Figure 1.5-5 Distillate Oil: Benzene Does Not Affect Fuel NO at High Air Preheat (44% Swirl; 315°F Air Preheat; 30°R Nozzle).

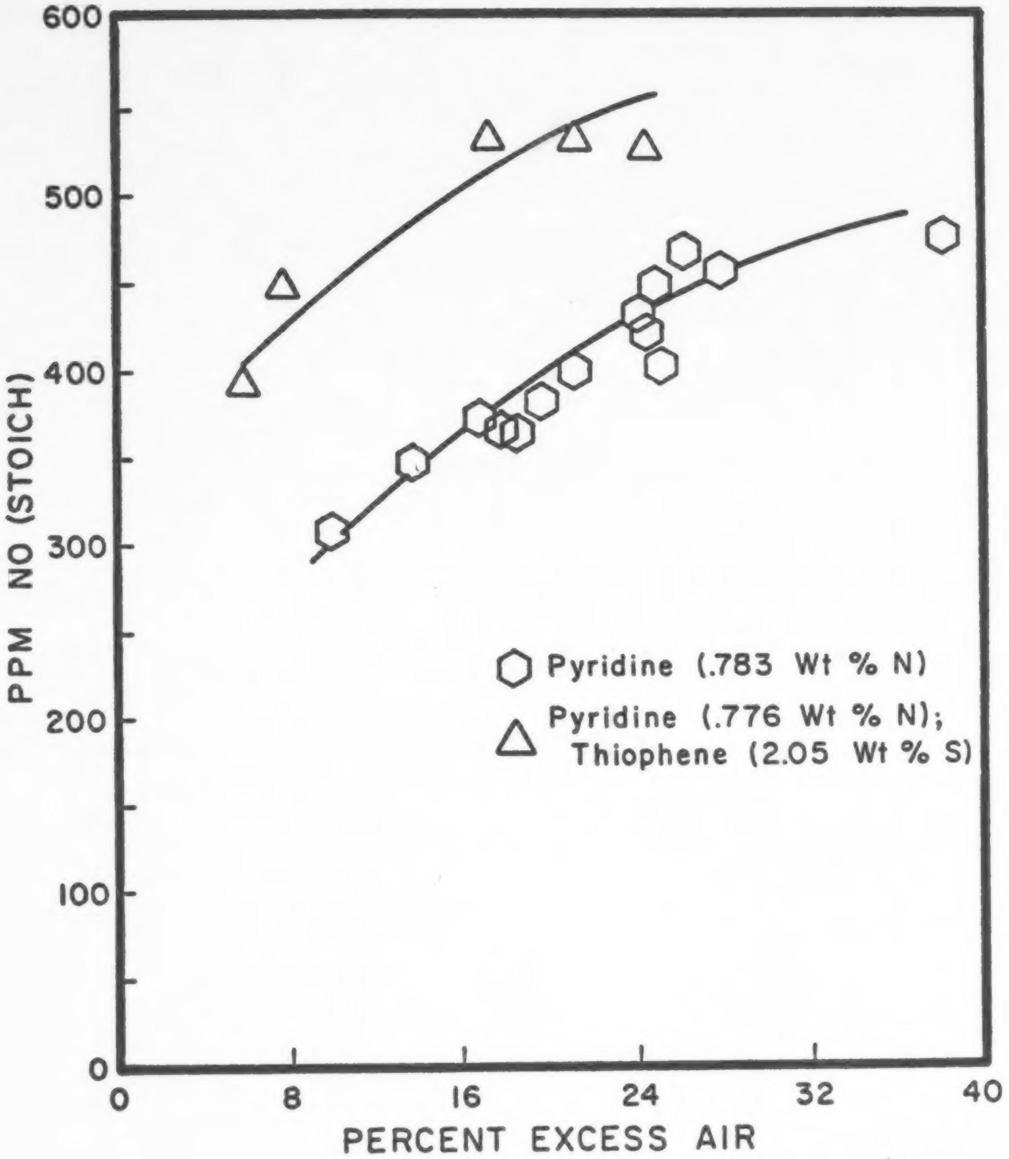

Figure 1.5-6 Distillate Oil: Thiophene Increases Fuel NO at High Air Preheat (40% Swirl; 310°F Preheat; 30°R Nozzle).

sulfur and fuel nitrogen levels are the same as those used for the "zero" air preheat studies.

Since an increase in NO emissions due to the presence of fuel sulfur was not anticipated, because of the findings at the "zero" air preheat conditions, this run was repeated. Figure 1.5-7 shows that an increase in NO emissions of 10 to 20 percent occurs due to the presence of fuel sulfur. The increase is about 60 ppm NO at 10 percent excess air and decreases to about 40 ppm at 24 percent excess air. Although the enhancement effect is less than that previously observed, it still occurs. The differences in the extent to which fuel sulfur enhances NO emissions may be partly due to different atomization characteristics of the nozzles used. Also, the data in Figure 1.5-7 were taken about 2 months later than those in Figure 1.5-6; there may have been subtle changes in the physical hardware which could have affected the results. It should be noted that the baseline data for the pyridine-oil mixture are 25 to 30 percent higher in Figure 1.5-7 than the values reported in Figure 1.5-6.

To gain information on the kinetic environment important in fuel NO formation, SO_2 was added to the air stream. It was also desired to determine whether SO_2 introduced to the fuel-lean side of the flame would have a similar enhancement effect on NO emissions as was observed when thiophene was added to the pyridine-oil mixture. Figure 1.5-7 shows the results of this study when SO_2 was added at a level to produce 3000 ppm SO_2 in the exhaust. As can be seen, the addition of SO_2 to the air causes an increase in NO emissions. Since it has already been shown that the addition of SO_2 reduces thermal NO for almost identical conditions

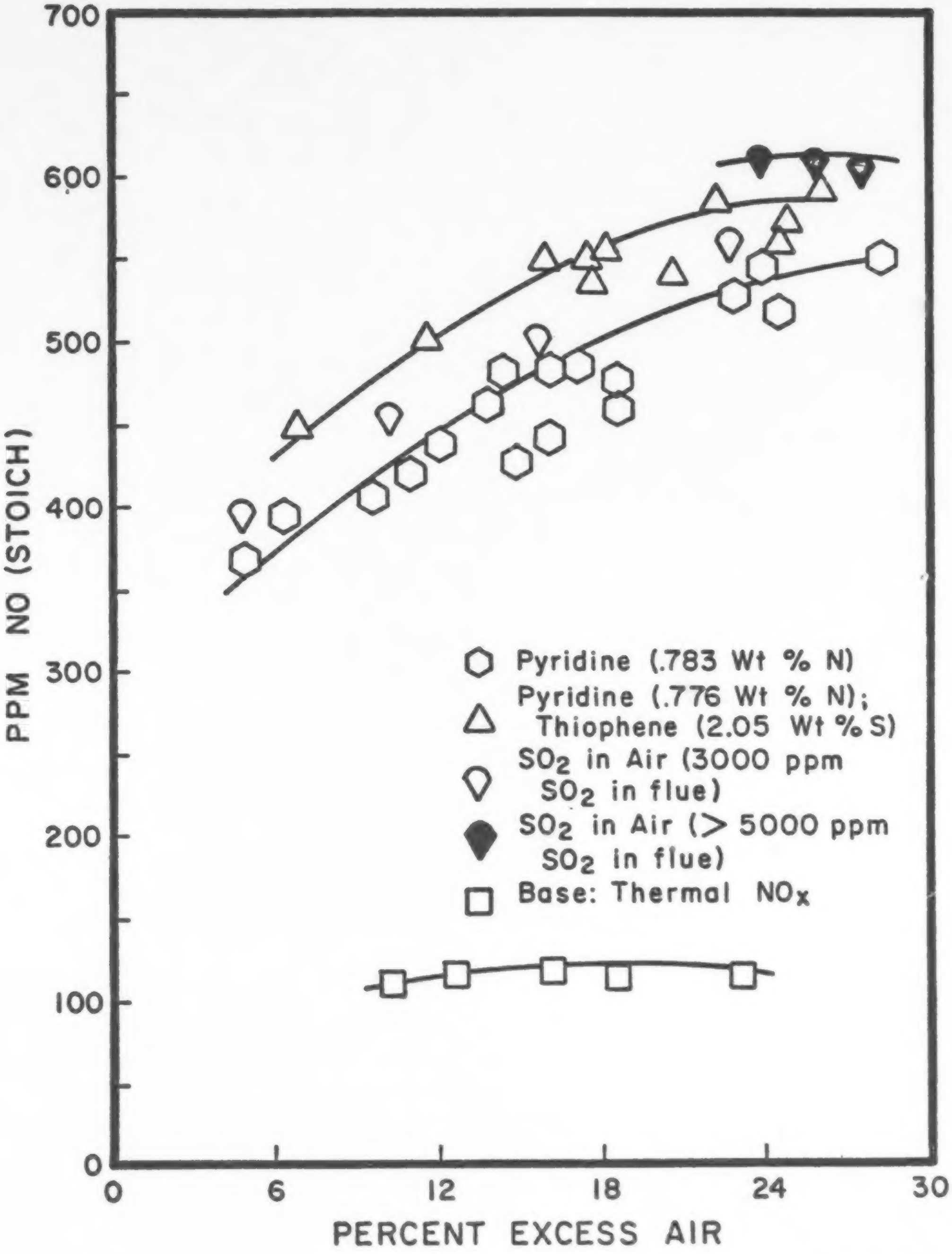

Figure 1.5-7 Distillate Oil: Fuel S and Fuel N Interactions of High Air Preheat (44% Swirl; 315°F Air Preheat; 30°R Nozzle).

(see section 1.4.4), it can be inferred that the enhancement is due to interactions of SO_2, or a reduced form of SO_2, with the fuel NO formation mechanism.

The enhancement effect observed when SO_2 is added to the fuel-lean side of the flame front is about one-half that observed when thiophene is added to the pyridine-oil mixture. This is significant inasmuch that the SO_2 level was 3000 ppm SO_2 in the exhaust as compared to 1100 ppm SO_2 in the flue when thiophene was used to simulate fuel sulfur. It may indicate that SO_2 must first diffuse to the fuel-rich side of the flame front before it, or a reduced form, can interact with fuel NO formation.

The SO_2 level was increased in order to determine what levels of SO_2 on the fuel-lean side of the flame front would produce similar increases on fuel NO exhaust levels as when thiophene was added. As Figure 5.7 shows, it was not until the flue measurements were greater than 5000 ppm SO_2 as measured (the upper limit of the SO_2 analyzer) that similar increases occurred. These SO_2 levels are at least four times greater than those achieved when thiophene was added to the pyridine-oil mixture. Since SO_2 in the air reduces thermal NO, and since the increased concentration of SO_2 should generate an increased concentration on the fuel-rich side of the flame front because of a greater driving force, it can be inferred from these data that fuel sulfur interacts with fuel NO formation on the fuel-rich side of the flame front. Since SO_2 achieves similar effects on fuel NO as chemically bound sulfur, these data indicate that SO_2, or a reduced form of SO_2, is important in the interaction.

The effect of fuel sulfur on fuel NO at high air preheat conditions was further investigated by varying the percent swirl value at a fixed excess air condition (21.3% excess air). As Figure 5.8 shows, fuel sulfur increases fuel NO emissions over the entire range of percent swirl values investigated. The increase was about 60 ppm NO and was fairly constant. The flame was detached below 35 percent swirl.

1.5-3 Natural Gas

To determine whether the effect of fuel sulfur on fuel NO at a high air preheat condition was peculiar to turbulent distillate oil diffusion flames, a study was conducted with natural gas doped with NH_3 and SO_2. The axial gas injector was used; the flame produced was long, narrow, and jetlike. The color of the flame was an intense blue-violet which indicated near-stoichiometric combustion conditions within the flame. To gain information concerning the kinetic environment important in fuel NO formation, SO_2 was also added to the air stream.

The results shown in Figure 1.5-9 indicate that the presence of SO_2 in the fuel to make 3350 ppm SO_2 in the exhaust significantly increases fuel NO emissions. However, part of the increase can be attributed to an increase in thermal NO as SO_2 in the fuel has already been shown to increase thermal NO at a high air preheat for the axial injector condition. It was shown in section 1.4-2 that for the same type flame with the same operating conditions and firing rate the increase in thermal NO was about 15 ppm NO. Therefore, even allowing for an increase in thermal

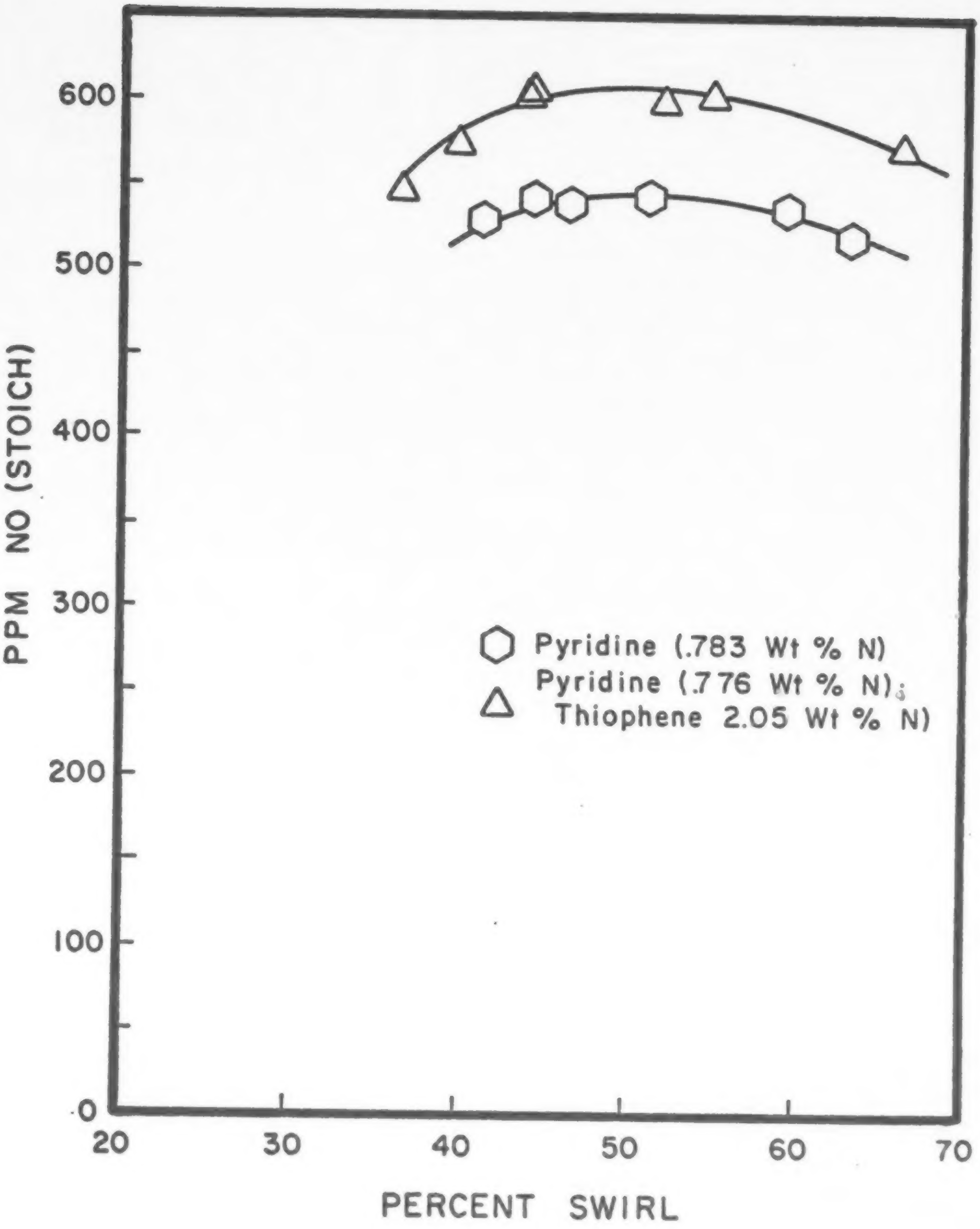

Figure 1.5-8 Distillate Oil: Effect of Swirl on Thiophene Enhancement of Fuel NO at High Air Preheat (21.3% Excess Air; 310°F Air Preheat; 30°R Nozzle).

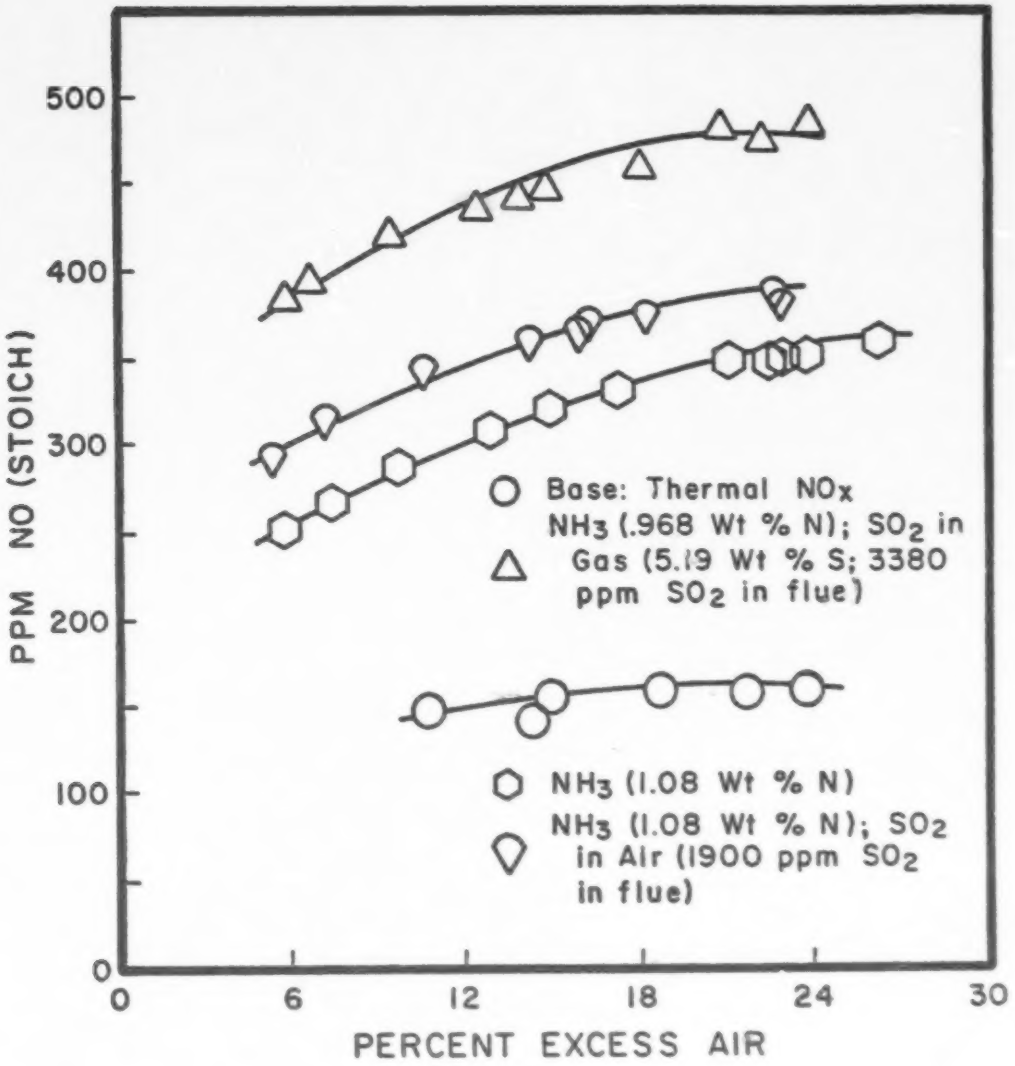

Figure 1.5-9 Natural Gas/Ammonia -- Axial Injector: SO_2 Increases Fuel NO at High Air Preheat (44% Swirl; 430°F Air Preheat).

NO, the addition of SO_2 to the fuel causes an increase of about 120 ppm NO for the entire range of excess air conditions investigated. Fuel nitrogen conversion to NO almost doubles when SO_2 is added to the fuel.

When SO_2 is added to the air, there is also an increase in fuel NO emissions. Since thermal NO is reduced by 10 to 20 percent when SO_2 is present in the air, the effect on fuel NO is probably greater than that indicated by the data in Figure 1.5-9. The smaller enhancement effect than when SO_2 is added to the fuel may be due to the lower SO_2 level. Since the flame color indicates locally near-stoichiometric conditions within the flame, and since this is an indication of fairly rapid mixing between the air and fuel streams, these data may indicate that SO_2 interacts with NH_3 conversion to NO in locally substoichiometric regions within the flame.

The above data indicate that in both turbulent gaseous and oil diffusion flames the presence of fuel sulfur enhances fuel NO formation at high air preheat conditions. The data also indicate that the interaction of fuel sulfur with the fuel NO formation mechanism takes place on the fuel-rich side of the flame front as was found for the distillate oil study. That increases were observed in fuel NO emissions even though the fuel nitrogen was introduced as different compounds, NH_3 and pyridine, may indicate that fuel sulfur is interacting with the same intermediary in both cases.

1.6 Fuel Nitrogen Conversion to NO

This chapter discusses overall conversion of fuel nitrogen to NO in turbulent distillate oil and gaseous diffusion flames. Factors which influenced the conversion of fuel nitrogen are also presented. Comparisons between the results of this study and those obtained by other investigators are made in order to demonstrate the consistency of the data acquired in the present study with that already published in the literature. Further information concerning the kinetic environment important in fuel NO formation is gained by contrasting the conversion data presented here with that for premixed flame studies.

1.6-1 Distillate Oil

In this particular study, only the fuel nitrogen content of the fuel was varied. Excess air conditions were maintained constant at 15.0 percent excess air. The study was conducted at a "zero" air preheat condition and a moderate percent swirl value. A 30°R, solid cone nozzle was used; the flame produced was short, bushy, and luminous. Locally substoichiometric conditions within the flame were indicated by the luminous nature of the flame.

The results of this study are presented in Figure 1.6-1. It is apparent that as the fuel nitrogen content increases from 0.166 wt % N to 1.55 wt % N the percent conversion decreases. Conversion was

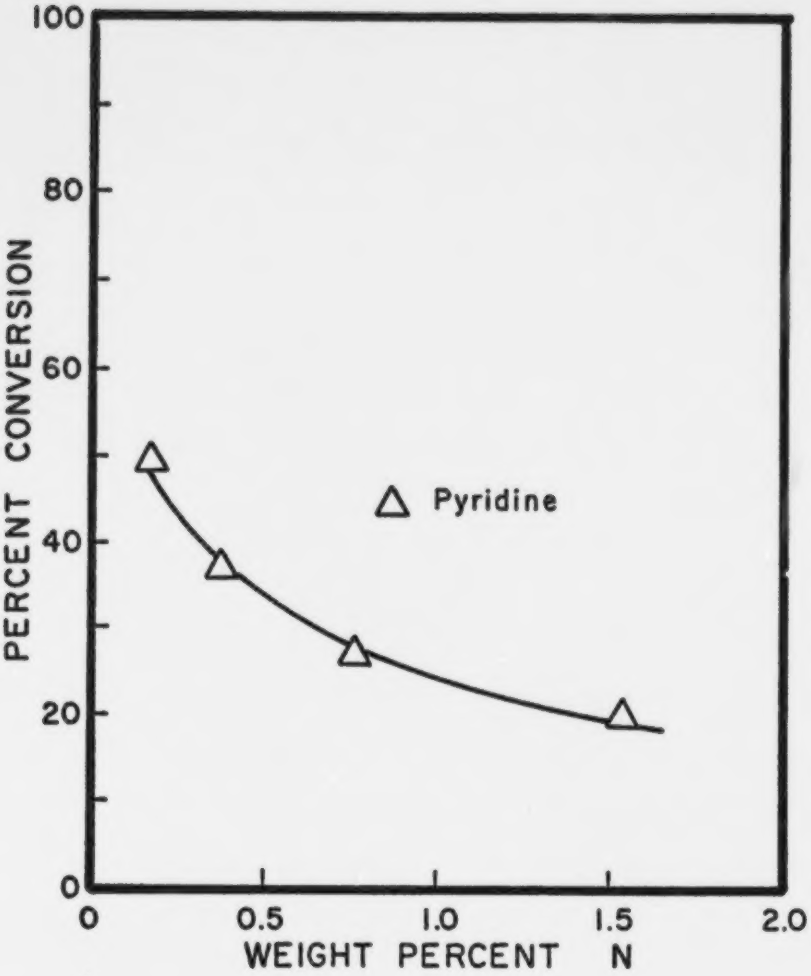

Figure 1.6-1 Distillate Oil: Conversion of Fuel N to Fuel NO at Various Fuel N Levels (15.0% Excess Air; 42% Swirl; 100°F Air Preheat; 30°R Nozzle; Thermal NO = 100 PPM).

approximately 50 percent at the lowest fuel nitrogen level and decreased to about 20 percent at the highest fuel nitrogen level. Although the percent conversion decreased as the fuel nitrogen content increased, the fuel NO emissions increased as the weight percent nitrogen in the fuel increased. At .166 wt % N, 100 ppm NO was measured, and at 1.55 wt % N, about 380 ppm NO was produced. The decrease in percent conversion of fuel nitrogen as the weight percent nitrogen increases and the increase in NO emissions with increasing weight percent nitrogen are consistent with the findings of other investigators working with oil (Turner et al., 1972; Martin and Berkau, 1972). However, the observed increase in NO emissions with increasing fuel nitrogen content is in contrast with recent data (Pershing, 1976) on coal in which it was found that NO emissions did not change significantly for different fuel nitrogen contents.

In calculating the percent conversion at various fuel levels of nitrogen, the thermal NO reading was subtracted from the overall NO emission data when pyridine was present. Since the mechanisms of thermal NO and fuel NO formation are additive and independent (Martin and Berkau, 1972), the resulting NO figure represents the contribution due to fuel nitrogen conversion. The fuel nitrogen levels used in this study .166 wt % N, .398 wt % N, .783 wt % N, and 1.55 wt % N, could produce the following fuel NO levels for complete conversion: 203 ppm NO, 488 ppm NO, 966 ppm NO, and 1926 ppm NO, respectively.

In Figure 1.6-2, fuel nitrogen conversion data from the present investigations (solid symbols) is compared to that of several other workers. All data presented in this figure were obtained from studies

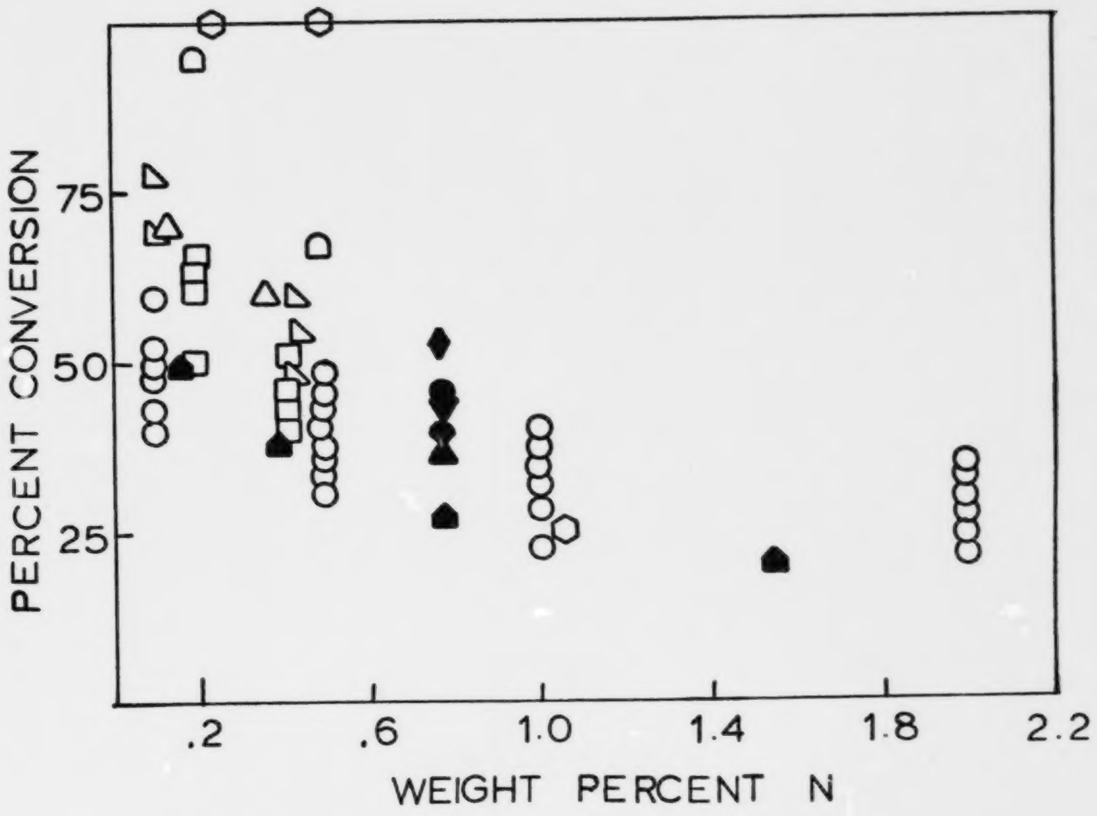

Figure 1.6-2 Comparison of Nitrogen Conversion to NO with That of Other Workers. -- Selected data taken from Sarofim and Flagan (1975).

with oil fuels. As can be readily seen, the decrease in fuel nitrogen conversion with increases in weight percent nitrogen in the fuel, and the extent of conversion of fuel nitrogen at a given weight percent nitrogen are at least qualitatively in good agreement with the data reported by others. More specific comparisons cannot be made, since the firing configurations, air preheats, and excess air conditions are not known for the data obtained by the other investigators.

Figure 1.6-2 also shows fuel nitrogen conversion data from a number of studies conducted at .78 wt % N. The data were taken at 15.0 percent excess air conditions, moderate percent swirl values, and both "zero" and high air preheat conditions. Since different 30°R, solid cone nozzles were used for each run, the effect of changing oil nozzles on fuel nitrogen conversion is also illustrated. In studies with kerosene doped with pyridine, Appleton and Heywood (1973) showed that atomization and initial fuel-air mixing were important in determining the conversion of fuel nitrogen to NO. It may, therefore, be that differences in atomization characteristics of the nozzles used with subsequent affects on fuel-air mixing are responsible for the variations in conversion observed. It is apparent that differences in the nozzles could be more significant than air preheat conditions.

As was shown in Section 1.5, the presence of fuel sulfur increased fuel NO emissions at high air preheat and a moderate percent swirl value. The solid triangles on Figure 1.6-2 represent data taken with the same oil nozzle, but with and without fuel sulfur. A comparison shows that fuel nitrogen conversion increased from 36.8 percent to 42.1 percent due to the presence of fuel sulfur.

Fenimore (1972, 1976) investigated NO emissions from premixed C_2H_4-O_2-inert flames doped with pyridine. For fuel-lean conditions, almost quantitative conversion of fuel nitrogen to fuel NO was observed. Conversion levels similar to those obtained in the present study of distillate oil flames doped with pyridine were observed for equivalence ratios of 1.5 to 1.7, i.e., about 60 to 70 percent of stoichiometric air requirements. Studies conducted on CH_4-air combustion in a jet-stirred combustor (Bartok et al., 1972) also indicate that fuel-rich conditions are necessary to obtain fuel nitrogen conversion data similar to those obtained in the present study. It can, therefore, be inferred that fuel-rich regions in turbulent distillate oil diffusion flames are important in the conversion of fuel nitrogen to fuel NO. Martin and Berkau (1972) draw the same inference from their data.

The data in Section 1.5 indicate a fairly strong dependence of fuel NO emissions and, therefore, fuel nitrogen conversion on excess air conditions. As the excess air is increased, the average driving force for oxygen diffusion also increases. An increase in air volume occurs with increasing excess air conditions, promoting turbulent mixing and aiding in dispersing fuel-rich regions within the flame. Since local oxidant levels are increasing, it is expected that conversion of fuel nitrogen to fuel NO should increase.

1.6-2 Natural Gas

A comprehensive study was not conducted on fuel nitrogen conversion to fuel NO in turbulent gas diffusion flames. However, limited data are available from the study on fuel sulfur effects on fuel NO (see section 1.5.3). The data were taken at 430°F air preheat and 44 percent swirl. The flame associated with these data was the near-stoichiometric, jetlike flame. Fuel nitrogen was simulated by NH_3.

At 1.08 wt % N in the fuel and 15.0 percent excess air, the conversion of fuel nitrogen to fuel NO was 11.4 percent. The exhaust measurements indicated 165 ppm fuel NO produced as compared to 1450 ppm NO for complete conversion of the fuel nitrogen. The dependence of fuel nitrogen conversion on excess air conditions was not as prominent as that observed for the distillate oil studies. At 12 percent excess air, conversion is 10 percent, while at 24% excess air the conversion is 15 percent. Since the flame associated with this natural gas-NH_3 data had near-stoichiometric regions within the flame, while locally substoichiometric regions were present in the distillate oil flame, an increase in excess air conditions may not have increased local oxidant levels to as great as an extent.

The effect of fuel sulfur on fuel nitrogen conversion to fuel NO is to increase conversion. At 15 percent excess air, the addition of SO_2 to the air stream (1900 ppm SO_2 in the exhaust) increases conversion from 11.4 percent to 14.5 percent. The addition of SO_2 to the fuel causes an increase in fuel nitrogen conversion to 20.4 percent.

Some insight as to where in the turbulent gaseous diffusion flame fuel NO formation occurs may be gained by comparing the conversion data of this study with the data available in the literature on premixed flame studies. Wendt and Sternling (1974) investigated CH_4-air flames doped with ammonia. For approximately .9 wt % N in the fuel conversion levels similar to those obtained in this study occurred below 80 percent of stoichiometric are requirements. Sarofim et al. (1975) investigated both premixed and diffusion CH_4-air flames doped with ammonia. Again, conversion levels of fuel nitrogen, for the same weight percent nitrogen as was used in this study, that were similar to the results reported here occurred only for substoichiometric conditions. It was also found that conversion of fuel nitrogen was less in diffusion flames than in premixed flames. It can be inferred from these data that fuel NO formation occurs in locally substoichiometric regions within turbulent gaseous diffusion flames.

1.7 Discussion

This section discusses reaction sequences which may be of importance in the interactions between fuel sulfur and thermal or fuel NO production. However, there is a lack of data and/or agreement concerning the kinetic mechanisms involved in the formation of SO_2 or NO from the combustion of organic sulfur or nitrogen compounds, respectively. It is, therefore, necessary to stress the speculative nature of the material presented.

1.7-1 Thermal NO

From the data presented in Section 1.4, it can be concluded that the effect of fuel sulfur on NO production in turbulent gaseous diffusion flames is dependent on local flame stoichiometry and local flame temperature. At "zero" air preheat and moderate percent swirl values, the addition of SO_2 to the fuel or to the air resulted in a decrease in NO emissions. Although this inhibition effect was observed for both the radial and axial injector studies, it was also observed that when SO_2 was added to the fuel in the axial injector study the decrease in NO emissions was not as great as when a smaller amount of SO_2 was introduced into the air stream. The flame produced by the axial injector was luminous, which is an indication of the presence of locally fuel-rich regions within the flame. Since Wendt and Ekmann (197) concluded that the inhibition effect of fuel sulfur on thermal NO production was due to mechanisms involving SO_2, a significant reduction of the SO_2 added to the fuel in the axial injector study could be anticipated to result in a decreased inhibition of NO formation.

However, in combustion studies of H_2S, it has been found that, even at 80 percent of stoichometric air requirements, 90 percent of the sulfur is present as SO_2 with the remainder almost entirely SO (Cullis and Mulcahey, 1972). It has also been determined that super-equilibrium hydrogen atoms in fuel-rich propane flames depress the concentrations of H_2S, HS, and S_2 below their equilibrium values (Cullis and Mulcahey, 1972); there is a corresponding increase in the concentrations of SO_2, SO, and S within the flame. From these data, it would appear that the decreased inhibition of NO formation, when SO_2 is added to the fuel in the axial injector study, cannot be attributed to a significant reduction of SO_2. These data do not preclude the possibility that the decreased inhibition effect is due to lower SO_2 concentrations in the regions of the flame important for NO formation via a Zeldovich-type mechanism.

At high air preheat conditions and moderate percent swirl values, an enhancement of NO production was observed for the axial injector studies when SO_2 was added to the fuel. The increase was more significant for the flame with locally substoichiometric conditions. It was also observed that a decrease in the inhibition of NO formation occurred in the radial injector study, when SO_2 was added to the fuel, as overall stoichiometric conditions were approached.

The production of thermal NO may be due to the fixation of molecular oxygen and nitrogen present in the combustion air or to fuel-rich induced prompt NO. Since the prompt NO mechanism is more important in fuel-rich hydrocarbon flames, and since Wendt and Ekmann (1974) report that the inhibition effect of SO_2 on NO formation, via the Zeldovich mechanism, is more significant at high air preheat conditions, it can be inferred that the enhancement of NO production is due to the interaction of fuel sulfur with the prompt NO mechanism. It can also be inferred that a reduced form of SO_2 is important in the interaction, since the enhancement is more pronounced in the flame with locally fuel-rich regions.

The possibility that fuel sulfur may enhance fuel-rich induced prompt NO formation provides an explanation for the results obtained with the axial injector at "zero" air preheat conditions. The fact that the addition of SO_2 to the fuel did not produce as great a decrease in NO emissions as when a smaller amount of SO_2 was added to the air stream may be an indication of a slight increase in the formation of fuel-rich induced prompt NO. However, it is also possible that, with the lower local flame temperatures expected at "zero" air preheat, the inhibition of NO formed via the Zeldovich mechanism is kinetically favored over the enhancement of prompt NO. Therefore, the presence of SO_2 on the fuel side of the flame may promote prompt NO formation while still acting to reduce thermal fixation of molecular oxygen and nitrogen present in the combustion air.

Although the addition of SO_2 to the fuel resulted in an enhancement or inhibition of overall NO formation, which depended upon the local flame stoichiometry and temperature, the addition of SO_2 to the air stream, the fuel-lean side of the flame front, always produced an inhibition of NO formation. The decrease in NO emissions occurred for both the radial and axial injector studies at all operating conditions investigated: "zero" and high air preheats; various percent swirl values; various overall excess air conditions; and for locally fuel-rich or near-stoichiometric flames. It seems reasonable to attribute this inhibition effect to the homogeneous catalysis of free radical recombination reactions by SO_2 (Wendt and Ekmann, 1974). The radicals involved are important in the Zeldovich mechanism or directly affect species which are important. The probable reactions sequence responsible for this behavior is:

$$SO_2 + O + M = SO_3 + M \tag{7.1}$$

$$SO_3 + O = SO_2 + O_2 \tag{7.2}$$

$$H + SO_2 + M = HSO_2 + M \tag{7.3}$$

$$HSO_2 + OH = H_2O + SO_2 \tag{7.4}$$

Even though the inhibition effect of SO_2 on NO formation can be readily explained in terms of the above reactions, it still remains to provide a reasonable explanation of the enhancement effect. It has been postulated that reduced SO_2 species affect the formation of fuel-rich induced prompt NO. The key to prompt NO production is:

$$CH + N_2 \rightarrow HCN + N \tag{7.5}$$

However, production of HCN is only the initial step in prompt NO formation (Haynes et al., 1975). Merryman and Levy (1975) indicate that CN or NH is the principal source of prompt NO; Fenimore (1972) postulated that CN does not directly form NO but forms NH_2, NH, or N, which then are oxidized to form NO.

The decay of HCN to products more likely to directly form NO may be as follows:

$$HCN + H = CN + H_2 \tag{7.6}$$

$$CN + O_2 = OCN + O \tag{7.7}$$

$$CN + CO_2 = OCN + CO \tag{7.8}$$

$$OCN + H = CO + NH \tag{7.9}$$

$$OCN + H_2 = CO + NH_2 \tag{7.10}$$

Studies conducted at Rocketdyne show that OCN is probably the intermediate involved in NO formation from HCN for fuel-lean and fuel-rich conditions.

It appears that for SO_2, or reduced SO_2 species, to enhance prompt NO formation the concentrations of H, H_2, O_2, and CO_2 in the flame must be influenced. Another potential path would be an enhancement of the formation rate of CH, which is the key to prompt NO formation. Results of H_2S combustion studies show an inhibition of H_2 combustion due to the relatively stable SO radical (Sachyan et al., 1967). Since Cullis and Mulcahey (1972) indicate that within 1 millisecond after completion of the primary flame reactions the distribution of sulfur species is the same whether SO_2 or H_2S is added to the flame, the delay in H_2 combustion may also apply to this study. The SO radical becomes more stable with increasing flame temperature (Cullis and Mulcahey, 1972) and may, therefore, be more important at the high air preheat conditions. It can be seen that at least reaction 7.10 would be affected by an increase in H_2.

Bauer et al. (1971) studied the oxidation of CO to CO_2 by SO_2. The following reaction scheme was proposed:

$$2CO + SO_2 = 2CO_2 + S(g) \tag{7.11}$$

Another reaction path also exists for the oxidation of CO to CO_2:

$$SO_2 + SO_2 \rightarrow SO_3 + SO \tag{7.12}$$

$$SO_3 + CO \rightarrow CO_2 + SO_2 \tag{7.13}$$

$$SO + CO \rightarrow CO_2 + S(g) \tag{7.14}$$

Regardless of which reaction mechanism actually takes place, it is immediately apparent that the concentration of CO_2 could be increased. Fuel sulfur may, therefore, increase the formation of the intermediate OCN (reaction 7.8).

Since the enhancement effect is more significant for the locally fuel-rich flame, reduced SO_2 species, such as SO or S, may be of importance. It is known that species such as SH or S are excellent hydrogen abstractors. It might, therefore, be anticipated that an increase in CH formation is caused by their presence. Reactions which might proceed are as follows:

$$CH_3 + S = CH_2 + SH \tag{7.15}$$

$$CH_2 + S = CH + SH \tag{7.16}$$

$$CH_2 + SH = CH + H_2S \quad (7.17)$$

Preliminary kinetic investigations indicate that reaction 7.17 could readily explain the increase in NO formation. The enhancement increased dramatically with increasing temperature.

The ability of S or SH to participate in hydrogen abstraction reactions may also be of importance in considering NO formation from NH or NH_2 species produced in reactions 7.9 and 7.10. Sarofim et al. (1975) indicate that hydrogen abstraction reactions are important in the production of NO from NH_3. It would seem reasonable to also assume the importance of such reactions in the reduction of NH to N atoms or NH_2 to NH and, subsequently, N atoms.

The above discussion has been mainly concerned with indicating how the rates of reactions 7.5 to 7.10 could be affected by fuel sulfur. However, species such as S or SO may provide alternate reaction paths for the formation of NO or directly oxidize species such as N atoms to produce NO. Other reactions which may contribute to the enhancement effect of fuel sulfur on prompt NO are:

$$S + CN \rightarrow SC + N \quad (7.18)$$

$$S + NH \rightarrow SN + H \quad (7.19)$$

$$S + HN \rightarrow SH + N \quad (7.20)$$

$$N + OS \rightarrow NO + S \quad (7.21)$$

$$O + NS \rightarrow ON + S \quad (7.22)$$

The material presented (reactions 7.5 through 7.22) indicates possible ways in which the addition of SO_2 to the fuel could promote the formation of fuel-rich induced prompt NO. The reactions are listed in

Table 7.1; the rate coefficients are presented along with the activation energy for each reaction. For comparative purposes, the rate coefficients are evaluated at 2000 K.

The data for distillate oil turbulent diffusion flames may also be explained by the mechanisms described above. When thiophene was added to the fuel at "zero" air preheat, and when SO_2 was introduced into the air stream at high air preheat, an inhibition of overall NO formation was observed. This inhibition effect can be attributed to the homogeneous catalysis of the recombination of super-equilibrium atoms -- O, OH, H atoms.

Although there are no data at high air preheat conditions for distillate oil doped with thiophene, it might be anticipated that an enhancement effect would be observed. Since fuel-rich regions are likely to occur in sprays, it could be expected that fuel-rich induced prompt NO would be important. Also, SO has been identified in diffusional flames of organic sulfur compounds; the optical spectrum is emitted more strongly in fuel-rich hydrocarbon flames containing sulfur compounds (Cullis and Mulcahey, 1972). With the introduction of species such as SO or S, it is not unreasonable to assume that an enhancement would take place.

1.7-2 Fuel NO

From the data presented in Chapter 5, it can be concluded that the effect of fuel sulfur on fuel nitrogen conversion to NO is a function of local flame temperature. The data also indicated that the interaction with the fuel NO mechanism occurred in fuel-rich regions of the flame.

Table 1.7-1 Summary of Proposed Reactions.

Reaction		$K_f = K_0 T^n \exp[-E_f/RT]$ (=) cm^3/gm-mole-sec				
		K_0	n	E_f (=) Kcal/gm-mole	$K_f\vert_{2000\ K}$	Source
$CH + N_2 \rightarrow HCN + N$	(7.5)	$2.0x10^{13}$	0	48.0	$1.14x10^8$	
$HCN + H = CN + H_2$	(7.6)	$9x10^{13}$	0	21.2	$4.34x10^{11}$	Mulvihill and Philips (1975)
		$9x10^{12}$	0	22.6	$3.05x10^{10}$	Mulvihill and Philips (1975)
$CN + O_2 = OCN + O$	(7.7)	$6x10^{13}$	0	1.67	$3.94x10^{13}$	Mulvihill and Philips (1975)
$CN + CO_2 = OCN + CO$	(7.8)	$3.7x10^{12}$	0	~ 0	$3.7x10^{12}$	Haynes et al. (1975)
$OCN + H = CO + NH$	(7.9)	$2x10^{13}$	0	0	$2x10^{13}$	Mulvihill and Philips (1975)
$OCN + H_2 = CO + NH_2$	(7.10)	--	--	--	--	--
$2CO + SO_2 = 2CO_2 + S_{(g)}$	(7.11)	--	--	--	--	--
$SO_2 + SO_2 \rightarrow SO_3 + SO$	(7.12)	--	--	--	--	--
$SO_3 + CO \rightarrow CO_2 + SO_2$	(7.13)	--	--	--	--	--
$SO + CO \rightarrow CO_2 + S_{(g)}$	(7.14)	--	--	--	--	--

Table 1.7-1 Summary of Proposed Reactions. -- Continued.

Reaction		$K_f=K_0T^n\exp[-E_f/RT]$ (=) cm^3/gm-mole-sec			$K_f\vert_{2000\ K}$	Source
		K_0	n	E_f (=) Kcal/gm-mole		
$CH_3 + S = CH_2 + SH$	(7.15)	6.04×10^{14}	0	29.0	4.06×10^{11}	Estimated
$CH_2 + S = CH + SH$	(7.16)	3.35×10^{14}	0	12.96	1.28×10^{13}	Estimated
$CH_2 + SH = CH + H_2S$	(7.17)	3.21×10^{14}	--	9.79	2.73×10^{13}	Estimated
$S + CN \rightarrow SC + N$	(7.18)	6.31×10^{11}	.5	0	2.82×10^{13}	Benson et al. (1975)
$S + NH \rightarrow SN + H$	(7.19)	6.31×10^{11}	.5	0	2.82×10^{13}	Benson et al. (1975)
$S + HN \rightarrow SH + N$	(7.20)	6.31×10^{11}	.5	8.0	3.77×10^{12}	Benson et al. (1975)
$N + OS \rightarrow NO + S$	(7.21)	6.31×10^{11}	.5	8.0	3.77×10^{12}	Benson et al. (1975)
$O + NS \rightarrow ON + S$	(7.22)	6.31×10^{11}	.5	8.0	3.77×10^{12}	Benson et al. (1975)

At "zero" air preheat conditions, the addition of thiophene to a pyridine-oil fuel mixture had no discernible effect on fuel NO emissions. Although it has already been determined that thiophene does inhibit thermal NO formation in distillate oil turbulent diffusion flames, the scatter in the data does not permit definite conclusions to be drawn concerning the effect of fuel sulfur on fuel NO at "zero" air preheat conditions.

However, at high air preheat conditions, the addition of thiophene to the pyridine-oil fuel mixture did significantly affect fuel nitrogen conversion to fuel NO. The extent of the observed enhancement was a function of the initial atomization of the fuel. Fuel sulfur, introduced as SO_2, was also shown to enhance fuel NO formation in natural gas flames doped with NH_3.

Before considering the ways in which fuel sulfur may interact with the fuel NO mechanism, some comments need to be made concerning the fate of chemically bound fuel nitrogen in flames. In studies conducted by Axworthy (1975) on the pyrolysis products of pyridine, it was found that above 1100°C all of the fuel nitrogen was recovered as HCN. This suggests that at higher temperatures typical in actual combustion processes most of the volatile fuel nitrogen may form HCN before reaching the flame front. These data also indicate that HCN is a likely precursor to formation of fuel NO in flames.

Work by Fenimore (1976) on premixed fuel-rich flames shows "that fuel nitrogen fed as pyridine, and not yet converted to NO or N_2, exists in large part as HCN" (Fenimore, 1976, p. 250). Merryman and Levy (1975) studied flat methane flames doped with pyridine. The presence of CN and NH species was spectroscopically determined. A thermally stable intermediate was produced during oxidation which was rapidly consumed in the O-atom region of the flame; it was postulated that HCN and NH_3 were likely compounds for the intermediate.

Fenimore (1976) also conducted studies of premixed fuel-rich flames doped with NH_3. It was again concluded that the fuel nitrogen not converted to NO or N_2 existed in large past as HCN. Since HCN is manufactured by the partial combustion of rich NH_3-hydrocarbon mixtures, this finding was not unreasonable. De Soete (1975) also studied flat premixed hydrocarbon/oxygen-argon (or helium) flames doped with NH_3. It was determined that the relative importance of HCN as an intermediate in the fuel NO mechanism increased according to the following sequence of primary fuel nitrogen compounds: ammonia, cyanogen, and molecular nitrogen.

The above discussion indicates the feasibility of considering the possible interactions of fuel sulfur with mechanisms producing NO from HCN or NH_3. It has already been stated that the SO radical is present in fuel-rich hydrocarbon flames containing sulfur compounds. Experimental evidence has also been presented (section 1.5-2) that indicates SO_2, or a reduced form of SO_2, produces similar increases in fuel NO formation as fuel sulfur introduced as thiophene. Since HCN and sulfur species such as SO_2, SO, and S are probably present in the flame, it would appear reasonable to assume that similar interactions as were noted for prompt

NO should be applicable in explaining the enhancement of fuel NO by fuel sulfur (see reactions 7.6 through 7.22 and discussion in section 1.7-1).

Further insight into how fuel sulfur interacts with fuel NO formation is provided by examining the fuel nitrogen data of this study in terms of a simplistic reaction mechanism for NO formation. Fenimore (1972) proposed the following reaction scheme:

$$\mathrm{NI} + \mathrm{Ox} \xrightarrow{K_1} \ldots \rightarrow \mathrm{NO} + \tag{7.23}$$

$$\mathrm{NO} + \mathrm{NI} \xrightarrow{K_2} \ldots \rightarrow \mathrm{N_2} + \tag{7.24}$$

In this model, nitrogen compounds are assumed to yield nitrogeneous intermediates (NI) which react with oxidants (Ox) to form NO. The same or similar intermediates also participate in reactions which reduce NO to N_2.

Using the same assumptions as Fenimore, the following equation may be developed:

$$[\mathrm{NO}] = \alpha\{1 - \exp(-\frac{[\mathrm{NO}] + [\mathrm{N}]}{2\alpha})\} \tag{7.25}$$

where

$[N]$ = nitrogen compound added expressed as ppm NO if all N formed NO;

$[NO]$ = ppm NO actually formed from the additive; and

$\alpha = (K_1/K_2)[Ox]$, a constant.

Fenimore (1976) indicates that the local value of α remains constant through a considerable thickness of gas.

Calculations show that when thiophene is added to the pyridine-oil fuel mixture (315°F air preheat, 15.0% excess air) the value of α increases from 470 to 600 ppm. The addition of SO_2 to the ammonia-natural gas mixture (430°F air preheat, 15.0% excess air) also causes an increase in the value of α -- from 166 to 315. Since α is directly proportional to the local oxidant level, it would appear that fuel sulfur acts to increase the oxidant levels within the fuel. Although [Ox] has been tentatively identified with the concentration of O-atoms or O_2 (de Soete, 1974), it is known that SO_2 reduces O-atom concentrations within the flame. It would appear more reasonable to assume that reduced sulfur species such as S or SO, which are oxidizing species, are responsible for the observed increase in the values of α.

Such a conclusion would be consistent with the hydrogen abstraction reactions attributed to sulfur species such as S or SH. It was observed that the conversion of NH_3 to NO increased from 11.4% without fuel sulfur to 20.4% when SO_2 was added to the fuel. If reactions such as:

$$NH_m + S = NH_{m-1} + SH \tag{7.26}$$

or

$$NH_m + SH = NH_{m-1} + H_2S \tag{7.27}$$

were taking place, the increase in species such as NH or N, which are readily oxidized to NO, could readily explain the increase in conversion observed. It should be noted that reactions 7.26 and 7.27 are oxidation reactions.

The increase in local oxidant levels could also be attributed to the SO radical which is more stable at the higher air preheat conditions. It is reasonable to assume that the SO radical could directly oxidize N atoms to NO (see reaction 7.21) and, therefore, also enhance the formation of NO. The oxidation of species such as NH_m by S or SH might also influence the rate of NO formation by lowering concentrations of species which participate in reactions as the following to reduce NO to N_2:

$$NH_2 + NO = N_2 + H_2O \tag{7.28}$$

$$NH + NO = N_2 + OH \tag{7.29}$$

By examining fuel nitrogen conversion to NO in terms of a simplistic reaction scheme, information has been gained concerning the effect of fuel sulfur on fuel NO formation. Fuel sulfur introduces oxidizing agents which are not already present in the flame. These oxidizing species may participate in hydrogen abstraction reactions or act to directly oxidize nitrogeneous species to NO. The participation of SO_2 or SO in oxidizing CO to CO_2 may also be of importance in determining the enhancement effect of fuel sulfur (see reactions 7.11 to 7.14 and reaction 7.8).

1.8 Conclusions

The addition of SO_2 to turbulent gaseous diffusion flames may enhance or inhibit thermal NO formation. The particular effect observed and the extent to which it occurs is dependent upon the local flame stoichiometry and the local flame temperature.

Inhibition of thermal NO formation was observed for flames with rapid mixing between fuel and air streams. The introduction of SO_2 into the air stream, i.e., the fuel-lean side of the flame front, also produced an inhibition of thermal NO formation. This particular effect can be attributed to the homogeneous catalysis of free radical recombination reactions, in particular super-equilibrium oxygen atoms, by SO_2.

The addition of SO_2 to the fuel produced an enhancement of NO formation for flames with poor mixing between fuel and air streams. The effect was observed at high air preheat conditions and was more significant for the flame with locally substoichiometric regions within the flame. The enhancement can be attributed to the interaction of SO_2 and reduced SO_2 species, such as SO and S, with the fuel-rich induced prompt NO mechanism.

The addition of thiophene, to simulate fuel sulfur, to turbulent distillate oil diffusion flames resulted in an inhibition of thermal NO formation at "zero" air preheat conditions. Again, the inhibition can be attributed to the homogeneous catalysis of super-equilibrium oxygen atom recombination reactions by SO_2.

The presence of thiophene in turbulent distillate oil diffusion flames doped with pyridine indicated that fuel sulfur had no discernible effect on fuel NO formation at "zero" air preheat conditions.

An enhancement of fuel NO formation was observed at high air preheat conditions when thiophene was added to the pyridine-distillate oil mixture. The extent of the increase varied from 10 percent to 20 percent in less fuel-rich flames to 30 percent to 50 percent in more fuel-rich flames. The enhancement effect can be attributed to the interaction of SO_2 and reduced SO_2 species, such as SO and S, with the mechanism for NO formation from HCN. The apparent local oxidant level increases with the addition of fuel sulfur. Oxidizing agents resulting from fuel sulfur -- SO_2, SO, and S -- may reduce nitrogeneous intermediates to species readily oxidized to NO or directly oxidize nitrogeneous species to form NO.

The addition of SO_2 to a turbulent gaseous diffusion flame doped with NH_3 resulted in a significant enhancement of fuel NO formation at high air preheat conditions. The increase can be attributed in part to the ability of reduced sulfur species to participate in hydrogen abstraction reactions important in the formation of NO from NH_3.

The conversion of fuel nitrogen to NO decreases as the weight percent nitrogen in the fuel increases; the actual NO emissions increase with increasing weight percent nitrogen in the fuel. Conversion of fuel nitrogen to fuel NO demonstrates a strong dependence on excess air conditions. The conversion to fuel NO is also a function of the atomization characteristics of the oil nozzle which affect the initial mixing between the fuel and the air stream. The resulting changes in local oxidant levels can significantly change levels of conversion.

The experimental results are especially significant from a practical point of view. Fuel desulfurization may have an adverse effect on thermal NO emissions for systems with rapid mixing between fuel and air streams. For systems with relatively poor mixing between the fuel and the air streams, fuel desulfurization may have a beneficial effect on thermal NO emissions.

However, of more importance are the results concerning possible interactions between fuel sulfur and fuel NO formation. Most fuels containing chemically bound nitrogen also contain chemically bound sulfur. Staged combustion is widely employed as an abatement technique for decreasing fuel NO formation. The experimental results of this study indicate that for fuel-rich flame conditions fuel sulfur can enhance fuel NO production. It can, therefore, be seen that fuel desulfurization should have decidedly beneficial effect on fuel NO emissions from staged oil combustion processes employing significant levels of air preheat.

The experimental results obtained in this study suggest several areas of future research on fundamental and practical levels. Three general areas which should be particularly important are:

1. Kinetic mechanisms: This work established that fuel sulfur could enhance prompt NO and fuel NO formation. The effect was influenced by local flame stoichiometry and temperature. Laboratory studies need to be conducted to determine the mechanisms for this interaction. Theoretical studies should be conducted in conjunction with the experimental work to test hypotheses and provide further insight into the processes. Questions which should be answered are: How does the effect depend on sulfur concentration? What stoichiometries reduce the interaction? At what flame temperatures does the interaction become important? Which sulfur species are involved?

2. Turbulence: To apply the results of research concerning kinetic mechanisms to practical combustion processes, turbulence must be accounted for. However, there is a lack of data about the role of turbulence in flames. Fundamental research needs to be undertaken to characterize the important features of turbulence as applied to combustion processes. Questions which would hopefully be answered are: How can turbulence be quantitatively related to the mixing phenomenon occurring in a flame? How does turbulence influence kinetic mechanisms in the flame?

3. Pilot combustor studies: The present research was concerned with fuel sulfur interactions on thermal and fuel NO formation in single-stage combustion processes. The possible interactions of fuel sulfur with fuel NO formation under staged combustion conditions should also be investigated to determine whether similar effects would be observed. Studies could also be conducted in conjunction with the fundamental research proposed above. The results could be used to evaluate turbulence models or to calibrate theoretical models. Such investigations could hopefully provide the bridge between laboratory flame studies and practical combustion processes.

1.9 References for Section 1

Appleton, J. P., and J. B. Heywood. "The Effects of Imperfect Fuel-Air Mixing in a Burner on NO Formation from Nitrogen in the Air and the Fuel." Fourteenth Symposium (International) on Combustion, The Combustion Institute, Pittsburgh, Pennsylvania (1973).

Axworthy, A. E. "Chemistry and Kinetics of Fuel Nitrogen Conversion to Nitric Oxide." AIChE Symposium Series No. 148, 71 (1975).

Bartok, W., A. R. Crawford, A. R. Cunningham, H. J. Hall, E. H. Manny, and A. Skopp. "Systems Study of Nitrogen Oxide Control Methods for Stationary Sources." Research Engineering Company, Final Report - Volume II, NAPCA (Now EPA) No. APTD 1286 (NTIS PB192-789) (1969).

Bartok, W., V. S. Engleman, R. Goldstein, and E. G. Del Valle. "Basic Kinetic Studies and Modeling of NO Formation in Combustion Processes." AIChE Symposium Series No. 126, 68 (1972).

Bauer, S. H., P. Jeffers, A. Lifschitz, and B. P. Yadava. "Reaction Between CO and SO_2 at Elevated Temperatures: A Shock-Tube Investigation." Thirteenth Symposium (International) on Combustion, The Combustion Institute, Pittsburgh, Pennsylvania (1971).

Benson, S. W., D. M. Golden, R. W. Lawrence, R. Shaw, and R. W. Woolfolk. "Estimating the Kinetics of Combustion: Including Reactions Involving Oxides of Nitrogen and Sulfur." Stanford Research Distitute, Pub. No. EPA-600/2-75-019 (NTIS PB 245-054) (1975).

Bowman, C. T. "Investigation of Nitric Oxide Formation Kinetics in Combustion Processes: The Hydrogen-Oxygen-Nitrogen Reaction." Combust. Sci. Technol., 3 (1971).

Bowman, C. T. "Kinetics of Nitric Oxide Formation in Combustion Processes." Fourteenth Symposium (International) on Combustion, The Combustion Institute, Pittsburgh, Pennsylvania (1973).

Bowman, D. T. "Non-Equilibrium Radical Concentrations in Shock Initiated Methane Oxidation." Fifteenth Symposium (International) on Combustion, The Combustion Institute, Pittsburgh, Pennsylvania (1975).

Bowman, C. T., and D. J. Seery. "Investigation of NO Formation Kinetics in Combustion Processes: The Methane-Oxygen-Nitrogen Reaction." Emissions from Continuous Combustion Systems, edited by W. Cornelius and W. G. Agnew, Plenum (1972).

Cullis, C. F., and M. F. R. Mulcahey. "The Kinetics of Combustion of Gaseous Sulfur Compounds." Comb. Flame, 18 (1972).

de Soete, G. G. "Formation and Decomposition of Nitric Oxide in Combustion Products of Hydrocarbon Flames." Paper presented at the AFRC American Flame Days, Chicago, Illinois (1972).

de Soete, G. G. "Overall Reaction Rates of NO and N_2 Formation from Fuel Nitrogen." Fifteenth Symposium (International) on Combustion, The Combustion Institute, Pittsburgh, Pennsylvania (1975).

Durie, R. A., G. M. Johnson, and M. Y. Smith. "The Effect of Sulfur Dioxide on Hydrogen-Atom Recombination in the Burnt Gas of Premixed Fuel-Rich Propane-Oxygen-Nitrogen Flames." Comb. Flame, 17 (1971).

Duxbury, J., and N. H. Pratt. "A Shock Tube Study of NO Kinetics in the Presence of H_2 and Fuel-N." Fifteenth Symposium (International) on Combustion, The Combustion Institute, Pittsburgh, Pennsylvania (1975).

Ekmann, J. M. M. S. Thesis, Department of Chemical Engineering, University of Arizona, Tucson (1974).

Engleman, V. S. "Survey and Evaluation of Kinetic Data on Reactions in Methane/Air Combustion." Exxon Research and Engineering Co., Pub. No. EPA-600/2-76-003 (NTIS PB 248-139) (1976).

Fenimore, C. P. "Formation of Nitric Oxide in Premixed Hydrocarbon Flames." Thirteenth Symposium (International) on Combustion, The Combustion Institute, Pittsburgh, Pennsylvania (1971).

Fenimore, C. P. "Formation of Nitric Oxide from Fuel Nitrogen in Ethylene Flames." Comb. Flame, 19 (1972).

Fenimore, C. P. "Reactions of Fuel-Nitrogen in Rich Flame Gases." Comb. Flame, 26 (1976).

Flagan, R. C., S. Galant, and J. P. Appleton. "Rate Constrained Partial Equilibrium Models for the Formation of Nitric Oxide from Organic Fuel Nitrogen." Comb. Flame, 22 (1974).

Haynes, B. S., D. Iverach, and N. Y. Kirov. "The Behavior of Nitrogen Species in Fuel Rich Hydrocarbon Flames." Fifteenth Symposium (International) on Combustion, The Combustion Institute, Pittsburgh, Pennsylvania (1975).

Iverach, D., K. S. Basden, and N. Y. Kirov. "Formation of Nitric Oxide in Fuel-Lean and Fuel-Rich Flames." Fourteenth Symposium (International) on Combustion, The Combustion Institute, Pittsburgh, Pennsylvania (1973).

Levy, A., and E. L. Merryman. "The Microstructure of Hydrogen Sulphide Flames." Comb. Flame, 9 (1965).

Malte, P. C., and D. T. Pratt. "Measurement of Atomic Oxygen and Nitrogen Oxides in Jet-Stirred Combustion." Fifteenth Symposium (International) on Combustion, The Combustion Institute, Pittsburgh, Pennsylvania (1975).

Martin, G. B., and E. E. Berkau. "An Investigation of the Conversion of Various Fuel Nitrogen Compounds to NO in Oil Combustion." AIChE Symposium Series No. 126, 68 (1972).

Martin, G. B., D. W. Pershing, and E. E. Berkau. "Effects of Fuel Additives on Air Pollutant Emissions from Distillate-Oil-Fired Furnaces." Environmental Protecton Agency, Office of Air Programs, Pub. No. AP-87 (NTIS PB 213-630) (1971).

Merryman, E. L., and A. Levy. "Kinetics of Sulfur-Oxide Formation in Flames: II. Low Pressure H_2S Flames." J. Air Poll. Control Assoc., 17 (1967).

Merryman, E. L. "Nitrogen Oxide Formation in Flames: The Roles of NO_2 and Fuel Nitrogen." Fifteenth Symposium (International) on Combustion, The Combustion Institute, Pittsburgh, Pennsylvania (1975).

Mitchell, R. E., and A. F. Sarofim. "Nitrogen Oxide Formation in Laminar Methane-Air Diffusion Flames." Paper presented at the Fall Meeting, Western States Section, The Combustion Institute, Palo Alto, California (1975).

Mulvihill, J. N., and L. F. Philips. "Breakdown of Cyanogen in Fuel-Rich $H_2/N_2/O_2$ Flames." Fifteenth Symposium (International) on Combustion, The Combustion Institute, Pittsburgh, Pennsylvania (1975).

Myerson, A. L. "The Reduction of Nitric Oxide in Simulated Combustion Effluents by Hydrocarbon-Oxygen Mixtures." Fifteenth Symposium (International) on Combustion, The Combustion Institute, Pittsburgh, Pennsylvania (1975).

Newbold, F. R., and N. R. Amundson. "An Analysis of Chemical Reactor Stability and Control -- XV: The Multicomponent Spray Reactor." Chem. Eng. Sci., 28 (1973).

Onuma, Y., and M. Ogasawara. "Studies on the Structure of a Spray Combustion Flame." Fifteenth Symposium (International) on Combustion, The Combustion Institute, Pittsburgh, Pennsylvania (1975).

Perry, R. H., C. H. Chilton, and S. D. Kirkpatrick (eds.). Perry's Chemical Engineers' Handbook, 4th ed., McGraw-Hill Book Company, New York (1963).

Pershing, D. W. Ph. D. Dissertation, Department of Chemical Engineering, University of Arizona, Tucson (1976).

Pershing, D. W., and E. E. Berkau. "The Chemistry of NO_x Formation and Control through Combustion Modifications." Pollution Control and Energy Needs, edited by R. M. Jimeson and R. S. Spindt, American Chemical Society, Washington, D. C. (1973).

Pershing, D. W., G. B. Martin, and E. E. Berkau. "Influence of Design Variables on the Production of Thermal and Fuel NO from Residual Oil and Coal Combustion." AIChE Symposium Series No. 148, 71 (1975).

Pershing, D. W., and J. O. L. Wendt. "Pollutant Control through Staged Combustion of Pulverized Coal." U. S. ERDA Report No. 1817-2, U. S. ERDA Technical Information Center, Oak Ridge, Tennessee (1976).

Sachyan, G. A., Y. M. Gershenzon, and A. B. Nalbandyan. "Multistage Nature of Combustion in Dilute Hydrogen Sulfide Flames." Dokl. Aked. Nauk SSSR, 175 (1967) [English version, 175 (1967)].

Sarofim, A. F., and R. C. Flagan. "Nitrogen Oxide Control Techniques," Air Quality and Stationary Source Emission Control. A Report by the Commission on National Resources, National Academy of Sciences, National Academy of Engineering, National Research Council, Serial No. 94-4, U. S. Government Printing Office (1975).

Sarofim, A. F., and J. H. Pohl. "Kinetics of Nitric Oxide Formation in Premixed Laminar Flames." Fourteenth Symposium (International) on Combustion, The Combustion Institute, Pittsburgh, Pennsylvania (1973).

Sarofim, A. F., G. C. Williams, M. Modell, and S. M. Slater. "Conversion of Fuel Nitrogen to Nitric Oxide in Premixed and Diffusion Flames." AIChE Symposium Series No. 148, 71 (1975).

Satterfield, C. N., M. Modell, and J. F. Mayer. "Interactions between Catalytic Hydrodesulfurization of Thiophene and Hydrodenitrogenation of Pyridine." AIChE J., 21 (1975).

Sternling, C. V., and J. O. L. Wendt. "On the Oxidation of Fuel Nitrogen in a Diffusion Flame." AIChE J., 20 (1974).

Turner, D. W., R. L. Andrews, and C. W. Siegmund. "Influence of Combustion Modification and Fuel Nitrogen Content on Nitric Oxides Emissions from Fuel Oil Combustion." AIChE Symposium Series No. 126, 68 (1972).

Wendt, J. O. L., and J. M. Ekmann. "Catalytic Inhibition of Nitrogen Oxide Formation by Sulfur Dioxide." Paper presented at 67th Annual Meeting AIChE, Washington, D. C. (1974) [Session 31, paper No. 310].

Wendt, J. O. L. "Effect of Fuel Sulfur Species on Nitrogen Oxide Emissions from Premixed Flames." Comb. Flame, 25 (1975).

Wendt, J. O. L., and C. V. Sternling. "Catalysis of SO_2 Oxidation by Nitrogen Oxides." Comb. Flame, 21 (1974).

Zeldovich, Y. B., P. Y. Sadovnikov, and D. A. Frank-Kamenetskii. "Oxidation on Nitrogen in Combustion." Academy of Sciences of USSR, Institute of Chemical Physics, Moscow-Leningrad, translated by M. Shelef (1947).

2. INTERACTIONS OF FUEL SULFUR AND FUEL NITROGEN IN FUEL RICH PREMIXED LAMINAR FLAMES

2.1 Purpose and Scope

The abatement of nitrogen oxide emissions by combustion modification is an important national problem. Chemically bound nitrogen is the main contributor to NO_x emissions from dirty fuels and so knowledge of mechanisms forming this fuel NO_x is important.

Most fuels containing nitrogen compounds also contain sulfur species. However, previous work on fuel NO_x formation mechanisms has neglected the possible effects of sulfur on these emissions. Therefore, there exists the need for studies on fuel NO_x mechanisms in the presence of fuel sulfur.

This work is part of a larger project in which SO_x/NO_x interactions in turbulent diffusion flames were investigated (see Section 1). Results from that work indicated that sulfur additives may have an important enhancement effect on fuel NO_x under fuel-rich conditions. Thus, this phase deals with an investigation of SO_x/NO_x interactions in a premixed environment focusing primarily on fuel-rich combustion of methane. Its purpose was to better define the combustion conditions at which these interactions occurred. In addition, insight was gained on the importance of fuel quality, that is, the influence of sulfur content of a fuel on the effectiveness of combustion modifications. Fuel-rich combustion of dirty fuels is a proven technique for achieving low fuel NO_x.

Therefore, the role of sulfur on the effectiveness of this type of combustion modification is of great interest.

This section of the report describes in detail the design and operation of a versatile, premixed, flat-flame burner system. Measurement of flame temperature by sodium D-line reversal, and sampling and analysis interfences are discussed in detail.

It is hoped that this study will provide some indications of the mechanisms necessary to explain the observed fuel sulfur/fuel nitrogen phenomenon. No attempt was made to analyze for intermediate species that may be important for a complete understanding of the reactions. However, the trends and parameters as discussed in this study may serve as a basis for future studies and also provide enough understanding to interpret already available data.

2.2 Background

In this section, current theories on the fate of fuel nitrogen and fuel sulfur are reviewed, in the light of the objectives of this study. Available evidence indicates the importance of addressing the formation of nitric oxide from chemically bound nitrogen. Pershing, Martin, and Berkau (1975) burned a low-sulfur residual oil in argon/oxygen and inferred that about half of the total NO measured under normal conditions was the result of fuel nitrogen oxidation. Pershing and Wendt (1977) showed that over 80% of total NO emissions from pulverized coal combustion resulted from fuel nitrogen oxidation, and that this conclusion held for a wide variety of coal types and combustion configurations.

Fenimore (1971) added pyridine to a premixed ethylene/oxygen/inert flame of 0.58 stoichiometric ratio. Whether argon or molecular nitrogen was substituted for the inert, the amount of nitric oxide formed was essentially the same, and exceeded the concentration appropriate to the equilibrium $N_2 + O_2 = 2NO$. He concluded that the formation of NO was independent of N_2 for this particular gas mixture and temperature, and depended solely on the fuel nitrogen content.

Experimental studies have indicated, to some extent, those factors which influence conversion of fuel nitrogen to NO. Various investigators have observed that the conversion of fuel nitrogen is independent of the additive type (Fenimore, 1971; DeSoete, 1973; Sarofim et al., 1975). Under lean conditions, fuel nitrogen present in amounts less than 1% is largely converted to NO (Fenimore, 1971). Under fuel-rich conditions, only part of combined nitrogen in the fuel is oxidized to NO and the rest is converted to N_2. The yield of NO is increased when: the concentration of combined nitrogen is low, the flame becomes leaner, and the temperature is high (Morley, 1976).

Although significant progress has been made recently in identifying the mechanism and kinetics of fuel nitrogen conversion to nitric oxide, there are still gaps in the understanding of the processes involved. Studies on premixed flames show that HCN is the dominant nitrogen compound other than NO which survives the primary reaction zone under fuel-rich conditions. This is supported by the data of DeSoete (1975) on the profiles of bound nitrogen species in premixed, rich ethylene flames seeded with C_2N_2, NO, ammonia, and various amines; and that of Haynes (1975) for premixed flames seeded with pyridine, ammonia, and nitric oxide. Fenimore (1976) also reports HCN as the principal bound nitrogen compound other than NO in the primary reaction zone of premixed flames of ethylene and methane to which ammonia and pyridine had been added.

In the post-flame gases of rich hydrocarbon flames, work by Haynes, Iverach, and Kirov (1975) led to the identification of cyano (CN) and amine (NH_i) species as well as nitric oxide. Thus, it is generally argued (Haynes, 1977; DeSoete, 1975) that, since the final products of fuel nitrogen in flames is either N_2 or NO, the amine species is the intermediate nitrogen radical that reacts with either NO to form N_2 or with an oxidizing radical, perhaps OH, to form NO. The scheme for fuel nitrogen conversion is presented as

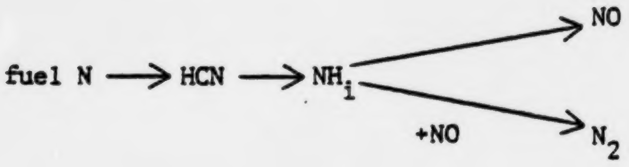

Although oxidation of chemically bound sulfur in the fuel can result in significant sulfur oxide emissions, there is little or no data concerning the pertinent mechanisms involved. The combustion of H_2S has been studied extensively (Levy and Merryman, 1965; Merryman and Levy, 1967; Sachyan, Gershenzon, and Nalbandyan, 1967). There is good agreement on the mechanisms involved in forming SO_2 from H_2S, and on the sulfur species present at different stages of the combustion process. The limited data available on combustion of organic sulfur compounds indicate the presence of sulfur species identified in the combustion of H_2S

(Cullis and Mulcahey, 1972). Due to the general lack of data, it would appear necessary to treat bound sulfur in the fuel as if it were H_2S to analyze the possible interactions with NO formation. Furthermore, there is evidence (Cullis and Mulcahey, 1972) that sulfur species are equilibrated under fuel-rich conditions. Intermediate products are SO, S, and SH. Addition of SO_2 to a fuel to simulate sulfur will produce a distribution of intermediates not very different from those produced using H_2S, especially in the post-primary reaction zone.

Wendt and Sternling (1973) suggested that oxidation of sulfur in flames could affect the nitrogen oxidation reactions. Indeed, in premixed flames with molecular nitrogen present, an inhibition of thermal NO formation was observed by Wendt and Ekmann (1975) for high levels of SO_2 or H_2S in lean mixtures. An enhancement of "prompt NO" formation in rich hydrocarbon flames at low levels of sulfur and high flame temperatures was noted by DeSoete (1975). The discrepancies in these data remain to be resolved.

Studies concerning fuel sulfur and fuel nitrogen are sparse. DeSoete (1975) added both NO and NH_3 to $CH_4/O_2/Ar$ flames containing both SO_2 and H_2S to investigate the influence of sulfur compounds on fuel NO formation. He found that the influence of sulfur compounds on fuel NO depends upon the stoichiometric ratio. For fuel-rich mixtures, the presence of H_2S enhances fuel NO emissions for both NO and NH_3. A similar effect, but less pronounced, was noted for SO_2 as the sulfur additive. In stoichiometric mixtures, there was no effect. For lean mixtures, the presence of sulfur inhibited the formation of fuel NO.

Remaining problems to be solved are: 1) Can DeSoete's results be reproduced with another fuel nitrogen compound? 2) How does the amount of fuel nitrogen additive affect the SO_x/NO_x interactions? 3) What influence do various sulfur levels have on the effect? 4) How important is temperature on the fuel NO_x emissions? The research reported herein addresses these problems.

2.3 Hardware

2.3.1 Burner System

Two burner designs were tested for these premixed, flat-flame studies. The first design, decribed by Morcomb (1977) was unsatisfactory because it did not yield sufficiently flat profiles of NO/NO_x across its diameter. The peak-to-edge measurements differed as much as 15 ppm. Unless sampling followed the centerline precisely, the data were not reproducible.

The second design freed the centerline sampling region of edge effects. The NO/NO_x profiles across its 5 cm diameter grid area indicated flat regions within ± 1 cm of the centerline. Variations in the readings differed as little as 1 ppm. Details can also be found in Morcomb (1977).

Figure 2.3-1 shows the final configuration of the burner system. The surrounding quartz chimney was 60 cm high and 15 cm in diameter. Its inside surface was purged with nitrogen to prevent soot deposition during fuel-rich studies. This was important because the soot could interfere with the optical temperature measurement technique described in Section 2.5. A coating of soot decreased the light transmission through the chimney, making temperature readings erroneous. The nitrogen purge also served to keep water from condensing in the cooler bottom portion of the quartz chimney. A film of water made sampling height difficult to

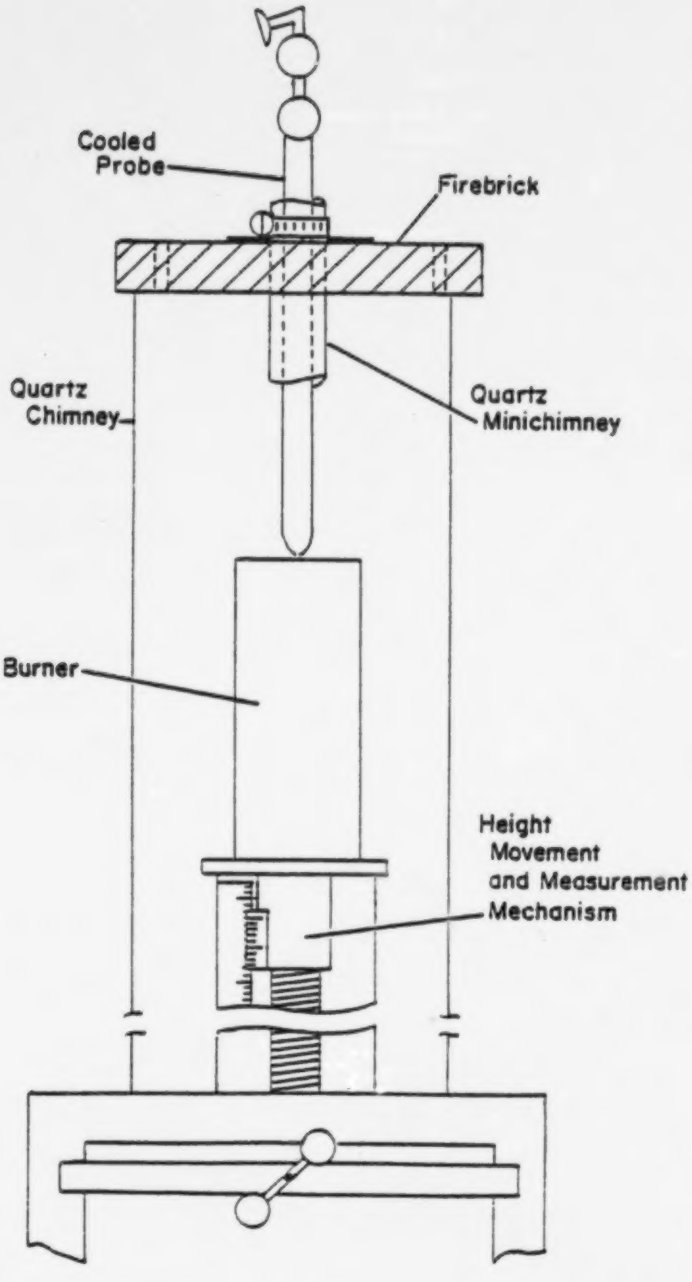
Cooled Probe
Firebrick
Quartz Chimney
Quartz Minichimney
Burner
Height Movement and Measurement Mechanism

Figure 2.3-1 Schematic of Burner and Position of Probe.

read from the vernier scale attached to the burner support. The nitrogen purge, plus much of the exhaust flow, exited the burner system through a series of 10, 6 mm diameter holes in the firebrick. The holes were arranged in a circular pattern just inside the edge of the quartz chimney.

The burner moved vertically on its support, allowing 15 cm of sampling height through the flame. To reach additional heights, the sampling probe could be moved upward to a maximum of 28 cm. At 20 cm, the probe entered the minichimney. This was a 13 cm length of 2.5 cm diameter quartz tubing supported by the firebrick so that 5.7 cm of its length was exposed below the brick. The minichimney extended the range of sampling without allowing dilution from the surrounding air.

In its position as indicated in Figure 2.3-1, the minichimney had no effect on the NO readings. Passage of the probe to sampling heights within the minichimney did not produce discontinuities in the nitric oxide profiles.

2.3-2 Sampling and Analysis Systems

Sampling from the flame was accomplished by hot and cooled quartz probes. Figure 2.3-2 is a drawing of the hot probe. The exact taper for the tip as indicated in the figure was not mandatory, nor was the tip opening precisely 1.5 mm. Indeed, after frequent use in the hot combustion gases, the tip of the probe became crusty white. The tip could be reformed, but the opening varied from 1 to 2 mm. The sample line, 1/4 in. O.D. Teflon, attached to the probe via a ball and socket arrangement. The quartz socket was fused to the 5 mm O.D. tubing at

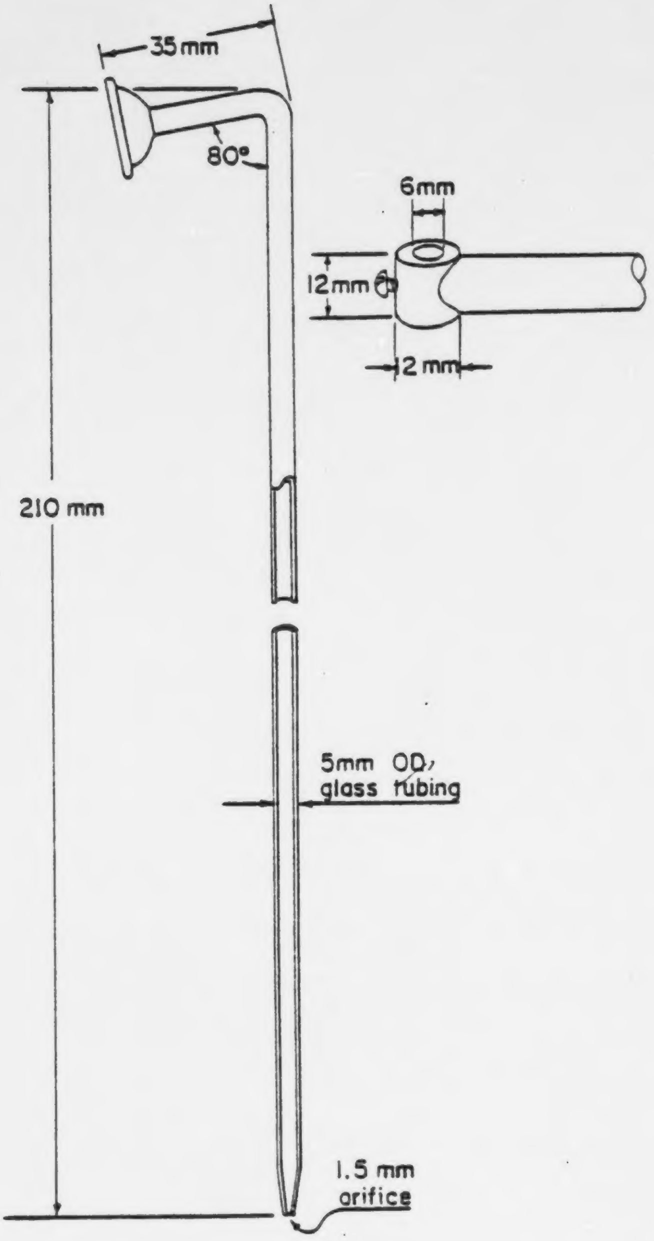
35mm
80°
6mm
12mm
12 mm
210 mm
5mm OD,
glass tubing
1.5 mm
orifice

Figure 2.3-2 Schematic of Hot Quartz Probe and Probe Holder.

approximately an 80° angle to encourage any water that might collect to drain into the sample line. The stem of the Pyrex ball was reduced until it fitted snugly inside the Teflon line. This joint was then sealed with silicon rubber sealer. The ball and socket arrangement was held firmly together with a Thomas No. 12 clamp. Stopcock grease on both parts improved the sealing.

During sampling in fuel-rich flames, the hot quartz probe collected a layer of soot on its outside and inside surfaces. To remove this layer, the probe was held over a Bunsen burner. A stream of air blown through the probe oxidized the soot, and also forced dislodged particles out of the tubing.

The hot probe was supported by an annular steel cylinder 12 mm long. The probe slid into the 6 mm O.D. center, and was held in place by a screw. For cushioning, asbestos string was wrapped around the probe. The support was positioned in the upper 6 cm of the probe.

Figure 2.3-3 is a diagram of the cooled quartz probe. It was designed to be the same length as the hot probe. Indeed, the cooled probe was the hot probe surrounded by a quartz cooling jacket.

Sample entered through a 1.5 mm opening at the cooled probe tip into a 4 mm O.D. quartz tube. This inner tube was sealed to the outermost 12 mm O.D. tube. The sample gases exited through a ball and socket arrangement identical to that of the hot probe.

The cooling jacket was formed from 8 and 12 mm O.D. tubes. Water entered through a ball and socket joint into the inner 8 mm O.D. tube, circulated to the tip, and exited through the 12 mm O.D. tube. The stems

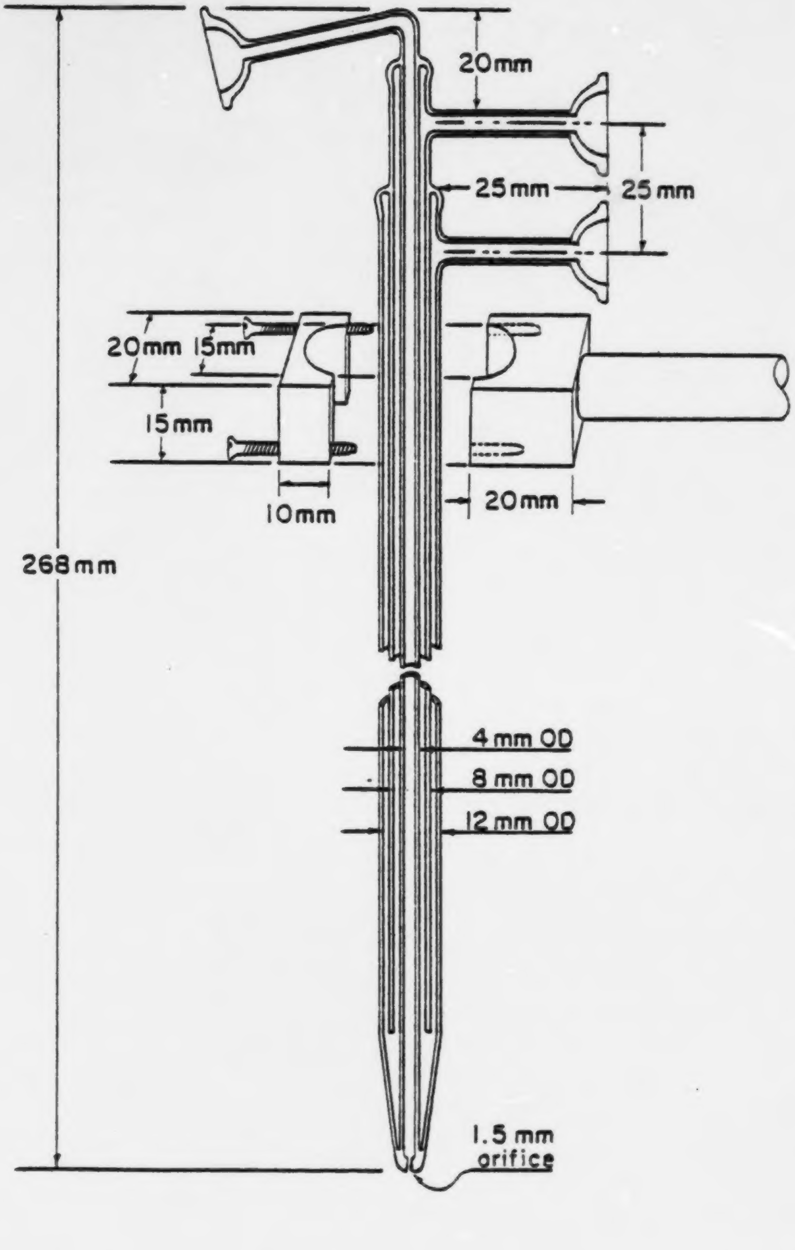
20mm
25mm
25mm
20mm
15mm
15mm
10mm
20mm
268mm
4 mm OD
8 mm OD
12 mm OD
1.5 mm orifice

Figure 2.3-3 Schematic of Water Cooled Quartz Sampling Probe and Its Holder.

of the Pyrex balls on the cooling water ports were reduced to fit inside 3/8 in. O.D. Tygon line. The Tygon tubing was pushed onto the stems and held with wire.

The cooling water rate was set by inspection. When the cooled probe was in the flame, its tip was watched for the formation of bubbles. The water rate was adjusted until the bubbles no longer appeared. The average rate was 3.5 l/min. Trials showed that deviations from this average did not affect the sample readings.

Even in fuel-rich studies, soot deposition was not a problem with the cooled probe. However, sulfur coated the inner surfaces of the 4 mm tube. Carbon disulfide was a convenient reagent for dissolving this coating.

For support, the cooled probe was clamped between two blocks of aluminum, forming a 15 mm diameter hole when together. For cushioning and ensuring a firm press, asbestos string was wrapped around the probe. A shield of asbestos was placed below the aluminum support to prevent fire damage to the metal.

After being sampled from the flame, the gases entered the rest of the analysis system as shown in Figure 2.3-4. Water from the sample collected in a 250 ml flask immersed in an ice bath. A Nupro S.S. inline filter casing filled with glass wool removed particles of soot and sulfur which would possibly clog the sample rotameter. This Fisher-Porter rotameter did not actually control the flow, but indicated variations in the sample flow due to probe and filter clogging. Under normal operation, the flow regulated at 1.3 l/min. Next, any minute particles were removed from the sample gases by a 7 micron Nupro S.S. inline filter. The

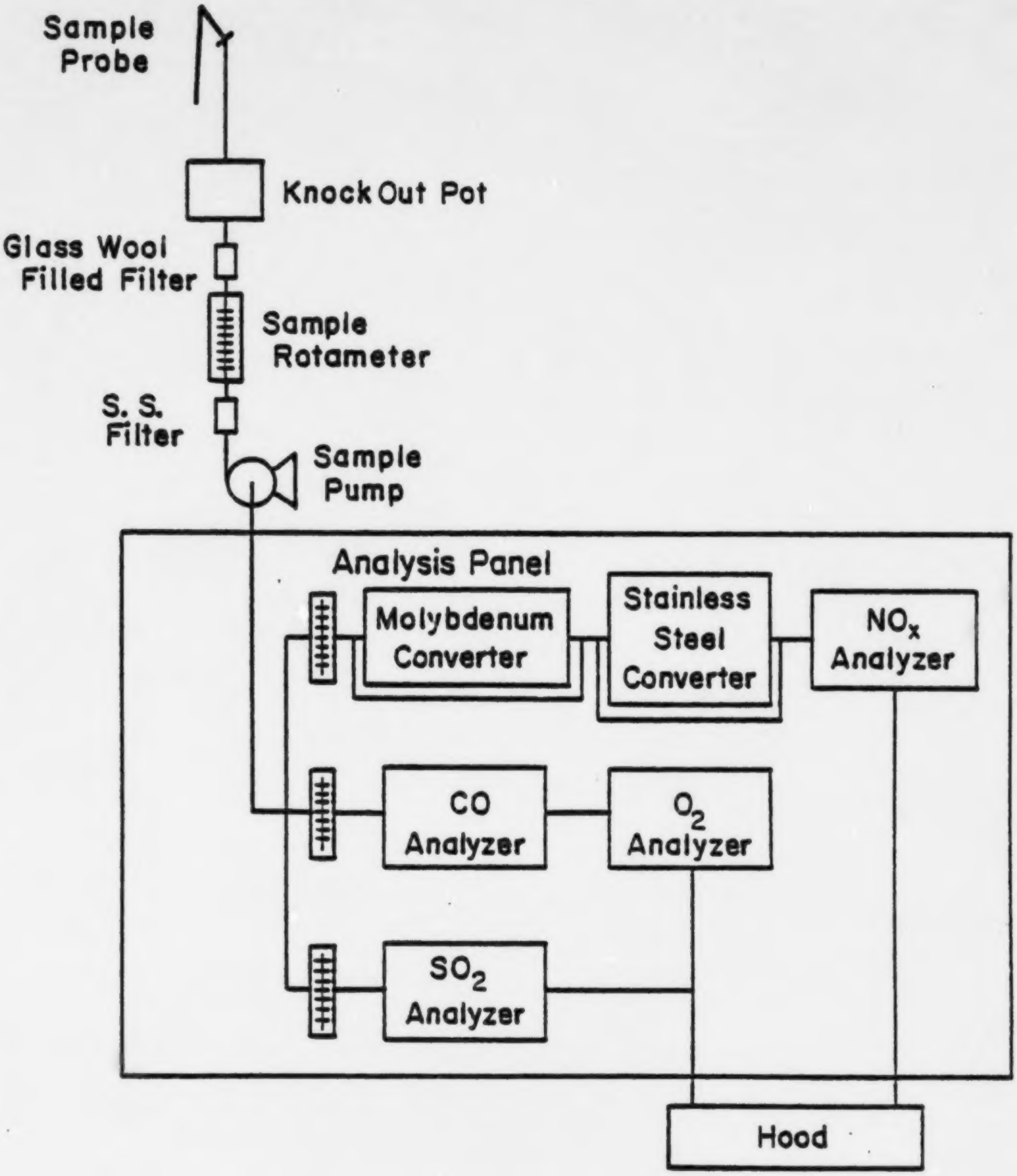
Sample Probe
Knock Out Pot
Glass Wool Filled Filter
Sample Rotameter
S. S. Filter
Sample Pump
Analysis Panel
Molybdenum Converter
Stainless Steel Converter
NO_x Analyzer
CO Analyzer
O_2 Analyzer
SO_2 Analyzer
Hood

Figure 2.3-4 Schematic of the Sampling and Analysis System.

pump responsible for flow through the sampling and analysis system was a Metal Bellows pump. This model MB-41 is an all stainless steel pump with stainless steel reed values.

The instrument section consisted of three systems in parallel. One flow system was the Thermo Electron Model 10A, Self-Contained Chemiluminescent NO-NO_x Gas Analyzer. To measure NO_x, the sample could be routed through either a Thermal Electron Model 300, Molybdenum Converter, or the stainless steel converter in the analyzer itself. The former converter was designed primarily for fuel-rich studies, and the latter for fuel-lean studies. The molybdenum converter, however, after sufficient exposure to sample gases from fuel-rich combustion, performed incorrectly, showing significantly lower NO_x concentration than the NO concentrations. In addition, the NO_x indication continued to decrease with time. An article supplied by Thermo Electron Co. discussed an investigation of this observation (Summers, 1976). Carbon monoxide in amounts greater than 10% by volume was found to be the species which interfered with the NO_x to NO conversion. The article suggested an oxygen bleed to negate the CO-NO_x interaction, but this was not attempted. However, since emphasis in this work is on NO, rather than on NO_2, the converters were seldom used.

The TECO was sensitive to flow and pressure variations of the sample. Therefore, the rate to this system was regulated by a rotameter. Calibration gases were ordered from Matheson Gas Products of Cucamonga, California. Two standards were used, 93 ppm NO/N_2 and 980 ppm NO/N_2.

Another flow system consisted of a Beckman Model 864 CO Infrared Analyzer, and a Beckman Model 715 Process Oxygen Monitor. The CO analyzer had two operating scales, 0-2% and 0-10%. For several of the fuel-rich studies, even the latter range was not high enough to register the carbon monoxide content. Beckman personnel suggested ways to extend the range of the instrument. This allowed at least approximate values. The calibration gases were from Matheson, 1.79% CO/N_2 and 8.09% CO/N_2.

The oxygen monitor operated on a polarographic principle. Consequently, the electrochemical process was sensitive to partial pressure of oxygen. The exit from the monitor was necessarily to the atmosphere. The monitor was sensitive to certain interfering gases such as SO_2 and H_2S, resulting in erroneous readings. H_2S, in particular, contaminated the sensor. Thus, during sulfur additions, the oxygen instrument was by-passed to prevent damage. Since fuel-rich studies were the predominate conditions investigated, the oxygen readings were close to zero. Calibration gases were compressed air available from University Stores Compressed Gases Section, and 4.33% O_2/N_2 from Matheson.

The last remaining flow system consisted of the Thermo Electron Model 40 Pulsed Fluorescent SO_2 Analyzer. In fuel-rich studies, this instrument was not reliable. The high amounts of CO in the sample gases interfered significantly with the detection system. Although TECO suggested that a correction for such interferences might be possible, such a method was not pursued.

All three parallel flow systems could not be operated at once due to limitations in the amount of sample that could be supplied compared to flow required by each instrument. Thus, during data acquisition, the $CO-O_2$ and the NO_x systems could be run simultaneously. To take SO_2 readings, the flow to the NO_x system was shut off, the $CO-O_2$ flow system left open, and the SO_2 analyzer allowed to sample. In this mode, the readings from the $CO-O_2$ system were not reliable. Only excess gases not needed by the SO_2 system passed through $CO-O_2$ system, and were insufficient to reach their necessary flow requirements.

2.3-3 Flow Panel

A variety of flow meters were used to control the inlet gases to the burner system. Figure 2.3-5 is a schematic of this flow arrangement. The entire experimental apparatus, compressed gas bin, flow panel, and burner system were housed in a University-constructed hood system approved for extra hazardous chemicals. All piping in the flow panel was 1/4 in. O.D. seamless S.S. tubing.

The cylinders of argon were available from University Stores Compressed Gases Section. Its flow was filtered through a 7 micron Nupro inline filter. Regulation was accomplished by a rotameter, calibrated to a 20 psi inlet pressure. By simultaneous adjustment of values upstream of the gauge and downstream of the rotameter, a desired setting at 20 psi could be obtained. The calibration chart is shown in Appendix C. The argon flow continued through a preheater and then to the burner through insulated tubing. The insulation was a durablanket ceramic fiber, Fiberfrax, manufactured by The Carborundum Company.

The methane and oxygen flows were both controlled by sonic orifices. The methane was C.P. grade, 99.0% purity from Matheson. The oxygen was available from University Stores Compressed Gases Section. The jewelled sapphire orifices were from Aurile Gatti Incorporated. They were pressed into Teflon holders and the entire holder inserted into

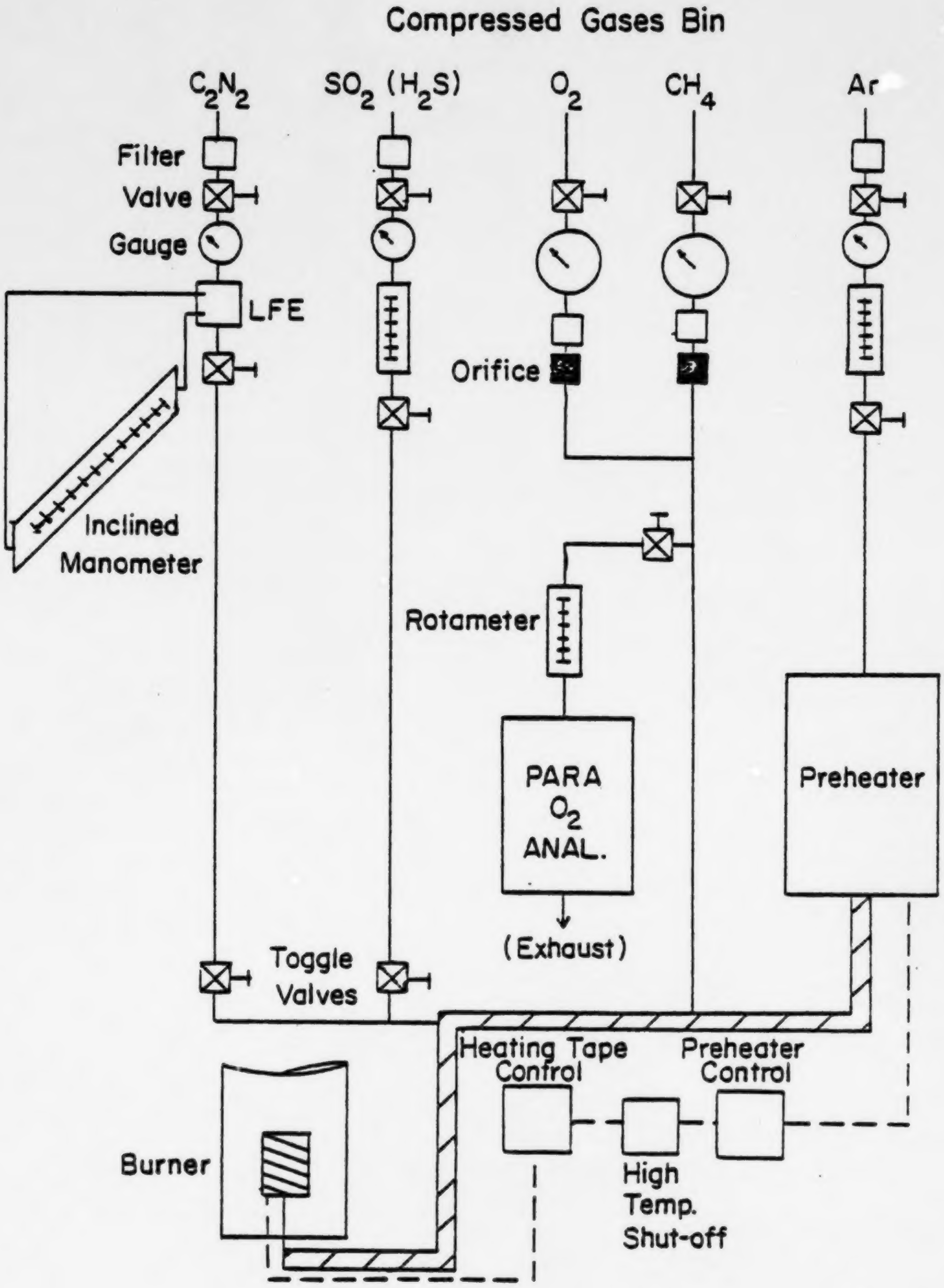
Compressed Gases Bin
C_2N_2
SO_2 (H_2S)
O_2
CH_4
Ar
Filter
Valve
Gauge
LFE
Orifice
Inclined Manometer
Rotameter
PARA O_2 ANAL.
(Exhaust)
Preheater
Toggle Valves
Heating Tape Control
Preheater Control
Burner
High Temp. Shut-off

Figure 2.3-5 Schematic of Flow System.

a specially machined, 1/4 in. S.S. union. To prevent particles from collecting on their edges, 7 micron filters were placed upstream of the orifices. Flow regulation was accomplished by precise setting of the upstream pressure on S.S. Master gauges from the Marsh Instrument Co. by Brooks NRS Needle Valves. The percent oxygen in the combined methane/oxygen stream was monitored directly by a Beckman Model F3 Paramagnetic Oxygen Analyzer. This procedure offered more accurate reproducibility of the methane/oxygen ratio.

The calibration charts for the orifices are in terms of "nitrogen" flow at standard conditions. Nitrogen was chosen as a calibration basis, but conversion to another desired gas flow is accomplished by multiplying by density ratios and by an orifice factor.

The sulfur additive, either SO_2 or H_2S, was added via a rotameter arrangement similar to that of argon. The SO_2, anhydrous, 99.98% purity; and the H_2S, C.P. grade, 99.5% purity, were both Matheson products. When the sulfur additive was not desired in the flame, its flow could be shut off via a toggle valve near the burner.

The cyanogen, 98.5% Matheson technical purity was regulated by an inclined manometer, Meriam Model 40H35. It measured a pressure drop in inches of water across a laminar flow element designed by Meriam Instrument Company. It utilizes a stainless steel capillary cemented into a stainless body. Unfortunately, the fluid designated specifically for the manometer could not be used. It was water based. Cyanogen reacts with water to form brown, amorphous azulmic acid plus other compounds, which precipitated in the glass tubing. Instead, the manometer was filled with No. 100 Blue King Indicating Liquid sp. gr. 1.000 at 20°C. This fluid did not respond as rapidly as the original Meriam fluid. However, it was a petroleum base and did not react with the cyanogen. The calibration of the manometer was done at a 20 psi inlet pressure. As before, this was accomplished by simultaneous adjustment of two fine metering valves located before the gauge and after the LFE.

The preheat system was not used extensively for the studies presented in this report. However, its construction is also presented in Figure 2.3-5. A Chromalox circulation heater Model GCH-210 was designed for raising the temperature of a argon stream to a maximum of 550°F. However, due to heat loss problems from the preheater and from the lines leading to the burner, an additional heating section was required. This was accomplished by wrapping heating tape around the burner. A further improvement was replacement of the glass beads by 316 S.S. balls of the same diameter. This improved the heat transfer to the incoming gases and enabled higher preheat temperatures.

The Chromalox heater was regulated by a factory-specified thermostat and bulb detector located near the exit port of the unit. The heating tape was regulated by a Chromalox Model 74 proportional temperature controller. The associated iron-constantin thermocouple was located inside the burner, measuring the gas temperature close to the bottom of the porous disc. For safety, power to both heating units was regulated by a Chromalox Model CNOF-76 on-off controller. Upon detecting a high temperature limit of approximately 900°F from a thermocouple placed between the wrappings of the heating tape, operation of the system was interrupted.

2.4 Flame Temperature Measurement

The development of optical methods for the measurement of flame temperatures is based on the radiating property of hot gases. In nonluminous flames, these radiations originate from energized particles in translations. For the reversal technique, an excitable metal, sodium, is introduced into a nonluminous flame. The sodium atoms become energized and radiation originates from an electronic transition. Therefore, the resulting temperature is called the electronic temperature. This value can be extended to describe the true thermodynamic flame temperature only when thermal equilibrium prevails in the hot gases. This situation has been investigated (Schmidt, 1909; Griffiths and Awbery, 1929). The conclusion has been that the sodium line reversal technique yields the thermodynamic temperature.

In the reversal technique, the temperature of the flame is measured by comparing its radiation at the wavelength of the excited sodium line with radiation of a black body of known temperature. The image of the black body, constituted by a tungsten lamp, is projected on the nonluminous flame. The flame is supplied with a sodium salt. The combined intensities of the tungsten filament and the excited sodium is then projected onto a monochromator scanning the wavelength region of the sodium doublet emission. The lamp intensity is varied until it matches that of the flame. At this point, temperature of the flame is equal to the temperature of the tungsten lamp. Mathematically this can be stated as

$$E(\lambda,S)[1 - \alpha(\lambda)] + e(\lambda,T) = E(\lambda,S) \tag{4.1}$$

where

$E(\lambda,S)$ = the spectral radiance at the sodium wavelength and at temperature S of the tungsten lamp. Spectral radiance is defined as the energy radiated by a body in a particular direction per unit time per unit wavelength per unit projected surface area per unit solid angle.

$\alpha(\lambda)$ = the spectral absorption coefficient or the fraction of incident energy absorbed by a body at a particular wavelength (sodium here).

$e(\lambda,T)$ = the spectral radiance of the sodium emission in the flame at the flame temperature, T.

The above equation states that, at reversal, the radiance of the black body transmitted through the flame plus the radiance of the sodium lines of the flame equals the radiance of the black body. The equation can be rewritten as

$$\frac{e(\lambda,T)}{\alpha(\lambda)} = E(\lambda,S) \tag{4.2}$$

This is Kirchoff's law stating that the radiance $e(\lambda,T)$ of a body is equal to the black body radiance $E(\lambda,T)$ at the same temperature and wavelength, times the absorption coefficient $\alpha(\lambda)$ of the body. Thus, T = S for equation (4.2) to be true. That is, the temperature of the lamp is equal to the temperature of the flame.

There are several advantages to this optical technique. Flow patterns in the flame are not disrupted as with measurements with thermocouples. High temperatures to 2300 K can be measured. This is above the suggested limits of many thermocouples. The technique is rapid and enables data acquisition to be smoother and continuous.

Although the reversal technique is orthodox and is used quite frequently in combustion work, detailed descriptions are not easily found in literature. The hardware is experimentally difficult, at least in its early stages. Noise in the system can arise from both the optics and the electronics. A sturdy rigid platform of Unistrut with a heavy aluminum channel base dampened vibrations from other machinery that would otherwise interfere with the optics. Lenses and diaphragms were firmly supported, but adjustable. Alignment of the optics was critical in ensuring a strong signal. Best results were obtained by focusing a laser beam through the monochromator and the rest of the system.

The apparatus used for the sodium line reversal technique is shown in Figure 2.4.1. The tungsten filament lamp was a GE 30A/T24, 6-volt, pyrometer lamp and was powered by a 44-amp d.c. source. The original source was a.c. However, the sinusoidal pattern caused fluctuations in the intensity from the tungsten lamp. These were detected by the electronics and became additional noise. The line voltage to the power supply was regulated by a constant voltage standard sinusoidal type

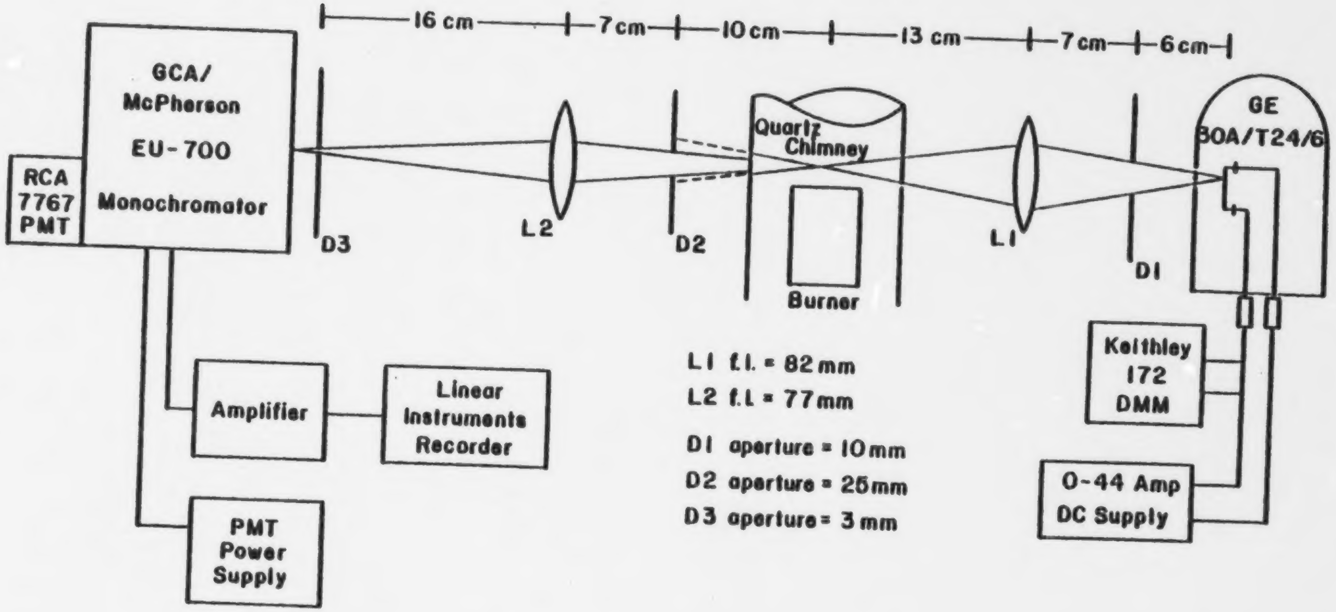
16 cm
7 cm
10 cm
13 cm
7 cm
6 cm
GCA/
McPherson
EU-700
Monochromator
RCA
7767
PMT
D3
L2
D2
Quartz
Chimney
Burner
L1
D1
GE
30A/T24/6
Keithley
172
DMM
0-44 Amp
DC Supply
Amplifier
Linear
Instruments
Recorder
PMT
Power
Supply
L1 f.l. = 82 mm
L2 f.l. = 77 mm
D1 aperture = 10 mm
D2 aperture = 25 mm
D3 aperture = 3 mm

Figure 2.4-1 Optical System for Flame Temperature Determination.

transformer manufactured by Sola Electric. This 1000 VA, 60 Hz unit was capable of regulating the 120 V output to ± 1% or less with a total input line voltage variation of ± 15%. In addition, it has less than 3% total rms harmonic content at full load. The Sola transformer eliminated as much a.c. noise as possible before the line entered the lamp power supply.

The image of the tungsten filament was focused on the flame through lens L1. The image from the flame was, in turn, focused on the slit of the monochromator by lens L2. These lenses were placed between the lamp and the flame as well as the flame and the slit to give approximately a one-to-one magnification. The monochromator used throughout this work was a GCA/McPherson EU-700 series equipped with a 1180 lines per mm grating blazed for 2500 Å. The slits in the instrument were ground and polished straight knife edges. The entrance and exit slit widths were gauged to a single control. The variable slit width counter was adjusted to 85 microns. The entrance slit height was set at 3 mm by a special aperture disc. For temperature measurements, the monochromator operated at a scanning rate of 0.2 Å/sec, between the wavelength region of 5880 Å and 5894 Å.

The light signal from the monochromator was detected by a RCA 7767 photomultiplier tube with a S-11 spectral response. Its maximum sensitivity was near the sodium doublet region. The tube was magnetically shielded for more efficient operation and less loss of signal. The tube was powered by a variable voltage supply. Its output was amplified and transmitted to chart recorder Model 252 manufactured by Linear

Instruments Corp. With the recorder speed of 2 cm/min, the recording interval calibrated at 6 Å/cm.

The temperature of the tungsten filament was measured with an optical pyrometer sighted through lens L1 and aperature D1. To allow for the additional correction of the large quartz chimney surrounding the burner, sightings were taken with and without the chimney in the optical path. The temperature drop due only to the chimney averaged 30°C. Half of this temperature drop was added to the temperature measured with the chimney in the optical path. This was done because only one side of the chimney was responsible for interference of the light intensity from the lamp before reaching the flame.

To make a temperature measurement using the sodium line reversal method, the grid was wetted by a few drops of $NaHCO_3$ in water. The drops were placed near the center of the grid so that the excited sodium atoms color the center portion of the flame. The monochromator was set to scan the sodium doublet region beginning at 5880 Å. The PMT voltage supply and the PMT signal amplifier were adjusted to give the best outline of the sodium peaks. The "best" outline was judged by the greatest amplification but with the least amount of electronic noise and the least amount of base line slant. The base line slant was due to the behavior of the RCA 7767 PMT. The sodium doublet falls on the portion of its spectral response curve after the maximum response at 4400 Å. Thus, the slant in the sodium doublet traces is due to the diminished detection capability of the PMT at longer wavelengths. Depending on the relative temperatures of both the lamp and the flame, traces were obtained similar to those illustrated in Figure 2.4-2. If the flame temperature was lower than the filament temperature, the doublet was seen in absorption against the lamp background. If the converse was true, the doublet would be seen in emission. When both temperatures are equal, the reversal temperature was found.

Certain characteristics of this sodium system became apparent after repeated use. Literature cites the sodium doublet to peak at 5890 Å and 5896 Å, the more intense line being the former. The peak wavelengths in the current system are 5886 Å and 5891 Å, with the first setting exhibiting the strongest emission. The difference between the literature and experimental values is probably due only to an error in monochromator calibration.

Normally, both lines of the sodium doublet reversed simultaneously. However, in some temperature determinations, the 5886 Å line tended to blend into the base line before the second line. In these cases, the 5886 Å line was chosen as the basis for determing the temperature.

Unfortunately, temperatures could only be taken when sulfur compounds were not being added to the flame. On the addition of either H_2S or SO_2, the yellow emission of sodium was eliminated. Upon shutting off the additive flow, the sodium color slowly revived itself. Other investigators have noted the same effect (Durie, Johnson, and Smith, 1971), attributing the disappearance of the yellow coloring to a reaction

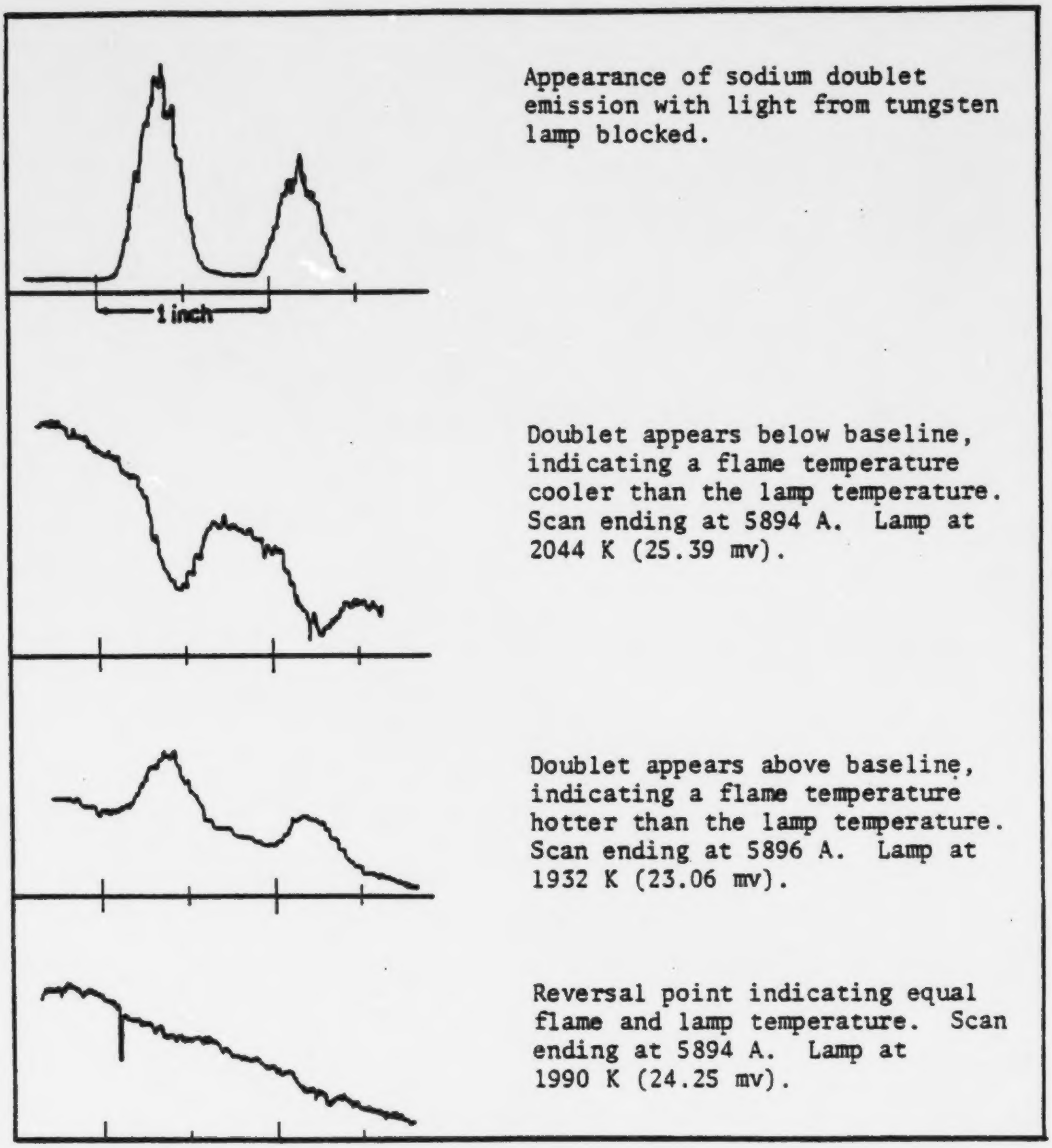

Appearance of sodium doublet emission with light from tungsten lamp blocked.

Doublet appears below baseline, indicating a flame temperature cooler than the lamp temperature. Scan ending at 5894 A. Lamp at 2044 K (25.39 mv).

Doublet appears above baseline, indicating a flame temperature hotter than the lamp temperature. Scan ending at 5896 A. Lamp at 1932 K (23.06 mv).

Reversal point indicating equal flame and lamp temperature. Scan ending at 5894 A. Lamp at 1990 K (24.25 mv).

Figure 2.4-2 Chart Recorder Traces of a Temperature Determination by Sodium Reversal Method. -- Peaks of sodium doublet appear at 5886 A and 5891 A. Chart speed set at 6 A/inch.

between sulfur and either Na or NaOH. In fuel-rich flames, the reaction of interest is

$$NaOH + S = NaS + OH$$

A convenient method for reviving the sodium coloring without shutting off the flame in order to add more of the aqueous solution was to drop a few grains of NaCl crystals onto the top of the grid. At times, with large flows of argon, the crystals would not land in the center of the flame as desired but near the edges. This may have biased the readings towards the lower temperatures of this portion of the flame. However, it was felt this effect would not add sufficient error because of the flat profile exhibited by the burner.

The temperatures at points in the flame were reproducible to ± 5°C. Once the burner system had reached thermal equilibrium, usually 20 to 30 minutes, this amount of accuracy was given to the temperature determinations.

2.5 Interferences in Sampling and Analysis System

The sampling and analysis system was tested for possible alterations to the sample gases between entry into the probe and analysis by the instruments. Investigated were the possibilities of interference in the chemiluminescent NO analyzer by sulfur species, of low temperature reactions occurring in the sampling system, and of the distinctions between hot and cooled probe behaviors. The system was divided into units as shown in Figure 2.5-1. Attention was focused onto each unit to determine its possible interference.

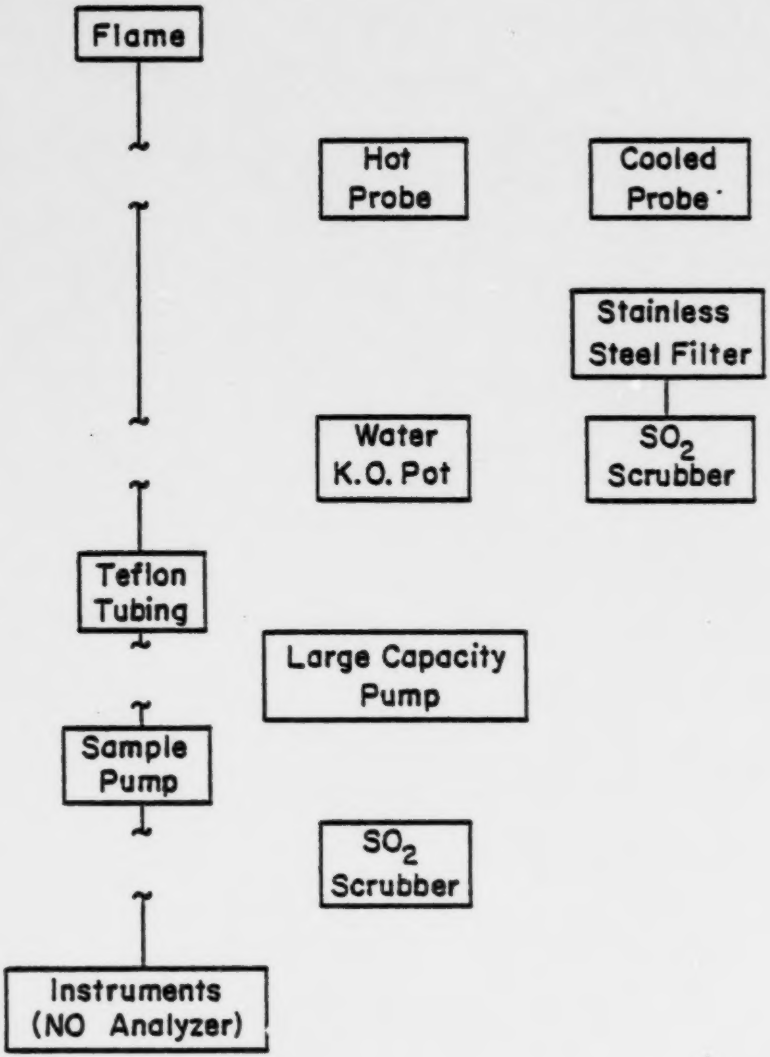
Flame
Hot Probe
Cooled Probe
Stainless Steel Filter
Water K.O. Pot
SO_2 Scrubber
Teflon Tubing
Large Capacity Pump
Sample Pump
SO_2 Scrubber
Instruments (NO Analyzer)

Figure 2.5-1 Units and Their Substitutes in the Sampling and Analysis System to Determine Possible Interferences.

Removal by sulfur was accomplished by bubbling the sample gases through an aqueous solution of 0.1 M NaOH contained in a 1000 ml Pyrex flask. Tests showed that, under non-flame conditions, this scrubber was very efficient in absorbing SO_2 concentrations of 400 ppm. NO values of 100 ppm and 1000 ppm ranges (in nitrogen) were decreased by 10%. O_2 and CO values of 4% and 8%, respectively, were not affected. Under flame conditions, the scrubber had no effect on the NO readings. Thus, corrections were not required. As indicated by the figure, the scrubber was entered into the sampling system at two positions. Its location just before the instruments verified that sulfur species did not interfere with operation of the NO analyzer.

In its second position, the scrubber alternated with the water knock-out pot to remove sulfur as well as water from the sample gases after they had exited the probe. The stainless steel filter was required before the scrubber to prevent particles of soot and sulfur from clogging the micro-pore glass bubbler. The NO values were not altered with the scrubber at this location. Thus, no low temperature reactions with sulfur species were occurring in the sampling system after the probes. These tests also indicated that the stainless steel filter before the scrubber did not behave as a catalyst at low temperatures for SO_x/NO interactions.

A 2.7 m section of Teflon 1/4 in. O.D. tubing as shown in the figure was replaced with new tubing. Similar tubing had acquired a coating of sulfur on the inside surfaces. Speculation was that perhaps a catalysis was occurring at room temperature. However, the NO analyzer showed no indication of this possibility.

The effect of sampling rate was investigated by introducing an additional pump in the system. This large capacity pump was able to pull more than twice the normal sampling rate. To maintain the same flow of sample through the instruments, thus ensuring correct readings, the sampling pump withdrew a portion of outlet stream of the large capacity pump. The excess gases were exhausted. In a study where a region of constant exhaust NO values were realized in the flame, the various sampling rates had no effect on the NO values. This indicated again that no reactions were occurring in the sampling system.

A consistent observation was designated as a probe effect and served as the only distinction between data taken by a hot probe versus that taken with a cooled probe. This behavior was noted in the profiles of base NO values. Figures 2.5-2 and 2.5-3 are studies of stoichiometric ratio 0.46 showing duplicate base values and values for a low SO_2 addition (13 ml/min). Refer to Figure 2.6-2 for curves of all SO_2 additions.

The data of the former figure were acquired with a hot probe. Sampling was begun at the lowest height, 1.27 cm. At each height, the initial base value, denoted by "i," was recorded, then increasing levels of SO_2 added, and the base value repeated, as denoted by "f" for "final." At 2.5 cm, the hot probe sensitization occurred. That is, the final base value was lower than the initial value by 7 ppm. This phenomenon was unique to the hot probe. It occurred after its inner surfaces had acquired a coating of soot and were exposed to a sufficient amount of sulfur. This sensitization, also, only affected base line NO values, i.e., when no sulfur was in the flame. After sensitization, base values followed a 3 ppm base line. At 18 cm, the base values had begun to

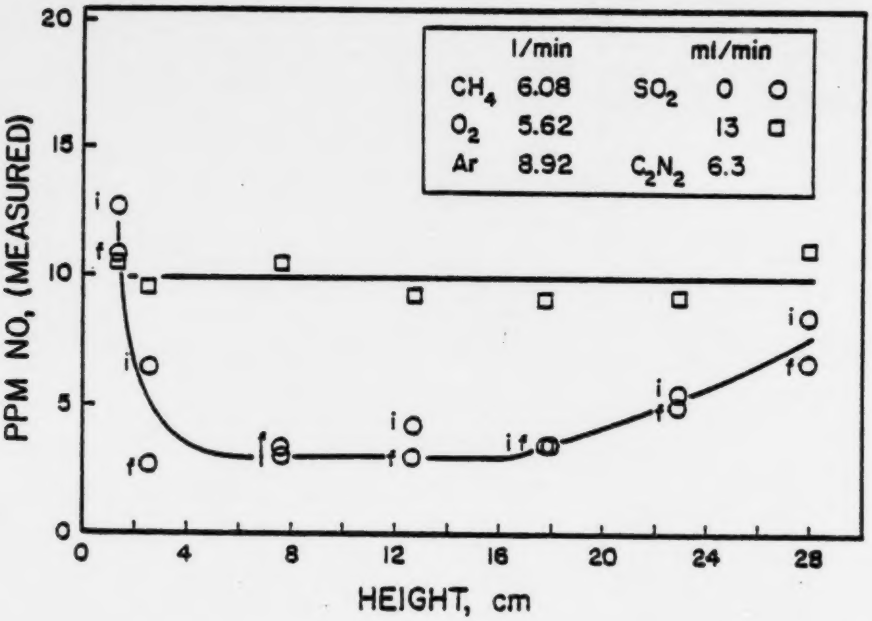

Figure 2.5-2 Hot Probe Effect Shown at a 0.46 Stoichiometric Ratio. -- Initial (i) and final (f) indices refer to base NO values before and after sulfur addition.

increase. This trend continued to the 28 cm height, the base line approaching the SO_2 addition values. At the higher sampling heights, more of the hot probe length was exposed to the cooler, outside environment. This cooling caused the increase in NO readings.

Indeed, the cooled probe accomplishes the same type of surface cooling, but with a water jacket. Figure 2.5-3 shows that the base values and the low SO_2 values did lie along a constant line of 12 ppm at sampling heights above 2 cm. Thus, the trend established by the hot probe was fully realized by the cooled probe, and the base line drift was avoided.

The above discussion established the distinction in probe behaviors as to interferences occurring to the sample gases when inside the probes. The probes could also affect the flame reactions by altering temperatures between the grid and itself by its mere presence and operation in the combustion system. Figures 2.5-4 and through 2.5-7 show the value of the temperature at a point in the flame as a function of the distance of a probe from that point. Common to all the figures are curves for two modes of probe operation: one for no flow through the probe, and one for a normal sampling rate of 1.3 l/min. Also, the latter three figures have the point temperature recorded without the probe in the flame. This point is the actual point temperature unaltered by interferences. The two modes of operation establish the error bounds for this temperature since its value fell within the limits of these two curves in the latter three figures.

Figures 2.5-4 and 2.5-5 deal with the cooled probe effects in low and high temperature flames, respectively. At the low temperature study, the error bound was zero. The point temperature was unaffected once the

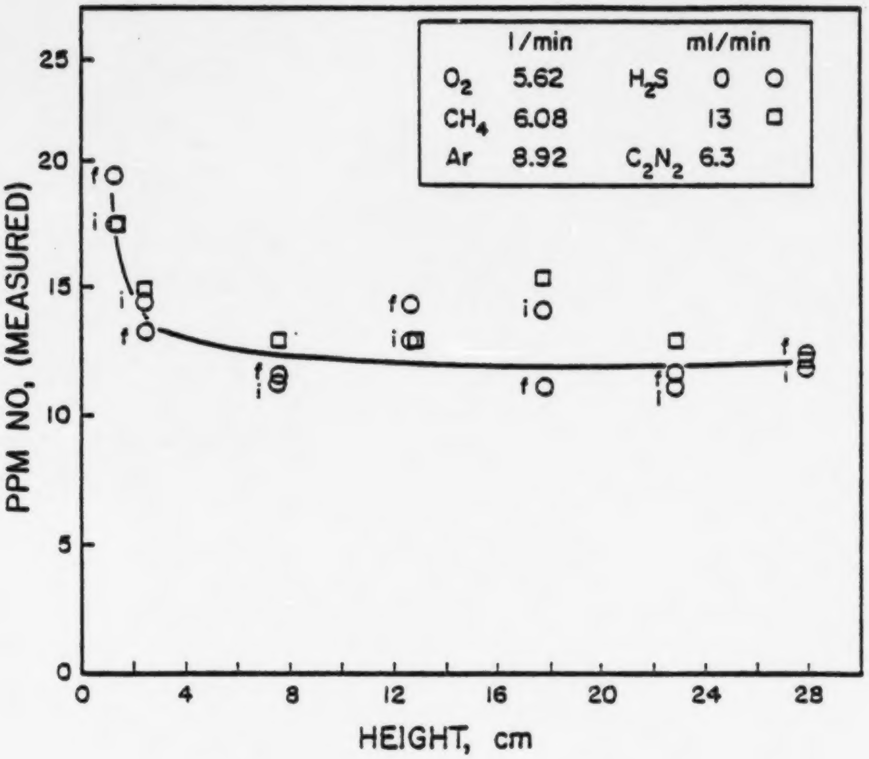

Figure 2.5-3 Behavior of Cooled Probe Sampling at a 0.46 Stoichiometric Ratio. -- Initial (i) and final (f) indices refer to base NO values before and after sulfur addition.

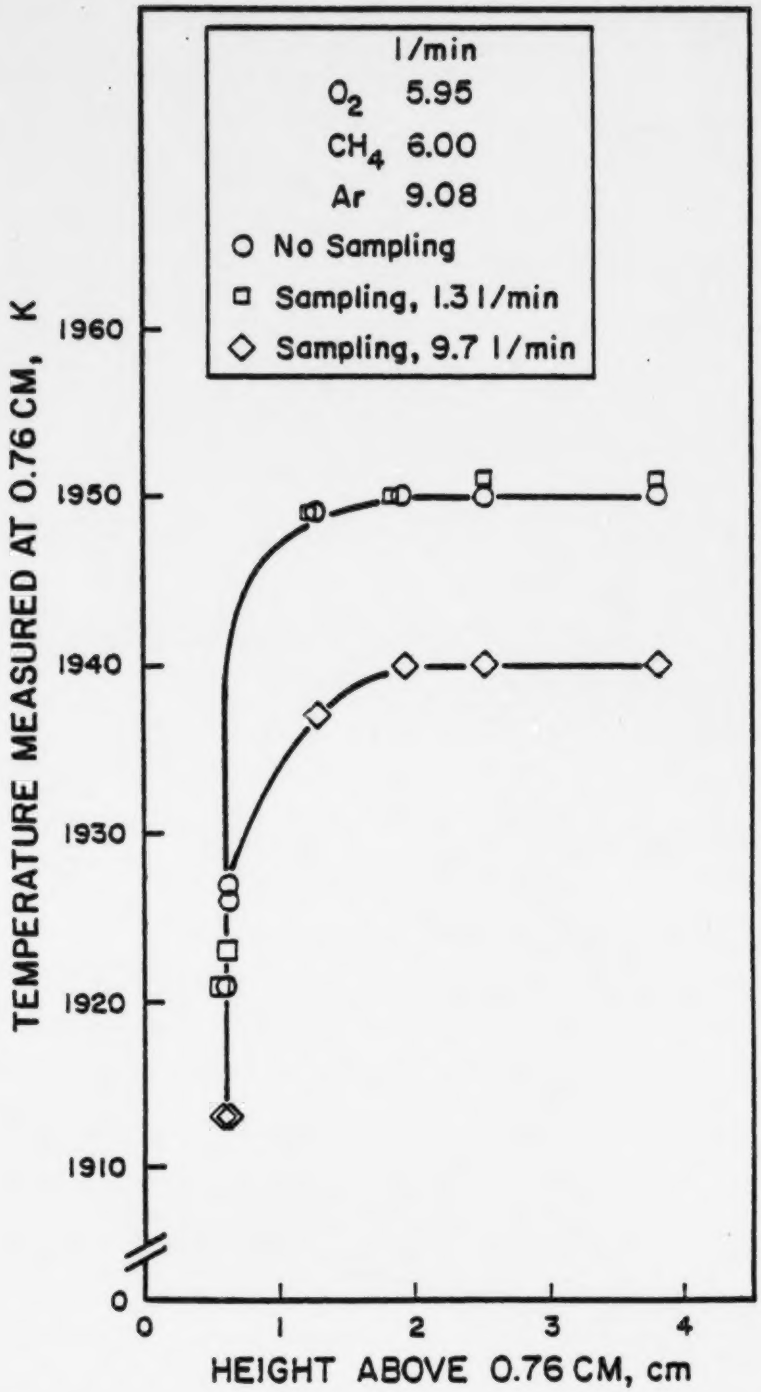

Figure 2.5-4 Effect of Cooled Probe on Temperature at a Point Low Temperature Study, S.R. = 0.50.

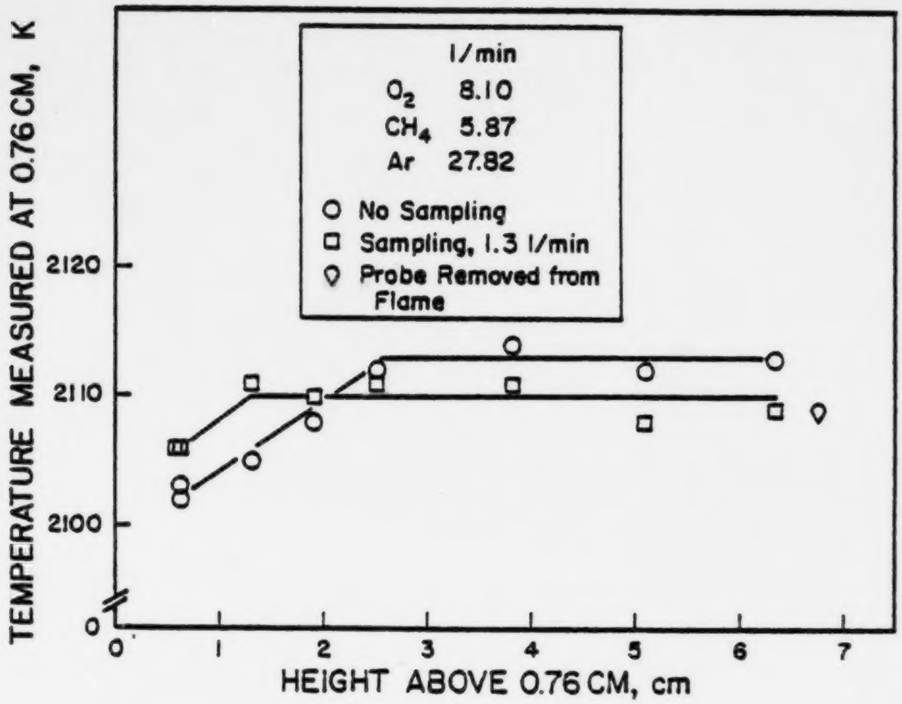

Figure 2.5-5 Effect of Cooled Probe on Temperature at a Point High Temperature Study, S.R. = 0.69. -- Peak temperature of 2114 K at grid level with probe removed.

cooled probe was 2 cm distant. However, in this amount of probe travel, the point temperature variation was an increase of 30 K. Also shown in Figure 5.4 is a high sampling rate curve yielding a constant temperature 10 K below the other curves. For the gas flows of this study, this large sample rate disrupted the aerodynamics, causing reactions to be altered and/or cooler gas to be pulled into the region of the temperature determination.

The high temperature study, Figure 5.5, shows an error of 3 K, and a rise of 7 K over a 2 cm travel.

Figures 2.5-6 and 2.5-7 show 5 K and 4 K error bounds, respectively, for the hot probe during low and high temperature studies. There is a 3 K temperature rise over less than 1 cm travel in Figure 2.5-6, and no rise in Figure 2.5-7.

Thus, the hot probe causes less interference to point temperatures than the cooled probe. However, the cooled probe caused, at most, a 30 K drop in point temperatures, and unless the flame reactions are very temperature sensitive, this change should be insignificant. In addition, since the cooled probe showed no sensitization, nor base line drift, it was concluded that this probe was the more reliable means of sampling in fuel-rich flames.

Conclusions from this chapter are that sulfur species did not interfere in the chemiluminescent analyzer, nor were they involved in low temperature reactions in other parts of the sampling system. Stainless steel fittings and Teflon lines did not serve as catalyst for further reactions of the combustion species. Sampling rate studies reinforced these findings. Although no significant alterations to NO readings were due to the hot probe behavior, the cooled probe was determined as the

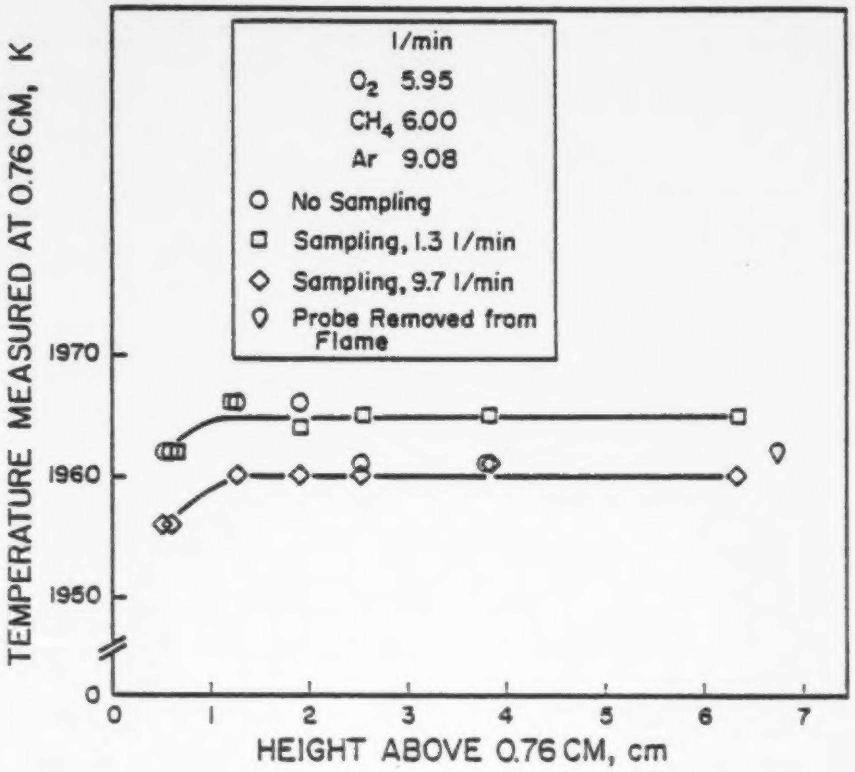

Figure 2.5-6 Effect of Hot Probe on Temperature at a Point Low Temperature Study, S.R. = 0.50. -- Peak temperature of 2022 K at grid level.

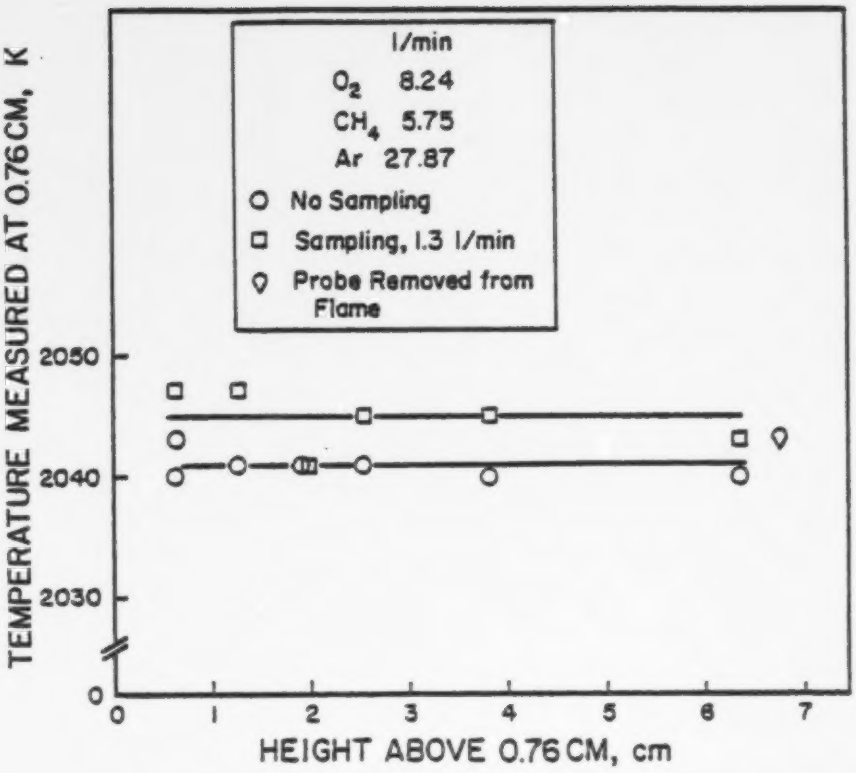

Figure 2.5-7 **Effect of Hot Probe on Temperature at a Point High Temperature Study, S.R. = 0.72. -- Peak temperature of 2076 K at grid level with probe removed.**

more reliable sampling means. The cooled probe decreased the temperature by a maximum of 30 K in the gases immediately upstream of its sampling position.

2.6 Results

In the previous chapter, the various units of the sampling and analysis system were checked for their possible interference with respect to sulfur/nitrogen interactions. Through those studies, several factors emerged as being important for obtaining the most reliable and reproducible data. These data are presented in this chapter.

Each of the figures to follow shows a profile of nitric oxide values to a 28 cm height above the burner grid for a particular stoichiometric ratio flame. Each profile is complete with base NO values, and with NO values affected by the additions of SO_2 and/or H_2S. These values are those recorded by the chemiluminescent analyzer and have not been reduced to some arbitrary basis. Only nitric oxide values are noted. All previous indications with the molybdenum converter showed that NO and NO_x readings to be the same. The high 28 cm sampling range was necessary and adequate to observe the trends of the interactions studied. It may be noted that, in some figures, even at such heights above the grid, exhaust values are still not suggested by some of the curves. To extend the profiles to this range, the final configuration of the burner used the minichimney. Unless otherwise stated, the NO values above 20.3 cm have been sampled inside the minichimney. The cooled probe was used for most data points. Those that were taken with the hot probe will be appropriately indicated.

The studies were made with methane/oxygen/argon flames of stoichiometric ratios ranging from very fuel-rich, 0.40, to fuel-lean, 1.2. The studies used the same methane flow, 6.08 st. 1/min. Standard conditions refer to 273 K and 1 atm. All flows in the figures are at these conditions although not specifically noted. The oxygen flow was varied to obtain the desired stoichiometric ratio. The argon flow was determined by that amount of inert necessary to support the flame on the grid to prevent flashback. The fuel nitrogen additive was cyanogen, C_2N_2. Figures 2.6-1 through 2.6-10 deal with cyanogen flows of 6.3 ml/min, giving a fuel nitrogen mole fraction of the methane flow of 0.21%. Figures 2.6-11 and 2.6-12 deal with 1.05% mole fraction fuel N. The sulfur additives, as mole fractions of the methane flow, range from 0 to 4.54% for sulfur dioxide, and from 0 to 3.75% for hydrogen sulfide.

Temperatures were taken by the sodium D-line reversal technique as discussed. These measurements were possible only in the absence of sulfur additives in the flame because both SO_2 and H_2S react with sodium atoms, and prevent the yellow light emission required for the reversal technique to function. Profiles were recorded from 0 to 11 cm. The 11 cm height was the maximum travel of the burner and thus limited the extent of the temperature profile. Also, in several flames studied, the sodium emission was not visible above a height of 11 cm. The heat loss from the system had decreased the energy in the flame sufficiently to suppress the excitation of the sodium atoms.

Information pertaining to a specific study is found in figure captions. Residence times and ppm NO corresponding to complete

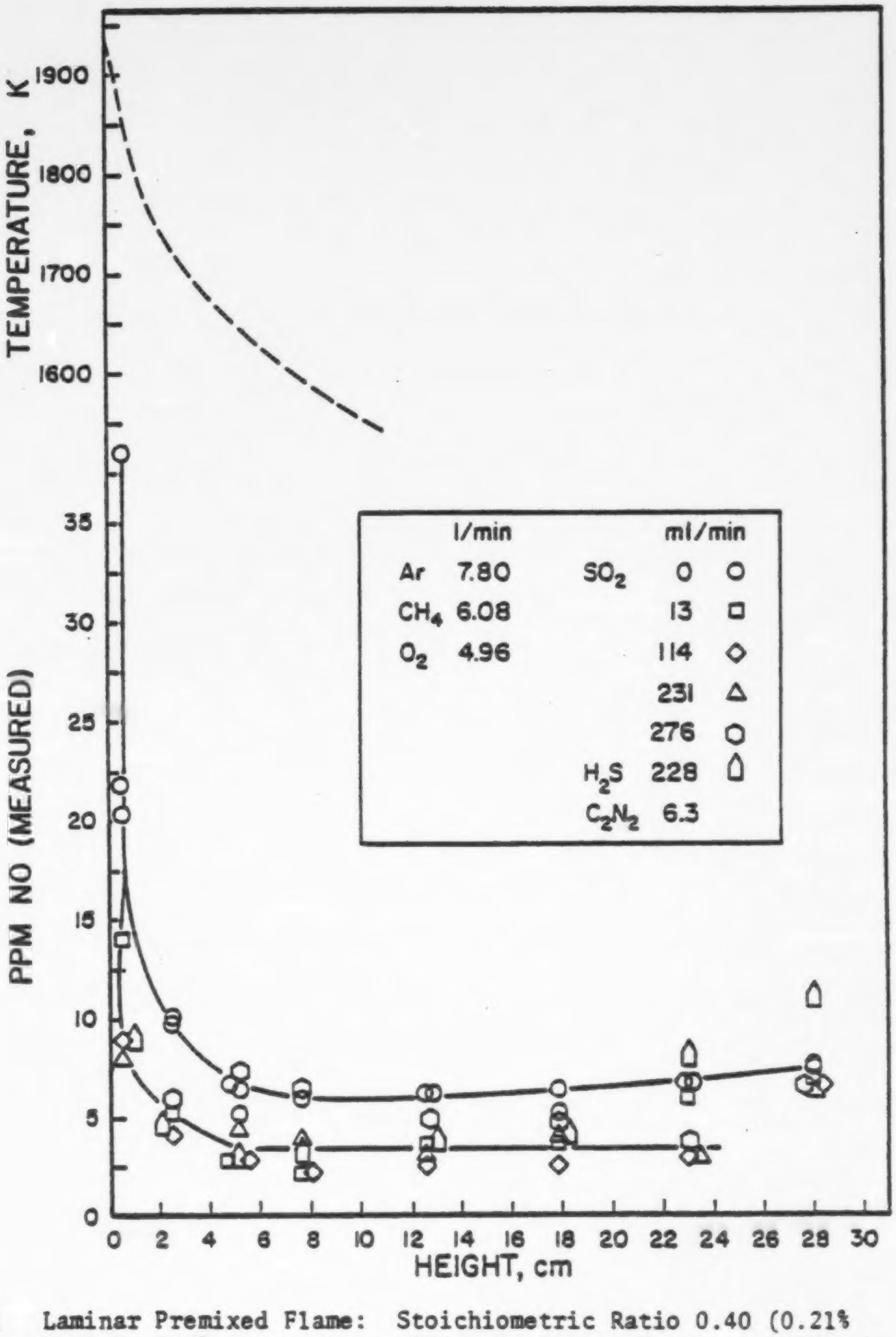

Figure 2.6-1 Laminar Premixed Flame: Stoichiometric Ratio 0.40 (0.21% Fuel N, 100% Conversion ≈ 554 ppm, 1 cm ≈ 7.56 ms at 1930 K, SO_2, H_2S as Fuel S).

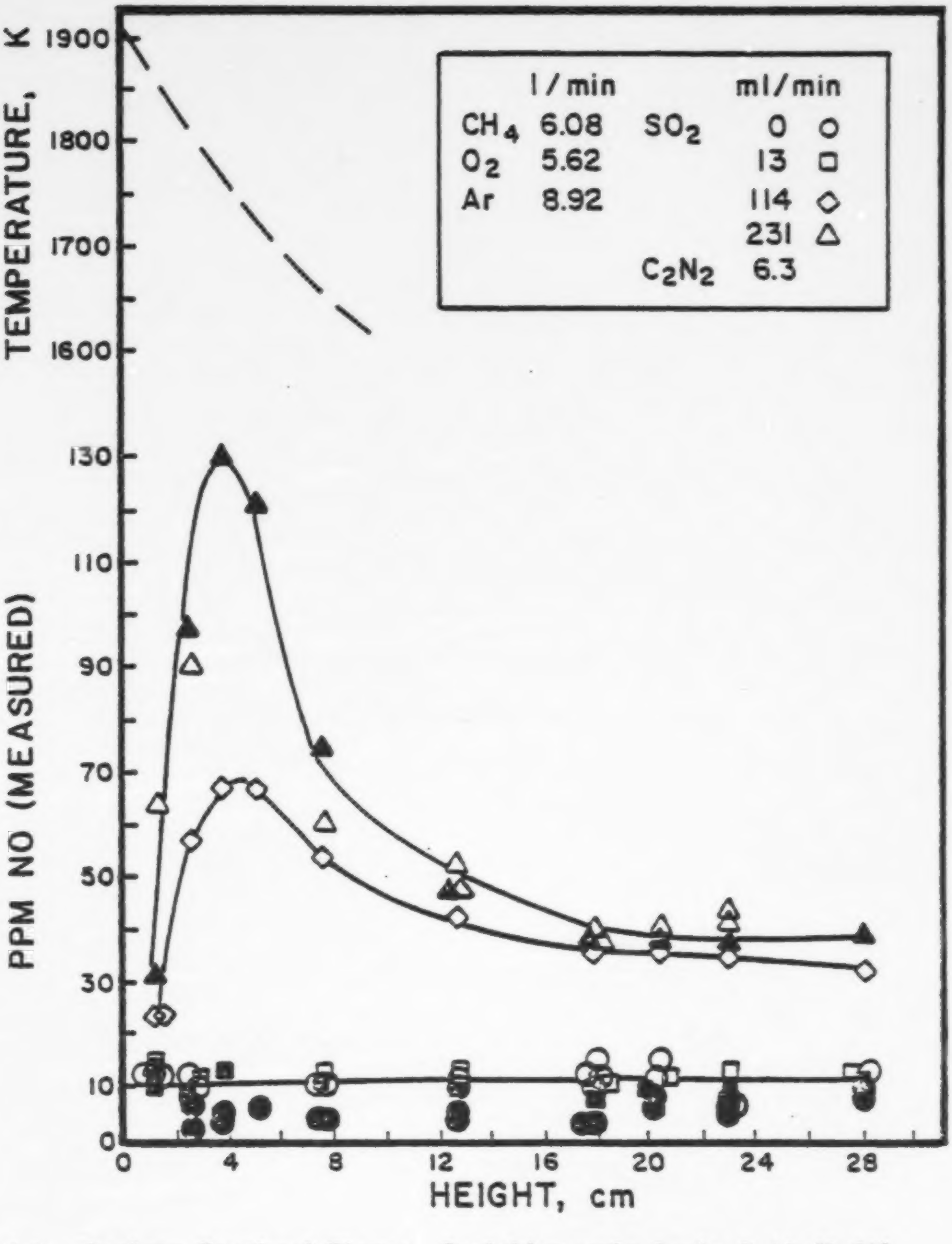

Figure 2.6-2 Laminar Premixed Flame: Stoichiometric Ratio 0.46 (0.21% Fuel N, 100% Conversion = 553 ppm, 1 cm = 7.67 ms at 1900 K, SO_2 as Fuel S).

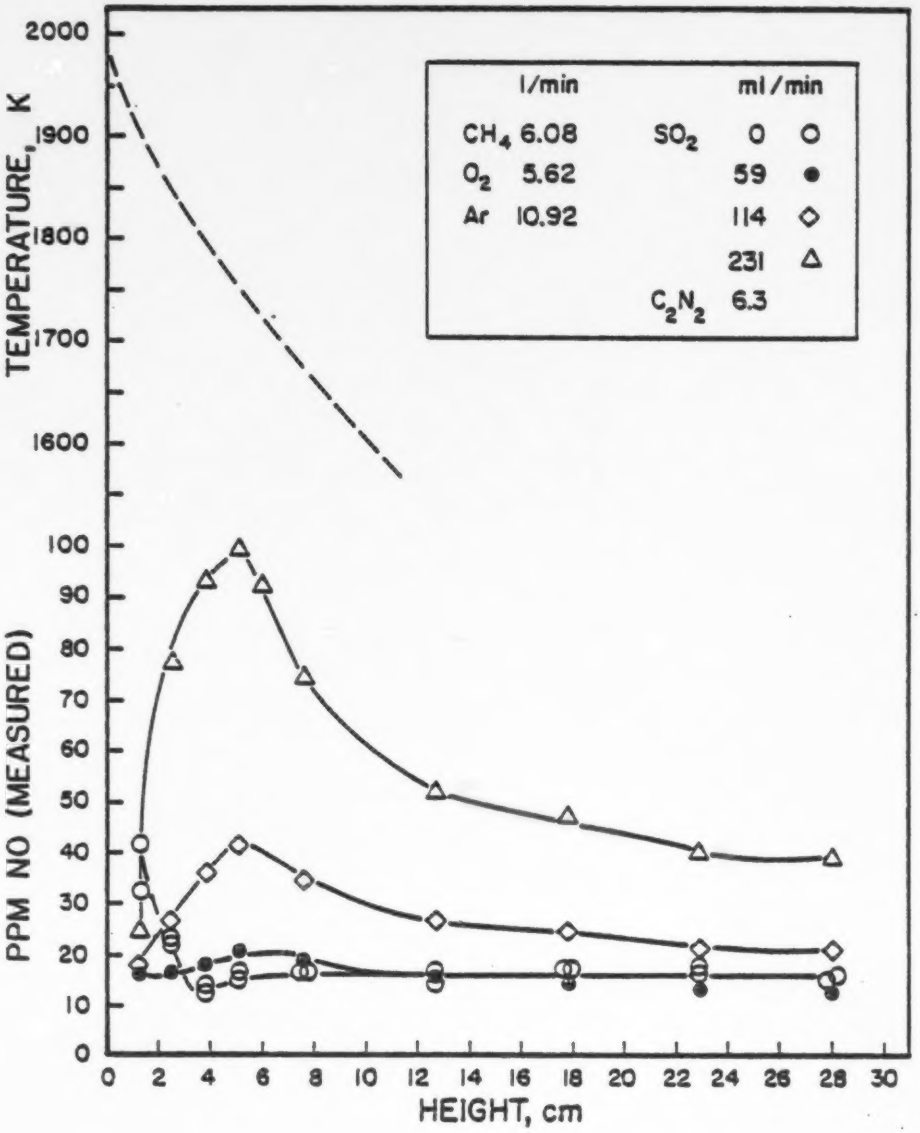

Figure 2.6-3 Laminar Premixed Flame: Stoichiometric Ratio 0.46 (0.21% Fuel N, 100% Conversion = 509 ppm, 1 cm = 6.81 ms at 1970 K, SO_2 as Fuel S).

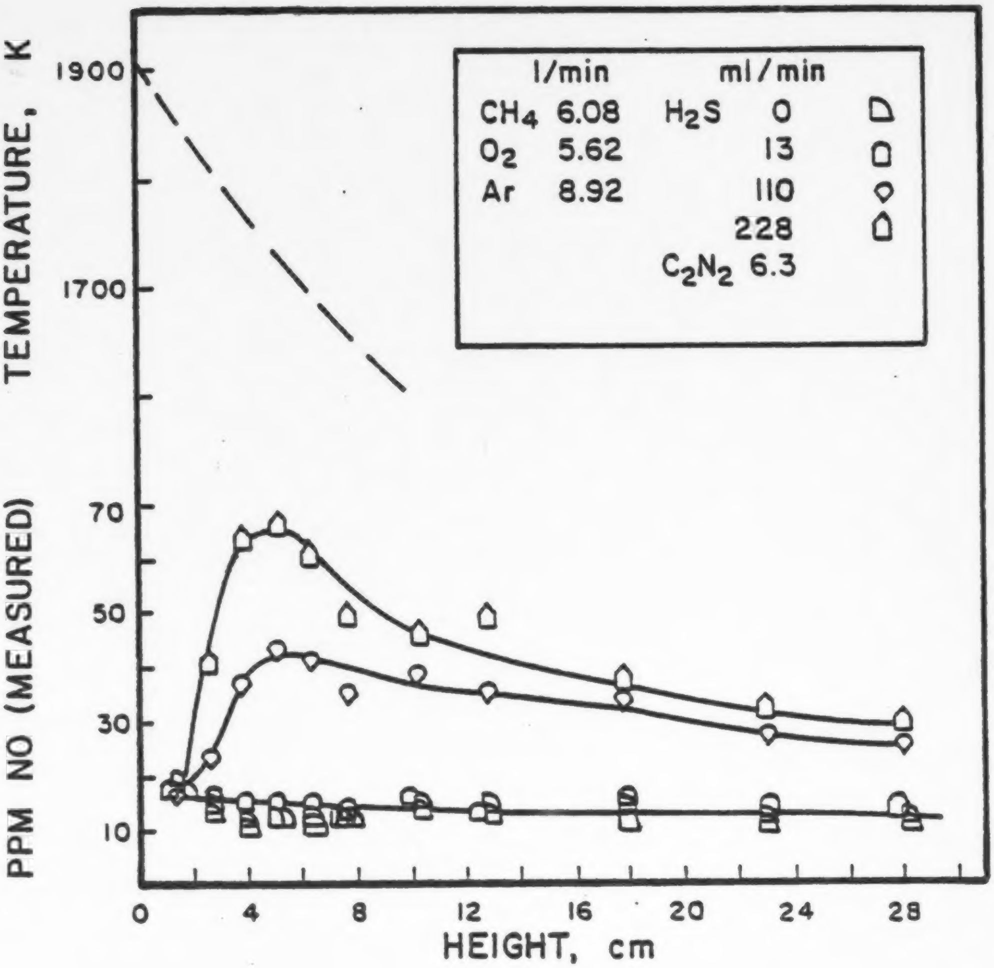

Figure 2.6-4 Laminar Premixed Flame: Stoichiometric Ratio 0.46 (0.21% Fuel N, 100% Conversion = 553 ppm, 1 cm = 7.67 ms at 1900 K, H_2S as Fuel S).

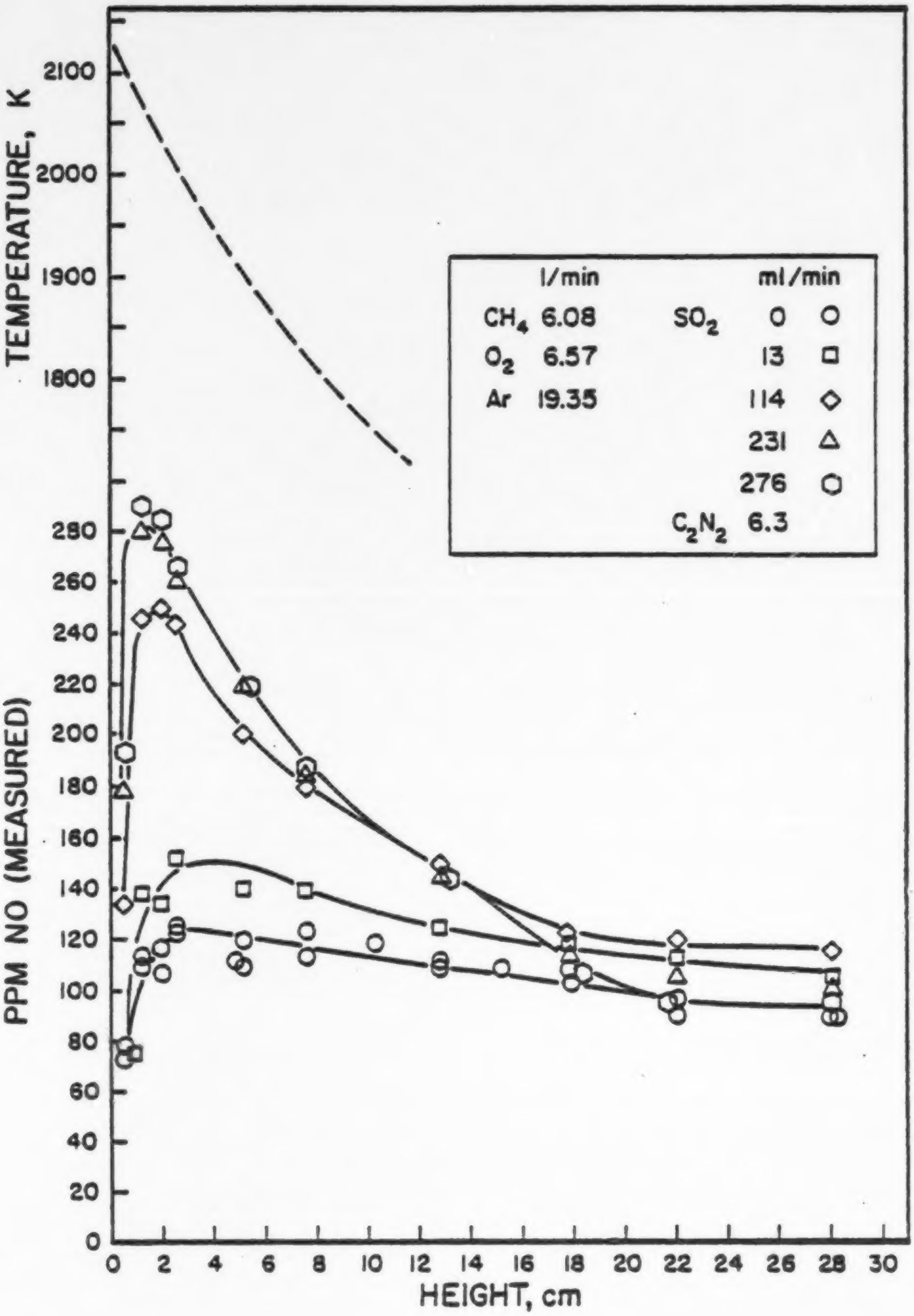

Figure 2.6-5 Laminar Premixed Flame: Stoichiometric Ratio 0.54 (0.21% Fuel N, 100% Conversion = 399 ppm, 1 cm = 4.10 ms at 2150 K, SO_2 as Fuel S).

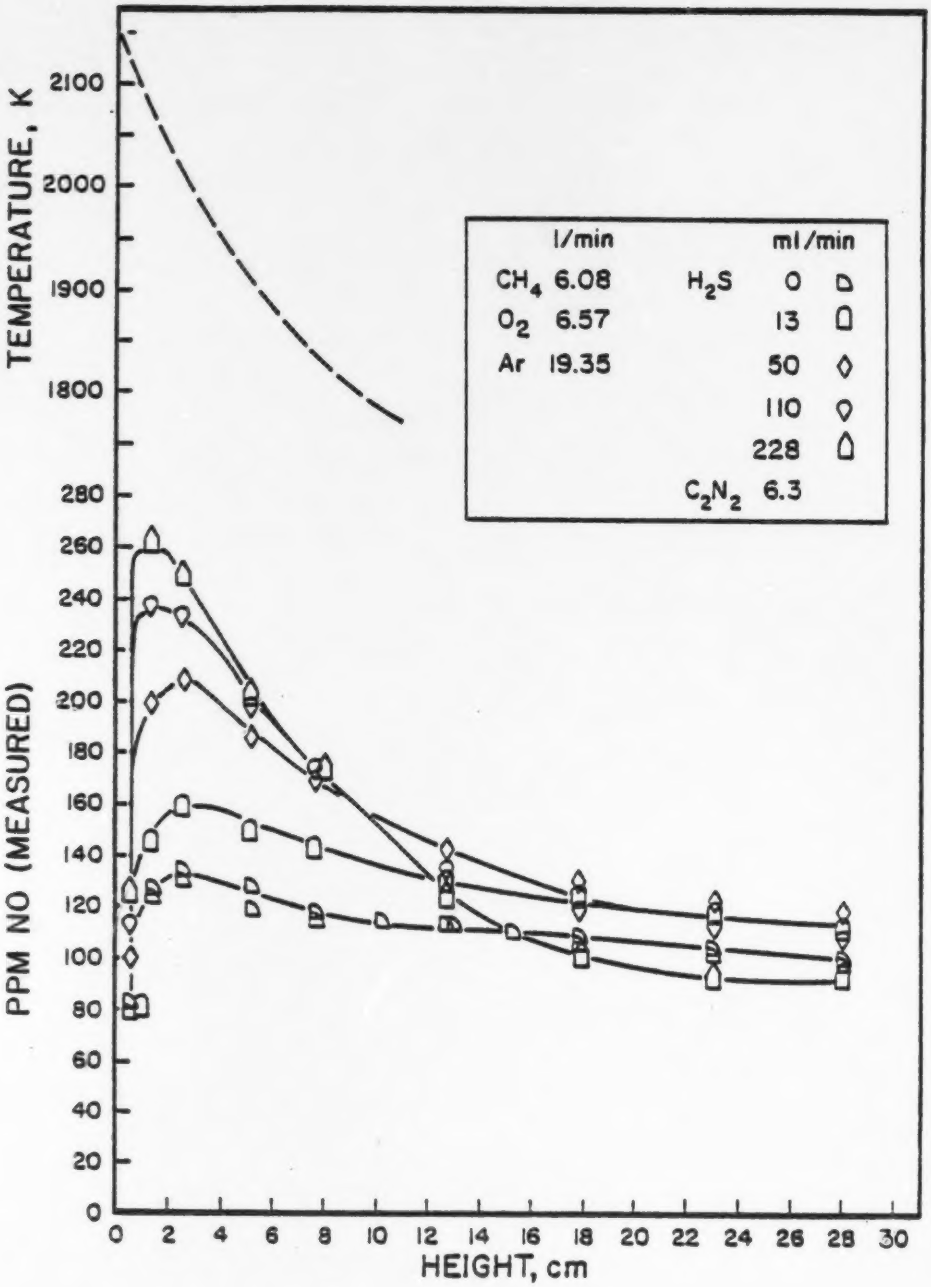

Figure 2.6-6 Laminar Premixed Flame: Stoichiometric Ratio 0.54 (0.21% Fuel N, 100% Conversion = 399 ppm, 1 cm = 4.10 ms at 2150 K, H_2S as Fuel S).

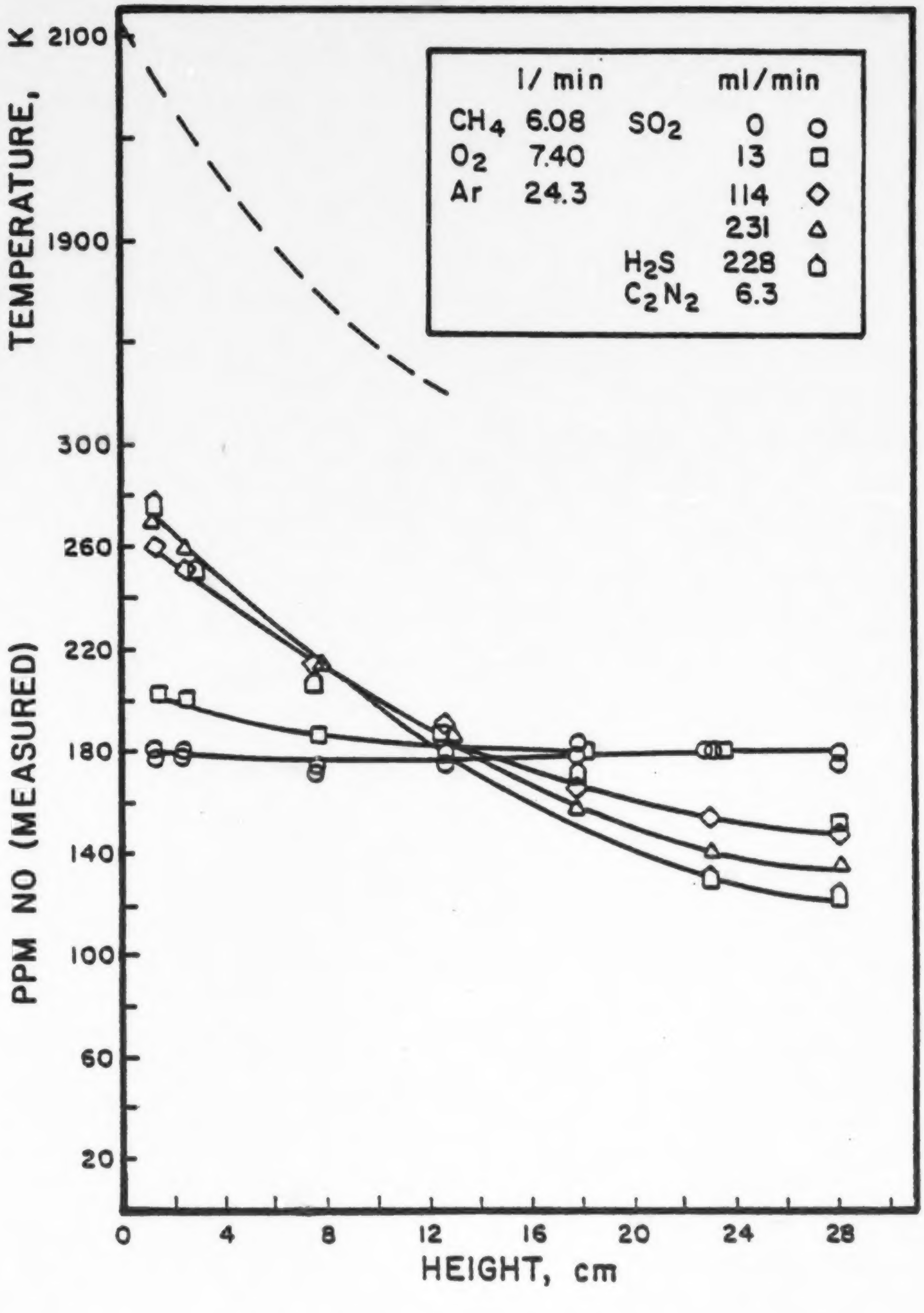

Figure 2.6-7 Laminar Premixed Flame: Stoichiometric Ratio 0.61 (0.21% Fuel N, 100% Conversion = 357 ppm, 1 cm = 4.47 ms at 2100 K, SO_2, H_2S as Fuel S).

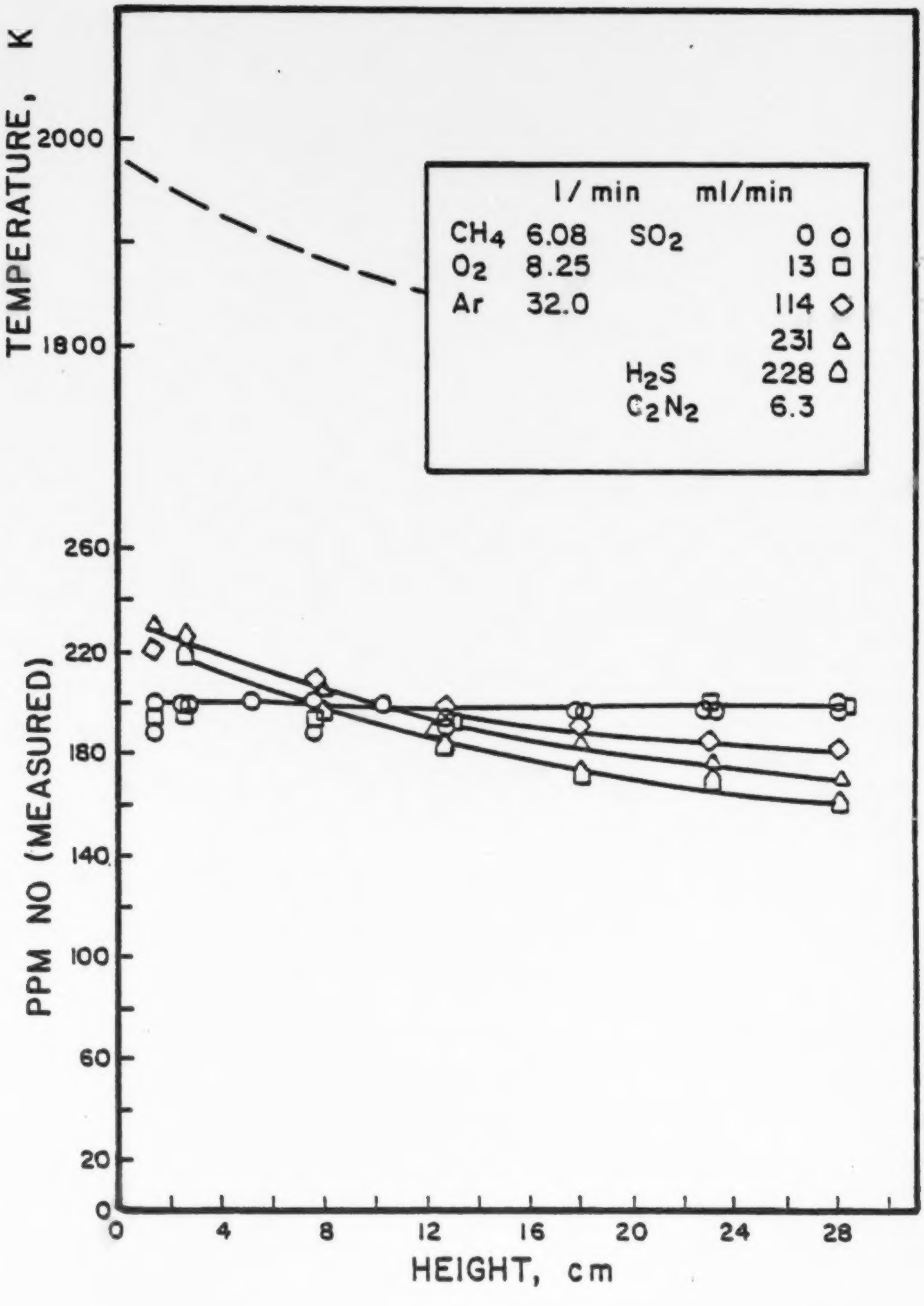

Figure 2.6-8 Laminar Premixed Flame: Stoichiometric Ratio 0.68 (0.21% Fuel N, 100% Conversion = 300 ppm, 1 cm = 4.00 ms at 1980 K, SO_2, H_2S as Fuel S).

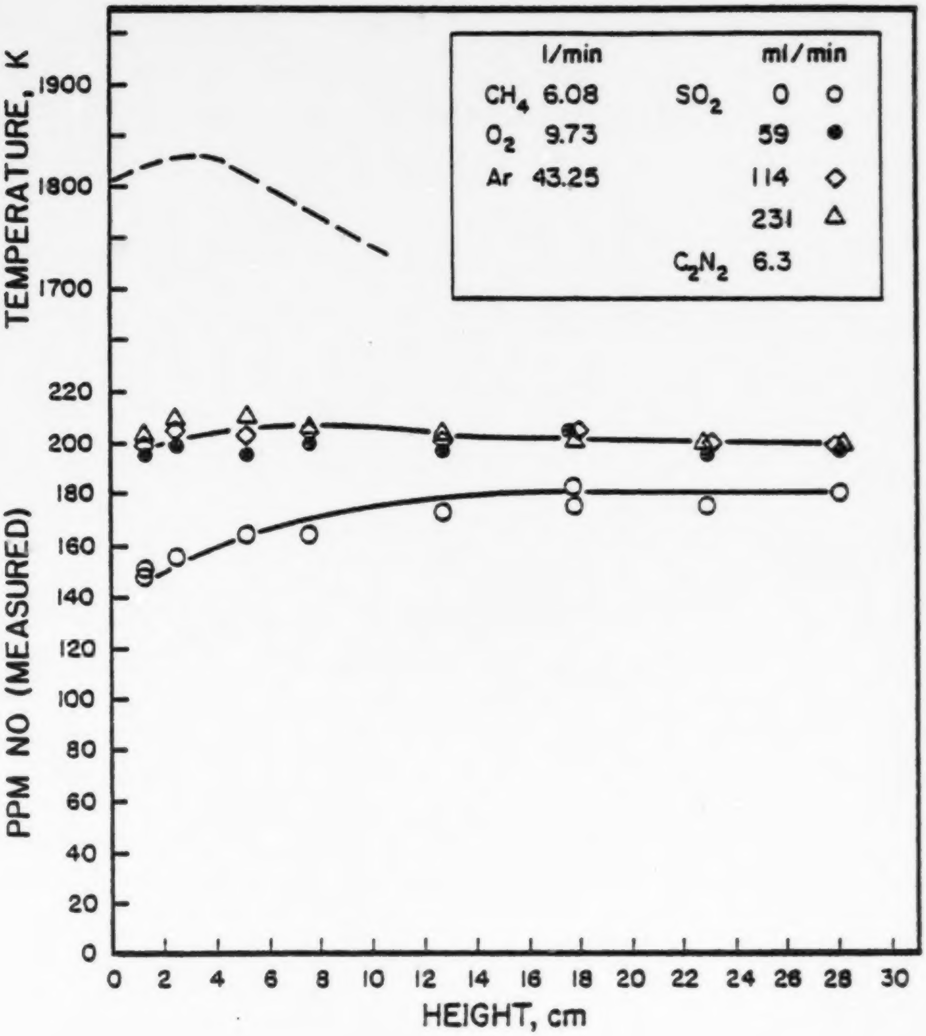

Figure 2.6-9 Laminar Premixed Flame: Stoichiometric Ratio 0.80 (0.21% Fuel N, 100% Conversion = 245 ppm, 1 cm = 3.53 ms at 1830 K, SO_2 as Fuel S).

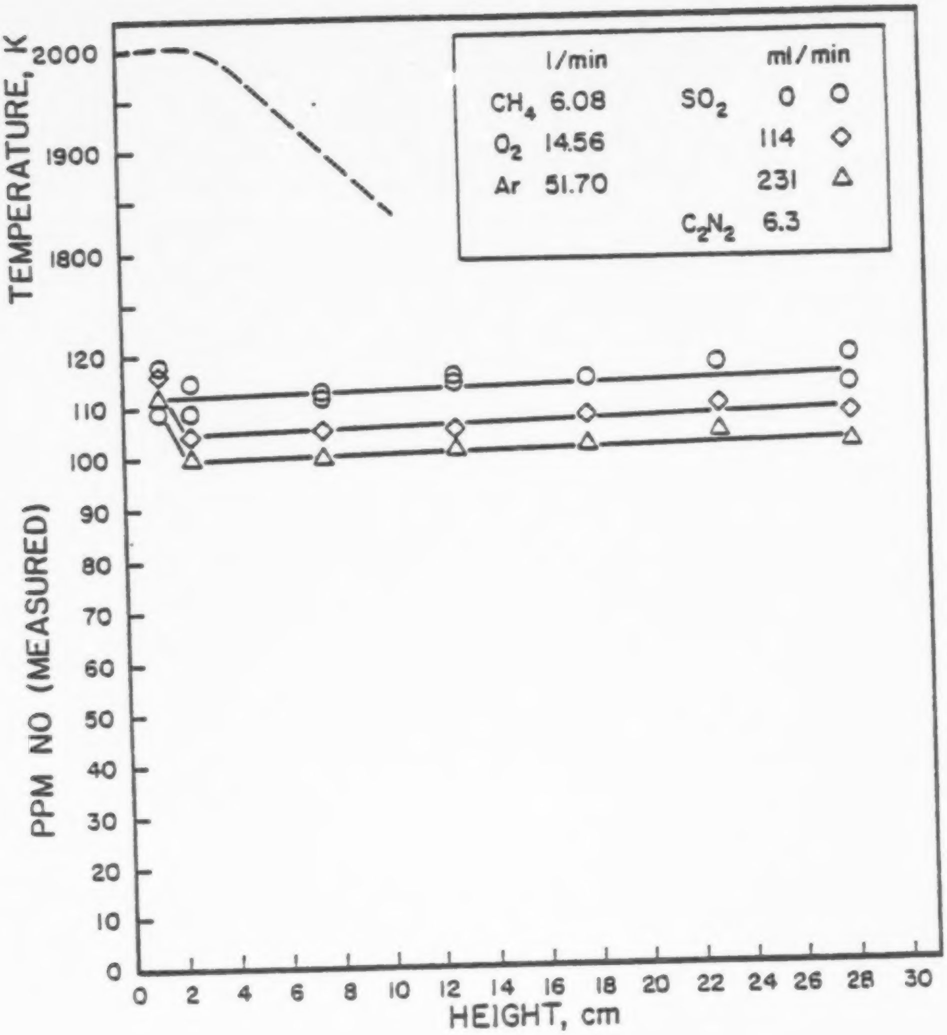

Figure 2.6-10 Laminar Premixed Flame: Stoichiometric Ratio 1.2 (0.21% Fuel N, 100% Conversion = 208 ppm NO, 1 cm = 2.74 ms at 2000 K, SO_2 as Fuel S).

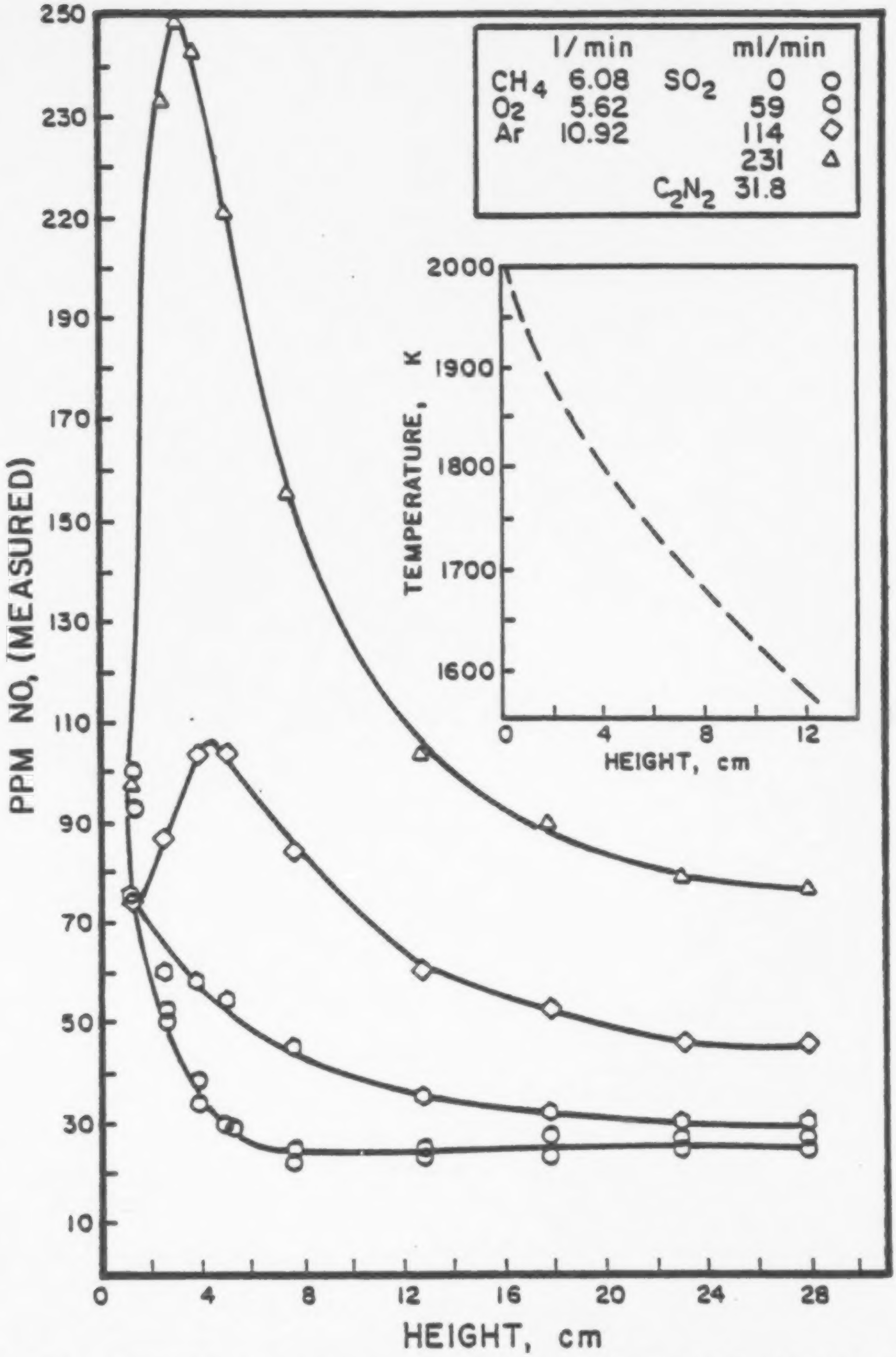

Figure 2.6-11 Laminar Premixed Flame: Stoichiometric Ratio 0.46 (1.05% Fuel N, 100% Conversion = 2559 ppm, 1 cm = 6.68 ms at 2000 K, SO_2 as Fuel S).

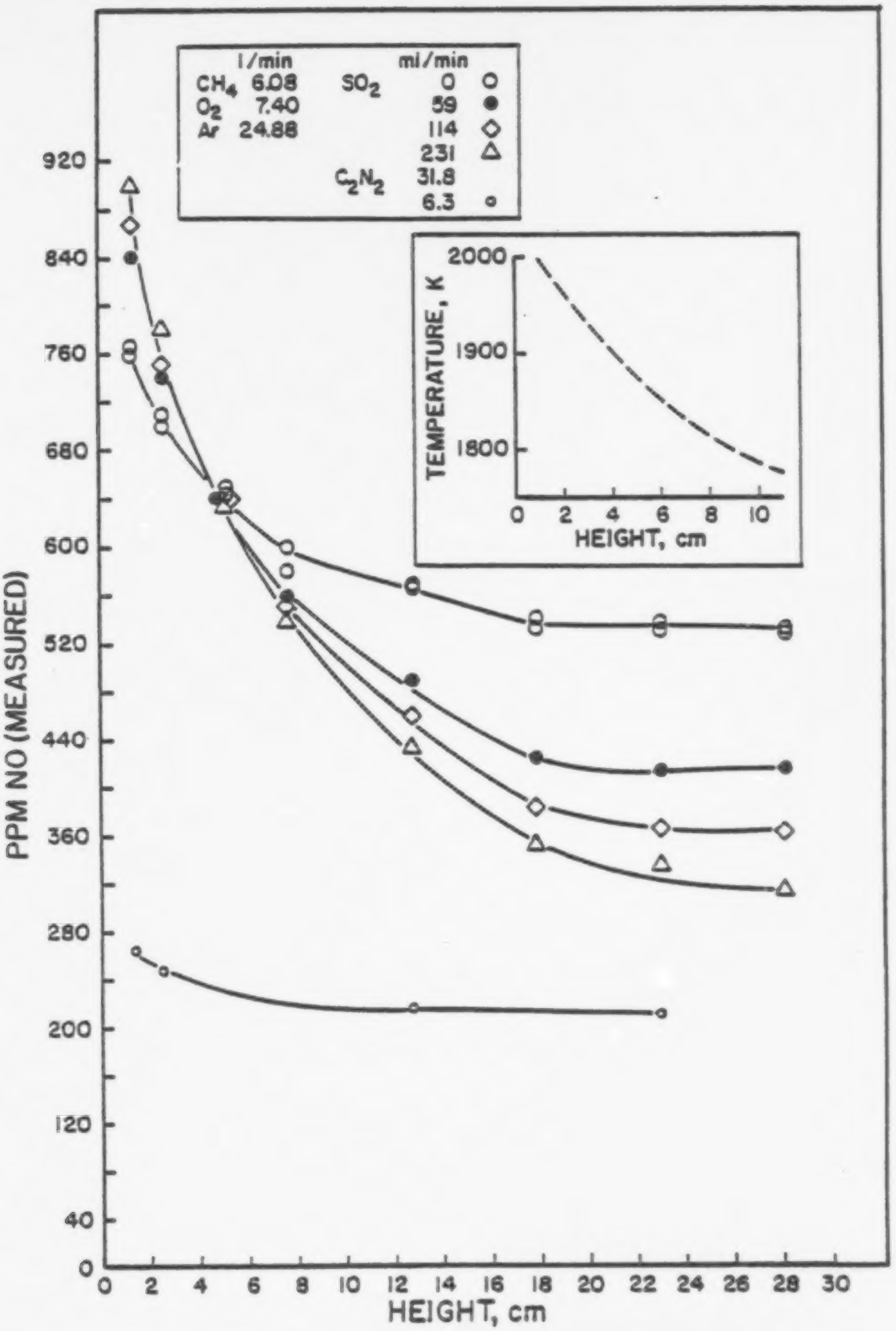

Figure 2.6-12 Laminar Premixed Flame: Stoichiometric Ratio 0.61 (1.05% Fuel N, 100% Conversion = 1751 ppm, 1 cm = 4.74 ms at 1940 K, SO_2 as Fuel S).

conversion of the fuel nitrogen were calculated using dry molar flow rates based on chemical equilibrium.

Figure 2.6-1 shows the results of a 0.40 stoichiometric ratio study. Most of the NO values, with and without the presence of sulfur, lie within a span of 2.5 ppm to 7.5 ppm. The base NO values have a rapid decline at the low sampling heights, indicating that the peak of the curve is very close to the grid. The curves of H_2S and various SO_2 additions are below the base line.

This study may be a limiting case for reliable data in the fuel-rich region. Such small quantities of NO are being formed that the reactions of fuel nitrogen and fuel sulfur are not possible.

During the course of this study, the cooled probe had become very sooty on the outside. Probably more soot had collected on its inside, or at least near the tip. Perhaps the combination of soot and sulfur caused, or contributed to, the NO/SO_x reduction effect in this figure.

Figure 2.6-2 shows NO values from a study at 0.46 stoichiometric ratio. The open symbols refer to points sampled with the cooled probe. The darkened symbols indicate sampling done with the hot probe. The base NO values show the probe effect. That is, the base NO values taken with the hot probe lie below the NO values at the lowest SO_2 addition. In comparison, the cooled probe yields the same base NO values as those at the lowest SO_2 addition. The figure indicates that differences in probe behaviors are not apparent at the higher SO_2 additions, where both the hot and cooled probes yield the same NO readings.

The lowest SO_2 addition does not change the NO values from their base line level. However, the two higher SO_2 additions, corresponding to 1.88 and 3.80 mole percent of the methane flow, significantly enhance the NO emissions. The curves exhibit sharp peaks near the 4 cm height, reaching maximums of 70 ppm and 130 ppm NO. They follow a rapid decay, achieving exhaust values near the 18 cm height of 35 ppm and 40 ppm NO. Even in this exhaust region, where temperatures are below 1600'K, the enhancement of NO is still apparent.

Figure 2.6-3 shows another study at stoichiometric ratio 0.46 with SO_2 as the sulfur additive. The curves duplicate the trends of the previous figure although some differences are noticeable. The peaks of the two higher SO_2 additions are 30 ppm lower than their peaks in Figure 2.6-2. The peaks occur at 5 cm. This can be explained by the movement of the flame front by the increased argon flow, 11 l/min in this figure compared to 9 l/min of Figure 2.6-2. The curves decay to exahust values of 40 ppm and 70 ppm NO; the values becoming constant at 23 cm.

Figure 2.6-4 shows a study of S.R. 0.46 but with H_2S as the sulfur additive. Hydrogen sulfide causes the same trends as does sulfur dioxide; however, the magnitude of the enhancement is less.

The next two figures show NO values at S.R. 0.54. Figure 2.6-5 deals with NO interactions with SO_2. The peaks in the curves have moved closer to the grid, between the heights of 1 and 2 cm. The curves show steep decays, grouping together at heights above 20 cm. However, the two highest sulfur levels no longer remain above the curves of lower sulfur levels. For example, the highest SO_2 addition, 276 ml/min, 4.54 mole percent of the methane, yields NO values that are equivalent to the base NO values in the higher flame regions.

Figure 2.6-6 shows that again H_2S gives the same trends as SO_2, but the peak NO values are lower in magnitude.

At S.R. 0.61, Figure 2.6-7, the inhibition effects of SO_2 and NO, hardly noticeable at the previous S.R. 0.54 studies, are now apparent. The enhancement effect of NO by the two high SO_2 additions, and the H_2S addition decreases from its peak at grid height of 270 ppm to the base NO value of 180 ppm at 13 cm. Above the 13 cm height, the various sulfur additions cause the NO values to be lower than their base NO points. This inhibition effect increases with increasing SO_2 levels. An equivalent mole percent of H_2S compared to SO_2, 3.75% H_2S to 3.80% SO_2, gives a greater inhibition of NO.

Sulfur additives at a more fuel-lean condition, S.R. 0.68, again influence both the production of NO in the grid region of the flame and the reduction of NO in the exhaust region. Figure 2.6-8 shows these effects. Both are not as strong as in the previous figure.

Figure 2.6-9 shows NO values of S.R. 0.80. All NO/SO_2 curves merged together, but lie above the base NO value. It was expected that the NO/SO_2 curves and the base NO curve would lie together. Instead, an enhancement is shown. Notice also that, in this study, the temperature profile has changed. In the previosu figures, the peak temperatures are at grid level. In this study, the highest temperature is recorded at a 3 cm height.

Figure 2.6-10, S.R. 1.20, shows all SO_2 additions inhibiting the NO emissions at all flame heights. The temperature profile remains fairly constant to the 3 cm height, where it peaks slightly, and then decreases rapidly.

Higher cyanogen levels were investigated at two stoichiometric ratios. Figure 2.6-11 shows a repeat of the study at S.R. 0.46, but for a cyanogen flow of 31 ml/min. The fuel nitrogen content is now 1.05 mole percent of the methane flow, 5 times the value of Figure 2.6-3. The peak NO values for the 1.88% SO_2 and the 3.80% SO_2 curves are 105 ppm and 250 ppm NO, respectively. These are approximately 1.5 and 2.0 times the corresponding values in Figure 2.6-3. The curve of base NO values drops from its peak at the grid to an exhaust value of 25 ppm NO at 8 cm.

The high fuel N study at S.R. 0.61 is shown in Figure 6.12. The peak NO values of the curves for 1.88% SO_2 and 3.80% SO_2 are 3.3 times the corresponding peaks in Figure 2.6.7. The base line follows a decline from its peak at the grid to its exhaust value of 530 ppm NO at 18 cm. For comparison, the base values were repeated for the low, 0.21%, fuel N case. This curve, at the bottom of the figure, has a much less pronounced decline.

2.7 Discussion

To aid in discussing the data of the previous chapter, a quantity termed percent yield is defined. This is the ratio of a measured ppm NO value to the ppm of NO corresponding to complete conversion of the fuel nitrogen. The basis for this calculation was the assumption of chemical equilibrium at the peak flame temperature and in the absence of sulfur additives. The equilibrium computer program used is described by Cortes-Chavez (1976).

Nitric oxide is seen to form and to decay rapidly in this study. The presented NO profiles indicate that without sulfur species the fuel N is converted immediately to NO. This growth is in the flame front located near the grid. In this region the temperature is also maximum. Thus, nitric oxide appears to form via a short-lived species present only at high temperatures. Fenimore (1971) proposed that this oxidant species was probably OH in fuel-rich flames. Instead of the OH initiating a reaction directly with the fuel nitrogen compound, he suggested a mechanism whereby a nitrogenous intermediate reacts rapidly with the oxidant to form NO:

$$I + Ox \rightarrow NO + \ldots \qquad (7.1)$$

where I is the nitrogeneous intermediate and Ox is the oxidant species (probably OH). Although the hydroxide species were not measured in this study equilibrium studies indeed confirm that OH exists at high temperatures and that its concentration in these studies would decay rapidly as do the temperature profiles.

The base NO curves flatten in the exhaust regions of the flame. Mechanistically, Fenimore further proposed that the NO once formed was reduced to N_2 by the same nitrogeneous intermediate responsible for its growth:

$$I + NO \rightarrow N_2 + \cdots \qquad (7.2)$$

Thus, NO is kinetically limited by competition between the NO-forming (reaction 7.1), and the destroying (reaction 7.2) reactions. In the reaction zone, the concentration of NO is low and that of the oxidant species is relatively high, causing reaction (7.1) to predominate. Then, as NO formation slows, either as Ox is all consumed, or as the reduction of NO becomes more important, the base NO curve achieves its exhaust values.

The nitrogeneous intermediate(s) is suggested to be the amine species (NH_i, $i = 0, 1, 2, 3$). Investigators (Haynes et al., 1975) have identified the cyano (CN) and the amine species as well as nitric oxide in the post-flame gases of fuel-rich hydrocarbon flames. Thus, the overall fuel nitrogen conversion is proposed to be

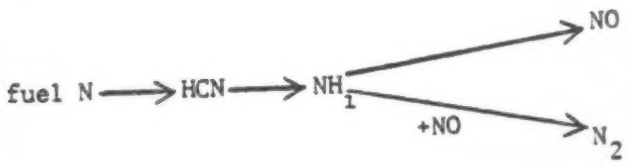

As predicted by equilibrium, and as shown by Haynes (1977), the NH_i system is temperature sensitive. As temperature is reduced, the amine species reaches its maximum concentration further downstream of the grid. Thus, in these studies, the rapid decrease in the temperature profile may imply a significant concentration of the species responsible for NO reduction in the exhaust regions of the flames.

With the addition of fuel sulfur, nitric oxide is again seen to form and to decay. However, distinct behavior of the NO profiles indicates a significant interaction between fuel sulfur and fuel nitrogen species. The NO profiles again peak in the early flame, but achieve values of magnitudes greater than their base values. This enhancement increases with the fuel richness, and with the amount of sulfur. Also, as the flame is made richer, the peaks tend to move away from the grid, indicating that sulfur species may lengthen the duration of a particular species in the flame front.

A plot of peak NO yields shown in Figure 2.7-1 emphasizes the dependency of the fuel sulfur and fuel nitrogen interactions on stoichiometric ratio. High levels of both SO_2 and H_2S, respectively 3.80% and 3.75% of the methane flow, significantly increase the peak yield of nitric oxide at fuel-rich conditions. At 0.55 S.R., the yield is doubled by the addition of sulfur. As suggested by the figure, the effect of sulfur on peak NO formation disappears at a fuel-rich limit of 0.40 S.R., and at a fuel-lean limit of 1.0 S.R. The fuel-lean limit was noted by DeSoete (1975). At stoichiometric ratios greater than 1.0, the formation of NO early in the flame is slightly inhibited.

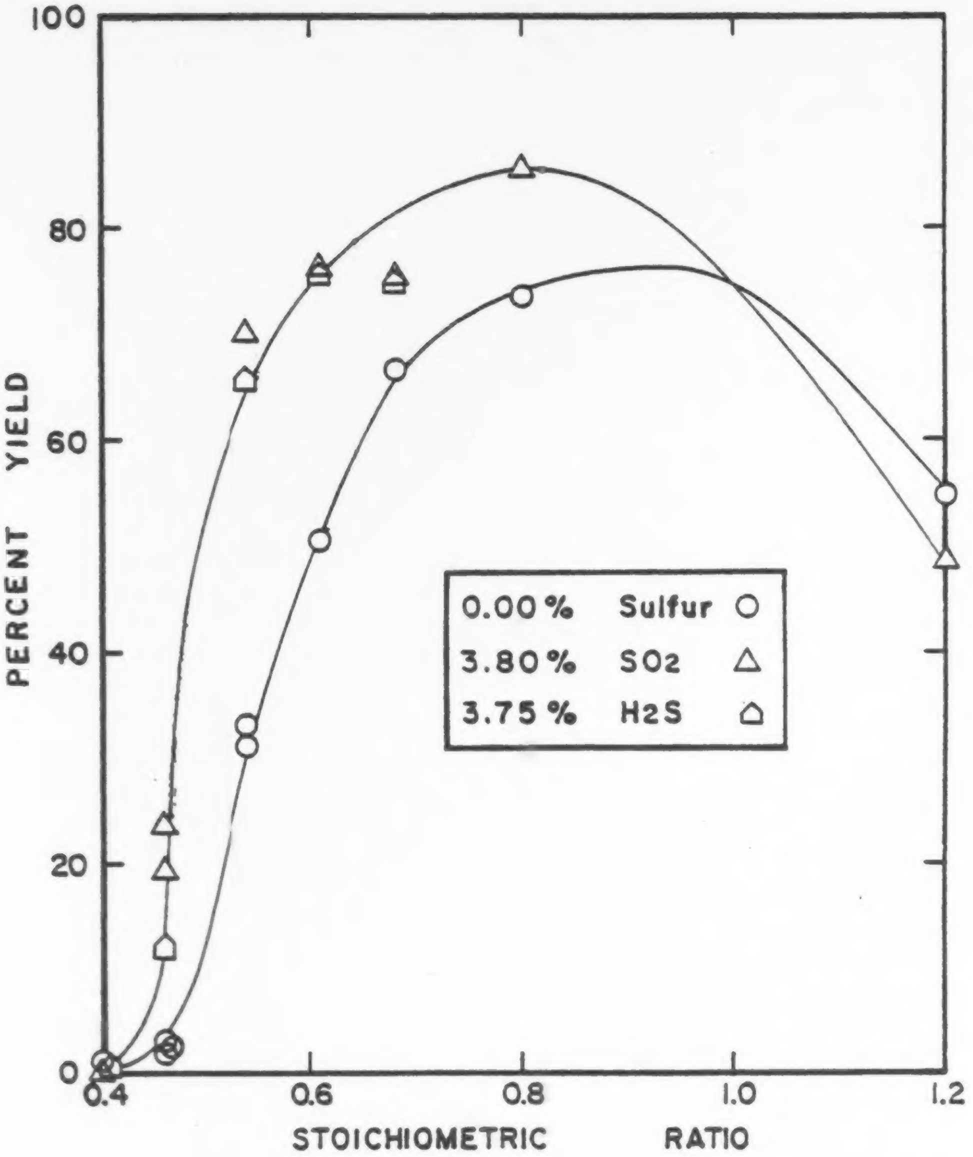

Figure 2.7-1 Enhancement of Peak Fuel NO by Sulfur Additives at Fuel-Rich Conditions. -- Sulfur given as mole percent of inlet fuel.

The two sulfur additives used in these studies had similar effects on the NO profiles. However, SO_2 caused a greater increase in the production of NO than did an equivalent molar flow of H_2S. For fuel-rich conditions, Figure 2.7-2 indeed shows that, with sulfur levels above 2 mole percent of the methane, SO_2 enhances the peak yield of NO more than H_2S. However, it should be noted that addition of H_2S decreases the stoichiometric ratio for given CH_4 and O_2 flow rates.

The figure also shows that there is an asymptotic yield of NO as sulfur additive level is increased. This trend is more apparent at fuel-leaner conditions.

Once nitric oxide has reached its peak production with sulfur present, it follows a decay in the exhaust region of the post-flame gases. Indeed, in the NO profiles leaner than 0.54 S.R., the reduction of NO continues to a greater extent than that achieved by the base NO values. H_2S affects the reduction more than SO_2. Figure 2.7-3 shows this effect for different stoichiometric ratios. There are limits for the fuel-rich conditions at 0.40 S.R., and at 1.0 S.R. All fuel-lean conditions exhibit a slight reduction of NO in the exhaust regions.

In view of the current theories of fuel NO formation, the observed SO_x/NO_x interactions may be explained in two ways. Since the formation of NO is greatly enhanced in the early portion of the flame, the sulfur species becomes involved in reactions which increase the amount or type of oxidant necessary to convert fuel N to NO. According to equilibrium calculations, the OH species is not affected by the presence of sulfur. However, under actual flame conditions, super-equilibrium

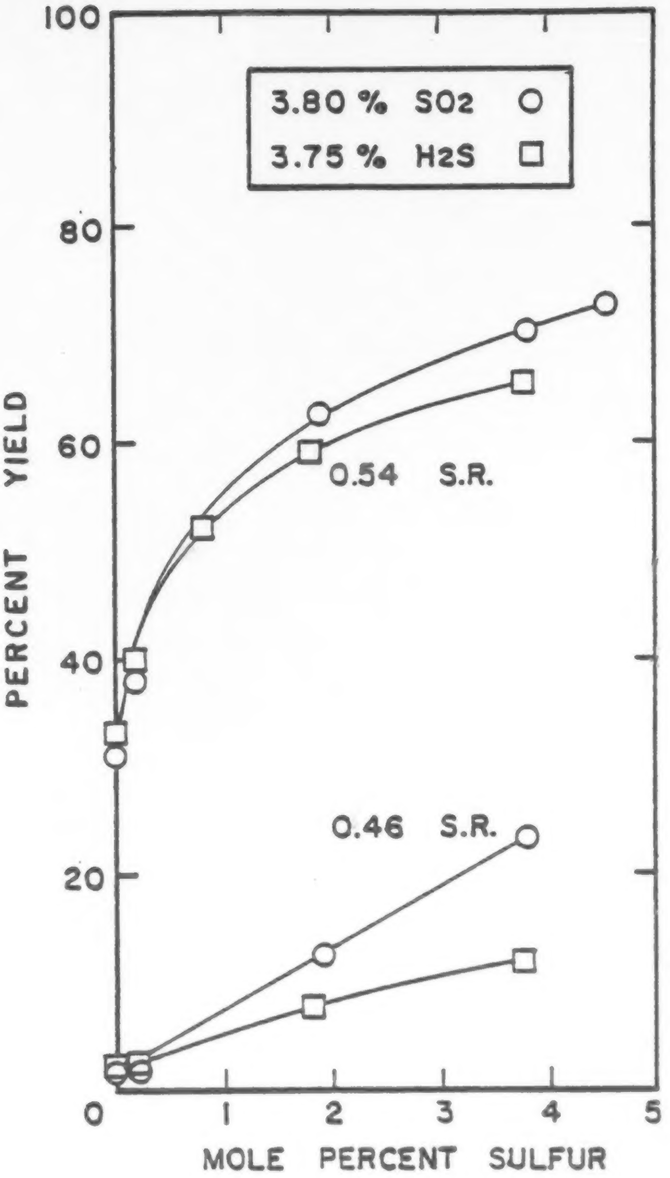

Figure 2.7-2 Higher Mole Percent Fuel Sulfur Contents Increase Peak Fuel NO Yields for Two Rich Stoichiometric Ratios.

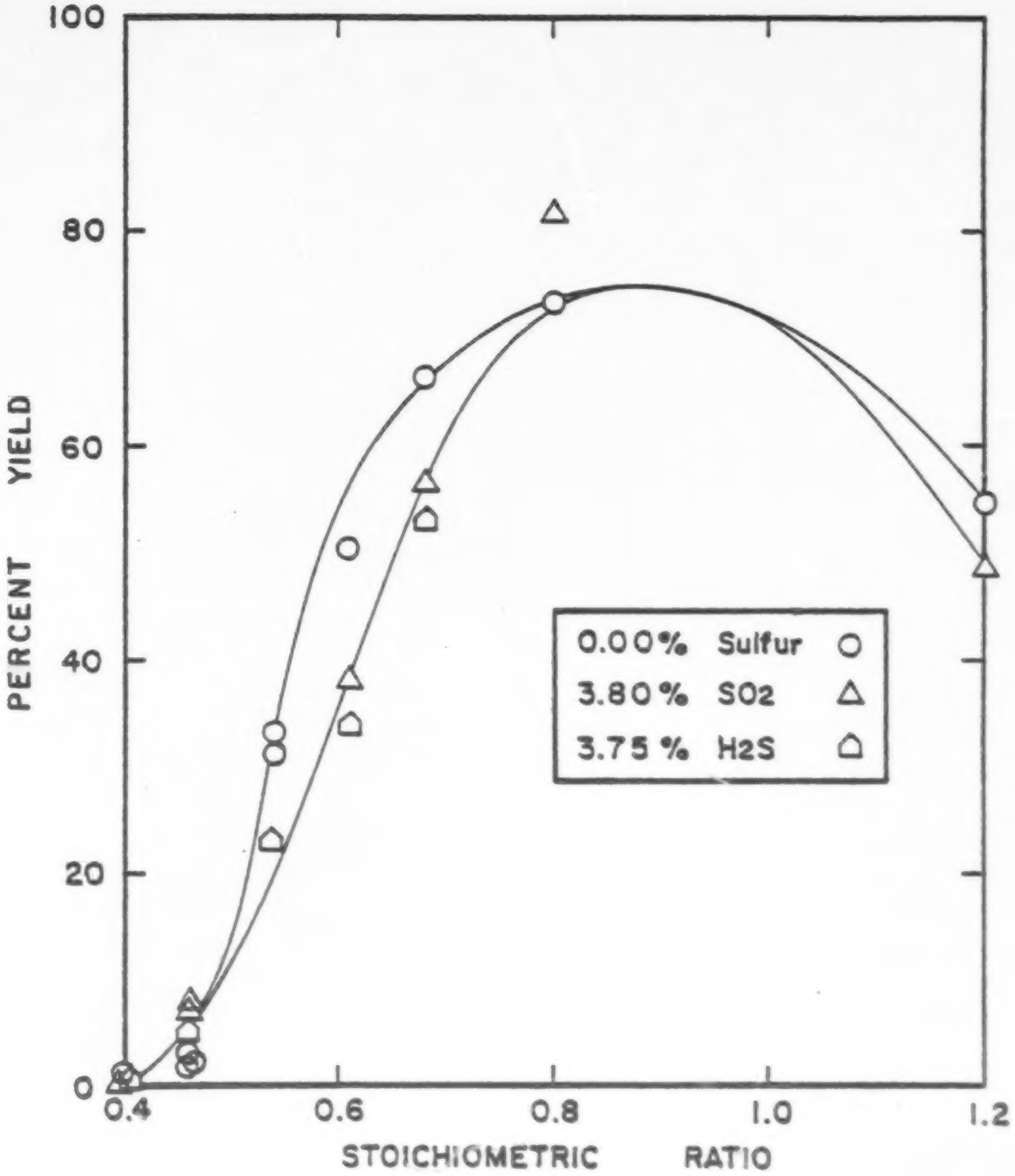

Figure 2.7-3 Sulfur Additives Cause a Greater Reduction in Exhaust Fuel NO at Most Stoichiometric Ratios.

concentration of hydroxyl radical may be produced. Alternatively, a new oxidant may be introduced or become important. Referring again to equilibrium studies of fuel-rich conditions, the oxygen atom concentration does increase slightly due to the addition of sulfur species. Even more significant is the increase in the sulfur radical SO to amounts of 10 times the OH concentration at high temperatures. Its reaction with the amine system could yield NO:

$$NH + SO \rightarrow NO + SH \tag{7.3}$$

$$N + SO \rightarrow NO + S \tag{7.4}$$

The rapid decay following the initial formation of NO is due to the reduction mechanism by a nitrogeneous species as proposed by Fenimore (reaction 7.2). Perhaps additional sulfur compounds aid in this reduction scheme:

$$NS + NO \rightarrow N_2 + SO \tag{7.5}$$

A second explanation of the SO_x/NO_x interactions deals with the effect of sulfur species on the nitrogeneous intermediate involved in reactions (7.1) and (7.2). Sulfur species enable the conversion of fuel nitrogen to I to be more efficient. Thus, this intermediate in increased concentrations in the flame front reacts with the oxidant species to give significant NO formation. In the post-flame region, the nitrogeneous intermediate is again involved in the reduction of NO. Due to its higher concentration, with additional effects by sulfur species possible, the reduction of NO occurs below the values observed in the absence of sulfur.

As already mentioned, the amine system is sensitive to lower temperatures. Thus, the addition of sulfur may decrease the temperature profile to an extent that permits the reactions with the nitrogeneous intermediate, recognizing it as part of the amine system, to become more significant in all regions of the flame. In the studies presented, flame temperatures were variable and no attempts were made to control this parameter. However, Figure 2.7-4 suggests some preliminary indications that low temperature interactions become important upon the addition of sulfur compounds. Peak temperatures of three studies at S.R. 0.46 varied within a narrow range of 100 K. Yields of base NO did not appear temperature sensitive within this range. However, yields at 1.88% and 3.80% SO_2 tended to increase as temperature decreased.

The two explanations proposed for the fuel sulfur interactions with the fuel NO mechanism focus either on reactions with the oxidant species or on reactions with the amine species. Evidence for occurrence of both possibilities were presented. However, to clarify the importance of either explanation, a study of intermediates is appropriate. The flame history of amine species, say NH_3, of nitrogen species, N_2, and of sulfur species would be useful for further understanding of the fuel N mechanism.

The NO profiles presented for fuel-rich flames with increased fuel nitrogen show higher concentrations of base NO leaving the reaction

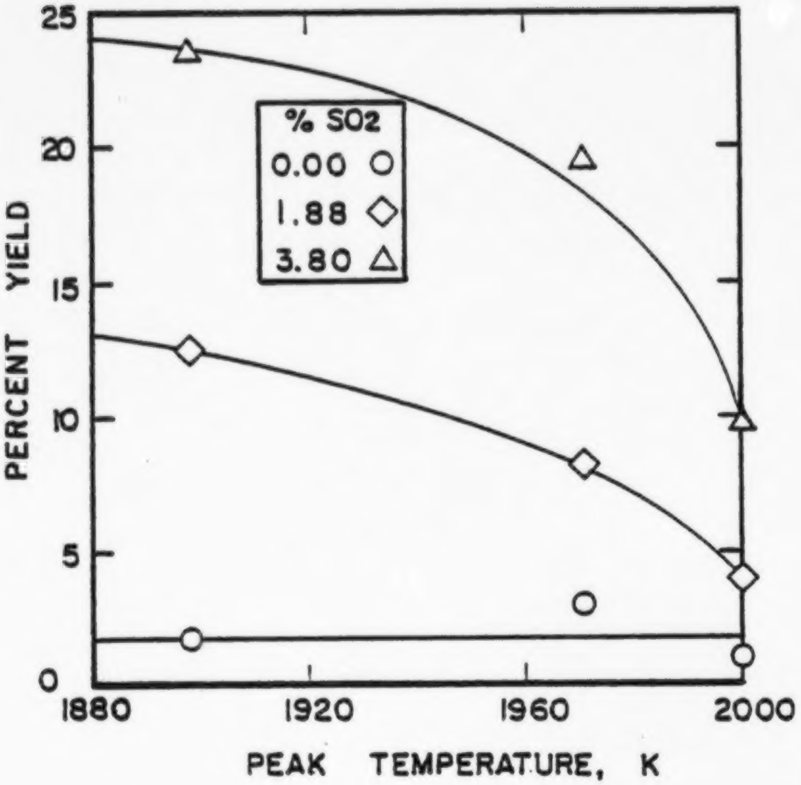

Figure 2.7-4 Peak NO Yields in the Presence of SO_2 Decrease with Increasing Peak Flame Temperatures. -- 0.46 stoichiometric ratic.

zone, but decaying rapidly to exhaust values. With sulfur species present, the trends of NO formation and reduction resemble those at the lower fuel N. A comparison of yields indicates the percent conversion of fuel N to NO decreases with increasing fuel nitrogen concentration.

An immediate application of these studies might be in the staged combustion of pulverized coal, where homogeneous fuel nitrogen mechanisms are likely to occur under fuel rich conditions in the presence of sulfur. However, the present work which focuses on NO profiles alone, is insufficient to determine the fate of other XN species, such as NH_3 and HCN. This latter aspect can be equally (or possibly even more) important in determining the optimum staged combustion configuration for fuels containing both chemically bound sulfur and nitrogen.

Furthermore, in order to elucidate kinetic mechanisms pertinent to the phenomena observed in this work, it is essential to obtain measurements of all nitrogeneous species, and if possible, to close the nitrogen balance. The effect of fuel sulfur on N_2 formation is, in many respects, of more practical interest than that on NO formation and destruction. The purpose of combustion modifications is to convert fuel N to N_2 rather than merely to inhibit NO formation (at the expense of other nitrogenous species). In view of this, further work is required to determine the role of fuel sulfur in converting fuel nitrogen not only to NO, but also to HCN, NH_3 and N_2. Subsequent sections of this report are concerned with this aspect of the problem.

2.8 References for Section 2

Axworthy, A. E., G. T. Schneider, M. D. Shuman, and V. H. Dayan. "Chemistry of Fuel Nitrogen Conversion to Nitrogen Oxides in Combustion," Rocketdyne/Rockwell International Report EPA-600/2-76-039 (NTIS PB 250-373) (1976).

Braker, W., and A. L. Mossman. Matheson Gas Data Book, 5th Edition. New Jersey: Matheson Gas Products (1971).

Corley, T. L. "Fuel Sulfur Effects on NOx Formation in Turbulent Diffusion Flames." M.S. Thesis, University of Arizona, Tucson, (1976).

Cortes-Chavez, R. N. "A Computer Program for the Calculation of Complex Chemical Equilibria." M.S. Thesis, University of Arizona, Tucson (1976).

Cullis, C. F., and M. F. R. Mulcahey. "The Kinetics of Combustion of Gaseous Sulfur Compounds." Comb. Flame, 18 (1972).

deSoete, G. European Combustion Symposium, 693 (1973).

deSoete, G. G. "Overall Reaction Rates of NO and N_2 Formation from Fuel Nitrogen." Fifteenth Symposium (International) on Combustion, Pittsburgh, pp. 1093-1102 (1975).

Durie, R. A., G. M. Johnson, and M. Y. Smith. "The Effect of Sulfur Dioxide on Hydrogen-Atom Recombination in the Burnt Gas of Premixed Fuel-Rich Propane-Oxygen-Nitrogen Flames." Comb. Flame, 17 (1971).

Fenimore, C. P. "Formation of Nitric Oxide in Premixed Hydrocarbon Flames." Thirteenth Symposium (International) on Combustion, Pittsburgh (1971).

Fenimore, C. P. "Reactions of Fuel-Nitrogen in Rich Flame Gases." Comb. Flame, 26, 249 (1976).

Griffiths, E., and J. H. Awbery. "The Measurement of Flame Temperatures." Proc. Roy. Soc., A123, 401-421 (1929).

Haynes, B. B. "The Formation and Behavior of Nitrogen Species in Fuel Rich Hydrocarbon Flames." Ph.D. Dissertation, University of New South Wales, Sydney, Australia, 1975.

Haynes, B. S. "Reactions of Ammonia and Nitric Oxide in the Burnt Gases of Fuel-Rich Hydrocarbon-Air Flames." Comb. Flame, 28, 81 (1977).

Haynes, B. S., D. Iverach, and N. Y. Kirov. "The Behavior of Nitrogen Species in Fuel-Rich Hydrocarbon Flames." Fifteenth Symposium (International) on Combustion, Pittsburgh (1975).

Levy, A., and E. L. Merryman. "The Microstructure of Hydrogen Sulfide Flames." Comb. Flame, 9 (1965).

Merryman, E. L., and A. Levy. "Kinetics of Sulfur-Oxide Formation in Flames. II. Low Pressure H_2S Flames." J. Air Poll. Control Assoc., 17 (1967).

Morcomb, J.T., "Interactions of Fuel Sulfur and Fuel Nitrogen in Fuel Rich Flames", MS Thesis, University of Arizona (1977).

Morley, C. "The Formation and Destruction of Hydrogen Cyanide from Atmospheric and Fuel Nitrogen in Rich Atmospheric-Pressure Flames." Comb. Flame, 27, 187 (1976).

Perry, R. H., and C. H. Chilton. Chemical Engineers' Handbook, 5th Edition. New York: McGraw-Hill Book Company, 1973.

Pershing, D. W., G. B. Martin, and E. E. Berkau. "Influence of Design Variables on the Production of Thermal and Fuel NO from Residual Oil and Coal Combustion." AIChE Symposium Series No. 148, 71 (1975).

Sachyan, G. A., Y. M. Gershenzon, and A. B. Nalbandyan. "Multistage Nature of Combustion in Dilute Hydrogen Sulfide Flames." Dokl. Aked. Nauk SSSR, 175 (1967) [English version, 175 (1967)].

Sarofim, A. F., G. C. Williams, M. Modell, and S. M. Slater. "Conversion of Fuel Nitrogen to Nitric Oxide in Premixed and Diffusion Flames." AIChE Symposium Series No. 148, 71 (1975).

Schmidt, H. "Verification of Radiation Laws of Bunsen Flames." Verhandl. Deutsch. Physik. Ges., 11, 87-102 (1909).

Summers, R. L. "NO_x Destruction by CO in NO_x to NO Converters of Chemiluminescent NO Analyzers." NASA Technical Memorandum NASA TMX-74480, July 1976.

Wendt, J. O. L., and J. M. Ekmann. "Effect of Fuel Sulfur Species on Nitrogen Oxide Emissions from Premixed Flames." Comb. Flame, 25 (1975).

Wendt, J. O. L., and C. V. Sternling. "Catalysis of SO_2 Oxidation by Nitrogen Oxides." Comb. Flame, 21 (1973).

3. POST FLAME BEHAVIOR OF NITROGENOUS SPECIES IN THE PRESENCE OF FUEL SULFUR. I. RICH, MOIST, $CO/Ar/O_2$ FLAMES

3.1 Introduction

Kinetic mechanisms governing the fate of fuel nitrogen during the fuel rich gas phase combustion of various fuels have been intensively studied by a number of investigators [1]-[7]. These studies, conducted primarily on hydrocarbon flames, have revealed two main paths for the formation of N_2 from fuel nitrogen:

$$N + NO \rightarrow N_2 + O \quad \text{[Reverse Zeldovich]} \qquad (1)$$

and

$$NO + NH_i \dashrightarrow N_2 + \qquad (2)$$

Recent work by Morley [8] indicates that, in a high temperature (1790-2100K) hydrogen flame, reaction (2) does not play an important role.

This chapter focuses on N_2 formation mechanisms occurring in the post flame gases and in the presence of sulfur compounds in fuel rich premixed flat flames with CO (with a known trace of hydrogen) as the fuel. Motivation for this work lies in 1) the observed reduction and decay of NO that occurs in the first stage of a staged pulverized coal combustor [9] and 2) previous work with hydrocarbon fuels presented in Section 2 that indicated significant post flame behavior of nitrogenous species in the presence of sulfur. Carbon monoxide was chosen as the fuel in the experiments reported here because first, its kinetics are relatively well understood; second, the phenomena observed and modeled here comprise a subset of those observed in the earlier work on hydrocarbon flames; and third, the results may pertain to the combustion of low Btu gases. Furthermore, in "premixed" pulverized coal char flames, a reduction of NO was observed [11] in the absence of ammonia, hydrocarbons or large quantitites of hydrogen, and although that reduction was atrributed to an heterogeneous mechanism [11] it is important to determine whether equivalent homogeneous mechanisms involving primarily CO oxidation could play a role under similar conditions.

In this work, post flame mechanisms destroying NO and forming N_2 were examined both experimentally and theoretically. The experimental results focus on closure of the nitrogen balance and so considerable effort was expended to obtain accurate measurements of N_2 in the ppm range. This is described in some detail. It was felt that closure to a given degree of accuracy would confirm that, indeed, all major nitrogenous species had been sought and accounted for. The specific topics addressed in the experimental portion of this work are 1) the effect of fuel nitrogen type, 2) the effect of temperature and 3) the influence of fuel sulfur on NO destruction and N_2 formation rates.

Theoretical modeling employed detailed chemical kinetics and focused entirely on the post flame region. Therefore, no attempt was made to model the in-flame species profiles in detail. In this work the purpose of kinetics modeling was not to use the experimental data obtained to derive specific rate coefficients but rather to determine consistency between our data and one of the best available sets of kinetic mechanisms and rates. Detailed kinetic mechanisms from the literature comprise many more reactions than are absolutely necessary to explain the observed phenomena. For example, mechanisms leading to NO destruction and N_2 formation may involve up to 41 reactions in addition to those describing CO combustion. In using kinetic modeling to obtain insight into which reactions are controlling the observed phenomena, we employed the following approach: first one of the currently most comprehensive set of reactions describing NO formation and N_2 destruction was drawn from the literature and utilized to determine consistency with our data; second, the reactions and species which did not contribute to the predicted NO destruction and N_2 formation rates were eliminated and results from the reduced set were compared to data. This approach allowed the relative importance of reactions (1) and (2) to be determined, as well as the applicability of pseudo stationary state hypotheses for intermediate species and other simplifications to be examined. From this, a simplified mechanism describing the fate of nitrogenous species in the post flame region of moist CO flames was deduced.

3.2 Experimental Burner

The premixed flat flame burner was similar to that utilized in section 2 of this report. Nominally 5 cm ID, with a coarse 10x10 mesh stainless screen for flame stabilization, the burner was enclosed in a 15 cm ID, 60 cm high quartz chimney, the inside surfaces of which were purged with Argon in order to prevent soot deposition and entrainment of room air. The quartz chimney was enclosed at the top by a firebrick which allowed the Argon purge and much of the exhaust flow to exit through 10 6 mm holes, situated near the quartz wall, and the remaining exhaust flow, including the center streamline to exit through a 2.5 cm hole in the center. This configuration allowed radial species profiles to be flat over at least one quarter of the burner diameter up to an axial distance of 12.7 cm from the grid.

Temperature measurements were made with sodium D-line reversal and flows of major (O_2, CO, Ar) and minor species (H_2, C_2N_2, NH_3, NO, SO_2) were controlled and metered with sonic orifices, rotameters and laminar flow elements where appropriate. In order to attempt a nitrogen closure, all gases utilized, including chromatograph carrier gas, had to be essentially N_2 free (less than 20 ppm). SO_2 bottles were bled prior to use in order to purge dissolved air in the liquid SO_2.

Sampling and Analysis

Samples were withdrawn along the centerline axis of the flame through a water cooled quartz probe with a 1.5 mm orifice. The normal sampling rate was 1.3 liters/minute. Water, if present, did not condense in the probe. The sample was then delivered either to a 1 ml sample loop of a Perkin Elmer Sigma 2 gas chromatograph, or to a Thermo Electron Model 10 NO/NO_x Chemiluminescence Analyzer as shown on Figure 3.2.1. The gas in the chromatograph sample loop was pressurized to 15 psi using an inert gas supply and delay tubing, as shown. Samples at this pressure were found to cause minimum pressure disturbances in the detectors when the gas sample valve was turned, and the delay tubing prevented the pressurizing gas from entering the sample loop.

A chromatographic procedure was developed for measurement of a large number of non-polar and polar flue gas constituents, some of which were present in trace quantities. Emphasis was on measurement of trace quantities of N_2. Two columns were used: 45-60 mesh molecular sieve 5A, 3.6 m long, 0.635 cm OD for the non-polar species; Porapack T, 1.8 m long, 0.317 cm OD for the polar species. An expendable molecular sieve trap prevented polar species from irreversibly contaminating the 1.8 m molecular sieve column.

Temperature programming was rejected because of baseline stability problems at the very high detector sensitivities required in this work. The best isothermal method of operation was that of column switching (as contrasted to sequence reversal or column trapping) in which two samples are used to gain complete analysis at one point in the flame. The sample is directed either to the molecular seive or to the Porapak column, while the other column not in use, acts as a conduit for the reference carrier gas. Throughout, great

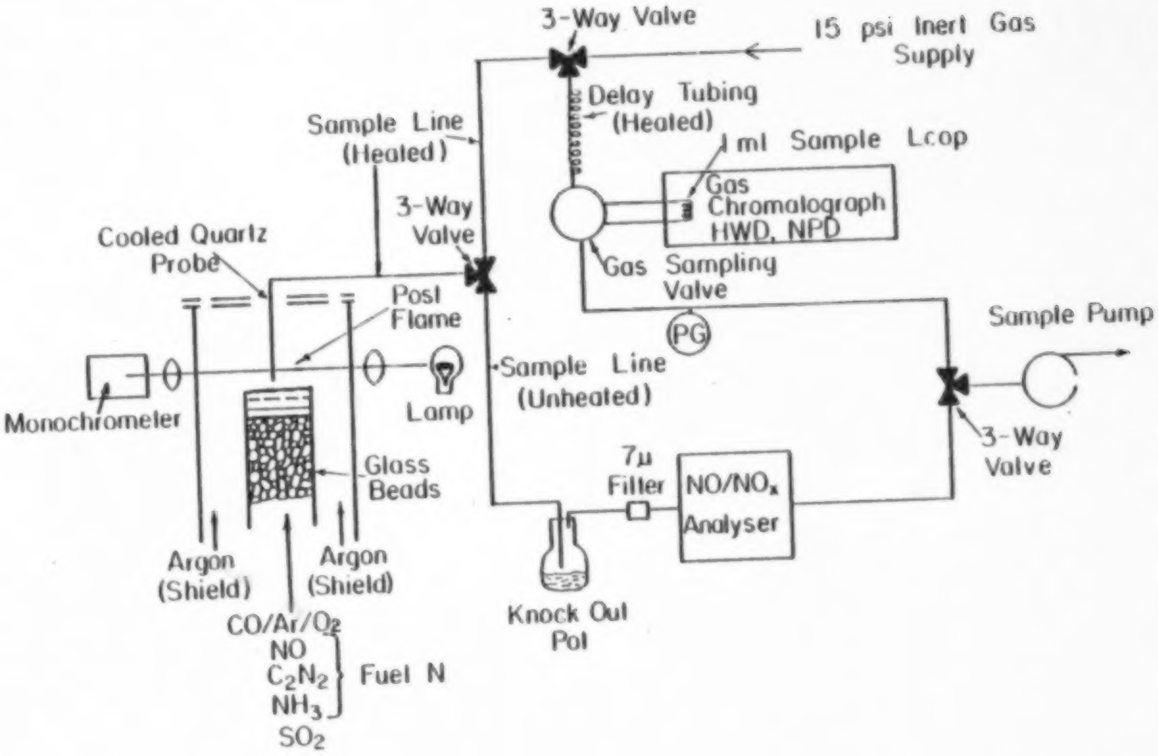
3-Way Valve
15 psi Inert Gas Supply
Delay Tubing (Heated)
1 ml Sample Loop
Sample Line (Heated)
Gas Chromatograph HWD, NPD
3-Way Valve
Cooled Quartz Probe
Gas Sampling Valve
Post Flame
Sample Pump
PG
Sample Line (Unheated)
Monochrometer
Lamp
3-Way Valve
Glass Beads
7µ Filter
NO/NO$_x$ Analyser
Argon (Shield)
Argon (Shield)
Knock Out Pot
CO/Ar/O$_2$
NO
C$_2$N$_2$
NH$_3$
Fuel N
SO$_2$

Figure 3.2-1 Schematic of flat flame apparatus and analysis system

care was exercised to prevent even minute air leaks into any part of the sampling systems or carrier gas.

Figure 3.2-2 shows a chromatogram of a sample containing 1000 ppm H_2, 1000 ppm N_2 and 1000 ppm CO in Argon. The N_2 is eluted on the Argon tail. The lower limits of detection of N_2 and CO are 20 ppm for each species. Precision in N_2 concentration measurement was ±20 ppm, although this did depend on the relative N_2 to Argon concentration and the height of the Argon chromatogram tail. Oven temperature was 110°C, hot wire current setting was at 240 mA and carrier gas flow rate was 60 ml/min. A hot wire detector was used for permanent gases, while a nitrogen-phosphorous detector, which was specific to compounds with a C-N bond, was used to increase sensitivity for trace HCN levels. In the absence of appreciable quantities of water, ammonia could be separated on the Porapak column. Since all flames studied here were hydrogen poor, very little water was formed and in these cases ammonia was detectable with the hot wire detector. This would not be true for gas samples with a higher water concentration, as in hydrocarbon flames.

3.3 Experimental Results

Results from six flames are presented. Flames 1 through 4, conditions for which are shown in Table 3.3-1, were at high temperature. Flames 5 and 6 had significantly lower temperatures, due to increased diluent flows, and had inlet conditions shown in Table 3.3-2. The influence of fuel nitrogen species type on post flame species profiles was examined at both high (Flames 1 and 2) and low (Flames 5 and 6) temperatures. Only at high temperatures was a decay of NO in the post flame region observed. Therefore, investigation of the effect of fuel sulfur on the post flame distribution of nitrogenous species was restricted to high temperature conditions and Flames 3 and 4 were used to study

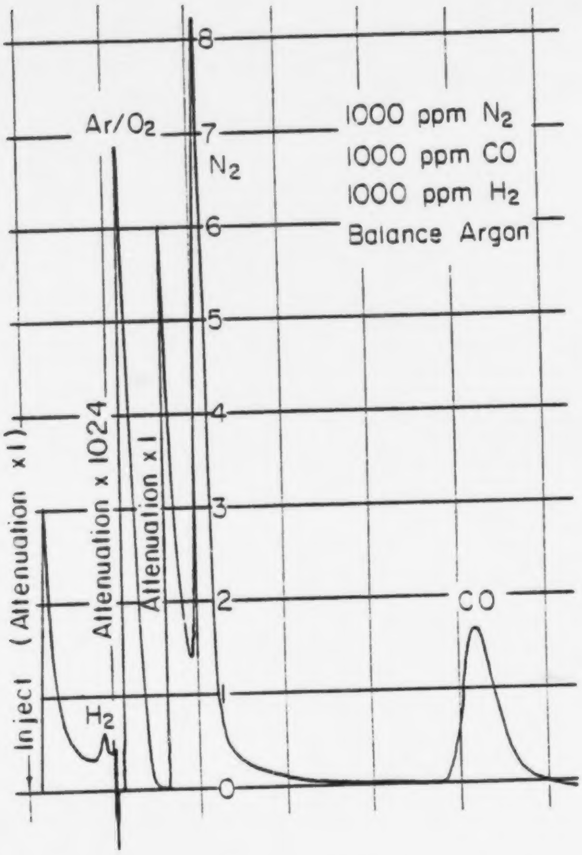

Figure 3.2-2 Sample chromatogram for trace N_2 analysis

Table 3.3-1 High Temperature Flame Conditions

	Flame 1	Flame 2	Flame 3	Flame 4
Flow Rates (sml/min, 1 atm. 298K)				
CO	15040	15040	15030	15040
O_2	3450	3450	3450	3450
Argon	8060	7720	10640	9690
H_2	12.8	12.8	12.8	12.8
Fuel Nitrogen Type	NO	C_2N_2	C_2N_2	C_2N_2
Flow Rate (sml/min)	98.2	51.4	52.2	6.6
Sulfur Added as SO_2 A)	NO	NO	NO	NO
B)	--	--	YES	YES
Flow Rate SO_2	--	--	255.0	252.0
ϕ (equivalence ratio)	2.17	2.17	2.17	2.17

Table 3.3-2 Low Temperature Flame Conditions

	Flame 5	Flame 6
Flow Rates (sml/min, 1 atm., 298K)		
CO	15040	15020
O_2	3450	3440
Argon	21840	24240
H_2	12.8	165.1
Fuel Nitrogen Type	NH_3	NO
Flow Rate (sml/min)	99.2	100.2
ϕ (equivalence ratio)	2.17	2.17

this facet of the problem for two different inlet levels of fuel nitrogen as C_2N_2.

a) NO Destruction at High Temperature

The major species for Flame 1, and the temperature profile are shown in Figure 3.3-1. The measured values of CO, CO_2 and H_2O in the post flame region were very close to their equilibrium values denoted in the figure by shaded symbols. The adiabatic flame temperature was 2613 K and measured temperatures were therefore correspondingly high, decaying from 2500 K to 2000 K over 8 cm (approximately 50 msec). Flames 2 through 4 gave similar results for major species.

Profiles of NO, N_2 and the nitrogen balance for C_2N_2 and NO as fuel nitrogen compounds are shown in Figure 3.3-2. The nitrogen balance was satisfied to within 7% in both cases over most of the post flame region of interest. Near the flame front, the nitrogen balance was low, possibly because of the steep gradients in that region. Very far from the flame front, at a distance greater than 8 cm, the nitrogen balance was occasionally high due to sporadic injestion of tiny amounts of surrounding air. The NO and N_2 post flame profiles are very similar for both C_2N_2 and NO as the parent nitrogen compound. In each case NO decays in the post flame zone, to form only N_2. There was no evidence of NH_3 or HCN at any point in this region, which is not surprising given the hydrogen poor composition of the fuel and the absence of hydrocarbons. Therefore, the post flame behavior of fuel nitrogen in these flames can probably be simply modeled by considering routes from NO to N_2 only, regardless of the nature of the fuel nitrogen compound. The in-flame conversions of fuel nitrogen to NO and N_2 were also remarkably independent of fuel nitrogen species type, a result which is consistent with Morley's [2] hydrocarbon flames, but

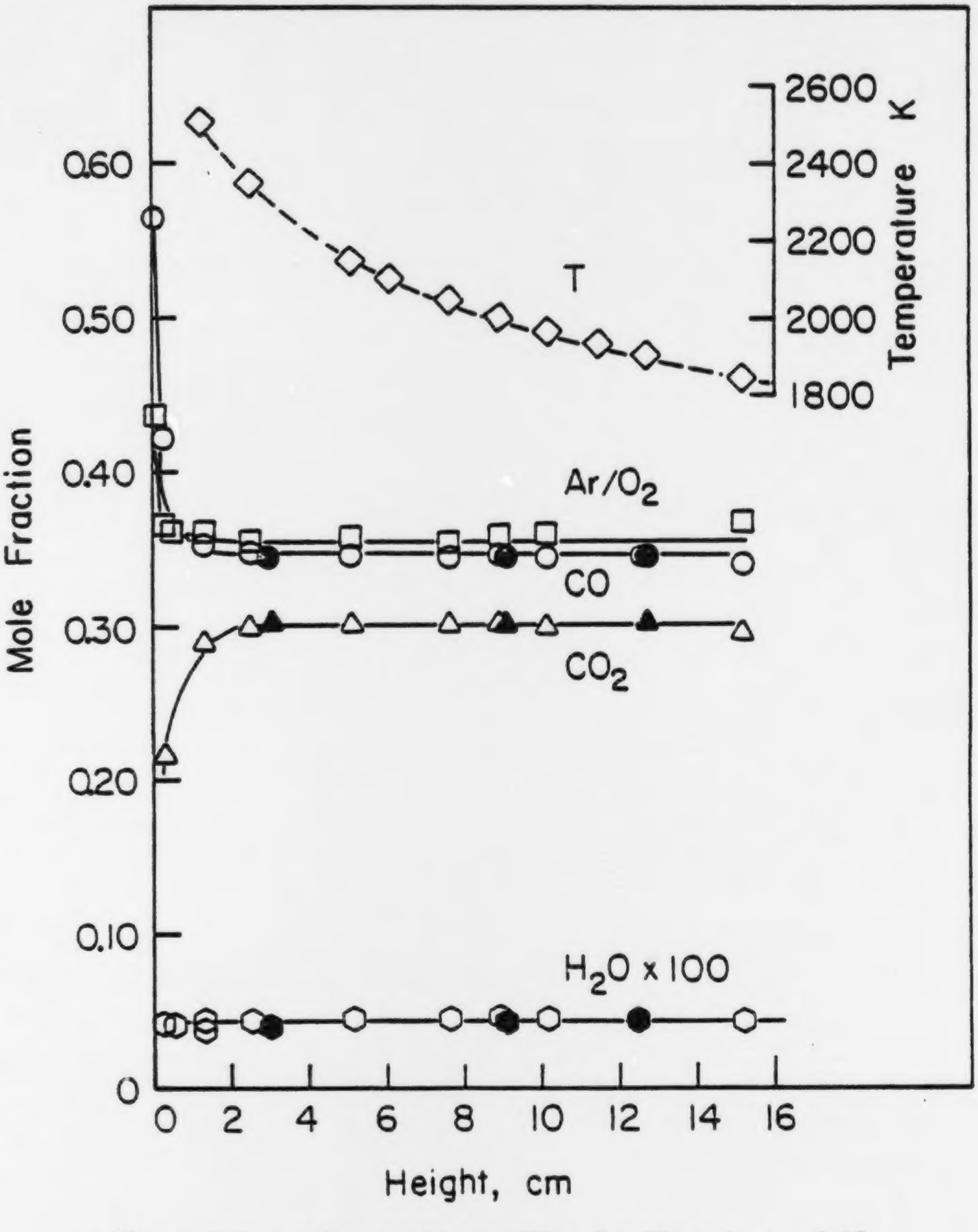

Figure 3.3-1 Major species profiles for Flame 1, $\phi = 2.17$. Shaded symbols denote equilibrium values at the local temperature.

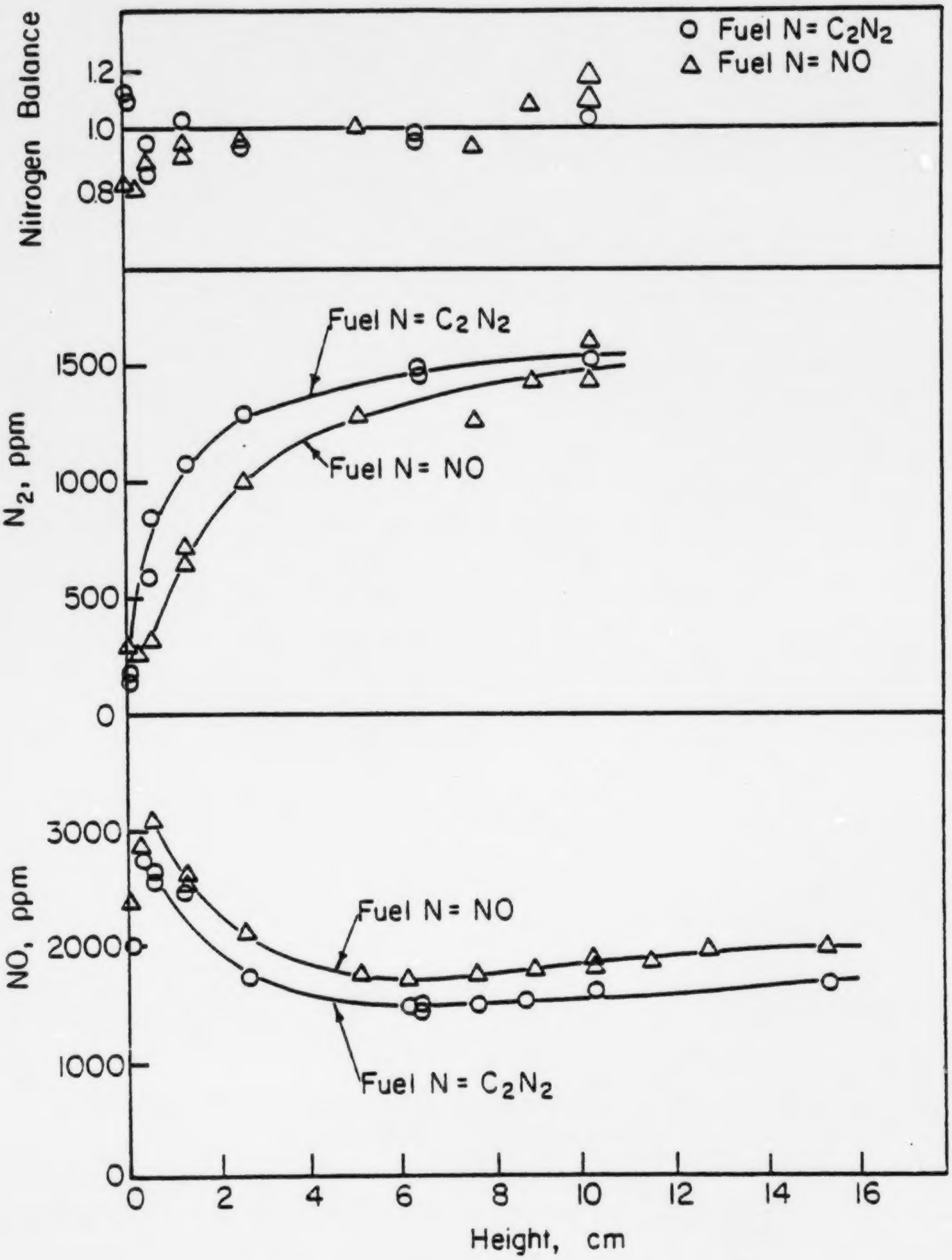

Figure 3.3-2 Nitrogenous species and nitrogen balance in post flame: Effect of fuel nitrogen species type.

Flames 1 and 2, ϕ = 2.17.

which is not intuitive for these slightly moist CO flames. The apparent small minimum in the NO profile at 6 cm is not significant and probably represents experimental error.

b) Low Temperature Phenomena

The lower temperature flames (Flames 5 and 6) contained more hydrogen (either through NH_3 as the fuel additive or through H_2 directly), much more Argon, and had peak temperatures of 1852 K decaying to 1700 K over 8 cm. The adiabatic flame temperature for these flames was 2057 K. Major species mole fractions were essentially at their equilibrium values (y_{CO}=0.22, y_{CO_2}=0.18, y_{H_2O}=0.0034) and the peak NO values were 1768 ppm (corresonding to 61% conversion of fuel N as NH_3 in Flame 5) and 1970 ppm (corresponding to 75% conversion of fuel N as NO in Flame 6). In contrast to the high temperature flame results, NO did not decay, N_2 did not rise in the post flame region and profiles with either NH_3 or NO in the fuel were similar. This will be discussed further in the modeling section below. The nitrogen balance was twenty percent low throughout in this experiment because of inaccuracies in the N_2 measurement, caused by the large quantity of Argon in the chromatograph sample, the low concentrations of N_2 and the fact that N_2 is eluted on the Argon chromatogram tail.

c) Influence of Fuel Sulfur

Only those flames in which mechanisms destroying NO and forming N_2 in the post flame were in evidence, were used to examine the influence of fuel sulfur on the destruction of nitrogenous species. Therefore, we restrict the presentation of results in this segment of the work to high temperature flames (Flames 3 and 4), in which the effect of sulfur on the fate of both high and low concentrations of C_2N_2 in the fuel was examined. Sodium D line measurements of flame temperature were not made when sulfur was added, because sulfur quenches the sodium emission under fuel rich conditions. However, adiabatic flame temperature calculations showed that the level of sulfur added would change that temperature by only -25 K. Therefore, it may be reasonable to assume that the addition of sulfur did not change the post flame temperature profile significantly.

Because of the paucity of hydrogen, essentially 100% of the sulfur is measured in the post flame gases as SO_2, even though the equivalence ratio is 2.17. NO, N_2 and nitrogen balance profiles for both high and low inlet C_2N_2 levels and with and without SO_2 are shown in Figure 3.3-3 SO_2 has a small but significant influence on the decay of NO, causing slightly lower NO levels and correspondingly higher N_2 levels, at the high C_2N_2 inlet concentration. At low C_2N_2 inlet levels there was negligible measureable effect and, indeed, only a very small decay of NO under sulfur free conditions. The nitrogen balance was satisified reasonably well in both cases, except at points greater than 8 cm from the burner grid, where entrainment of a small quantity of surrounding air was obviously a problem. The results should be contrasted with those presented previously for hydrocarbon flames, in which the effect of sulfur was much greater with regard to post flame NO behavior.

3.4 Kinetic Modeling

Complete analysis of complex chemical kinetics in a premixed flame zone environment is complicated by effects of diffusion and flame holder heat loss. In this work we are concerned wholly with post flame phenomena. This region can be modeled as a plug flow reactor, provided the proper initial conditions, at a point downstream of the flame front are specified.

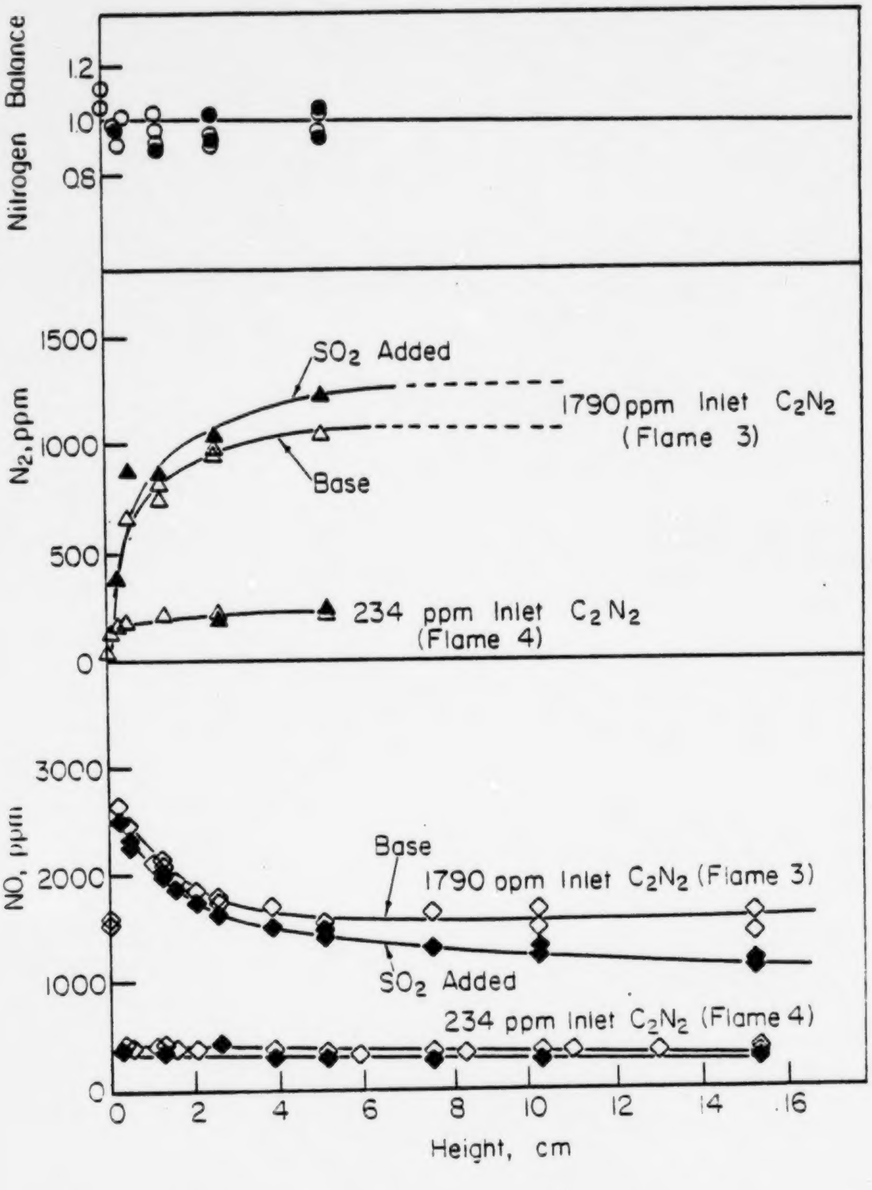

Figure 3.3-3 Nitrogenous species and nitrogen balance in the post flame: Effect of fuel sulfur and fuel nitrogen level.

Here we use experimental data for major species, NO, and temperature to set a portion of the necessary post flame initial conditions. We predict initial free radical concentrations by simulating the flame zone by a well stirred reactor at the measured peak temperature and of mean residence time of 3 msec, which gave the correct major species concentrations. This is a better estimate of free radical concentrations than equilibrium, and is a correct estimate if the in-flame profiles are quadratic functions of axial distance [12]. Our initial condition, therefore, corresponds to data taken at 0.75 cm from the grid, or after a residence time of 3 msec.

The reaction set describing the combustion of moist CO contained 28 reactions and 10 species (CO, CO_2, HCO, H_2, H_2O, H_2O_2, H, O, OH, HO_2) and is identical to that found by Corley and Bowman. According to Corley and Bowman, the kinetic model was able to predict flame velocities, ignition delay times, and species profiles in shock tube and flame combustion studies of a large number of $CO/O_2/H_2$ mixtures. Since this paper is not directed towards a verification of CO combustion kinetics, the reader is directed to the above reference for further specifics on the fuel oxidation mechanisms and the parameters utilized.

The nitrogen chemistry contained the reverse Zeldovich mechanisms

$$N + NO = N_2 + O \tag{1}$$

$$H + NO = N + OH \tag{2}$$

$$O + NO = N + O_2 \tag{3}$$

as well as 38 additional reactions involving the formation and destruction of NH, NH_2, NH_3, HCN, CN, NCO, N_2O, HNO and NO_2. This augmented reaction mechanism included Fenimore's [5] estimate for the global step

$NH_2 + NO \rightarrow N_2 + H_2O$ (2')

and Engleman's [13] estimate for

$HNO + CO \rightarrow CO_2 + NH$ (5)

NO Reduction in the Absence of Sulfur

The calculated initial conditions for the plug flow reaction model of Flame 1 and the corresponding equilibrium concentrations are shown in Table 3.4-1 It can be seen that the radical species are above their equilibrium values. The plug flow reactor calculation predicted NO and N_2 profile denoted by the solid curve shown in Figure 3.4-1. This should be compared to the experimental data points on the same figure. Agreement between prediction and experiment is good but not perfect. However, the purpose of the kinetic modeling was not to derive reaction rate coefficients but rather to check consistency of a given kinetic mechanism with the data. One can conclude that the reaction set described above is largely consistent with the experimental data of Flame 1. In order to provide insight, the kinetic model was then used to determine which reactions are controlling and what simplications might be appropriate, within the context of the reaction set utilized here.

The plug flow reactor calculation showed that at a typical point (3 cm, 15 msec) along the axis, the computed rates for NO destruction and N_2 formation were:

$R_{NO} = - 0.985 \times 10^{-7}$ moles/cm^3 -sec

$R_{N_2} = 0.493 \times 10^{-7}$ moles/cm^3-sec

Analysis of the reaction network showed that the only important reaction producing N_2 is the reverse Zeldovich reaction:

Table 3.4-1 Inlet, Calculated Plug Flow Inlet and Equilibrium Mole Fractions. Flame 1

	Inlet to Burner mole fractions	Initial Conditions to Plug Flow Reactor mole fractions	Equilibrium mole fractions
CO	0.566	0.421	0.352
O_2	0.123	0.339E-01	0.159E-02
Argon	0.303	0.330	0.34
H_2	0.481E-03	0.800E-05	0.489E-04
H	0	0.483E-03	0.220E-03
O	0	0.196E-01	0.728E-03
CO_2	0	0.195	0.296
CHO	0	0.137E-07	0.129E-06
H_2O	0	0.338E-04	0.265E-03
OH	0	0.481E-02	0.252E-03
NO	0.367E-2	0.283E-02	0.106E-03
N_2		0.251E-03	0.169E-02

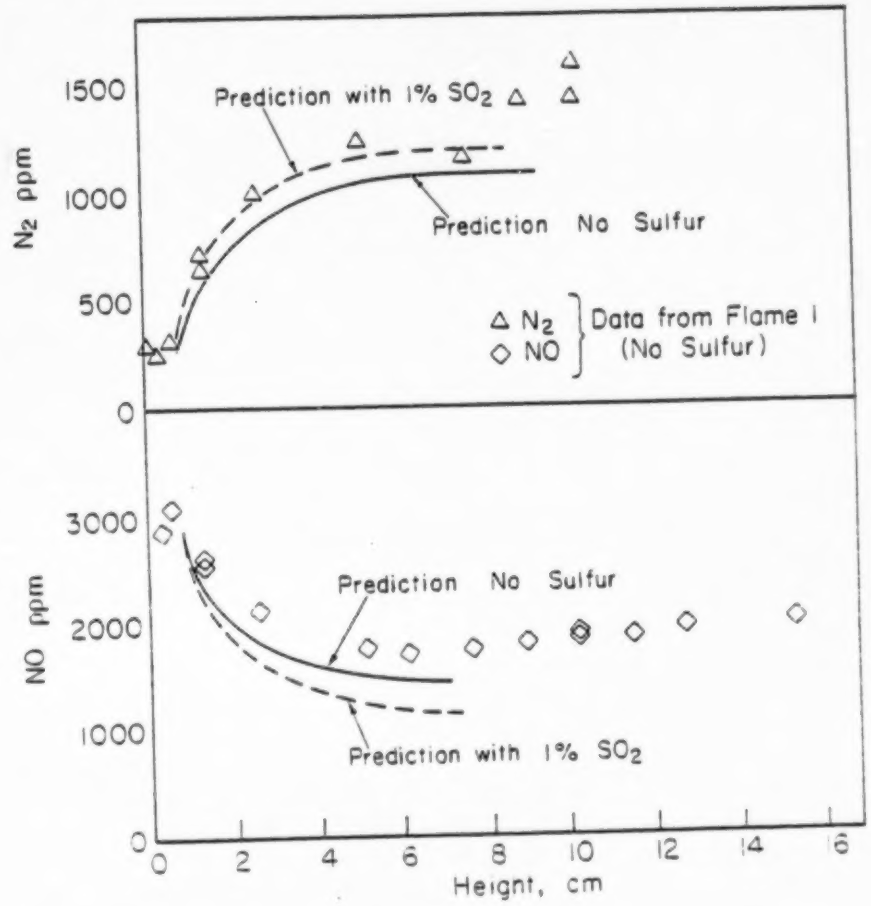

Figure 3.4-1 Experimental and predicted NO and N_2 profiles in the high temperature (2400-2000 K) post flame.

$$N + NO \xrightarrow{k_{1f}} N_2 = 0 \qquad (1)$$

with a computed undirectional net rate of 0.491 x 10^{-7} moles/cm^3-sec. Nitrogen atoms are produced through

$$H + NO \underset{k_{3r}}{\overset{k_{3f}}{\rightleftarrows}} N + OH \text{ ; net rate} = 0.254 \times 10^{-7} \frac{\text{mole}}{\text{cm}^3\text{sec}} \qquad (3)$$

$$O + NO \underset{k_{4r}}{\overset{k_{4f}}{\rightleftarrows}} N + O_2 \text{ ; net rate} = 0.235 \times 10^{-7} \frac{\text{mole}}{\text{cm}^3\text{sec}} \qquad (4)$$

and are essentially at a pseudo-stationary state. These computations showed that no other reactions influence the N atom concentration, the rate of NO destruction or the rate of N_2 formation.

The above information permits the following simplified expression for N_2 formation to be developed

$$R_{N_2} = \frac{[k_{3f}(H) + k_{4f}(O)](NO)}{1 + \dfrac{k_{3r}(OH) + k_{4r}(O_2)}{k_{1f}(NO)}}$$

which varies between first and second order in NO, depending on the NO concentration, temperature, and radical concentrations. At a lower intitial NO concentration of 394 ppm the model predicted a post flame reduction to 323 ppm after 0.1 sec compared to the experimental values (Flame 4) of 394 ppm to 332 ppm (see Figure 3.3-3).

For the low temperature flame (Flame 6) the reaction set predicted a decay in NO although no reduction was observed experimentally as shown in Figure 3.4-2. Examination of the reaction mechanism indicated that in this case was formed via

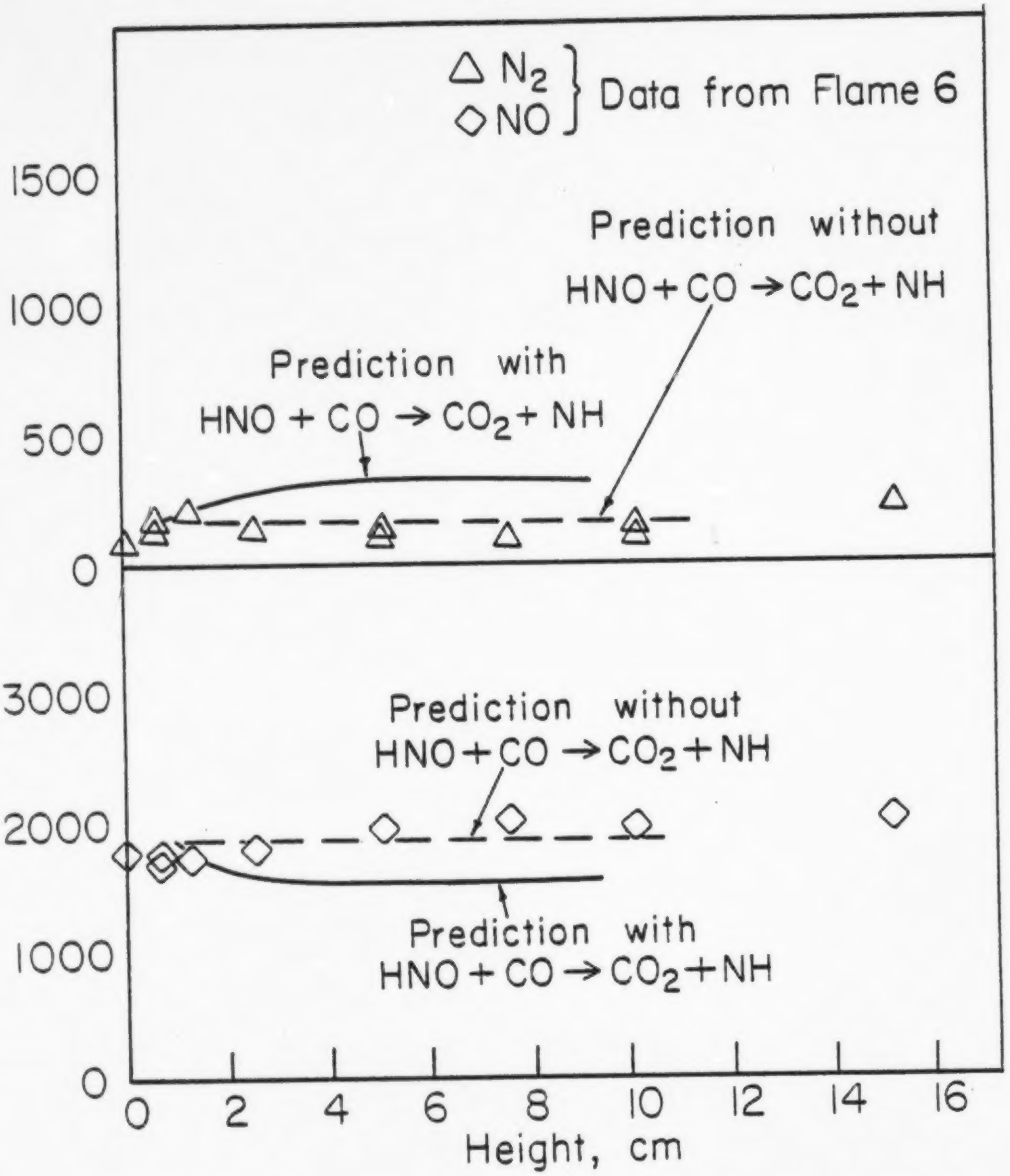

Figure 3.4-2 Experimental and predicted NO and N_2 profiles in the low temperature (2000-1700 K) post flame. The role of HNO + CO → CO_2 + NH.

$$NH_2 + NO \rightarrow N_2 + H_2O \qquad (2')$$

as has been previously hypothesized [5]. Further analysis showed that the production of NH_2 and, therefore, the predicted decay of NO was due to the use of Engleman's estimate for the rate coefficient of

$$HNO + CO = CO_2 + NH \qquad (5)$$

With reaction (5) omitted no decay was predicted and, as in the high temperature case, reaction 2' appeared to play no role. This information indicates that the rate expression used for reaction (5) is probably too rapid, and should not be used with the presently available reaction set.

These results show that for slightly moist CO flames with fuel nitrogen, the post flame behavior of NO can be reasonably accurately modeled using the reverse Zeldovich reactions alone. There was neither theoretical nor experimental evidence for other N_2 production mechanisms being operative in these hydrogen poor flames at either the high or the low temperature conditions studied. Therefore, the 38 additional reactions used in the augmented nitorgen mechanisms were deleted in subsequent modeling of the effect of sulfur on NO reduction and N_2 formation.

NO Reduction in the Presence of Sulfur

Experimental data for moist CO flames (with C_2N_2 as the fuel nitrogen, ϕ=2.17) show, Figure 3.3-5, that 1% SO_2 in the inlet mixture accelerates NO reduction and N_2 formation slightly. Therefore, the effect of SO_2 must be to increase the rate of N atom production. To model the effect of sulfur the additional reactions shown in Table 3.4-2 were added to the kinetic mechanism (for the plug flow reactor calculation only). The rate coefficients for reactions involving HSO are crude estimates, but extreme accuracy is not

Table 3.4-2 Sulfur Chemistry[a)]

Number		A_f	n_f	Θ_f	Ref. #
32	$H_2S + M = HS + H + M$	2.(14)	0	37.2(3)	16
33	$H_2S + H = HS + H_2$	9.03(12)	0	0.855(3)	17
34	$H_2S + O = HS + OH$	4.36(12)	0	1.66(3)	18
35	$H_2S + OH = HS + H_2O$	1.4(13)	0	.443(3)	19
36	$HS + HS = H_2S + S$	1.0(14)	0	.715(3)	est.
37	$HS + H = H_2 + S$	6.31(11)	0.5	0.	14
38	$HS + O = SO + H$	6.31(11)	0.5	0.	14
39	$HS + O = S + OH$	6.31(11)	0.5	4.03(3)	14
40	$HS + S = S_2 + H$	6.31(11)	0.5	0.	14
41	$S + O_2 = SO + O$	6.31(11)	0.5	0.	14
42	$S + OH = SO + H$	6.31(11)	0.5	0.	14
43	$S_2 + O = SO + S$	6.31(11)	0.5	0.	14
44	$S + S + M = S_2 + M$	1.(18)	-1.	0.	14
45	$SO + O_2 = SO_2 + O$	1.81(11)	0.	2.82(3)	17
46	$SO + OH = SO_2 + H$	6.46(14)	0.	1.05(3)	est[b)]
47	$SO_3 + O = SO_2 + O_2$	2.8(14)	0.	6.04(3)	17
48	$SO_2 + O + M = SO_3 + M$	4.(20)	-4.0	2.65(3)	20
49	$SO + O + M = SO_2 + M$	1.2(22)	-1.84	0.	21
50 (6)	$N + SO = NO + S$	6.31(11)	0.5	1.01(3)	see text
51 (7)	$NO + S = NS + O$	1.(12)	0.5	17.5(3)	14
52 (8)	$NS + O = SO + N$	6.31(11)	0.5	4.03(3)	14
53	$N + NS = N_2 + S$	6.31(11)	0.5	0.	14
54	$N + SH = NS + H$	6.31(11)	0.5	4.03(3)	14
55	$H + SO + M = HSO + M$	1.6(20)	-1.5	0.	est[c)]
56	$HSO + H = H_2 + SO$	5.(11)	0.5	1.11(3)	"
57	$HSO + H = H_2S + O$	5.(10)	0.5	2.26(3)	"
58	$HSO + H = HS + OH$	5.(11)	0.5	2.26(3)	"
59	$HSO + OH = H_2O + SO$	5.(13)	0.	.503(3)	"
60	$HSO + O = SO + OH$	5.(11)	0.5	1.11(3)	"
61	$HSO + O = HS + SO_2$	1.(14)	0.	13.1(3)	"
62	$HSO + O = HS + O_2$	5.(11)	0.5	2.26(3)	"
63	$HSO + O_2 = SO + HO_2$	5.(11)	0.5	1.11(3)	est
64	$H + SO_2 + M = HSO_2 + M$	7.26(16)	0.	0.	24
65	$HSO_2 + OH = H_2O + SO_2$	6.79(13)	0.	.886(3)	24

Table 3.4-2 continued ....

[a] Forward rate coefficients as $k_f = A_f T^{n_f} \exp(-\Theta_f/T)$ with units of cm^3 gm-mole, sec, K. Numbers in parentheses refer to powers-of-ten, i.e., $1.(13) = 1. \times 10^{13}$.

[b] Estimate used yields values for k_f in agreement with data reported in ref. 17.

[c] Thermochemistry for HSO radical from ref 22. Rate coefficients for reactions 55 thru 63 estimated by techniques in ref. 14 and 23 or by analogy with reactions of HNO and HO_2.

required since the reactions involving H_2S, SH, SO, etc. are expected to be partially equilibrated. The coefficient for the direct N/S interaction reaction

$$N + SO = NO + S \tag{6}$$

was estimated by combining the pre-exponential factor given by Benson et al [14] with the room temperature data of Jacob and Winkler [15] to obtain an activation energy of 2 kcal/mole. The reaction set shown on Table 4 includes known reactions in which sulfur compounds catalyse the recombination of O and H atoms and OH radicals.

Comparison between the solid (no sulfur) and dashed (sulfur added) curves on Figure 3.4-1, allows the computed effect of 1% sulfur in the mixture to be examined. The model predicted that the effect of SO_2 in the feed mixture is to accelerate NO destruction and N_2 formation. This predicted influence of sulfur should be compared to the experimental data in Fig. 5 which shows similar results for C_2N_2 as the fuel nitrogen species. Thus the sulfur reaction set of Table 3.4-2 can be viewed to be consistent with experimental observations under conditions reported here. The kinetic model was then used to isolate which reactions are likely to be responsible for the changes in the NO and N_2 profiles caused by the presence of sulfur.

The model showed that the direct interactions

$$N + SO = NO + S \tag{6}$$

$$NO + S = NS + O \tag{7}$$

$$NS + O = SO + N \tag{8}$$

were responsible for increased N atom concentrations and therefore increased N_2 formation. The reverse Zeldovich step was still the only reaction forming N_2. Since a pseudo stationary state was again found for nitrogen atoms, the following expression may be derived for the rate of N_2 production.

$$R_{N_2} = \frac{\left\{k_{3f}(H) + k_{4f}(0) + \left[k_{6r} + \frac{k_{8f}\,k_{7f}}{k_{7r}\,k_{8f}}\right](S)\right\}(NO)}{1 + \frac{k_{3r}(OH) + k_{4r}(0_2)}{k_{1f}(NO)} + \left[k_{6f} - \frac{k_{8f}\,k_{8r}}{k_{7r}+k_{8f}} + k_{8r}\right]\frac{(SO)}{k_{1f}(NO)}}$$

Although calculations showed a slight increase in (O) and (OH) when compared to the sulfur free case, this increase is not likely to account for the increase in R_{N_2} since the term containing (S) dominates in the numerator and the term with (SO) in the demoninator is of order one.

In a numerical test in which the direct interaction steps (reactions 6,7,8) were omitted, the model predicted a deceleration of NO decay (and a decrease in (O) and (OH), compared to the sulfur-free case) because of the homogeneous recombination of free radicals catalyzed by SO_2 (i.e., an indirect mechanisms influencing NO destruction). Since this is contrary to what was observed (Fig. 5), the small, but significant, acceleration effect of SO_2 is most likely to be due to the direct mechanism cited above.

3.5 Conclusions

Our results on 1700-2500 K moist CO flames, together with Morley's results on 1790 - 2100 K hydrogen flames are consistent with the view that at high temperatures, and in the absence of hydrocarbons, routes to form N_2 through NH and NH_2 are insignificant and N_2 formation occurs entirely through the reverse Zeldovich mechanism, although the dominant reaction forming N atoms may differ. This difference in N atom formation routes, as a function of fuel composition, may be important in hydrocarbon flames.

Closure of the nitrogen balance in the experiments, together with the kinetic modeling, indicates that the only significant nitrogenous species in the post flame are NO and N_2. NO does not decay at low temperatures in these hydrogen poor flames and routes towards N_2 via HNO are not in evidence. The most plausible effect of sulfur was to increase the steady state N atom concentration through direct reactions between NO and S. This can cause the observed accelerated decay of NO and formation of N_2. It should be cautioned, however, that these conclusions may be valid strictly only within the context of the original full reaction set utilized in the kinetic model described in this work.

These results should be distinguished from those describing the effect of sulfur on fuel nitrogen in hydrocarbon flames. In the latter case, interactions with NH_i species are more likely to play a role and the observed behavior is totally different from that described here [10]. Results on fuel rich hydrocarbon flames are to be reported in the next section. Future work should focus on the effect of increased hydrogen concentrations on the conclusions obtained here, especially on post flame behavior at lower temperatures where the higher hydrogen levels may influence the N atom concentration and/or increase the importance of reactions of NH_i species.

3.6 References for Section 3

1. Haynes, B.S., Combust. Flame 28:113 (1977).

2. Morley, C., Combust. Flame 27:177 (1976).

3. Haynes, B.S., Combust. Flame 28:81 (1977).

4. Haynes, B.S., in Alternative Hydrocarbon Fuels : Combustion and Chemical Kinetics (C.T. Bowman and J. Birkeland, Eds.), Progress in Astronautics and Aeronautics, Vol. 62, p. 359. Published by AIAA (1978).

5. Fenimore, C.P., Combust. Flame 26:249 (1976)

6. Fenimore, C.P., Seventeenth Symposium (International) on Combustion, The Combustion Institute, Pittsburgh, Pa., 1979, p. 661.

7. de Soete, G. G. Fifteenth Symposium (International) on Combustion, The Combustion Institute, Pittsburgh, Pa., 1975, p. 1093.

8. Morley, C., Eighteenth Symposium (International) on Combustion, The Combustion Institute, Pittsburgh, Pa., 1981, p. 23.

9. Wendt, J.O.L., Pershing, D.W., Lee, J.W., and Glass, J.W., Seventeenth Symposium (International) on Combustion, The Combustion Institute, Pittsburgh, Pa., 1979, p. 77.

10. Wendt, J.O.L., Morcomb, J.T. and Corley, T.L., Seventeenth Symposium (International) on Combustion, The Combustion Institute, Pittsburgh, Pa. 1979, p. 671.

11. Glass, J. W. and Wendt, J.O.L., The Destruction of Trace Nitrogenous Species During the Staged Combustion of Pulverized Coal Char, Paper presented at the 73rd Annual Meeting of the AIChE, Chicago, November, 1980

12. Sternling, C.V. and Wendt, J.O.L., Kinetic Mechanisms Governing the Fate of Chemically Bound Sulfur and Nitrogen in Combustion, Shell Development Co., Report No. EPA-650/2-74-017 (NTIS) PB 230-895, 1972.

13. Engleman, V. S., Survey and Evaluation of Kinetic Data on Reactions in Methane/Air Combustion, Exxon Research and Engineering Co., Report EPA-600/2-76-003 (NTIS PB 248-139) 1976.

14. Benson, S. W., Golden, D.M., Lawrence, R. W., Shaw, R., and Woolfolk, R.W., Estimating the Kinetics of Combustion, Including Reactions Involving Oxides of Nitrogen and Sulfur, Report EPA-600/2-75-019 (NTIS PB 254-054), 1975.

15. Jacob, A. and Winkler, C.A., Can. J. Chem. 48:1774 (1970).

16. Bowman, C.T. and Dodge, L.G., Sixteenth Symposium (International) on Combustion, The Combustion Institute, Pittsburgh, Pa., 1977, p. 971.

17. Schofield, K., J. Phys. Chem. Ref. Data 2:25 (1973).

18. Whytock, D.A., Timmons, R.B., Lee, J.H., Michael, J.V., Payne, W.A. and Stief, L.J., J. Chem. Phys. 65:2052 (1976).

19. Westenberg, A.A. and deHaas, N., J. Chem. Phys. 59:6685 (1973).

20. Troe, J., Ann. Rev. Phys. Chem. 29:223 (1978).

21. Grillo, A., Reed, R. and Slack, M.W., J. Chem. Phys. 70:1634 (1979).

22. White, J.N. and Gardiner, W.C., Jr., Chem. Phys. Lett. 58:470 (1978).

23. Tunder, R., Mayer, S., Cook, E. and Schieler, L., Aerospace Corp. Report No. TR-001 (9210-02), 1967.

24. Halstead, D.J., and D.R. Jenkins, Trans. Faraday Soc., 65:3013 (1969).

4. POST FLAME BEHAVIOR OF NITROGENOUS SPECIES IN THE PRESENCE OF FUEL SULFUR. II. RICH, $CH_4/He/O_2$ FLAMES

4.1 Introduction

Experimental data, on NO emissions from turbulent diffusion flames, shown in Part 1 of this report indicate that under hot poorly mixed conditions, the presence of sulfur increases the overall conversion of fuel nitrogen to NO. Additional laboratory experimental data on NO profiles in rich, premixed $CH_4/O_2/Ar$ flames, shown in Part 2 of this report, showed that fuel sulfur could have a radical influence on fuel NO formation mechanisms. Both enhancement and apparent inhibition of fuel NO were observed, depending on the stoichiometric ratio and the residence time at which the measurement was made.

Since these data contained information only on the NO concentrations, they provided little insight into which mechanisms controlling the conversion of fuel nitrogen into HCN, NH_3, or other nitrogenous species were affected by fuel sulfur. High levels of NO do not necessarily imply high levels of HCN and NH_3 with corresponding low levels of N_2. Therefore, the objective of this part of the project was to fill in these gaps in the previous data with special emphasis on closure of the nitrogen balance.

Knowledge on mechanisms involving fuel nitrogen/fuel sulfur interactions is extremely important in determining the influence of fuel quality on pollutant emissions. It is hoped that results generated from this part of the project will aid in the development of new combustion modifications for NO_x control from fuels containing both chemically bound nitrogen as well as chemically bound sulfur.

Three flames were studied at stoichiometric ratios of SR = .458, SR = 0.585 and SR = 0.693. In all cases the flames were composed of $CH_4/He/O_2$ mixture with C_2N_2 as the fuel nitrogen compound and SO_2 as the fuel sulfur compound. Previous work had shown that the nature of the sulfur compound was not important because sulfur species are partially equilibrated, and the addition of SO_2 does not change the overall stoichiometric ratio. The focus of this work is, as in Part 3, entirely on the post flame, at fairly long residence times 20 ms. Special emphasis was on closure of the nitrogen balance insofar as this was possible in view of the soot generated under some very rich conditions examined here.

4.2 Experimental Apparatus

The premixed flames burner was identical to that utilized in the earlier studies described in Parts 2 and 3. Nominally 5 cm ID, it utilized a porous metal disk rather than the course 10 x 10 mesh screen described in Part 3. Again, it was enclosed in a 15 cm ID, 60 cm high, quartz chimney, the inside surfaces of which were purged with helium to prevent deposition of soot or entrainment of air. The quartz chimney was enclosed at the top by a firebrick which allowed the helium purge and the exhaust flow to exit through a 3 cm hole in the center. The flame was exceedingly flat at the grid, without any appearance of tiny flamelets that tended to occur in the earlier work. The flame profiles were flat over half the burner diameter up to a distance of 5 cm from the grid, which was the furthest point at which data was taken. After 5 cm, small quantities of surrounding air were sometimes drawn into the post flame gases, and this disturbed the nitrogen balance.

It was found to be important to use glass beads rather than stainless steel beads as a packing to straighten the flow in the burner. Stainless steel appeared to adsorb C_2N_2 and SO_2 to form a sticky solid compound that caused erroneous nitrogenous species profiles. This problem delayed this project several months, until it was recognized and solved.

Temperature measurements were made with sodium D line reversal and were corrected for reflection from the walls of the glass chimney. Flows of major (O_2, CH_4, He) and minor species (C_2N_2, SO_2) were controlled and metered with sonic orifices, rotameters and laminar flow elements where appropriate. In order to attempt a nitrogen closure, all gases had to be essentially N_2 free (less than 20 ppm) and were tested for impurities prior to use. As before, SO_2 bottles were bled prior to use in order to purge dissolved air in the liquid SO_2.

Sampling and Analysis

Samples were withdrawn along the centerline axis of the flame through a water cooled quartz probe with a 1.5 mm orifice. The normal sampling rate was 1 liter/min. The sampling system consisted of a Sigma 2 chromatograph and Thermo Electron Model 10 NO/NO_x Chemilumenescent Analyzer as shown in Part 3, Figure 3.1-1. The sample loop conditions, columns and chromatograph operating conditions were identical to those described in Part 3. The columns used, however, had deteriorated over the time span of a year and were replaced. Separation of argon and small quantities of nitrogen were insufficient to obtain the desired resolution of 10 ppm N_2 in the mixture. Therefore, helium was utilized as the diluent gas for all flames investigated here, and this allowed excellent separation for N_2 measurements. Figure 4.2-1 demonstrates the

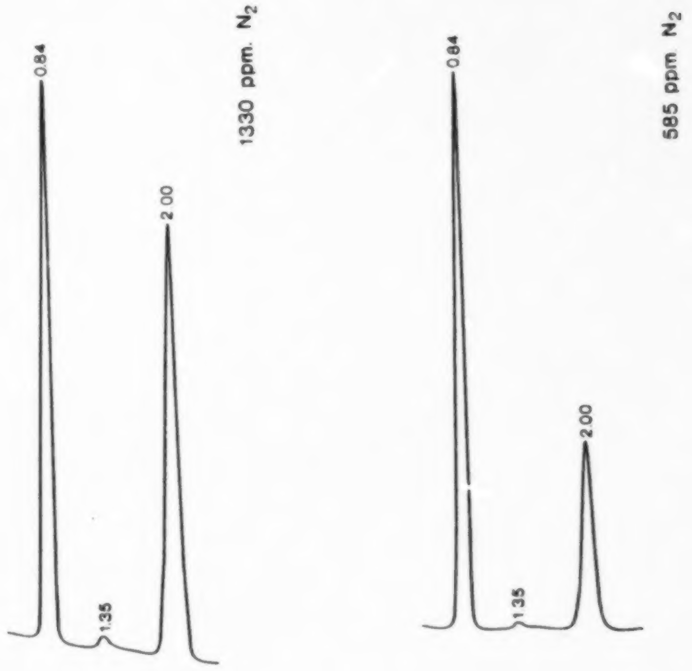

Figure 4.2-1 Chromatograms for N_2/He Mixtures. N_2 appears at 2.0 minutes.

resolution and separation achieved for N_2 measurements with helium as the diluent. No other gases present in the flame eluted near N_2 which ensured excellent sensitivity for this species.

4.3 Experimental Results

Experimental results are presented in three parts, each one corresponding to a specific stoichiometric ratio. The latter are 0.458, 0.585 and 0.693, respectively. Interim conclusions are presented at the end of each subsection.

a) Stoichiometric Ratio, SR = 0.458

The very fuel rich conditions of SR = 0.458 were chosen because the results in Part 2 showed that it was under these conditions that the effects of fuel sulfur on the NO profiles were the largest. However, these flames operated under strongly sooting conditions.

Figure 4.3-1 shows NO profiles for a flame with argon as the diluent, with and without SO_2 percent. The effect of sulfur was very smiliar as those presented in Part 2, only here we have greater resolution near the flame front. Without sulfur, a decay in NO is observed; with sulfur the NO first decreases, then rapidly increases to many times the sulfur free value. This run showed that the burner characteristics had not changed radically since Part 2 was completed, and that the sulfur effect was real and reproducible.

When the argon was replaced by helium as the diluent, the effect became less pronounced except at extremely high sulfur levels as shown on Figure 4.3-2. This may be due to the more rapid diffusion characteristics of species in the flame zone of this helium/fuel mixture, which may have greatly affected the post flame behavior. It should also be realized that the sooting characteristics of $CH_4/O_2/He$ flames are different than those of $CH_4/O_2/Ar$

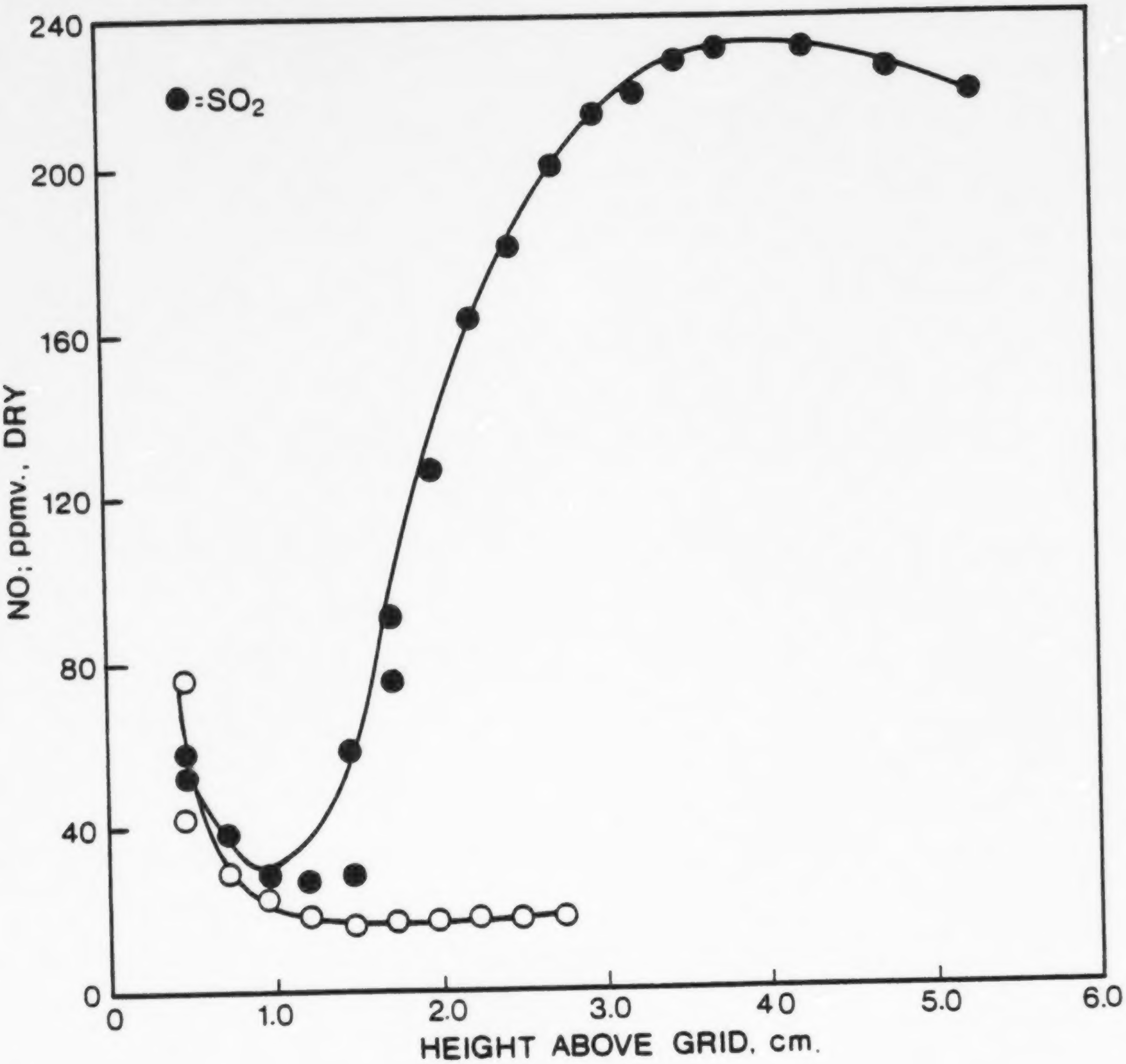

Figure 4.3-1 Influence of SO_2 on NO Profiles with Argon Diluent [Zero SO_2: $C_2N_2^o$ = 1906 ppm; with SO_2: $C_2N_2^o$ = 1409 ppm; SO_2^o = 9436 ppm; CH_4 = 6.08 ℓ/min; O_2 = 5.62 ℓ/min; Ar = 10.84 ℓ/min]

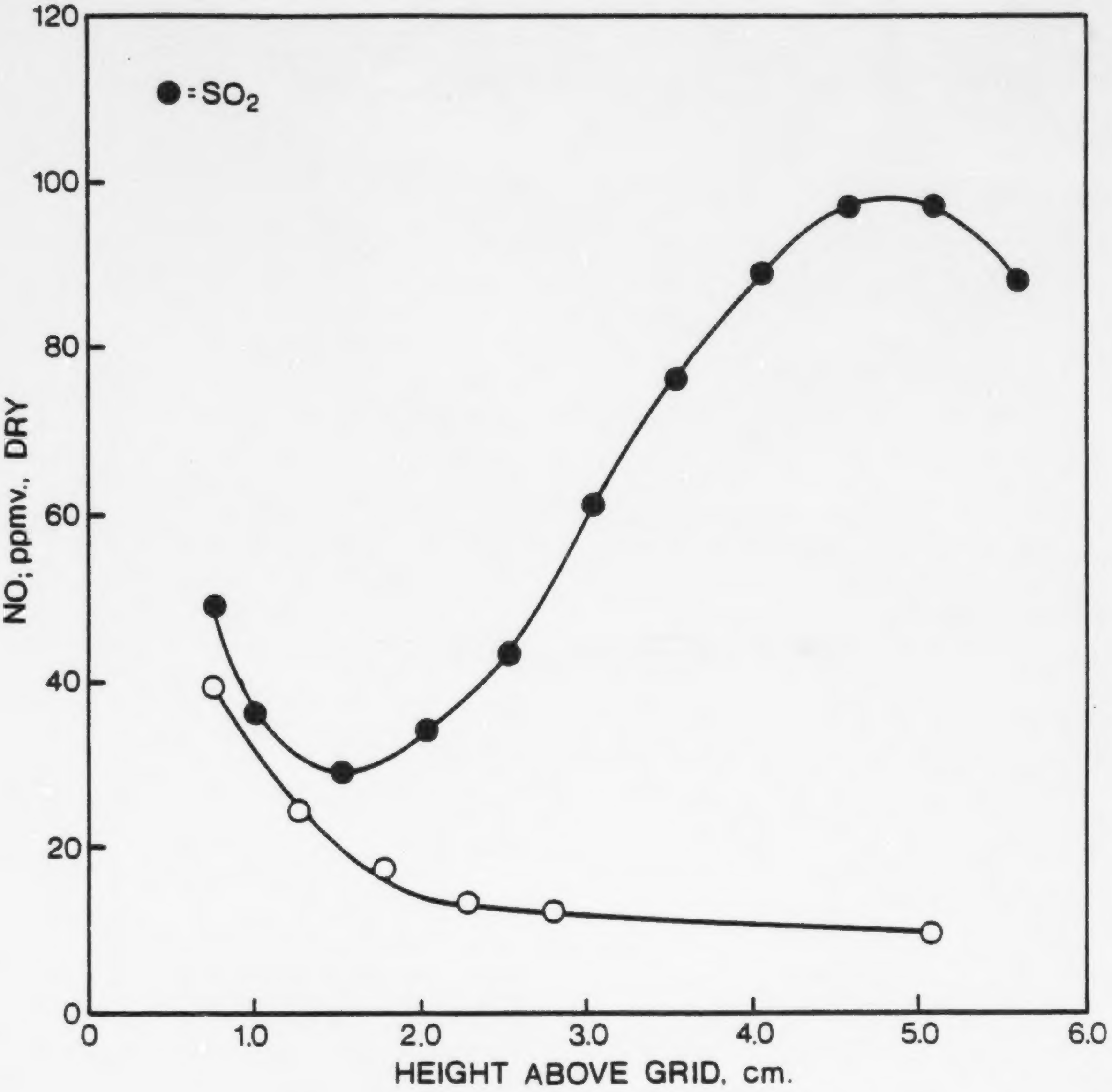

Figure 4.3-2 Influence of SO_2 on NO Profiles with Helium Diluent [Zero SO_2: $C_2N_2^o$ = 1906; with SO_2: $C_2N_2^o$ = 1884 ppm; SO_2^o = 11570 ppm]

flames (Haynes and Wagner, 1981). However, it was impossible to run the burner at these unnaturally high sulfur levels for sufficiently long times to allow us to gather all the chromatograph data necessary. This was because copious deposits of sulfur clogged up the sampling line, filters and chromatograph capillaries. Therefore, it was decided to investigate the sulfur effect at much lower sulfur levels, where, unfortunately, the effect itself was less pronounced.

Profiles of major species and minor hydrocarbon species are shown in Figure 4.3-3. Although CO and CO_2 concentrations change little throughout the flame with the addition of SO_2, the impact on levels of CH_4 and C_2H_2 is significant. The concentration of CH_4 surviving the flame front is lower with sulfur present. In addition, the rate of C_2H_2 disappearance is accelerated with SO_2 addition. Large amounts of soot were observed in this flame and depositions within the probe occurred.

Figure 4.3-4 shows the distribution of nitrogenous species measured with and without sulfur for the flame data presented in Figure 4.3-3. Although the effect of sulfur on the NO profiles is not as dramatic as that shown in Figure 4.3-2, it can be seen that HCN level is increased and that of N_2 decreased when SO_2 is added. HCN was the most abundant XN species in evidence. The peak temperature of 1820 K at 0.76 cm from the grid decayed linearly to 1660 K at 5.35 cm. It should be noted that the temperature profile is approximately 100 K lower throughout than that of the flame with the NO profile in Figure 4.3-2. The temperatures are also 50 K lower than those corresponding to the SR = 0.46 flame with argon presented in Section 2 of this report.

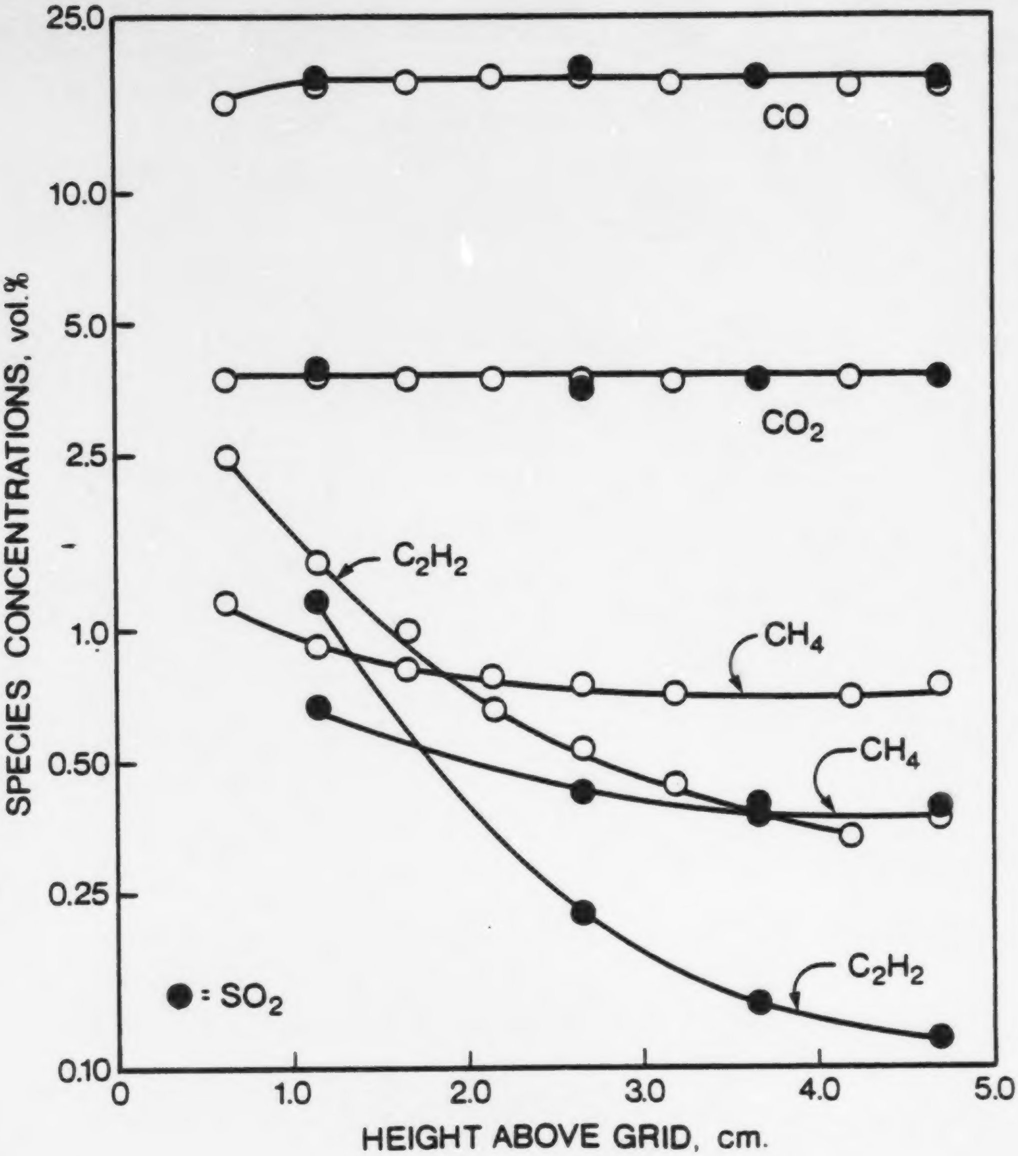

Figure 4.3-3 Influence of Sulfur on Major Species Profiles: SR = 0.458, Flame A [CH_4 = 6.18 ℓ/min, O_2 = 5.68 ℓ/min, He = 12.20 ℓ/min, SO_2 = 8850 ppm]

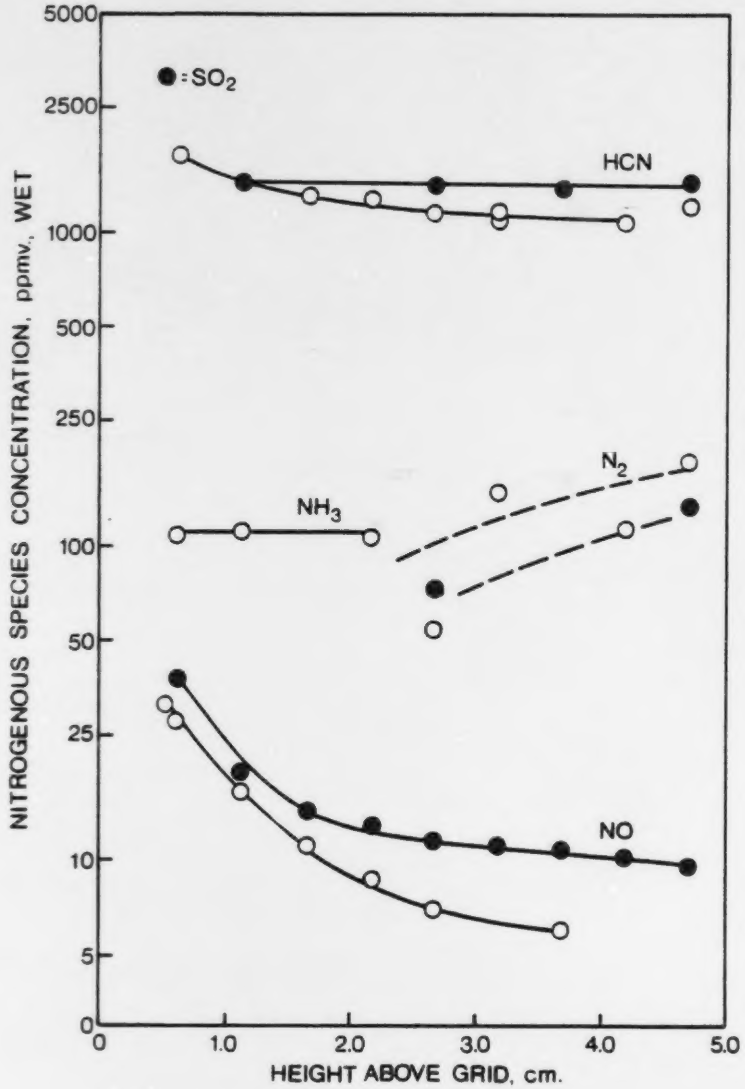

Figure 4.3-4 Effect of Sulfur on Nitrogenous Species SR = 0.458, Flame A [C_2N_2 = 1350 ppm, 1340 ppm with SO_2]

The highly sooting environment of this flame precluded the determination of an overall N_2 balance since carbon was used as a basis for those calculations. In addition, it was known from an analysis of the soot deposited within the quartz sample probe that some of the fuel nitrogen was present in the collected solid. Based on the ultimate analysis of this soot a composition of $C_1H_{3.0}N_{.0075}$ was calculated, which is different from the initial CH_4/C_2N_2 composition of $C_1H_{3.96}N_{.0104}$. The chemical identity of the nitrogenous compound(s) present in the soot is not known. A physically different nitrogenous compound whose composition was consistent with NH_4HSO_3 was collected on the outside of the cooled probe, downstream of the sampling point.

Figure 4.3-5 shows profiles for major species and minor hydrocarbon species for a different flame at SR = 0.458. The major difference between these data and those presented in Figure 4.3-3 is the temperature profile, which was approximately 130 K higher throughout the post flame region. Again fuel sulfur alters the hydrocarbon chemistry although the effect is less pronounced.

Figure 4.3-6 shows the distribution of nitrogenous species, measured with and without sulfur for the flame data presented in Figure 4.3-5. Although the effect of sulfur on the NO profiles is different from that shown on Figures 4.3-2 and 4.3-4 (NO concentrations are decreased), it is observed that HCN levels are again increased and N_2 levels decreased when SO_2 is added. The decreased conversion of fuel nitrogen to NO with increased flame temperature is qualitatively in agreement with the data presented in Section 2 of this report.

In each case examined at this stoichiometry of SR = 0.458, HCN formation was increased and N_2 formation decreased when SO_2 was added. This is consistent with the results in Part 1 of this report. The effect on the NO

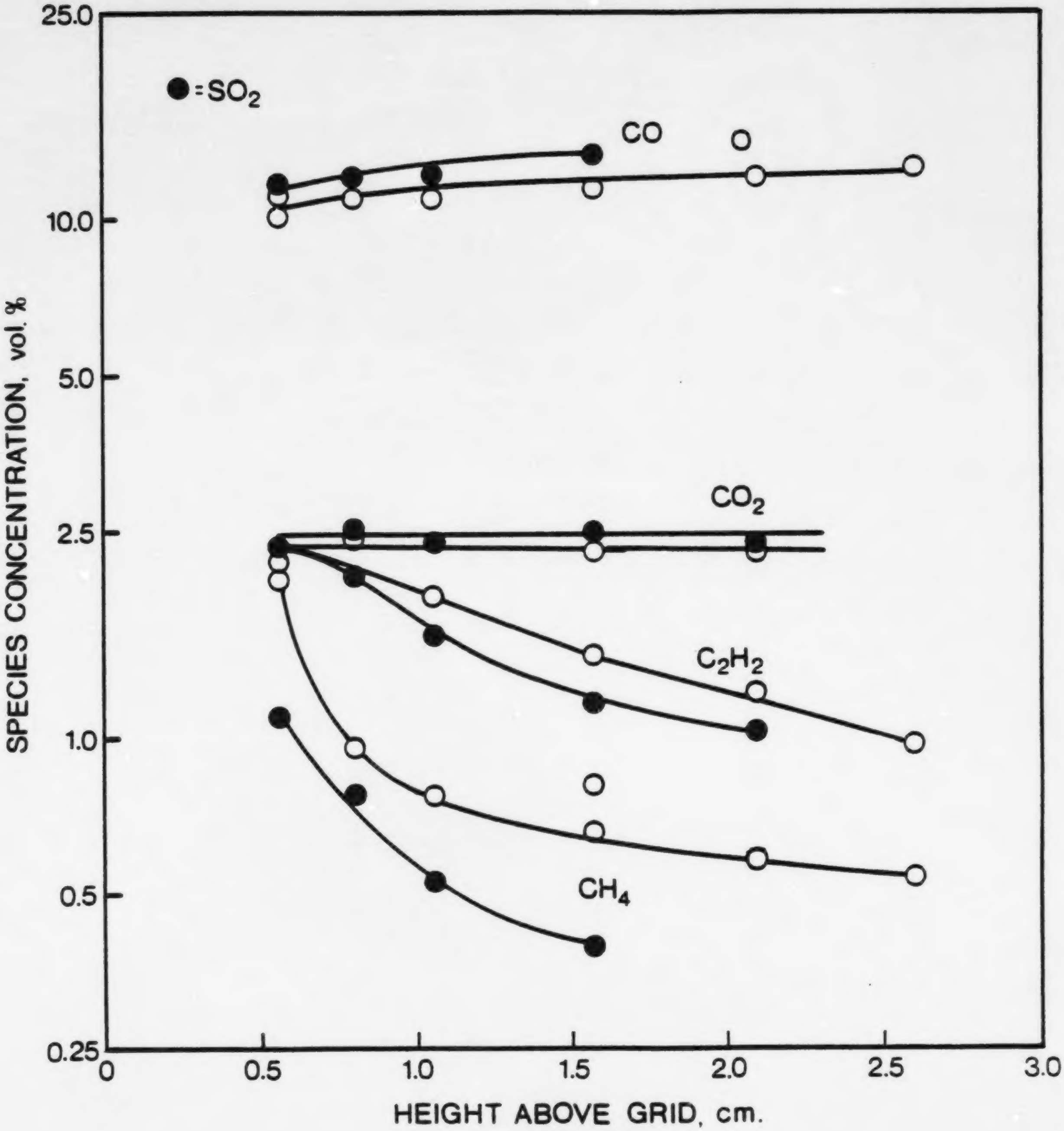

Figure 4.3-5 Influence of Sulfur on Major Species Profiles: SR = 0.458, Flame B [CH_4 = 7.12 ℓ/min, O_2 = 6.55 ℓ/min, He = 13.64 ℓ/min, SO_2 = 242 ℓ/min]

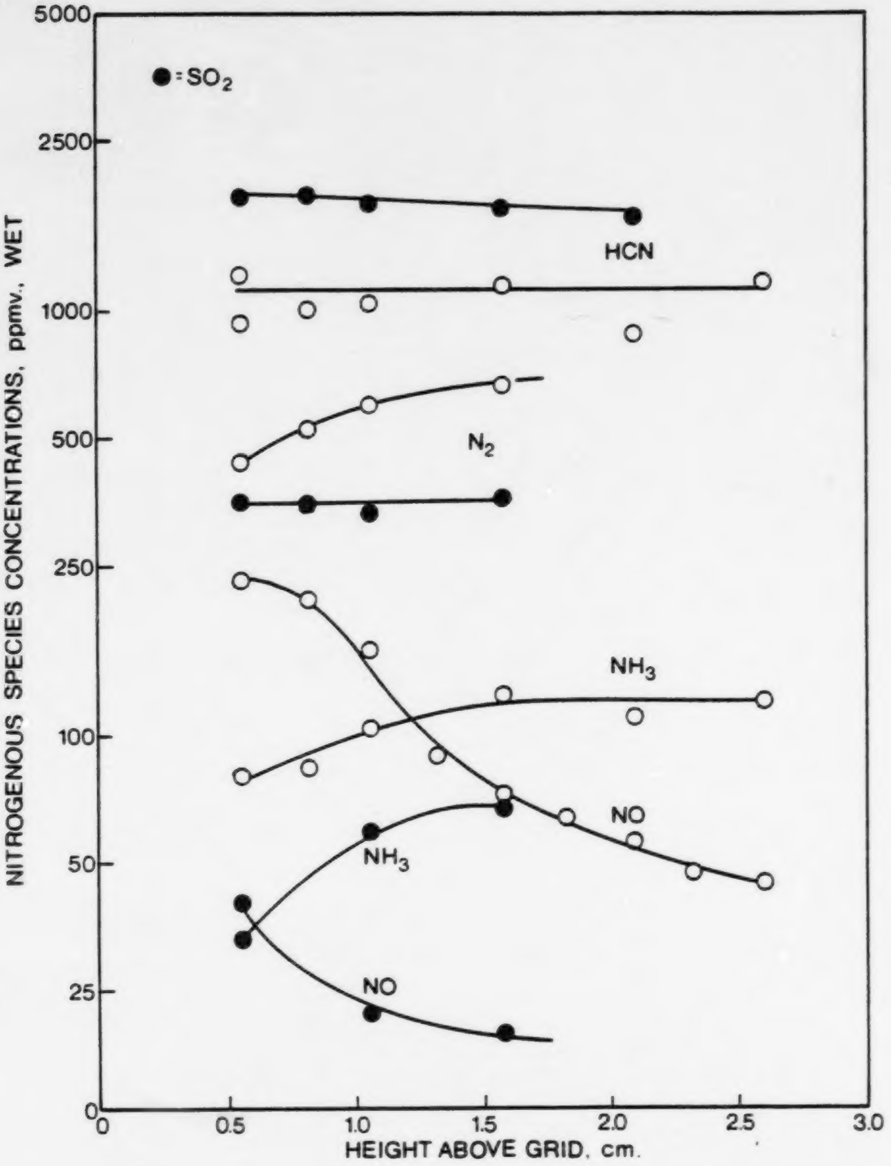

Figure 4.3-6 Influence of Sulfur on Nitrogenous Species Profiles, SR = 0.458, Flame B [C_2N_2 = 53.6 mℓ/min]

profile varied and apparently depended (at least) upon flame temperature and the nature of the diluent. It is also possible that the effect of sulfur on NO may be related to the sooting characteristics of these flames since nitrogen was found in samples of the soot produced, and soot formation appeared to be inhibited by SO_2.

b) Stoichiometric Ratio, SR = 0.585

At a stoichiometric ratio of SR = 0.585, the flame operated below visible sooting conditions, and this allowed the carbon balance to be utilized to calculate the flue gas molar flow rate and thus accurately determine the nitrogen balance. Therefore, data presented in this section are discussed in detail. Concentrations of H_2 and H_2O were not measured accurately (the former because of inadequate separation of He and H_2, the latter because of possible partial condensation in the heated sample line), but were calculated using the oxygen and hydrogen balance.

Figure 4.3-7 shows the major species profiles as functions of distance and Figure 4.3-8 the temperature profile. The levels of CH_4 and C_2H_2 were small (maximum 900 ppm CH_4; maximum 1500 ppm C_2H_2) in the sulfur free case and the addition of SO_2 reduced the concentrations of hydrocarbons to the detector limits. Figure 4.3-9 compares the temperature measured with Na D-line to that corresponding to a water gas shift equilibrium consistent with the CO, CO_2, H_2 and H_2O concentrations. The close agreement (within 50 K) indicates that the gases withdrawn from the flame were rapidly quenched in the probe and consequently that probe reactions were probably negligible.

Concentrations of nitrogenous species are plotted in Figure 4.3-10. NO profiles show similar behavior to that found by de Soete (1975) and by

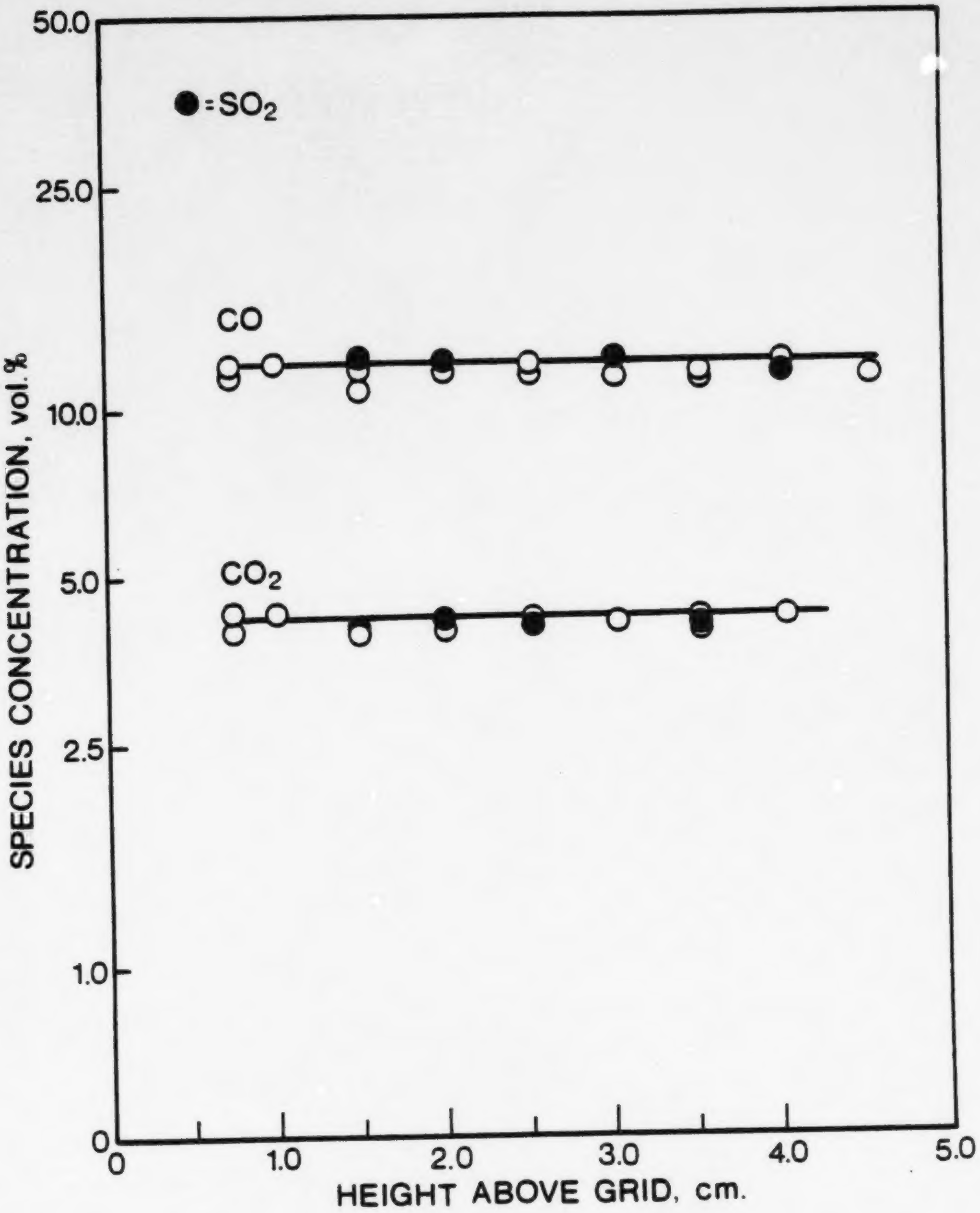

Figure 4.3-7 Major Species, SR = 0.585. [CH_4 = 7.12 ℓ/min, O_2 = 8.39 ℓ/min, He = 26.99 ℓ/min, SO_2 = 215 mℓ/min]

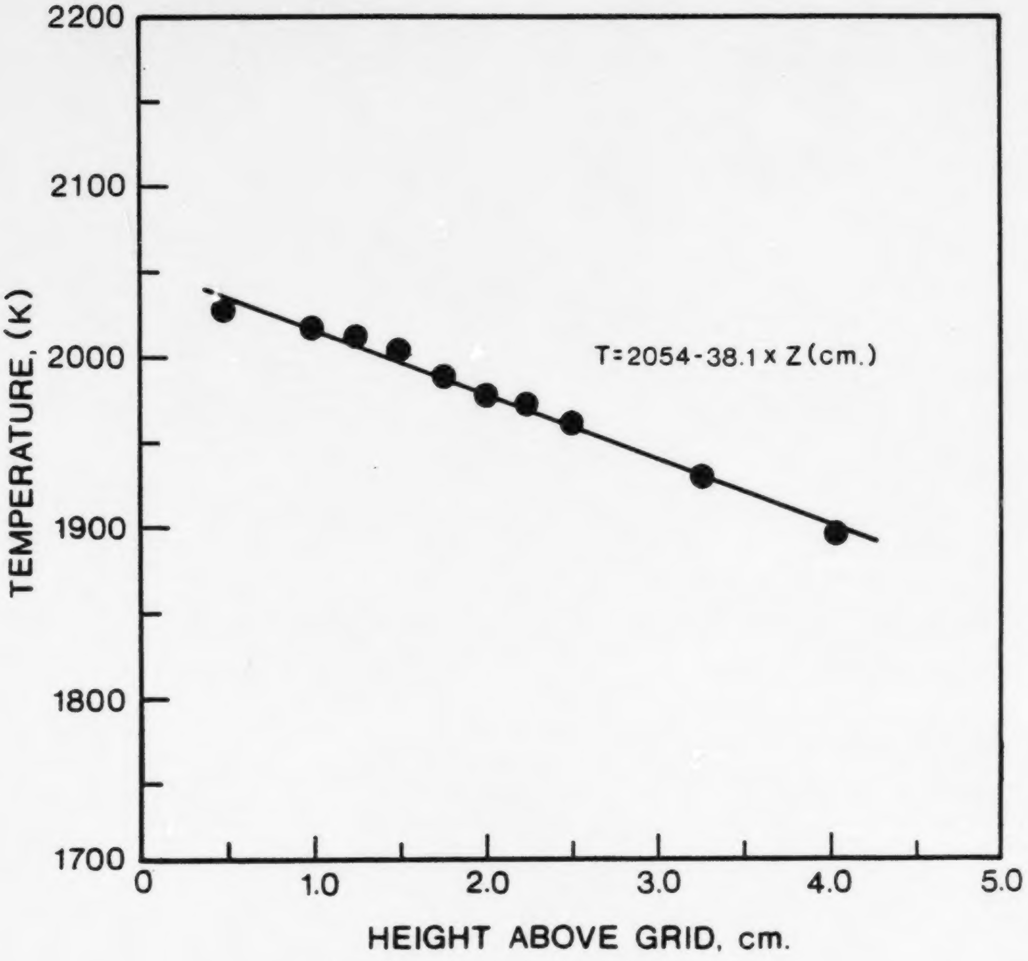

Figure 4.3-8 Temperature Profile: SR = 0.585

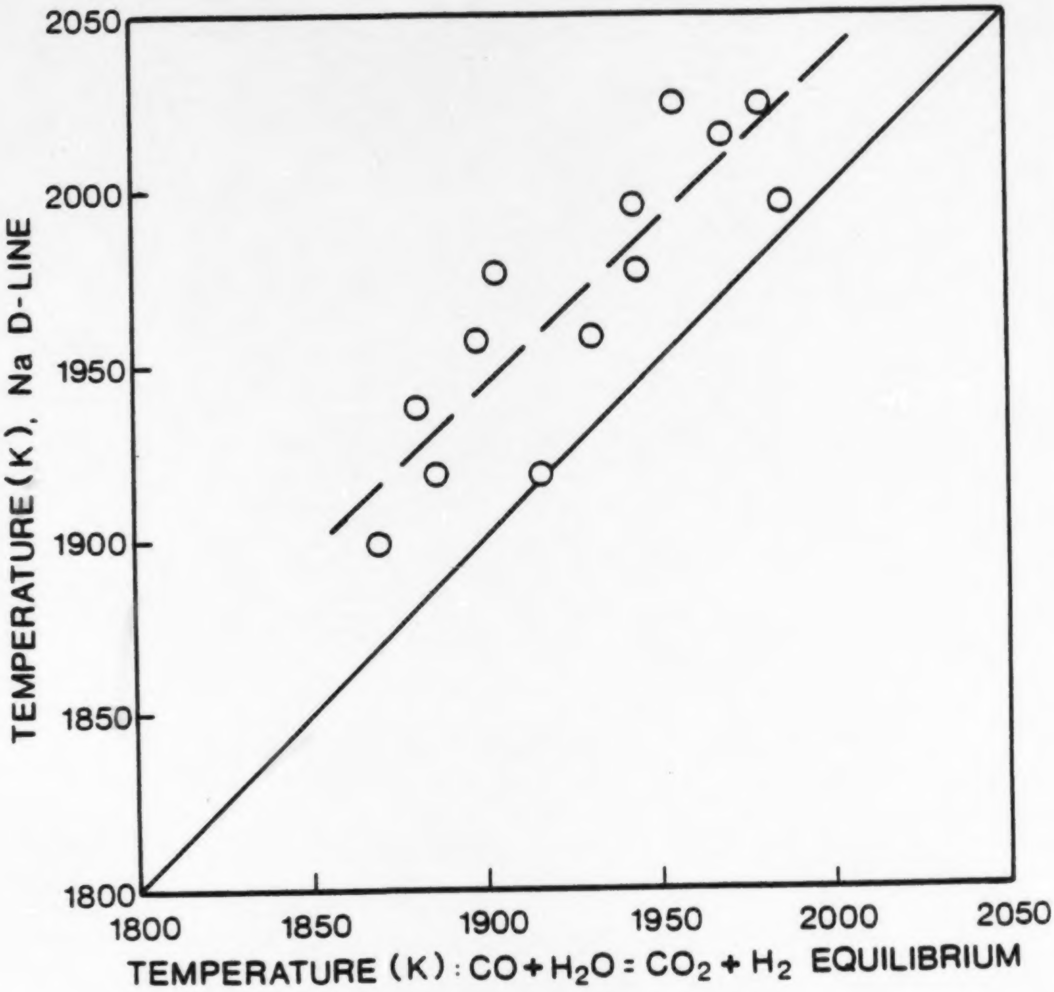

Figure 4.3-9 Comparison of Measured Temperature and Temperature Consistent with Water Gas Shift Equilibrium.

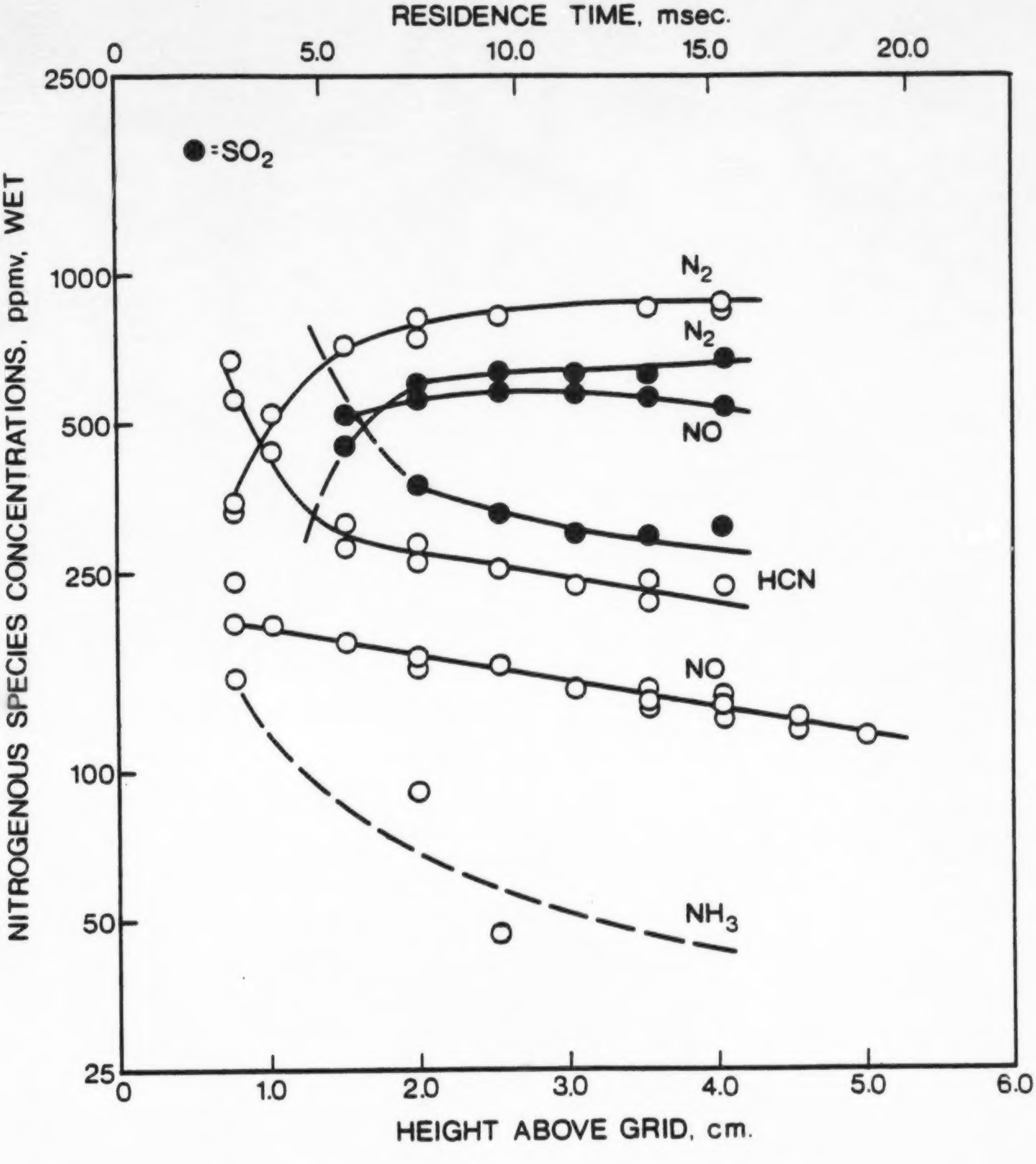

Figure 4.3-10 Influence of Sulfur on Nitrogenous Species, SR = 0.585 [C_2N_2 = 50.9 mℓ/min]

us in Part 2 of this report. The addition of sulfur increased the NO formed by over 300 ppm. Furthermore, the sulfur increased HCN concentrations and decreased N_2 formation significantly. NH_3 levels are low and decayed rapidly in the post flame.

The experimental ability to close the nitrogen balance in this flame is shown in Figure 4.3-11. At distances greater than 2.0 cm, or residence times greater than about 7 msec, closure to within 3% is obtained for most cases.

Early in the flame the discrepancy is as great as twenty five percent low. Since the maximum experimental error in nitrogenous species measurements (total N_2 balance) is ± 5%, the inability to close the nitrogen balance early in the flame is attributed to the presence of another nitrogenous species which was not measured.

The data of Houser and Lee (1980) on C_2N_2 oxidation at temperatures near 1273 suggest that the missing nitrogenous compound may be N_2O. These authors observed about 20% conversion of the reacted cyanogen to N_2O. Significant levels of N_2O from fuel nitrogen were also reported by Corlett et al (1979). Maclean and Wagner (1967) also observed early formation of N_2O in the pyrolysis zone of low-pressure ammonia-oxygen flames. Downstream, in the latter parts of the flame, the N_2O disappeared. Axworthy and Dayan (1977) measured N_2O product yields of 15 to 40% from the oxidative pyrolysis of pyridine and benzonitrile in a quartz reactor operated near 2000 K. Finally, definitive proof of the presence of N_2O in samples from this flame is contained in our chromatograms which show a small shoulder peak on the tail of the CO_2 peak. Separation was inadequate to quantify absolute amounts.

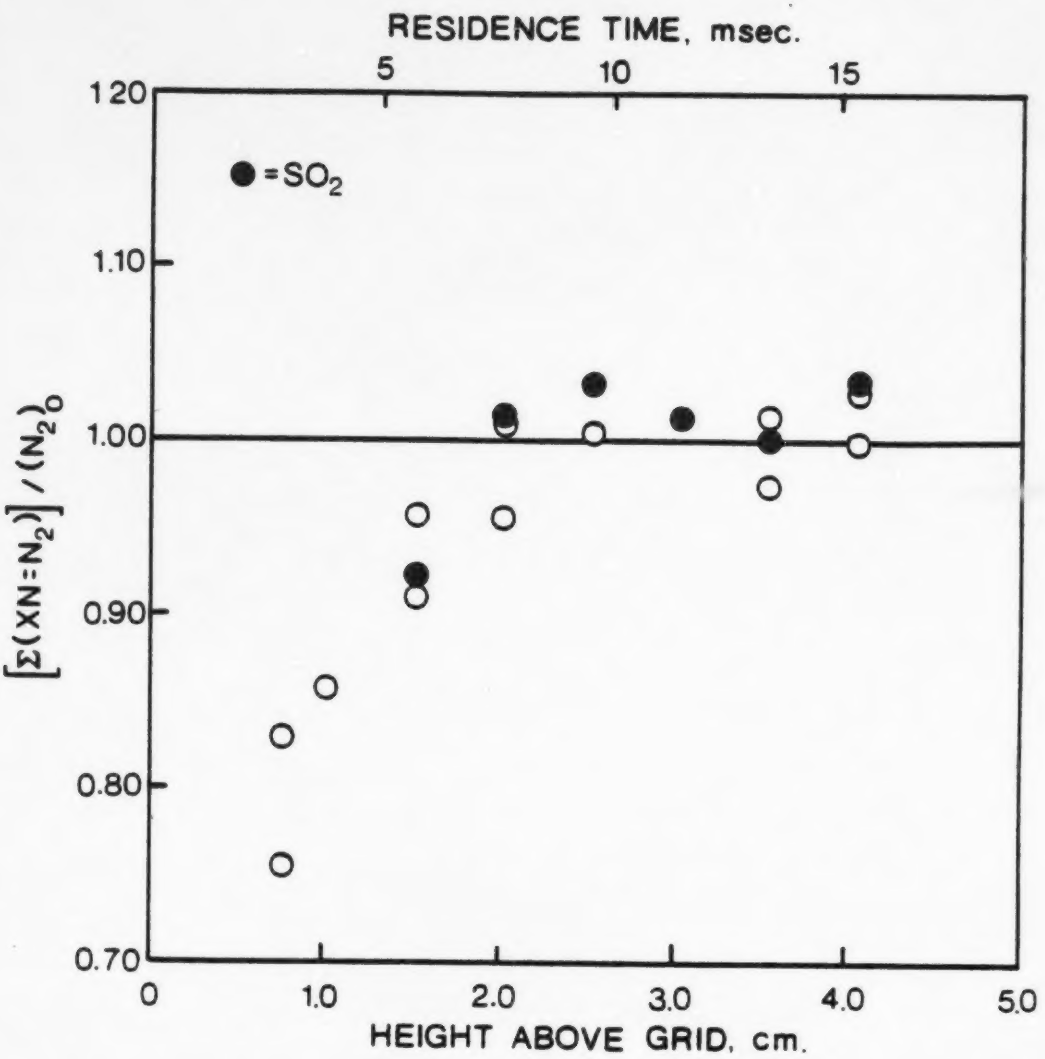

Figure 4.3-11 Closure of the Nitrogen Balance

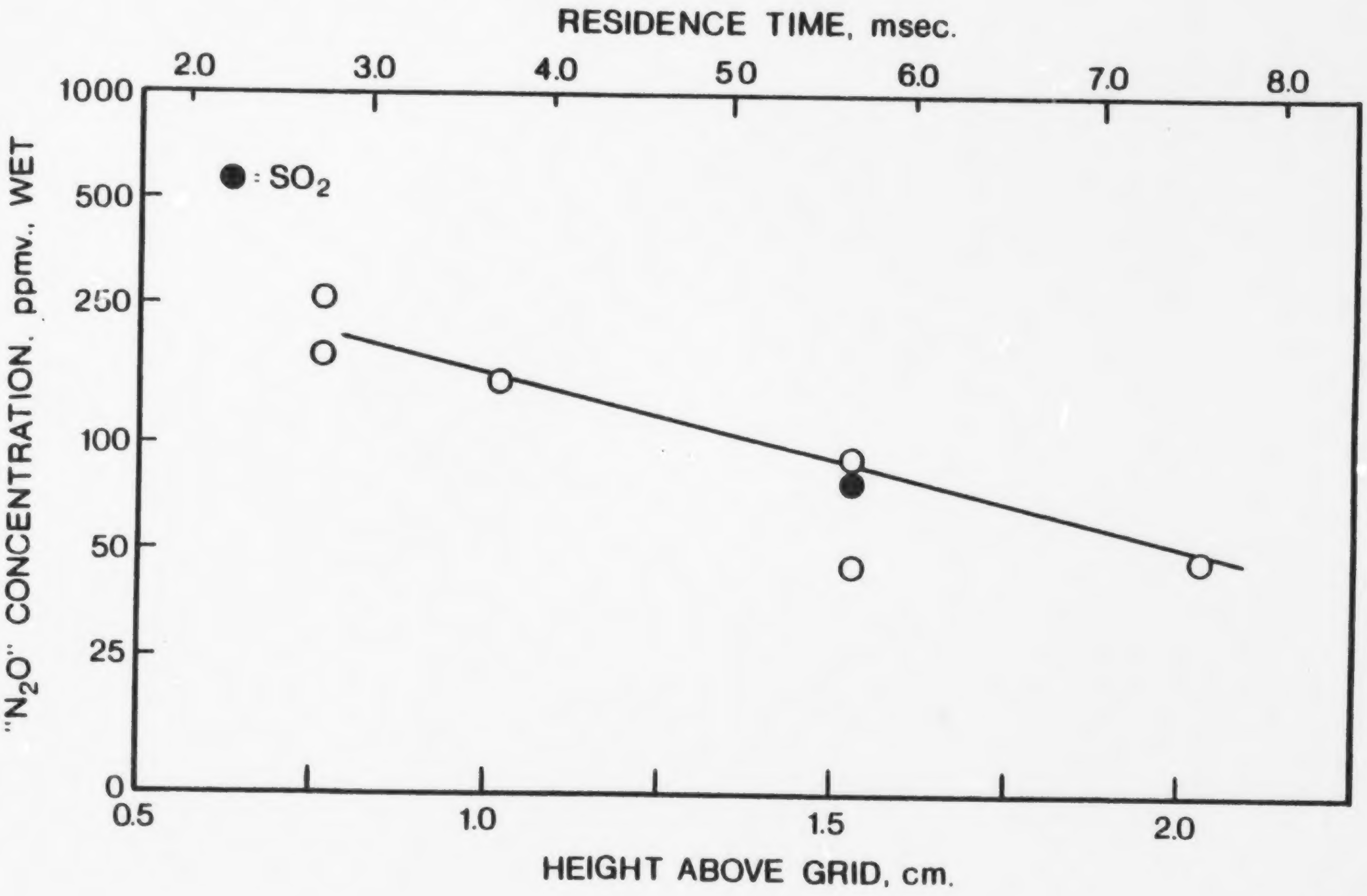

Figure 4.3-12 Decay of (Inferred) N_2O Concentration

These results strongly suggest that the (decaying) discrepancy in the nitrogen balance is caused by the formation of early N_2O and its subsequent destruction. Figure 4.3-12 shows the resulting profile for the missing nitrogenous species, which is assumed to be N_2O. Furthermore, analysis of the profiles of HCN, NH_3, NO, "N_2O" and N_2 early in the post flame, strongly suggest that "N_2O" is destroyed to form N_2 directly, indicating an important additional route to form N_2 from fuel nitrogen (as C_2N_2). Fuel sulfur does not appear to influence the "N_2O" profile, which suggests that the changes in the N_2 and NO profiles are due to an interaction between sulfur compounds and the steps connecting HCN destruction to N_2 formation. These data, therefore, are consistent with the data presented in Part 1 of this report, which indicates that sulfur can have a deleterious effect on NO_x emissions in poorly mixed or staged combustion conditions.

c) Stoichiometric Ratio SR = 0.693

At the stoichiometric ratio of 0.693 the sulfur effect becomes less pronounced as shown on Figure 4.3-13. However, the overall effect of fuel sulfur is still to increase HCN and lower N_2 profiles. These data are therefore consistent with those obtained in other phases of this project. In this flame there was no measurable CH_4 or C_2H_2 either with or without sulfur present. NH_3 levels were very low and the apparent increase shown is within the experimental error. The major stable species, CO and CO_2 were constant throughout the flame. The experimental temperature profile is given by: $T = 1964 - 30.4*Z(cm)$. The NO profiles are consistent with the data of de Soete (1975).

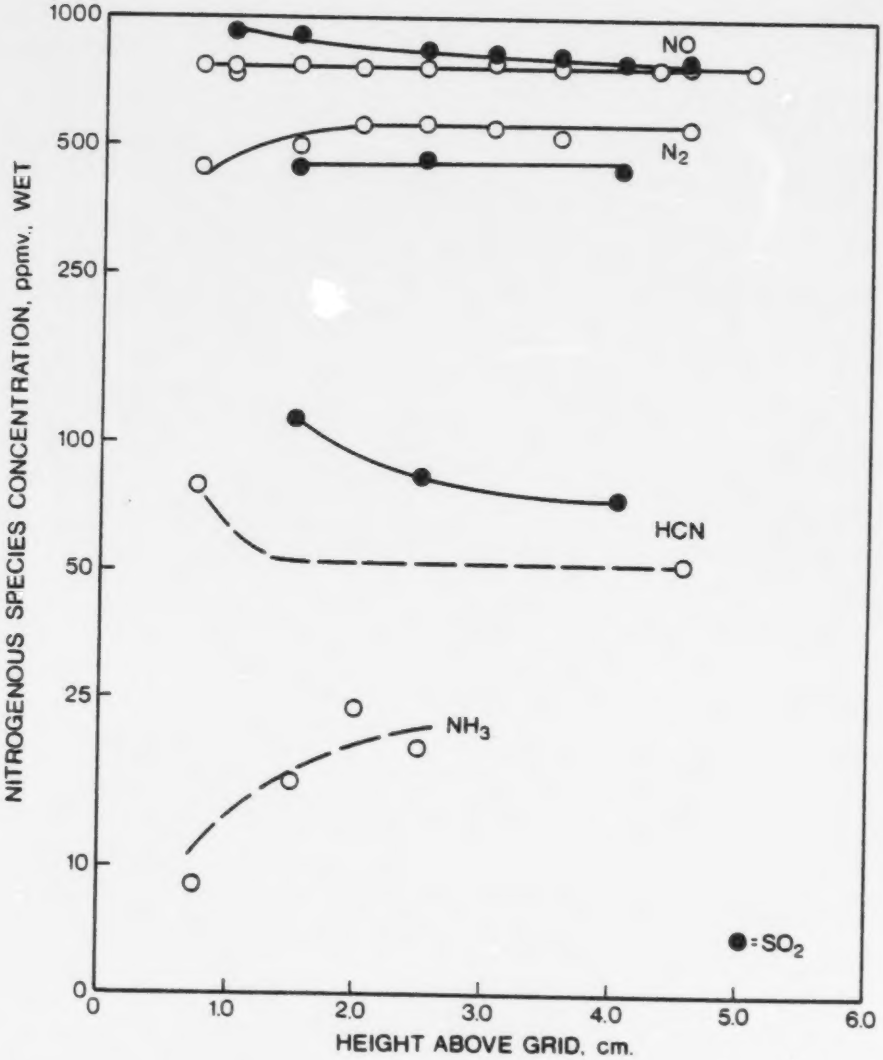

Figure 4.3-13 Nitrogenous Species Profiles, SR = 0.693 [CH_4 = 5.03 ℓ/min, O_2 = 7.04 ℓ/min, He = 39.67 ℓ/min, C_2N_2 = 983 ppm (979 ppm with SO_2), SO_2 = 4135 ppm]

4.4 Conclusions

The data presented in this part of the report shed light on the generality of the sulfur effect noted in Parts 1 and 2. In all cases sulfur raised HCN levels and lowered N_2 levels. Furthermore, the presence of sulfur influenced the hydrocarbon chemistry in the post flame. When soot is formed it contains nitrogenous compounds. We can conclude that sulfur will increase XN species and decrease N_2 species under hot fuel rich conditions. This has implications in attempts to develop optimum staged combustion configurations for fuels containing both chemically bound nitrogen and sulfur.

4.5 References for Part 4

1. Axworthy, A.E. and V.H. Dayan, Chemical Reactions in the Conversion of Fuel Nitrogen to NO_x: Fuel Pyrolysis Studies, Proceedings of the Second Stationary Source Combustion Symposium, Vol. 4, Fundamental Combustion Research. EPA-600/7-77-073d (NTIS PB 274-029), p. 39 (1977).
2. Corlett, R.C., L.E. Monteith, C.A. Halgren, and P.C. Malte, Molecular Nitrogen Yields from Fuel-Nitrogen in Backmixed Combustion, Comb. Sci. Tech., 19, 95 (1979).
3. de Soete, G., La Formation des Oxyde D'Azote Dans La Zone d'Oxydation des Flammes d'Hydrocarbures, Institut Francais due Petrole, Final Report No 23306, June 1975, Ruiell Malmaison, France.
4. Haynes, B.S. and H. Gg Wagner, Soot Formation, Prog. Energy Combust Sci., 7, 229 (1981).
5. Houser, T.J. and P.K. Lee, Oxidation of Cyanogen, Comb. Sci. Tech., 23, 177 (1980).
6. Maclean, D.I. and H.G. Wagner, The Structure of the Reaction Zones of Ammonia-Oxygen and Hydrazine-Decomposition Flames, Eleventh Symposium (International) on Combustion, p. 871, The Combustion Institute, 1967.